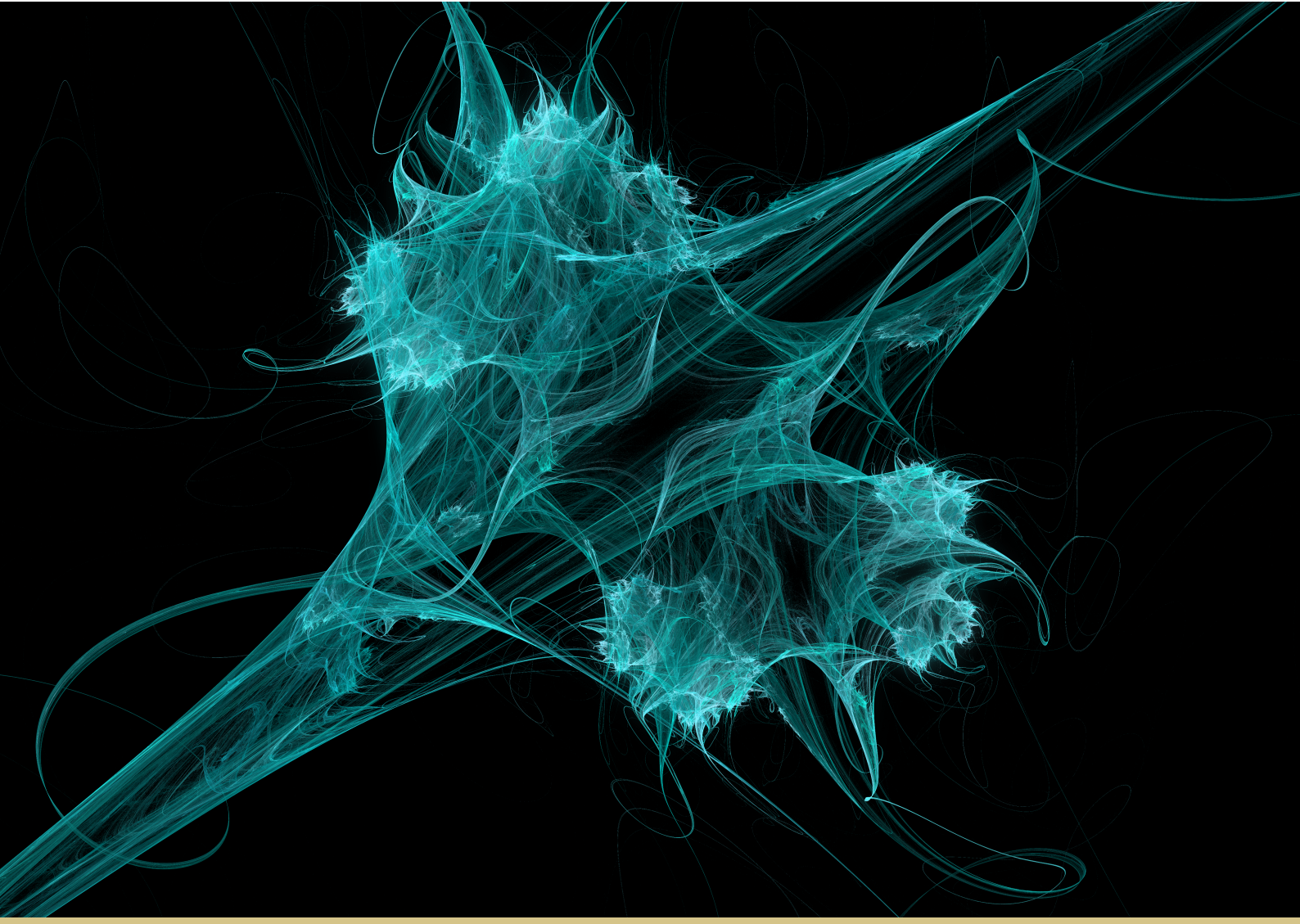

Sara Tavares de Sousa Melo Lima

INDUCTION OF DIFFERENT TYPES OF CELL DEATH BY THE ETHER LIPID EDELFOSINE IN GLIOBLASTOMA:
SIGNALLING CROSS-TALK CONTROLLING CELL DEATH COMMITMENT

Tese de Doutoramento em Ciências Farmacêuticas, especialidade de Biologia Celular e Molecular, orientada por Faustino Mollinedo e Maria Celeste Fernandes Lopes e apresentada à Faculdade de Farmácia da Universidade de Coimbra

2015

· U C ·

Universidade de Coimbra

INDUCTION OF DIFFERENT TYPES OF CELL DEATH BY THE ETHER LIPID EDELFOSINE IN GLIOBLASTOMA:

SIGNALLING CROSS-TALK CONTROLLING CELL DEATH COMMITMENT

Sara Tavares de Sousa Melo Lima

Tese de Doutoramento apresentada à Faculdade de Farmácia de Coimbra para obtenção do grau de Doutor em Ciências Farmacêuticas, especialidade de Biologia Celular e Molecular

· U C ·

UNIVERSIDADE DE COIMBRA

2015

Cover: Apoptosis, conceptual image. ©Laguna Design/Science Photo Library

Orientadores / Supervisors

Doutor Faustino Mollinedo
Instituto de Biología Molecular y Celular del Cáncer
Centro de Investigación del Cáncer, CSIC - Universidad de Salamanca
Salamanca, Espanha

Professora Doutora Maria Celeste Lopes
Faculdade de Farmácia, Universidade de Coimbra, Portugal
Centro de Neurociências e Biologia Celular (CNC), Universidade de Coimbra
Coimbra, Portugal

Instituições e financiamento / Institutions and funding

O trabalho experimental apresentado nesta tese de Doutoramento foi realizado no Centro de Investigación del Cáncer (CIC) da Universidade de Salamanca, Espanha, e no Centro de Neurociências e Biologia Celular (CNC) da Universidade de Coimbra, Portugal, tendo sido financiado pela Fundação para a Ciência e Tecnologia (FCT) através de uma Bolsa de Doutoramento (SFRH/BD/46330/2008).

The research work presented in this thesis was performed at the Center for Cancer Research, University of Salamanca, Spain, and at the Center for Neuroscience and Cell Biology, University of Coimbra, Portugal, and was funded by the Portuguese Foundation for Science and Technology, PhD fellowship (SFRH/BD/46330/2008).

FCT
Fundação para a Ciência e a Tecnologia
MINISTÉRIO DA CIÊNCIA, TECNOLOGIA E ENSINO SUPERIOR

Agradecimentos/Acknowledgements

Ao longo destes anos de Tese de Doutoramento tive a oportunidade de trabalhar e conviver com muitas pessoas que de várias maneiras me transmitiram novos conhecimentos e formas de ver e entender a vida. Gostaria de agradecer a todas essas pessoas que cruzaram e influenciaram o meu caminho e que contribuíram também para que este trabalho fosse possível:

Al Prof. Dr. Faustino Mollinedo, por darme la oportunidad de realizar este trabajo en su laboratorio y acogerme desde el primer momento con toda la amabilidad. Gracias por sus enseñanzas y por la confianza depositada em mí. Ha sido un largo trayecto, con muchas dificultades, pero querré recordar siempre el entusiamo y la ilusión con que discutimos los resultados de estas células "tan raras!"

À Prof. Dra. Celeste Lopes, pelo seu apoio ao longo deste difícil percurso e por estar sempre disponível para ajudar, mesmo não estando perto. Pela sua preocupação e interesse pela minha carreira, pelas generosas oportunidades que me tem proporcionado. O meu mais sincero agradecimento por transmitir-me a sua motivação e confiança, sem as quais provavelmente não teria podido levar este projecto até ao fim.

A la Dra. Consuelo Gajate, por su apoyo y disponibilidad a lo largo de estos años.

A todos mis compañeros de laboratorio: Mariana, Álvaro, Janny, Rúben, Rósula, Márcia, Xime, Ale, Ana, Vero, Amayita, Alberto y Adolfo. A los compis del labo 1, Sami, Alicia, Pilar, Fer, Carmela, los vecinos más animados y con la buena costumbre (o mala, para ellos quizás) de trabajar en festivos y horas tardías de la noche, facilitando siempre algún reactivo o una charla amistosa. La mayoría ya estaban ahí cuando llegué, otros llegaron después. Muchos se han marchado antes de mí...os recordaré siempre con mucho cariño. Recordaré también las fiestas, helados en la plaza mayor, idas de pinchos, tardes por el puente romano y noches de bailes de salsa. Gracias por ser mi familia en Salamanca y compartir conmigo momentos tan especiales. Gracias por vuestras ideas, consejos y risas. Por hacer la vida en el labo más fácil y divertida, por tantas horas en el cuarto de cultivos, en los sofas del CIC, en la biblioteca y en la calle. Vuestras formas distintas y coloridas de ver la vida y el mundo me han hecho entender también el mundo de una otra forma.

Un agradecimiento especial a mi querida amiga Alejandra, por escucharme siempre, apoyarme en los buenos y malos momentos, por compartir mi entusiasmo por la repostería creativa y otras locuras, por creer siempre en el suceso de mis tartas y de mis experimentos. Gracias por todo lo que he aprendido de ti, admiro tu fortaleza y tu fe, y agradezco haber podido compartir contigo y con tu bebé Paula tan buenos y tiernos momentos.

À minha Mãe e ao meu Pai, às minhas irmãs Sofia e Leonor, aos meus Avós. Por me terem trazido até aqui, por estarem sempre comigo mesmo estando longe. Por acreditarem em mim, por entenderem a minha ausência, por olharem pela minha Patas. Obrigada Mãezinha por me ouvires todas as noites ao telefone, descrevendo vias de sinalização e hipóteses aborrecidas sobre o mecanismo de acção da edelfosina, pelas tuas palavras de apoio e conforto em todos os momentos. Obrigada Pita, pelo teu sentido de humor e imitações de nuestros hermanos que sempre me fazem rir, e por estares quando eu não estou. Obrigada Pai por acreditares em mim e por convenceres a família a ir ver-me a Salamanca. À minha irmã loirinha e meu cunhado Paulo, por me perguntarem sempre "Quando é que acabas isso, pá?", finalmente posso responder-vos! À minha Avó que tanto se preocupa comigo, um agradecimento especial por me ter cedido o escritório nestes últimos meses para poder trabalhar mais ou menos sossegada, e por trazer-me sempre algum miminho para subir a glicémia. Ao meu Avô, que continua sempre comigo, por me ter ensinado a pensar com conversas amenas.

Ao meu João, por ter sobrevivido a esta tese comigo. Obrigada pela paciência, por todas as horas de LaTeX, noites sem dormir e sessões de Teamviewer. Perdoa-me por todos os prazos não cumpridos e planos não realizados. Posso prometer que agora já está! E já tenho voo :)

Esta tese, ou pelo menos aquilo que ela tiver de bom, é de todos vós também.

Summary

Glioblastoma is the most common and the most aggressive malignant primary brain tumor. The survival rate for this tumor is extremely low because of its aggressiveness, ranging from about 3-4 months without treatment to up to a median survival of about 12-15 months following current medical therapy (Johnson & O'Neill, 2012; Lwin *et al.*, 2013). Despite very important progresses in the understanding of the molecular pathogenesis of glioblastoma and technological advances in diagnostic and treatment strategies, glioblastomas almost invariably recur near their initial sites rapidly leading to death (Holdhoff & Grossman, 2011; Omuro & DeAngelis, 2013).

A number of survival signalling pathways can be activated constitutively in glioma cells, rendering these cells resistant to conventional chemotherapies and pro-apoptotic insults (Adamson *et al.*, 2009; Kanu *et al.*, 2009). The unfavorable prognosis for glioblastoma patients is also strongly correlated to the intrinsic apoptosis resistance of glioblastoma cells (Kögel *et al.*, 2010; Eisele & Weller, 2013). On these grounds, induction of alternative types of cell death could be an option for the treatment of glioblastoma. Autophagic cell death has been recently considered as an alternative and emerging concept to trigger glioma cell death and to exploit caspase-independent programmed cell death pathways for the development of novel therapies (Kögel *et al.*, 2010).

The ether phospholipid edelfosine (1-*O*-octadecyl-2-*O*-methyl-*rac*-glycero-3-phosphocholine, ET-18-OCH_3) is the prototype molecule of a family of unnatural lipids, collectively known as synthetic alkylphospholipid analogs, which promotes apoptosis in a variety of tumor cells (Mollinedo *et al.*, 1993; Gajate & Mollinedo, 2002). Edelfosine has been shown to be an effective *in vitro* and *in vivo* antitumor drug, which acts through the reorganization of membrane domains, termed lipid rafts, as well as through an endoplasmic reticulum stress response, leading to caspase- and mitochondria-mediated apoptosis in different hematological and solid tumor cells (Gajate & Mollinedo, 2001, 2007, 2014; Gajate *et al.*, 2004, 2012; Nieto-Miguel *et al.*, 2007).

On the first part of this study, we report that edelfosine induces mainly necroptosis in the U118 (U-118 MG) glioblastoma cell line, used as a brain tumor cell line model, whereas apoptosis and autophagy are relatively minor responses. Edelfosine-induced necroptototic response is very rapid and potent, suggesting a putative therapeutic role for necroptosis in brain tumor therapy. On the second part, we describe that inhibition of MEK1/2-ERK1/2 signalling pathway highly potentiates edelfosine-induced apoptosis in glioblastoma U118 cells

and switches the type of edelfosine-induced cell death from necrosis to apoptosis. The MEK1/2 inhibitor U0126 alone reduced ERK1/2 phosphorylation, but its effect was further potentiated when used in combination with edelfosine, leading to: RIPK1 degradation, likely underlying inhibition of necroptosis; RelA/NF-κB p65 degradation, thus inhibiting survival signalling; and caspase activation, leading to caspase-dependent apoptosis. The fact that ERK1/2 inhibition dramatically potentiates edelfosine-induced apoptosis in U118 cells, and turns either the survival or necrotic responses into potent apoptosis, suggests that edelfosine is a potent inducer of apoptotic signalling, and that this apoptotic response is highly modulated by ERK1/2 phosphorylation.

Next, we explored the impact of each cell death modality in overall survival, and its implications for the development of resistance. When incubated with edelfosine alone, ~20% of the cells remained intact regarding mitochondrial membrane potential ($\Delta\Psi_m$), and did not die through apoptosis or necrosis. These surviving cells expressed Bcl-x_L and incubation with the BH3 mimetic inhibitor ABT-737 after edelfosine treatment induced $\Delta\Psi_m$ loss and increased cell death. U0126 preincubation resulted in Bcl-x_L degradation with practically all the cells undergoing total $\Delta\Psi_m$ loss (~95%), and strong caspase-9 activation and apoptosis. Inhibition of ERK phosphorylation changed the type of cell death following edelfosine treatment and favored cell demise. ERK and Bcl-x_L inhibition resulted in increased apoptotic rates and decreased survival of resistant cells.

Through repeated exposure to edelfosine, we generated a resistant cell line from the sensitive U118 cell line, U118-R, and then performed a comparative analysis of some characteristics in order to gain insight into possible mechanisms of resistance.

In the last part of this work, we screened for different types of cell death induced by edelfosine in other glioblastoma cell lines and explored possible ways to increase cell death execution and/or abolish survival signalling, aiming to identify commonly altered pathways where to interfere in order to maximize cell death and avoid drug resistance.

This study, with several limitations, brings some contributions to the understanding of decisions in cell death commitment and its implications to cell death resistance, and reinforces the need to further explore the repertoire of antiapoptotic mechanisms in cancer and how survival signalling and cell death blockage contribute to tumor progression, deregulated cell proliferation and resistance to therapies. U118 cells can constitute a useful cell model to elucidate the mechanisms that dictate the cellular decision to undergo alternative cell death pathways, such as apoptosis or necroptosis, as well as the processes mediating the triggering and execution of necroptosis.

Unveiling the molecular and regulatory features of the early/primary cell death triggers and initiators, as well as of the switches leading to the different types of cell death, will be of major importance in delineating new approaches to trigger and modulate cell death processes of critical importance in the treatment of tumors, including GBM.

Sumário

Glioblastoma (GBM) é o tipo de tumor cerebral primário maligno mais comum e também o mais agressivo. O tempo médio de sobrevida dos doentes portadores deste tumor é extremamente baixo devido à agressividade do mesmo, variando entre 3-4 meses sem tratamento e 12-15 meses cumprindo a actual terapêutica de referência (Johnson & O'Neill, 2012; Lwin *et al.*, 2013). Apesar dos importantes progressos no conhecimento sobre a patogénese molecular do GBM, e em tecnologias de diagnóstico e tratamento, os glioblastomas quase invariavelmente recidivam em zonas próximas da localização inicial, conduzindo rapidamente à morte (Holdhoff & Grossman, 2011; Omuro & DeAngelis, 2013).

Várias vias de sobrevivência encontram-se constitutivamente activadas em células de glioblastoma, tornando estas células resistentes à quimioterapia convencional e a estímulos pró-apoptóticos (Adamson *et al.*, 2009; Kanu *et al.*, 2009). O prognóstico desfavorável em doentes com GBM está também fortemente correlacionado com a resistência intrínseca das células do tumor à apoptose (Kögel *et al.*, 2010; Eisele & Weller, 2013). Neste campo, a indução de tipos de morte celular alternativos poderia constituir uma opção para o tratamento do GBM. A morte celular autofágica foi recentemente considerada como uma forma alternativa para a indução de morte celular em glioblastoma, tendo este conceito vindo a ser explorado de forma a tirar partido de mecanismos de morte celular programada independente de caspases para o desenvolvimento de novas terapias (Kögel *et al.*, 2010).

O éter lípido edelfosina (1-*O*-octadecyl-2-*O*-methyl-*rac*-glycero-3-phosphocholine, ET-18-OCH_3) é a molécula protótipo de uma família de lípidos artificiais, conhecidos colectivamente como análogos alquilfosfolípidos sintéticos, que promove apoptose em células de distintos tumores (Mollinedo *et al.*, 1993; Gajate & Mollinedo, 2002). A edelfosina demonstrou ser um fármaco antitumoral eficaz *in vitro* e *in vivo*, actuando através da reorganização de domínios da membrana plasmática denominados *lipid rafts*, bem como através da resposta de stress do retículo endoplasmático, induzindo apoptose mediada por caspases e mitocôndria em diferentes células de tumores hematológicos e de tumores sólidos (Gajate & Mollinedo, 2001, 2007, 2014; Gajate *et al.*, 2004, 2012; Nieto-Miguel *et al.*, 2007).

Na primeira parte deste estudo, mostramos que a edelfosina induz principalmente necroptose na linha celular de glioblastoma U118 (U118-MG), utilizada como modelo de GBM, enquanto que a apoptose e a autofagia constituem respostas menos significativas para a execução da morte celular. A resposta necroptótica induzida por edelfosina é muito rápida e potente, sugerindo um possível papel terapêutico para a necroptose no tratamento de tumores

cerebrais.

Numa segunda parte, descrevemos que a inibição da via de sinalização de MEK1/2-ERK1/2 potencia fortemente a apoptose induzida por edelfosina nas células U118 e muda o tipo de morte celular de necrose para apoptose. Isoladamente, o inibidor de MEK1/2 UO126 reduz a fosforilação de ERK1/2 mas os seus efeitos são potenciados quando usado simultaneamente com edelfosina, conduzindo a uma série de eventos: degradação de RIPK1, provavelmente responsável pela inibição da necroptose; degradação de RelA/NF-κB p65, inibindo assim a sinalização de sobrevivência; activação de caspases, conduzindo à execução de apoptose dependente de caspases. O facto de que a inibição de ERK1/2 potencia dramaticamente a apoptose induzida por edelfosina nas células U118 e altera as respostas de sobrevivência ou necroptose para uma potente activação da apoptose, sugere que a edelfosina é um indutor potente de sinalização apoptótica e que a sua regulação é altamente modulada através da fosforilação de ERK1/2.

Em seguida, avaliámos o impacto da modalidade de morte executada na sobrevivência celular e as suas implicações para o desenvolvimento de resistência. Quando incubadas com edelfosina, ~20% das células permaneceram intactas no que diz respeito ao potencial de membrana mitocondrial ($\Delta\Psi_m$), e não morreram nem por apoptose nem por necrose. Estas células sobreviventes expressam Bcl-x_L e a sua incubação com o inibidor mimético de BH3 ABT-737 após tratamento com edelfosina, resultou na perda de $\Delta\Psi_m$ e no aumento da morte celular. A pré-incubação com U0126 resultou na degradação de Bcl-x_L com praticamente todas as células a perderem $\Delta\Psi_m$ (~95%) e em forte activação de caspase-9 e apoptose. A inibição da fosforilação de ERK alterou o tipo de morte após tratamento com edelfosina, favorecendo a morte celular. A inibição de ERK e de Bcl-x_L conduziu a taxas mais altas de apoptose e à diminuição da sobrevivência de células resistentes.

Através de exposição repetida à edelfosina gerámos, a partir da linha U118 originalmente sensível, uma linha celular resistente, U118-R, e fizémos uma análise comparativa de algumas características de forma a tentar compreender melhor possíveis mecanismos de resitência ao fármaco.

Na última parte deste trabalho, procurámos caracterizar diferentes tipos de morte celular induzidos pela edelfosina noutras linhas de glioblastoma e explorámos formas de aumentar a execução da morte celular e/ou abolir a sinalização de sobrevivência, tentando identificar vias de sinalização que se encontram mais frequentemente alteradas em GBM, onde interferir de forma a maximizar a morte celular e evitar o desenvolvimento de resistência ao fármaco.

Este estudo, apesar das limitações, traz algumas contribuições para a compreensão da "decisão de opção" entre distintos tipos de morte e possíveis implicações dessa decisão para o desenvolvimento de resistência à morte, e reforça a necessidade urgente de explorar detalhadamente o repertório de mecanismos antiapoptóticos no cancro e a forma como a sinalização de sobrevivência e o bloqueio da execução de morte celular contribuem para a progressão tumoral, desregulação da proliferação celular e resistência a terapêuticas. A linha celular U118 pode constituir um modelo útil para ajudar a esclarecer quais os mecanismos que ditam a decisão para a execução de um ou de outro mecanismo de morte, como a apoptose ou a

necroptose, e quais os processos que medeiam as fases de *triggering* e de execução da necroptose. Conhecer as características moleculares de iniciadores e reguladores de morte celular bem como dos "interruptores" que conduzem à execução de distintos tipos de morte será de extrema importância para o estabelecimento de novas formas de activação e modulação de mecanismos de morte essenciais para o tratamento mais eficaz de tumores, incluindo GBM.

Abbreviations/Abreviaturas: ERK, extracellular signal-regulated kinase; MAPK, mitogen- activated protein kinase; MEK1/2, MAPK/ERK kinase 1/2; NF- κB, nuclear factor kappa-light-chain-enhancer of activated B cells; RIPK1, receptor-interacting serine/threonine-protein kinase 1; U0126, 1,4-diamino-2,3- dicyano-1,4-bis[2-aminophenylthio]butadiene; ABT-737, 4-[4-[[2-(4-chlorophenyl)phenyl]methyl]piperazin-1-yl]-N-[4-[[(2R)-4-(dimethylamino)-1-phenylsulfanylbutan-2-yl]amino]-3-nitrophenyl]sulfonylbenzamide.

Glossary

A

ABC ATP-binding cassette
ADP Adenine dinucleotide phosphate
AEL Antitumor ether lipid
AEP Alkyl ether phospholipid
AIF Apoptosis-Inducing Factor
Akt/PKB Protein Kinase B
ALP Alkyl-lysophospholipid
AML Acute myeloid leukemia
ANT Adenine Nucleotide Translocase
AO Acridine orange
APAF1 Apoptotic Protease Activating Factor 1
2-APB 2-aminoethoxydiphenyl borate
APC Alkylphosphocholine
APL Alkylphospholipid
APO1/Fas/CD95 Apoptosis antigen 1/Fas/Cluster of Differentiation 95
ARF1 ADP-Ribosylation Factor 1
ASK Apoptosis Signal-regulating Kinase
ATG Autophagy-related gene
ATL Antitumor lipid
ATP Adenosine triphosphate
AVO Acidic vacuole organelle

B

BAF Bafilomycin A1
BAP31 B-cell receptor-Associated Protein 31
BBB Blood brain barrier
Bcl-2 B-cell lymphoma 2
BH-3 Bcl-2 Homology domain 3
Bid BH3-Interacting-Domain Death Agonist
BNIP3 Bcl2/Adenovirus E1B 19kDa Interacting Protein 3

C

CAD Caspase-Activated DNase
CCT CTP: phosphocholine cytidylyltransferase
CDKN2A/p16 p16-Cycline-Dependent Kinase Inhibitor 2A
CDP-choline Cytidine diphosphate-choline
CE Cholesteryl esters
CHEK/CHK Checkpoint Kinase
Cho Choline
CHOP/GADD153 C/EBP Homology Protein / Growth Arrest and DNA damage-inducible protein 153
CI Confidence interval
CLL Chronic lymphocytic leukemia
CMC Critical micellar concentration
CNS Central Nervous System
CQ Chloroquine
CREB cAMP Response Element-Binding Protein
CT Computed tomography
CTP Cytidine triphosphate
CYLD Cylindromatosis (Turban Tumor Syndrome)

D

DAG Diacylglycerol
DCC Deleted in Colorectal Carcinoma
DD Death Domain
DED Death Effector Domain
DHE Dihydroethidine
DIC Differential interference contrast
$DiOC_6(3)$ 3,3'-dihexyloxacarbocyanine iodide
DISC Death-Inducing Signaling Complex
DMEM Dulbecco's modified Eagle's medium
DMSO Dimethyl sulfoxide
DR Death Receptor
DTT Dithiothreitol

E

EBRT External beam radiation therapy
ECL Enhanced chemiluminescence
EDLF Edelfosine
EDTA Ethylenediaminetetraacetic acid
EGF Epidermal Growth Factor
EGFR Epidermal Growth Factor Receptor
EGFRvIII Epidermal Growth Factor Receptor variant III
EGTA Ethylene glycol tetraacetic acid
ENDOG Endonuclease G
ER Endoplasmic reticulum
ERBB2 Receptor tyrosine-protein kinase erbB-2
ERK Extracellular Signal-Regulated Kinase
ErPC Erucylphosphocholine
ErPC3 Erufosine
ET-18-OCH_3 Edelfosine

F

FADD Fas-Associated Death Domain-Containing Protein
FAK Focal Adhesion Kinase
Fas/APO1/CD95 Fas/Apoptosis antigen 1/Cluster of Differentiation 95
FasL/CD95L Fas/CD95 ligand
FasR Fas receptor/Fas/CD95/APO1
FBS Fetal bovine serum
FDA (United States) Food and Drug Administration
FITC Fluorescein isothiocyanate
c-FLIP cellular FLICE-inhibitory protein
FOX Forkhead transcription factor
FSC Forward scatter

G

GBM Glioblastoma multiforme
Gd-DTPA Gandolinium-diethylenetriamine pentaacetic acid
GELD Geldanamycin, Hsp90 inhibitor
GSK-3 Glycogen Synthase Kinase 3
GTP Guanosine triphosphate

H

HE Hydroethidine
HIF Hypoxia-Inducible Factor
HMGB1 High Mobility Group B1
HPC/miltefosine Hexadecylphosphocholine
HRP Horseradish peroxidase
Hsp90 Heat shock protein 90

I

IAP Inhibitor of Apoptosis
ICAD Inhibitor of Caspase-Activated DNase (CAD)
ICNIRP International Comission on No-Ionizing Radiation Protection
IDH1 Isocitrate dehydrogenase-1
IDO Indoleamine-2,3-dioxygenase
IEX IEX-1/IER3 - immediate early response 3
IF Immunofluorescence (immunocytochemistry)

IFN Interferon
IGF Insulin-like Growth Factor
IMS Intermembrane space

J

JNK c-Jun N-terminal kinase

K

KEGG Kyoto Encyclopedia of Genes and Genomes
KPS Karnofsky performance status

L

LC3B Light chain 3B
LDH Lactate dehydrogenase
LMP Lysosomal membrane permeabilization
LPC Lysophosphatidylcholine

M

MAPK Mitogen-Activated Protein Kinase
Mcl-1 Myeloid cell leukemia 1
MDC Monodansylcadaverine
MDM2 Mouse Double Minute 2 homolog
MDM4 Mouse Double Minute 4 homolog
MEK1/2 MAPK/ERK kinase 1/2
MET Mesenchymal Epithelial Transition factor
MFI Mean fluorescence intensity
MGMT O^6-methylguanine methyltransferase
MLKL Mixed-Lineage Kinase domain-like
MMP Mitochondrial membrane permeabilization
MOMP Mitochondrial outer membrane permeabilization
MPT Mitochondrial permeability transition
MRI Magnetic resonance image
MRS Magnetic resonance spectroscopy
mTOR Mammalian target of rapamycin

N

NAA N-acetylaspartate
NADP Nicotinamide adenine dinucleotide phosphate
NADPH Reduced form of nicotinamide adenine dinucleotide phosphate
NCCD Nomenclature Committee on Cell Death
Nec-1 Necrostatin-1
Nec-1s 7-Cl-O-Nec-1
NEMO NF- κB Essential Modulator
NF- κB/RelA Nuclear factor kappa-light-chain-enhancer of activated B cells
NF1 Neurofibromatosis type I
NF2 Neurofibromatosis type II
NSA Necrosulfonamide

O

OlPC Oleylphosphocholine

P

PA Phosphatidic acid
PARP Poly(ADP-ribose) polymerase
PBS Phosphate-buffered saline
PC Phosphatidylcholine
PDGF Platelet-Derived Growth Factor
PDGFR Platelet-Derived Growth Factor Receptor
PDK Pyruvate Dehydrogenase Kinase
PET Positron emission tomography
PFS Progression-free survival
PGAM5 Phosphatase phosphoglycerate Mutase family member 5
PH Pleckstrin homology
PI Propidium iodide
PI3K Phosphatidylinositol-4,5-bisphosphate 3-kinase
PIP3 Phosphatidylinositol (3,4,5)-triphosphate

PKB/Akt Protein kinase B
PKC Protein kinase C
PMSF Phenylmethylsulfonyl fluoride
PTEN Phosphatase and Tensin homologue
PTPC Permeability transition pore complex
PUMA/BBC3 Bcl-2 Binding Component 3
PVDF Polyvinylidene fluoride

R

RB Retinoblastoma
RelA/NFκB Nuclear Factor kappa-light-chain-enhancer of activated B cells
RHIM RIP Homotypic Interaction Motifs
RIPK/RIP1 Receptor Interacting Protein Kinase 1
ROS Reactive oxygen species
RT Radiotherapy

S

SAPK/JNK Stress-Activated Protein Kinase/ Jun amino-terminal Kinase
SD Standard deviation
SDS Sodium dodecyl sulfate
SMAC/DIABLO Second Mitochondria-derived Activator of Caspase
SphK Sphingosine kinase
SSC Side scatter
STAT Signal Transduction and Activator of Transcription
STS Staurosporine

T

TBST Tris-buffered saline with Tween
TCGA The Cancer Genome Atlas
TMZ Temozolomide
TNF Tumor Necrosis Factor
TNFR TNF Receptor
TNFRSF Tumor Necrosis Factor Receptor Superfamily
mTOR Mammalian Target Of Rapamycin
mTORC Mammalian Target Of Rapamycin Complex
TP53 Tumor protein p53
TRADD TNFRSF 1A-Associated via Death Domain
TRAF TNF Receptor Associated Factor
TRAIL TNF-Related Apoptosis-Inducing Ligand
TRAILR TNF-Related Apoptosis-Inducing Ligand Receptor
TSC1 Tuberous Sclerosis I
TSC2 Tuberous Sclerosis II
TUNEL Terminal deoxynucleotidyl transferase dUTP nick end labeling

U

UPR Unfolded protein response
UV Ultraviolet

V

VDAC Voltage-Dependent Anion Channel
VEFG Vascular Endothelial Growth Factor

W

WHO World Health Organization

X

XIAP X-Linked Inhibitor of Apoptosis

ABT-737 4-[4-[[2-(4-chlorophenyl)phenyl]methyl]piperazin-1-yl]-N-[4-[[(2R)-4-(dimethylamino)-1-phenylsulfanylbutan-2-yl]amino]-3-nitrophenyl]sulfonylbenzamide

BAPTA 1,2-bis(2-aminophenoxy)ethane-N,N,N′,N′-tetraacetic acid

DAPI 4′,6-Diamidino-2-phenylindole

Edelfosine 1-*O*-octadecyl-2-*O*-methyl-*rac*-glycero-3-phosphocholine

Et-BDP-ET (1-*O*-(11′-(6″-ethyl-1″,3″,5″,7″-tetramethyl-4″,4″-difluoro-4″-bora-3a″,4a″-diaza-*s*-indacen-2″-yl)undecyl)-2-*O*-metil-*rac*-glycero-3-phosphocholine

MTT 3-(4,5-Dimethylthiazol-2-yl)-2,5-diphenyltetrazolium bromide

Necrostatin-1 5-(1H-Indol-3-ylmethyl)-3-methyl-2-thioxo-4-imidazolidinone

Necrosulfonamide
(E)-N-(4-(N-(3-Methoxypyrazin-2-yl)sulfamoyl)phenyl)-3-(5-nitrothiophene-2-yl)acrylamide

U0126 1,4-diamino-2,3-dicyano-1,4-bis[2-aminophenylthio]butadiene

z-VAD/z-VAD-fmk carbobenzoxy-valyl-alanyl-aspartyl-[O-methyl]-fluoromethylketone

List of Figures

Contents

1 Introduction

"...the most acute, most powerful, and most deadly diseases, and those which are most difficult to be understood by the inexperienced, fall upon the brain."

Hippocrates

Glioblastoma overview

The tumors of the central nervous system (CNS) are grouped according to the type of their presumable cell of origin and are graded based on standard histopathological features (Pelloski & Gilbert, 2007). Among the neoplasms of the CNS, gliomas comprise a heterogeneous group of neuroectodermal tumors that arise from glial cells. Astrocytes, oligodendrocytes, and ependymal cells may give rise to astrocytomas, oligodendrogliomas, and ependymomas, respectively (Grier & Batchelor, 2006).

Glioblastoma, or glioblastoma multiforme (GBM) is one of the most frequently occurring tumors in the central nervous system, representing 12-15% of adult intracranial tumors and 50-60% of astrocytic neoplasms (Kleihues & Cavenee, 2000). Although "multiforme" is no longer part of the World Health Organization (WHO) designation, glioblastoma is still often abbreviated as "GBM", and this abbreviation will be also used along this work. GBM has had the name "multiforme" due to its variegated gross appearance (firm white areas, yellow necrotic areas, hemorrhagic areas and cystic areas) and diverse histological features (PathologyOutlines.com, 2013). It is now called only "glioblastoma" and is classified as a grade IV astrocytoma by the World Health Organization. The WHO classification of tumors of the CNS includes a grading scheme that is a 'malignancy scale' rather than a strict histological grading system, and Grade IV is the highest possible grade, being "assigned to cytologically malignant, mitotically active, necrosis-prone neoplasms that are typically associated with rapid pre- and postoperative disease evolution and a fatal outcome" (Louis

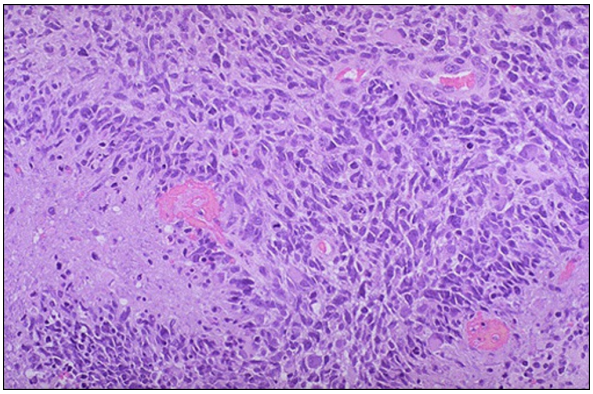

Figure 1.1: Histological specimen of a glioblastoma tumor stained with hematoxylin and eosin. The prominent vascularity, the extense area of necrosis at the left and the neoplastic cells palisading around it can be clearly seen. There is marked hyperchromatism and pleomorphism. *Image from University of Utah - Health Sciences Library (2015).*

et al., 2007). From the histological point of view, the system used by WHO is similar to the Sainte Anne/Mayo classification (Louis *et al.*, 2007). The next four morphologic criteria are used in the Sainte Anne-Mayo grading system to assign a grade:

a) nuclear atypia,
b) mitosis,
c) endothelial proliferation - "piled-up" endothelial cells. NOT hypervascularity
d) necrosis

Grades are assigned as following (Daumas-Duport *et al.*, 1988):

Grade 1 tumors - do not meet any of the criteria
Grade 2 tumors - meet one criterion, usually nuclear atypia
Grade 3 tumors - meet two criteria, usually nuclear atypia and mitosis
Grade 4 tumors - meet three or four of the criteria

Histologically, GBM can be distinguished from lower grade tumors by the presence of necrosis and microvascular hyperplasia (Brat, 2012). In GBM, small areas of necrotic tissue are typically surrounded by arrangements of anaplastic cells with elongated nuclei stacked in neat arrows - this alignment is known as "pseudopalisading". Perinecrotic palisading does not need to be present to identify GBM, but the pseudopalisading configuration is quite unique to malignant gliomas and has been recognized as an unfavourable prognostic factor (Rong *et al.*, 2006).

GBM is a highly anaplastic and morphologically heterogenous tumor, with an exceptionally infiltrative nature. Aberrant genetic events and altered signalling pathways contributing to this heterogeneity and to the infiltrative nature of GBM have been partially unriddled in the last years, however GBM treatment remains one of the most challenging tasks in oncology (Mrugala, 2013). Although important progresses were made, most patients diagnosed with this tumor die within one year from the diagnosis, and only ~5% survive more than 5 years despite pursuing aggressive therapies (Ostrom *et al.*, 2012).

Epidemiology

Compared to other types of cancer, brain and other nervous system cancers are relatively rare. According to the International Agency for Research on Cancer worldwide statistics, the estimated age-standardized rate of incidence for brain and other nervous system cancers was 3.4 per 100,000 in the year 2012 (IARC, 2015). GBM accounted for 15.4% of all primary brain and CNS tumors in the United States between the years 2007-2011 (Ostrom *et al.*, 2012) and these tumors are estimated to represent 1.4% of all newly diagnosed cancer cases in 2015 (SEER, 2014). Gliomas account for ~28% of all primary brain and CNS tumors, astrocytomas represent 75% of all gliomas (Ostrom *et al.*, 2012) and GBM constitutes the most frequently diagnosed astrocytoma. An estimated 14,930 deaths would be attributed to primary malignant brain and central nervous system tumors in the United States in 2013 (Siegel *et al.*, 2013).

Glioblastomas are slightly more common in men, with a male to female ratio of ~1.5:1, while meningiomas are more common among woman (Ostrom *et al.*, 2012). Because meningiomas harbor hormone receptors, an etiologic role for endogenous and exogenous hormones has been hypothesized for this cancer (Wiemels *et al.*, 2010) but the reason for the gender preponderance of both cancer subtypes is yet unknown.

Examination of incidence by race showed that Caucasians are at significantly higher risk for brain cancer than African-Americans (6.7 compared with 3.6 per 100,000); the corresponding relative risk was 1.86 (95% CI 1.78–1.94) (Sundeep Deorah *et al.*, 2006).

Most series report a median age at diagnosis of GBM in the mid-50s (Kleihues & Ohgaki, 1999; Simmons *et al.*, 2001). Although this tumor may affect people of all ages, less than 10% of children with central nervous system tumors have GBM and congenital cases are extremely rare (Iacob & Dinca, 2009).

The incidence of GBM is fairly constant worldwide, however there is a difference of around four fold in the incidence of primary malignant brain tumors between countries with a high incidence (e.g. Australia, Canada, Denmark, Finland, New Zealand and the US) and regions with a low incidence (e.g. Rizal in the Philippines and Mumbai in India) (Schwartzbaum *et al.*, 2006). Higher incidence rates are observed in countries with greater access to health care and better medical assistance but some of the geographic variations can not be easily attributable to this phenomenon (Schwartzbaum *et al.*, 2006). Evironmental factors are

expected to account at least for some of the observed geographic variation, but differences in diagnostic practices and completeness of reporting hamper geographic comparisons (Wrensch *et al.*, 2001).

Causes and risk factors for many common cancers have been established but the factors that contribute to brain tumorogenesis remain elusive despite a significant amount of research has been conducted to understand the etiology of primary brain tumors (Wrensch *et al.*, 2001).

Environmental risks

Studies investigating the etiology of primary brain tumors often produce conflicting results and the evidence for most of the explored associations remains to be conclusive (Gomes *et al.*, 2011). Different methodological issues arise when identifying environmental risk factors for brain tumors, namely: **1**. brain tumors are relatively rare, and cohort studies are not possible in many cases; even occupational and industrial cohort studies may have too few affected individuals to analyze exposure subgroups; **2**. case-control studies have problems such as misclassification of prior exposures and differential selection of cases and controls; **3**. many studies rely on proxy respondents, leading to further inaccuracies in prior exposures; **4**. possible recall bias for the affected patient, or even recall difficulties due to the own nature of the disease; **5**. the heterogeneity of primary brain tumors and the insufficient number of large-scale studies of homogeneous subtypes, etc. (Nelson *et al.*, 2004).

Occupational or industrial cohorts usually have many relevant exposures and identifying which chemicals or combination of chemicals/processes are responsible for observed risks is an extremely complex task. Environmental risk factors that were analyzed and for which the available evidence *has not excluded* the possibility of an association with brain tumors include: exposure to infectious agents, traffic related air pollution, residence near low frequency electromagnetic fields and volatile organic and non-organic compounds from landfills, exposure to ionizing radiation from diagnostic tests and hospital equipment and higher levels of exposure to petrochemicals, nitriles, nitrites, amides, lead, pesticides, herbicides and insecticides (Gomes *et al.*, 2011). Some of these organic and inorganic chemicals and metals are reported neuro-carcinogens (Gomes *et al.*, 2011) but a causal relationship between specific chemicals and primary brain cancers still remains to be established, even for known or putative carcinogens (Ohgaki & Kleihues, 2005).

Risk factors for which there is limited established biologic plausibility, such as electromagnetic fields, are even more equivocal than the risks associated with suspected chemical carcinogens (Nelson *et al.*, 2004). Association between brain tumors and cell phone usage, for example, appears to be inconclusive when the statistical significance is considered, although most of the studies reported an increased risk of brain tumors and a few studies reported no relationship between cell phone use and brain neoplasm (Gomes *et al.*, 2011). The International Commission on Non-Ionizing Radiation Protection, the International Committee on Electromagnetic Safety and the World Health Organization suggest that there is *no proven* health risk from cell phone use (ICNIRP, 1996, 2009; WHO, 2006) but further studies are

needed to address this question and improve the basis and reliability of the current safety standards (Leszczynski & Xu, 2010).

It is possible that synergy between different environmental factors influence GBM development, and also that these different environmental risk factors interact with genetic factors that are not uniform across different populations and different studies. This may explain the lack of meaningful information that could be extracted from all the epidemiological studies searching for risk factors and also justify contradictory results between some of them. If multiple factors contribute to the etiology of brain tumors and genetics control their influence, the weak association found between one factor and the development of brain tumors in a study could be diluted in new studies with more heterogeneity and different confounding factors, or it could represent just a chance finding; there are too many variables and not enough subjects to determine statistical significance. To better understand this interplay an interdisciplinary approach would be required, with the contribution of neurologists, oncologists, epidemiologists and molecular biologists; the new approaches should also consider better exposure assessment techniques, lifetime occupational exposures, genotypic and phenotypic characteristics and lifestyle and dietary habits (Gomes *et al.*, 2011).

Genetic risks

Studies linking candidate genes to brain tumor risk yielded the same mixed results as the ones for environmental factors. The difficulty of understanding the genetic basis of brain tumor risk arise from the same fundamental problems in finding environmental risk factors: limited number of brain tumor patients available for these studies, the possibility for necessary interactions of different genetic factors and/or of genetic and environmental factors that are not uniform across different populations and different studies (Reilly, 2009). Since studies of glioma epidemiology have generated inconsistent or null findings for most of the analyzed factors, risk factors for developing glioma remain poorly understood.

Only two relatively rare factors have so far been conclusively shown to affect glioma risk: exposure to high doses of ionizing radiation and inherited mutations of highly penetrant genes associated with rare syndromes (Schwartzbaum *et al.*, 2006).

Several genetic syndromes are strongly associated with glioblastomas, including Li-Fraumeni syndrome and Turcot syndrome, neurofibromatosis (I and II) and tuberous sclerosis. These patients have a much higher risk of developing malignant gliomas than the general population (Pelloski & Gilbert, 2007).

Li-Fraumeni syndrome is caused by mutations in the cell checkpoint genes *tumor protein p53* (*TP53*) and *checkpoint kinase 2* (*CHEK2*) (Van Meir *et al.*, 2009) and Turcot's syndrome is caused by mutations in genes involved in DNA repair (Hamilton *et al.*, 1995). Both syndromes may increase the risk for brain tumors since they cause a reduced ability to repair DNA mutation and also favor uncontrolled growth, due to the inhibition of different processes that prevent cells with mutated or damaged DNA from dividing. Neurofibromatosis is caused by mutations in *NF1* (*neurofibromatosis type I*) or *NF2* (*neurofibromatosis type II*) and

tuberous sclerosis by mutations in *TSC1* (*tuberous sclerosis I*) or *TSC2* (*tuberous sclerosis II*) (Reilly, 2009). Since *NF1*, *NF2*, *TSC1* and *TSC2* are involved in the downregulation of growth promoting signal transduction pathways (Reilly, 2009), their misregulation could facilitate cancer initiation and progression through unregulated cellular proliferation.

Regarding exposure to ionizing radiation, children treated with radiotherapy for leukemia and other cancers have an increased risk for developing CNS tumors, including malignant glioma (Neglia *et al.*, 2006). Adults with more benign brain tumors who are long-term survivors and received radiotherapy at the beginning of their treatment are also at higher risk of developing GBM (Mrugala, 2013).

Clinical presentation and diagnosis

The clinical manifestations of GBM depend on the age of the patient and on the location, size and rate of growth of the tumor (Zhang *et al.*, 2012). The clinical history of patients with glioblastoma multiforme is usually short, spanning less than 3 months in more than 50% of patients, except for the cases in which the neoplasm developed from a lower-grade astrocytoma (Kleihues & Ohgaki, 1999). Sometimes the patient may remain asymptomatic until the tumor has reached an enormous size (Iacob & Dinca, 2009). Like in other brain tumors, GBM produces symptoms by a combination of focal neurologic deficits from compression and infiltration of the surrounding brain, vascular compromise and raised intracranial pressure (Stadlbauer *et al.*, 2011). The most common presentation of patients with glioblastomas is a slowly progressive neurologic deficit, usually motor weakness, although the most common reported symptom is headache. The kind of symptoms depends highly on the location of the tumor, more so than on its pathological properties (Bala & Bhattacharjee, 2011). However, as with other CNS tumors, the most frequent symptoms include progressive headaches, dizziness, partial or generalized seizures in 30-60% of patients, contralateral slowly progressive hemiparesis, sudden onset of hemiplegia with depressed level of consciousness, sensory disturbances, subtle personality changes and visual field defects (Iacob & Dinca, 2009).

GBM occurs most often in the subcortical white matter of the cerebral hemispheres, although tumor infiltration into the adjacent cortex, basal ganglia or contralateral hemisphere is common (Bala & Bhattacharjee, 2011). With the progression of the disease, an increasing number of patients experience cognitive problems, neurologic deficits resulting from radiation necrosis, communicating hydrocephalus, occasionally cranial neuropathies and polyradiculopathies from leptomeningeal spread (Iacob & Dinca, 2009).

Imaging glioblastoma

The best imaging diagnostic method for GBM is a T1-weighted gadolinium-enhanced magnetic resonance image (MRI), particularly the three-planar images and diffusion tensor imaging (Zhang *et al.*, 2012).

The two most basic image types in magnetic resonance image are T1 and T2 images that can be obtained by manipulating two basic parameters, TR and TE. TR, repetition time, is the time between one radio frequency transmission, or excitation, and the next. TE, echo time, is the time between the excitation and when the coil is programmed to receive the resultant signal (Blink, 2004). Contrast-enhanced T1-weighted images (gadolinium-DTPA is the most commonly used contrast agent) are useful to evaluate blood-brain barrier (BBB) breakdown. Since gadolinium-DTPA does not cross the BBB, it will enhance only structures or lesions that are devoid of a BBB (Hesselink & Press, 1988). Contrast-enhanced computed tomography (CT) can delineate a disrupted BBB, but its sensitivity is much lower than that of MRI. Gd-DTPA MRI helps characterize and delineate the extent of lesions, and increases the sensitivity for detection of cerebral abnormalities (Hesselink & Press, 1988). Pathologies in the neighborhood of the skull base and the posterior fossa are better delineated by MRI because of the absence of artifacts caused by beam hardening in CT, in particular due to the petrous bone (Heiss *et al.*, 2011). As so, whenever possible, MRI image is preferred over CT scan for brain tumor image assessment (Zhang *et al.*, 2012).

Tissue asymmetries or a change in tissue density are diagnostic hints for space-occupying lesions: a slight increase in tissue density indicates an increase in tissue cellularity, a strong increase indicates calcification (commonly found in oligodendrogliomas), and decreased tissue density indicates low tumor cellularity or edema (Heiss *et al.*, 2011).

Glioblastoma MRI T1 images usually present an hypo to isointense mass within the white matter, with a central heterogeneous signal from necrosis or intratumoral hemorrhage. In enhanced MRI, enhancement is variable but is almost always present, typically peripheral and irregular with nodular components and completely surrounding necrosis (Gaillard, 2015). On T2-weighted images, GBM appears to be an heterogeneous mass with high signal intensity: again, this heterogeneous appearance may be due to central necrosis, hemorrhage and tumor vascularity. Vasogenic edema, surrounding the tumor and usually producing significant mass effect, is caused by abnormal neoplastic vessels that lack the normal blood-brain barrier, resulting in transudation of fluids and proteins into the extracellular space (Antonios, 2011).

The majority of GBMs are solitary lesions with multifocal and multicentric tumors occurring in about 10% and 1% of cases, respectively (Lafitte *et al.*, 2001). Multicentric tumors are widespread lesions in different lobes of the hemispheres without evidence of intracranial spread or microscopic connection, whereas those with either gross or microscopic continuity are defined as multifocal (Mechtler, 2009). Most commonly, GBMs disseminate along the white matter tracts to involve the contralateral hemisphere, especially across the corpus callosum and this symmetric extension through the corpus callosum gives rise to a butterfly appearance on MRI imaging (Urbańska *et al.*, 2014).

Due to its infiltrative nature, the tumor mass is usually not clearly distinguishable from the normal tissue and many gliomas contain areas of different de-differentiation degrees. By definition, the highest-grade component determines the grade of the tumor and, therefore, biopsy is best performed in contrast-enhanced areas, where it is more likely to find the most de-differentiated parts of the tumor. However, some apparently low-grade gliomas do contain anaplastic components that do not have yet a disrupted BBB and may be missed by biopsy (Delorme & Weber, 2006). Imaging tools like spectroscopy and perfusion-weighted imaging may help neurosurgeons locate the part of the tumor that probably contains the highest-grade component (Barker *et al.*, 1997). These modern MRI techniques, offering possibilities for the detection of functional information on metabolism and physiology, have been increasingly used to improve the sensitivity and specificity of diagnostics (Kurhanewicz *et al.*, 2000).

Magnetic resonance spectroscopy (MRS) can identify brain tumor masses with a marked increase in the choline (Cho) to creatine ratio, reduction of N-acetylaspartate (NAA) and the presence of a lactate-lipid peak (Horská & Barker, 2010). The less differentiated the tumor, the higher will be its choline concentration and the lower the NAA peak; a lipid or lactate peak may also indicate some higher degree of malignancy (Delorme & Weber, 2006). E.g., the presence of a central area with an increased Cho/NAA ratio and a lactate peak in a glioma MRS imaging without contrast enhancement (a low-grade lesion according to usual criteria), strongly indicates focal anaplasia and suggests a higher degree of malignancy (Delorme & Weber, 2006). A diffuse astrocytoma by biopsy that shows enhancement or evidence of necrosis on imaging should be monitored by MRI with the same frequency as a high-grade tumor, independently of the lower grade attributed by the pathology report (Mechtler, 2009). MRS can thus increase the diagnostic value of conventional MRI in non-invasive assessment of glioma grade (Bulik *et al.*, 2013) and also improve sensitivity of tumor diagnostics following other imaging assessments or biopsy.

MRI provides detailed morphologic information but still has limitations in identifying tumor grade, invasive growth into neighboring tissue, and treatment-induced changes, as well as recurrences. PET (positron emission tomography) can overcome some limitations of conventional MRI and be used to derive information on tumor hypoxia, necrosis, proliferative activity, or vasculature (Heiss *et al.*, 2011). Different PET modalities can be combined in order to evaluate these characteristics, including imaging of glucose metabolism, amino acid uptake, nucleoside uptake, and hypoxia. Diagnostic accuracy benefits from co-registration of PET results and MRI, enabling the fusion of high-resolution morphologic images with the corresponding biologic information (Heiss *et al.*, 2011).

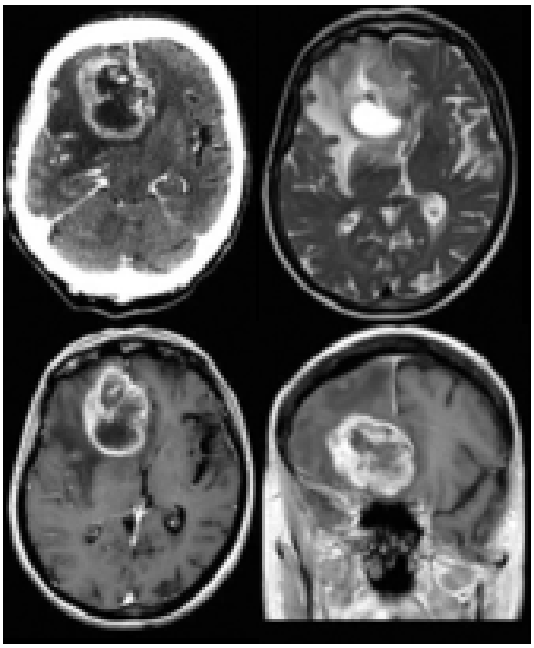

Figure 1.2: Upper pannel: Contrast-enhaced CT scan and T2-weighted MR images. The contrast-enhaced CT scan shows a peripherally enhancing lesion and T2WI shows a heterogeneous hyperintense mass and surrounding signal abnormality, probably related to tumor extension and edema. T1-weighted contrast-enhanced MR images are represented in the lower pannel showing a peripherally enhancing mass with surrounding mass effect and midline shift. The final diagnosis was glioblastoma multiforme WHO grade IV. *Images adapted from Heiss et al. (2011).*

Standard of care for newly diagnosed GBM

The standard of care for patients with newly diagnosed GBM includes maximal safe resection of the tumor followed by 6 week course of radiotherapy (typical dose ~60 Gy) with concomitant systemic therapy using the alkylating agent temozolomide (TMZ) (75 mg/m^2 daily), followed by the minimum of 6 months of adjuvant temozolomide (150/200 mg/m^2 for 5 days every 28 days) (Weller *et al.*, 2005).

Surgical resection alone results in a median survival of approximately 6 months. Combined surgical resection and radiotherapy (RT) extend median survival to 12.1 months and addition of temozolomide further extends the median survival to 14.6 months (Wilson *et al.*, 2014).

Surgery

The location of the disease and its complex and heterogeneous biology present major challenges to GBM therapy. Surgery is frequently inadequate given the diffuse nature of the tumor and inability to remove it without damaging the healthy brain: tumor locations such as the eloquent cortex, basal ganglia or brain stem may not be eligible for surgical intervention and typically exhibit worse prognosis (Mrugala, 2013). The main contraindications to resective surgery are poor performance status (Karnofsky performance status (KPS) <70), advanced age, eloquent location of the tumor or extensive bihemispheric involvement (Wilson *et al.*, 2014).

Although not proved in a phase III study, several studies support maximal, safe surgical resection (Lacroix *et al.*, 2001; Stummer *et al.*, 2006). Less tumor cells remaining after surgery represent a reduction in the number of cells that may be resistant to therapy, may undergo further malignant transformation or that may release growth factors and immune inhibiting agents, contibuting to unsuccessful treatment (Hentschel & Sawaya, 2003). The survival advantage found in some studies for younger patients with good Karnofsky scores when there was a 98% or greater resection may, however, reflect differences in tumor biology or patient performance status rather than the real impact of tumor removal (Pelloski & Gilbert, 2007). Although there is some discussion around the way many studies evaluated the value of extended resection, it is unlikely that additional, large-scale prospective randomized studies are either necessary or practical in the face of all the evidence that favors maximal resection (Gonda *et al.*, 2013).

Intraoperative magnetic resonance imaging, diffusion tensor imaging, awake craniotomy, cortical mapping, stereotactic guidance and fluorescent-guided resection represent amazing advances in peri-operative and surgical imaging techniques that have facilitated delineation of tumor borders and helped to optimize maximal safe surgical resection (Wilson *et al.*, 2014). Fluorescent-guided resection utilizes a pharmacologic agent that localizes to tumor but not to the surrounding normal brain and fluoresces when exposed to light of a specific wavelength, helping to distinguish tumor tissue that may otherwise appear normal (Wilson *et al.*,

2014). The use of fluorescence-guided resection was associated with improved outcome when compared to standard white light resection in different studies: patients were more likely to have a gross total resection and to be progression free at 6 months (Stummer *et al.*, 2006; Hoover *et al.*, 2010). Following these studies, intraoperative MRI- and fluorescence-guided surgery is increasingly being used to assist in achieving the goal of supra-maximum resection. It was observed that due to the significant reduction in mass effect, patients that undergo maximal resections tolerate radiotherapy better and experience fewer side effects (Hentschel & Sawaya, 2003).

Radiotherapy

Radiotherapy has long been the central component of adjuvant treatment in GBM, with improvement of patient survival times from ~14 weeks with surgery and supportive care to 36 weeks with the addition of external beam radiation therapy (EBRT) (Pelloski & Gilbert, 2007). Ionizing radiation induces single-strand and double-strand breaks in the DNA of proliferating cells, resulting in cell death of radiosensitive cancer cells. However, many aspects of radiotherapy, such as the dose, fractionation, target delineation and use of concurrent agents are still under investigation, in order to better understand and improve the benefits of this therapy. Several studies failed to reveal a survival advantage in doses above 60 Gy and also found no benefit from hyperfractionation, hypofractionation, or the use of Boron neutron capture; and from the existing studies emerged the standard dosing for GBM as 60 Gy at 1.8–2 Gy per fraction (Pelloski & Gilbert, 2007). Despite the fact that autopsy studies consistently show malignant cells that are at a significant distance from the primary site, more than 80% of tumors recur within the original tumor location (Pelloski & Gilbert, 2007). The radiation field remains restricted to the surgical cavity and to a 2 cm margin of surrounding brain tissue as studies demonstrated a higher incidence of treatment-induced brain injury with no survival improvement for whole-brain RT compared to regional radiation (Shapiro *et al.*, 1989).

Other methods for delivering RT besides EBRT have been investigated, such as a brachytherapy device and the use of radioactive seed implants. The brachytherapy device consists in a balloon catheter system that is inflated with radioactive liquid iodine; the balloon conforms to the shape of the surgical cavity and delivers a more uniform dose of radiation but it was not proven to be more effective than conventional radiotherapy (Pelloski & Gilbert, 2007). Radioactive seed implants may also be placed at the time of surgery but phase III studies did not demonstrate any survival benefit when this technique is used in combination with standard radiotherapy (Pelloski & Gilbert, 2007).

Chemotherapy

Chemotherapy has been extensively evaluated in the treatment of patients with GBM as a first-line therapy and for patients with recurrent disease (Pelloski & Gilbert, 2007). Studies failed to demonstrate any improvement in survival with the addition of nitrosourea chemotherapy such as semustine, lomustine or carmustine to radiotherapy treatment, and thus radiotherapy alone remained the standard of care after surgical resection (Anton *et al.*, 2012). A meta-analysis of over 3,000 patients comparing those who received radiation and chemotherapy with those receiving only radiation, demonstrated a very modest 6% improvement in the one-year survival rate (Fine *et al.*, 1993). Conventional chemotherapy for recurrent disease typically demonstrates a 5–15% objective response rate and a 15–25% six-month progression-free survival (PFS), suggesting that the majority of the patients do not respond to these therapies and that objective responses are often not durable for the few respondents (Pelloski & Gilbert, 2007).

In 2005, a clinical trial demonstrated for the first time a benefit from a chemotherapeutic agent for GBM patients. The phase III clinical trial conducted by the European Organization for Research and Treatment of Cancer and the National Cancer Institute of Canada demonstrated that concurrent radiotherapy and temozolomide followed by adjuvant temozolomide significantly prolonged the median survival more than radiation alone (14.6 months versus 12.1 months; $P < 0.001$) (Weller *et al.*, 2005). These findings established the therapeutic benefit of TMZ in combination with RT and the so-called "Stupp regimen" standard of care for GBM treatment (Wilson *et al.*, 2014).

The initial studies with temozolomide in patients with recurrent or progressive disease demonstrated an objective response rate of only 5% and a six-month PFS rate of 21% (Yung *et al.*, 1999). In patients with newly diagnosed GBM, a phase II study showed a high response rate (48%), but these responses were not durable being the median PFS at 3.6 months (Gilbert *et al.*, 2002). However, the therapy with TMZ demonstrated excellent oral bioavailability, no significant drug–drug interactions, no cumulative myelotoxicity and it remains, until now, the only drug that was shown to have an impact in overall survival of GBM patients (Pelloski & Gilbert, 2007).

The triazene compound temozolomide has been suggested to act through the methylation of O^6-guanine, leading to the formation of O^6-methylguanine in DNA, which mispairs with thymine during the next DNA replication cycle, thus leading to futile cell cycles of DNA mismatch repair resulting in cell death, likely by apoptosis (Friedman *et al.*, 2000). The methyl group added to O^6-methylguanine can be removed by O^6-methylguanine methyltransferase (MGMT), a DNA repair protein that functions to remove methyl groups from the O^6 position of guanine. Removal of this methyl group confers resistance of tumor cells to TMZ and to other alkylating chemotherapeutic agents, by protecting cells from their DNA-damaging effects (Wilson *et al.*, 2014). In some patients, MGMT expression has been decreased or silenced by methylation of the promoter regions of the MGMT gene,

preventing it from removing methyl groups from the O^6 position of guanine. It is now known that response to alkylating therapy with temozolomide differs among patients with the same histological diagnosis of GBM and depends on the methylation status of the MGMT promoter (Mrugala, 2013). Patients whose MGMT gene is inactivated (which occurs in 45% of patients) have a significantly greater chance of responding to TMZ than those for whom the gene is still functional (Hegi *et al.*, 2005). The median survival of patients with methylation *versus* lack of is 21.7 *vs* 15.3 months. For patients with an inactive gene, 2-year survival was 23% for those receiving radiation only, compared to 46% for those who received radiation and TMZ together and for those with an active MGMT gene the corresponding numbers were 2% and 14% (Hegi *et al.*, 2005). Despite these findings, almost all patients with newly diagnosed GBM receive irradiation with concomitant and adjuvant temozolomide, and it is not routine to test MGMT status outside of clinical trials (Mrugala, 2013). This issue is controversial, as some authors have disputed whether the status of the MGMT gene has predictive value (Blanc *et al.*, 2004), and the referred numbers suggest that the addition of TMZ provides some benefit even for patients with the active gene. It is also important to note that the MGMT gene is *only one* of several mechanisms by which chemoresistance is mediated.

TMZ has also been extensively investigated in combination with other cytotoxic agents and signal transduction modulators and some combinations suggest an enhancement of efficacy over TMZ alone (Pelloski & Gilbert, 2007).

Limitations of chemotherapies to address GBM

Many chemotherapeutics are not able to cross the blood-brain barrier making it difficult to efficiently deliver the drug to the brain parenchyma and the tumor itself (Misra *et al.*, 2003). Even the most active agents in glioma therapy achieve relatively low concentrations in the tissues surrounding the tumor (Ostermann *et al.*, 2004; Portnow *et al.*, 2009). Different factors influence drug access to the central nervous system: the size of the molecule, its lipophilicity, the integrity of the blood-brain barrier (that is typically damaged by invasive GBM) and the presence of active efflux pumps (Neuwelt *et al.*, 2011). Steroids and antiepileptic medication that many patients with glioblastoma receive may also interfere with the chemotherapeutics, reducing their efficacy and potentially exacerbating side effects (Mrugala, 2013).

In order to maximize efficient delivery of chemotherapeutics to the tumor, and fill the usual gap between surgery and radiotherapy, local treatments started to be administered at the time of the surgical resection. Local chemotherapy helps to bridge the unavoidable treatment gap between surgery and radiotherapy and to achieve extra reduction of the quickly dividing tumor cells (Wolbers, 2014). A biodegradeable polymer containing carmustine (bis-chloroethylnitrosourea - BCNU) has been approved for placement along the walls of the tumor resection cavity for both newly diagnosed and recurrent GBM. This wafer dissolves over two to three weeks, slowly releasing carmustine into the cavity walls (Pelloski & Gilbert, 2007). Carmustine wafers used in combination with radiation and TMZ were shown to

modestly prolong survival in subsets of patients but because of complications associated with their use (including infection, swelling, need for removal, and impairment of wound healing) wafers are not routinely used (Wilson *et al.*, 2014). Several other agents apart from carmustine are being evaluated in preclinical studies via local implants and gels, including taxanes, cyclophosphamide, adriamycin and irinotecan (Wolbers, 2014).

Another form of direct drug delivery that is being evaluated is convection-enhanced deliver, in which a catheter is placed into the brain parenchyma surrounding the tumor cavity followed by continuous delivery of treatment under pressure. Targeted agents such as antibody fragments and gene therapies are being studied using this delivery modality, allowing for diffusion of the treatment into areas that were not previously reachable by systemic delivery (Pelloski & Gilbert, 2007).

Managing recurrent glioblastoma

After initial therapy fails, therapeutic options are limited and generally not effective. To date, no regimen has been proved in terms of efficacy by randomized clinical trials in order to become the established standard of care; therefore, treatment options and decisions are often determined by the specific clinical situation and treatment availability (Mrugala, 2013). Median time to progression at this stage is about 10 weeks and overall survival ~30 weeks (Wong *et al.*, 1999).

Second tumor resection

The impact of radical tumor resection as first line therapy is beyond controversy, but the significance of a second resection in case of tumor-recurrence in GBM remains unclear (Quick *et al.*, 2014). Different series report that approximately 20–40% of patients with recurrent GBM undergo re-resection of tumor, but this greatly varies since there are no formal guidelines to assist in the decision; patients with a local recurrence in non-eloquent brain regions are more likely to undergo a second tumor resection (Pelloski & Gilbert, 2007).

Surgical resection can relieve mass effect and issues related to increased intracranial pressure, be helpful diagnostically (to distinguish between the necrotic treatment effect and active progressive tumor), and is also an opportunity for using a local therapy strategy (Pelloski & Gilbert, 2007). Carmustine impregnated wafers have been shown to increase time to progression in patients with recurrent GBM, and although the effect is rather modest, this treatment modality can be attractive in patients who cannot tolerate toxicity associated with systemic chemotherapy (Mrugala, 2013).

Quick *et al* (Quick *et al.*, 2014), in a recent study from 2014, defend that patients in good clinical condition with recurrent GBM amenable to complete resection should not be withheld second surgery as a treatment option.

Re-irradiation

Despite aggressive radiation therapy approaches, most GBM recurrences are within the high-dose field, limiting the ability to safely re-irradiate (Torok *et al.*, 2011). Historically, second course of radiotherapy was believed to be too toxic and was rarely recommended (Mrugala, 2013), but today re-irradiation is more frequently employed, since modern techniques like conformal radiotherapy, intensity-modulated radiotherapy, and advance planning imaging and software made re-irradiation more safe, and it was shown to provide survival benefit (Butowski *et al.*, 2006).

Different groups have shown that fractionated stereotactic radiosurgery/RT can benefit patients with recurrent GBM (Vordermark *et al.*, 2005; Torok *et al.*, 2011). Stereotactic radiosurgery/RT can be used close to or within the previous high-dose region for small volumes of recurrence that appear within a short period of time, and tumors outside of significant dose volumes can be treated three to six months after completion of the first RT course (Pelloski & Gilbert, 2007).

Chemotherapy

Patients with recurrent GBM often gain minimal benefit from conventional treatments. Objective response rates were reported in the 5–15% range, and response is frequently not durable (Pelloski & Gilbert, 2007). There is a great interest in developing new treatment regimens for this group of patients, since traditional cytotoxic chemotherapy agents such as cisplatin, carboplatin, procarbazine, and irinotecan have had rather disappointing results. Temozolomide, in the recurrent setting, has also shown very modest efficacy with an overall response rate of 10% with PFS-6 rate of 48% and median PFS of 21 weeks (Wick *et al.*, 2004).

More recently, signal transduction modulating agents have been evaluated, but the response to these drugs as single-agent therapies has been limited (Pelloski & Gilbert, 2007). FDA (United States Food and Drug Administration) has approved bevacizumab, an anti-VEGF (vascular endothelial growth factor) inhibitor, for use in recurrent GBM in 2009 (Cohen *et al.*, 2009). Bevacizumab is a recombinant monoclonal IgG1 antibody that selectively binds and neutralizes the biological activity of human VEGF, which can result in the reduction of tumor vascularization and consequent reduction in tumor growth (Cohen *et al.*, 2009). Physicians have been using it as a single agent or in combination with other drugs such as irinotecan, carboplatin, etoposide, and lomustine (Mrugala, 2013). The timing of cytotoxic therapy in relation to bevacizumab might be crucial in order to take advantage of the so called "vascular normalization window" (Jain & Meyer-Hermann, 2011) and further studies are being conducted to exploit different drug regimens.

The combination of different signal transduction modulators along with tumor molecular profiles research will hopefully result in individualized patient treatment (Pelloski & Gilbert, 2007). Different clinical trials *(www.clinicaltrials.gov)* are recruiting now patients to exploit immunotherapy approaches, such as dendritic cell immunotherapy (NCT00045968). Despite the increasing number of trials and agents being tested, the majority has not shown beneficial

results, and further research is urgently needed in order to better understand the limitations of current therapies.

Prognostic factors and clinical decisions

The single most important prognostic factor in GBM is patient age. Age has important implications regarding issues of patient management, including greater comorbidities, but patient age is also important because it correlates with differences in tumor biology and pathogenesis (Pelloski & Gilbert, 2007).

GBM can be classified as **primary**, if it occurs *de novo*, without evidence of a less malignant precursor, or as **secondary**, if GBM develops from a lower-grade glioma. Patients with primary glioblastoma tend to be older than patients with secondary glioblastoma. Although largely indistinguishable based upon histopathology, primary and secondary GBMs evolve from different genetic precursors and have distinct genetic alterations (Wilson *et al.*, 2014). Primary GBMs typically present amplification of the *epidermal growth factor receptor* (*EGFR*) gene, *phosphatase and tensin homologue* (*PTEN*) mutations, loss of chromosome 10 and a more aggressive clinical course (Ohgaki & Kleihues, 2007). Among younger patients, secondary GBMs are more common, and in many cases these patients have an established history of lower-grade gliomas (grades II–III). These tumors often display *isocitrate dehydrogenase 1* (*IDH1*) mutations, *TP53* mutations, and 19q loss (Wilson *et al.*, 2014). Secondary glioblastoma is associated with better prognosis and increased overall survival when compared with primary glioblastoma. Survival decreases with each additional decade of life at the time of diagnosis (Mrugala, 2013), making age the most relevant prognosis factor. The different genetic alterations between primary and secondary GBM and their impact on prognosis and disease will be discussed with further detail in the following chapter - *GBM molecular characterization*.

The patient's performance status is another important factor with prognostic value. Most studies have correlated a higher performance status with improved prognosis, which may reflect both the patient's ability to tolerate treatment and the extent of the tumor (Pelloski & Gilbert, 2007). Patients defined as high-risk patients present the worse prognosis and have poor performance status, large tumors that cause neurological dysfunction or important comorbid conditions (Pelloski & Gilbert, 2007). An hypofractionated radiotherapy regimen can be used (50 Gy in 20 fractions- 2.5 Gy/session) instead of the conventional radiation schedule (60 Gy in 2 Gy per fraction), achieving increased cell kill from a higher dose per fraction and shortening the overall treatment time with no increased toxicity or apparent impact on survival (Lanzetta & Minniti, 2010). The use of the standard tri-modality therapy must be even more critically evaluated in these cases and weighted against the potential toxicities, compromises and interference with quality of life (Pelloski & Gilbert, 2007).

The evaluation of prognosis remains essential in modern medical practice, meeting patient's needs for information about their future and providing a basis for rational medical

decisions (Mackillop, 2006). The fact that prognostic judgment is extremely important when considering treatment options for individual patients and when evaluating the efficacy of treatment regimens tested in clinical trials (Pelloski & Gilbert, 2007), underscores the importance of continuing to study prognostic factors in oncology.

GBM molecular characterization

It has been clearly demonstrated that GBM is highly anaplastic and a morphologically heterogeneous tumor with underlying distinct molecular phenotypes (Zhang *et al.*, 2012), but it remains unclear whether these differences relate to the cell of origin or molecular genesis of the tumor, or are a signature of different mechanisms of tumor progression (Carmo *et al.*, 2011).

In GBM, the most common genetic alterations include: *epidermal growth factor receptor* (*EGFR*) amplification, mutations in *tumor protein p53* (*TP53*), *cycline-dependent kinase inhibitor 2A* (*CDKN2A/p16*), *deleted in colorectal carcinoma* (*DCC*) and *retinoblastoma* (*RB*), and deletions associated with chromosomes 19q and 22q, chromosome 7 gain and chromosome 10 loss (Zhang *et al.*, 2012). DNA copy number changes affect gene expression either through overexpression of large amplification regions, or through inactivation of genes in deleted regions; loss of heterozigoty and different mutations seem to modify crucial cellular processes resulting in deregulation of growth signalling and cell cycle control (Carmo *et al.*, 2011).

Although highly heterogeneous, with particular genetic alterations occurring in some tumors and not in others, it was possible to identify different molecular subtypes of GBM (Liang *et al.*, 2005). Mainly, GBM profiling allowed identifying important differences in the molecular abnormalities observed between primary and secondary GBM, which are largely indistinguishable based upon histopathology.

Primary GBM

As already mentioned, GBM can be classified as primary if it occurs *de novo*, or as secondary if it develops from a lower-grade diffuse astrocytoma or from an anaplastic astrocytoma (WHO grades II and III, respectively) (Ohgaki & Kleihues, 2007). Before molecular profiling enabled the finding that the two groups harbored distinct genetic alterations, primary and secondary GBM were distinguished only based on clinical findings. Recent studies allowed the definition of a diagnostic molecular marker, more reliable and objective than clinical and/or pathological criteria (Ohgaki & Kleihues, 2013), as will be discussed next.

Primary GBMs typically harbor amplification and/or a high rate of *EGFR* mutations, *CDKN2A/p16* deletion in chromosome 9p, *receptor tyrosine-protein kinase erbB-2* (*ERBB2*) mutations and *phosphatase and tensin homologue* (*PTEN*) deletion in chromosome 10 (Carmo *et al.*, 2011). A low rate of *TP53* gene mutation and a high frequency of loss of the long arm of the chromosome 10 are also characteristics of primary glioblastoma (Fults & Pedone, 1993;

Watanabe *et al.*, 1996; Fujisawa *et al.*, 2000).

The most common type of mutation in *EGFR* is the mutant type-variant III (*EGFRvIII*), due to an in-frame deletion of exons 2-7 that results in constitutively active EGFR-mediated signalling, conferring cell proliferation and survival advantages (Carmo *et al.*, 2011). EGFRvIII expression is tightly correlated with the activation of downstream targets of the phosphatidylinositol-4,5-bisphosphate 3-kinase/protein kinase B (PI3K/Akt), including the mammalian target of rapamycin (mTOR), the forkhead transcription factor (FOX) family and S6 (Gan *et al.*, 2013). EGFRvIII was also shown to indirectly stimulate nuclear factor kappa-light-chain-enhancer of activated B cells (NF-κB) pathway and resistance to chemotherapy (Tanaka *et al.*, 2011). The effects of EGFRvIII via the PI3K/Akt pathway may be even facilitated by associated loss or mutation of the *PTEN* gene (a negative regulator of PI3K), which occurs in approximately 40% of the samples that express EGFRvIII (Gan *et al.*, 2013), resulting in increased survival, proliferation and invasion.

Secondary GBM

The following alterations are commonly found in secondary glioblastoma: mutations in the tumor suppressor gene *TP53* on chromosome 17p, abnormalities in the p16 and retinoblastoma pathways, loss of heterozigoty of chromosome 10q but no loss of 10p, and 19q loss (Fujisawa *et al.*, 2000; Carmo *et al.*, 2011).

In 2008, it was reported that *isocitrate dehydrogenase 1* mutations occur in a disproportionately large portion of younger patients and in the majority of patients with secondary GBM, and appeared to be associated with better prognosis and increased overall survival (Wilson *et al.*, 2014). Subsequent studies found that *IDH1* mutations were present in more than 80% of secondary GBM and in less than 5% of primary GBMs (Ohgaki & Kleihues, 2013). *IDH1* mutations are also frequent (>80%) in diffuse astrocytoma WHO grade II and anaplastic astrocytoma WHO grade III, the precursor lesions of secondary glioblastomas, as well as in oligodendroglial tumors (Ohgaki & Kleihues, 2013).

IDH1 is localized within the cytoplasm and peroxisomes (Zhang *et al.*, 2012) and is an enzyme that catalyzes the oxidative decarboxylation of isocitrate to alfa-ketoglutarate, while reducing NADP to NADPH and liberating CO_2 (Cairns & Mak, 2013). IDH1 deficiency was shown to increase lipid peroxidation, oxidative DNA damage, intracellular peroxide generation and to decrease survival after oxidant exposure (Reitman & Yan, 2010). Patients who have *IDH1* mutations have a high frequency (>70%) of *TP53* mutations and a very low frequency of mutations in other commonly altered GBM genes (Zhang *et al.*, 2012). Astrocytomas may develop in cells with *IDH1* mutations that subsequently acquire *TP53* mutations (Ohgaki & Kleihues, 2013). *IDH1* mutations may be the earliest detectable genetic alteration in precursor low-grade astrocytomas, and are proof that despite similar histologic appearence, primary and secondary GBMs are distinct entities with different origins that may require different therapeutic approaches (Ohgaki & Kleihues, 2013).

Refining GBM classification

The availability of large-scale microarray-based genomic profiling together with advances in bioinformatics allowed to refine GBM's classification (Carmo *et al.*, 2011). In 2010, Verhaak *et al* (Verhaak *et al.*, 2010) described a robust gene expression-based molecular classification for glioblastomas. On the basis of prior naming and considering the expression profiles observed; aberrations and gene expression of *EGFR*, *NF1*, and *PDGFRA (Platelet-Derived Growth Factor Receptor)/IDH1* defined **classical**, **mesenchymal**, and **proneural** GBM subtypes, respectively, as will be described in the following subsections and summarized in table 1.1.

Classical GBM

Classical GBMs have a characteristic profile of highly proliferative cells, common gains on chromosome 7 paired with losses on chromosome 10 and frequent focal losses on chromosome 9p21.3 (Carmo *et al.*, 2011). Chromosome 7 amplification paired with chromosome 10 loss is a highly frequent event in GBM and was seen in 100% of the classical subtype samples analyzed (Verhaak *et al.*, 2010). Although chromosome 7 amplification was seen in other subtypes, abnormally high levels of epidermal growth factor receptor characterized classical GBM tumors, whereas EGFR abnormalities occurred at a much lower rate in the three other GBM subtypes (Verhaak *et al.*, 2010). However, mutations in *TP53*, the most frequently mutated gene in GBM (TCGA, 2008), are nearly absent in classical GBM tumors (Carmo *et al.*, 2011). Neural precursor and stem cell marker nestin were highly expressed in the classical subtype (Verhaak *et al.*, 2010).

Clinically, the classical group demonstrates responsiveness to radiation and chemotherapies, likely because the p53 DNA damage response is intact, and this is the subtype of GBM in which the patients have the highest benefit from pursuing aggressive treatment (Van Meir *et al.*, 2009).

Proneural GBM

Proneural tumors are characterized by an expression profile reminiscent of gene activation in neural development, presenting a high level of expression of oligodendrocytic and proneural development genes (Van Meir *et al.*, 2009). In proneural tumors, *TP53* is significantly mutated (54%) and this is the group that presents more mutations in the *IDH1* gene (Evans, 2011). The finding of *IDH1* gene mutations in lower grade gliomas also suggests that secondary glioblastoma might belong to this subtype (Van Meir *et al.*, 2009) and that these tumors may derive from neural precursor cells. *PDGFRA* was mutated and expressed in abnormally high amounts only in the proneural tumors and not in other subgroups (Evans, 2011).

The proneural subgroup was significantly younger, and tended to survive longer than patients with other GBM subtypes, however, these patients received almost no benefit from aggressive therapies (Van Meir *et al.*, 2009).

Mesenchymal GBM

Mesenchymal tumors display overexpression of mesenchymal markers (Carmo *et al.*, 2011) and this subgroup contains the most frequent number of mutations in the *NF1* tumor suppressor gene (37%). Mutations in the *PTEN* and *TP53* tumor suppressor genes are also frequent (Evans, 2011). *NF1* and *PTEN* co-occurring mutations, both intersecting with the Akt pathway, are also observed.

Genes in the tumor necrosis factor (TNF) superfamily and NF-κB pathways are highly expressed in this subtype, being this fact possibly related to higher overall necrosis and associated inflammatory infiltrates (Carmo *et al.*, 2011).

Patients in the mesenchymal group have significant increases in survival after aggressive treatment and might be responsive to Ras, PI3K and angiogenesis inhibitors (Carmo *et al.*, 2011).

Neural GBM

The neural group is characterized by the expression of genes that are also typical of normal neurons (Carmo *et al.*, 2011). While presenting mutations in many of the same genes as the other groups, the neural group does not stand out as having significantly higher or lower rates of mutations (Evans, 2011), and seems to be less well defined.

Patients in the neural group were the oldest, on average, and also had some improvement in survival after aggressive treatment, but not as much as the classical or mesenchymal groups.

The Cancer Genome Atlas (TCGA) dramatically accelerated comprehensive understanding of the gene mutations and expression profiles of GBM, helping to narrow down the problem to a limited number of genes and pathways on which to focus further studies (Van Meir *et al.*, 2009). Comparison of the gene expression patterns of the four GBM subtypes with those of primary cultures of murine astrocytes, oligodendrocytes, neurons, and microglia suggests that the subtypes may reflect different cells of origin, but this hypothesis needs further substantiation (Van Meir *et al.*, 2009).

Despite the differences that allowed GBM classification into four subtypes, all subgroups commonly demonstrate inactivation of the p53 and retinoblastoma tumor suppressor pathways and activation of receptor tyrosine kinase pathways. Further studies linking the genetic alterations with consequent affected signalling pathways may be key to better understand the occurrence and progression of these tumors (Carmo *et al.*, 2011).

	Classical GBM	Mesenchymal GBM	Proneural GBM	Neural GBM
Genetic signature	Gains of chr 7 Loss of chr 10 Loss of chr 9p21	NF1 loss/mutation TP53 loss/mutation PTEN loss/mutation	TP53, CDKN2A and PTEN loss/mutation; PDGFRA amplification; IDH1 mutation; PIK3CA/PIK3R1 mutation	Not distinctive
Activated signaling pathways	Notch and Sonic Hedgehog pathways	TNF family and NF-kB pathways	HIF, PI3K, and PDGFRA pathways	Not defined
Treatment effect on patients' survival	Significantly improved	Significantly improved	No impact	Low impact

Table 1.1: GBM subtypes as defined by Verhaak *et al* (2010)

Commonly altered signalling pathways in GBM - possible therapeutic targets?

EGFR/Akt/PTEN

EGFR is commonly mutated or amplified in GBM. Amplification occurs in 40% of primary GBMs and EGFR overexpression is present in 60% of primary GBM (Ohgaki & Kleihues, 2007). EGFR amplicons are also often mutated, being the most frequent type the variant 3 (EGFRvIII) with an in-frame deletion of exons 2 to 7 within the extracellular ligand-binding domain (Gan *et al.*, 2013). This in-frame deletion leads to constitutive activation of the receptor and failure to attenuate signalling by receptor down-regulation (Van Meir *et al.*, 2009).

Constitutive activation results in several signal transduction pathways downstream of EGFR becoming activated such as the Ras/Raf/mitogen-activated protein kinase pathway (MAPK), the PI3K/Akt pathway, protein kinase C (PKC), the signal transduction and activator of transcription (STAT) and VEGF, among others. EGFRvIII confers enhanced tumorigenecity, possibly through multiple mechanisms that are mediated by these pathways, as EGFRvIII-transfected GBM cell lines show increased rates of proliferation, increased ability to form tumor xenografts, reduced apoptosis, increased angiogenesis and increased invasiveness compared with matched parental cell lines (Gan *et al.*, 2013).

EGFR has been a prime target for therapeutic intervention in GBM: small molecule kinase inhibitors (gefitinib, erlotinib), antibody-based immunotherapy (cetuximab) and small interfering RNA-directed neutralization of wild type EGFR or EGFRvIII allele were different strategies used with little success (Wilson *et al.*, 2014). The deletion in EGFRvIII engenders a unique codon, which is not found in the wild-type receptor, creating a tumor-specific epitope that could be exploited for therapeutic targeting (Van Meir *et al.*, 2009).

The constitutively active EGFRvIII may enhance cell proliferation through activation of the PI3K/Akt pathway. The action of PI3K enzyme is directly antagonized by a phosphatase encoded by the *PTEN* gene: PTEN acts as a negative regulator of the PI3K pathway by

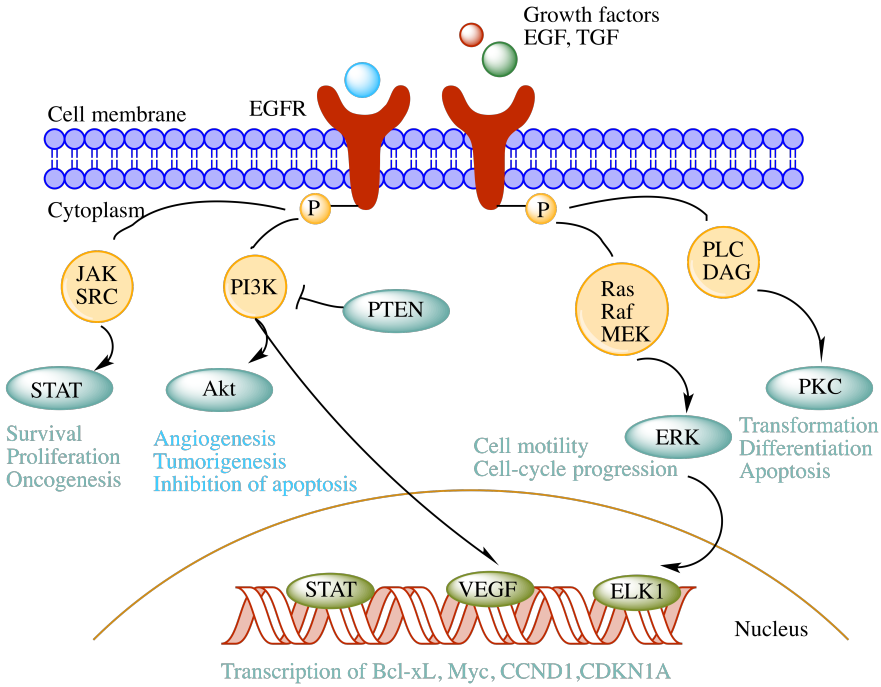

Figure 1.3: The figure shows signalling pathways that are activated by EGFR without including all the known components. PTEN can dephosphorylate PI3K and MKP1 (MAPK phosphatase 1), which can dephosphorylate ERK1/2. These signalling pathways also regulate the activity of transcriptional factors directly or indirectly, consequently affecting important cellular functions. *Image adapted from Nyati et al. (2006).*

removing the third phosphate from the inositol ring of PIP3 (phosphatidylinositol (3,4,5)-triphosphate) (Mellinghoff *et al.*, 2005). PTEN inactivation results in accumulation of PIP3 levels and persistent activation through the serine/threonine kinase Akt.

In many instances, unsuccess of EGFR-targeted therapies are linked to inactivation of PTEN and activation of PI3K/Akt (Mellinghoff *et al.*, 2005). PTEN loss could then promote resistance to EGFR kinase inhibitors by dissociating EGFR/EGFRvIII inhibition from downstream inhibition of PI3K signalling pathway. Activation of PI3K/Akt may also occur due to mutations; in up to 10% of GBMs, Akt activation is due to mutations that amplify or activate the catalytic and regulatory subunits of PI3K (Carmo *et al.*, 2011). PI3K might also be activated by c-MET (mesenchymal epithelial transition factor) and PDGFR (platelet-derived growth factor receptor), which are often co-activated in EGFR-amplified tumors (Furnari *et al.*, 2007).

mTOR

mTOR integrates signals such as deprivation of glucose and aminoacids, ATP depletion, hypoxia and lack of growth factors, in order to generate adaptative cellular responses (Ronellenfitsch *et al.*, 2009). Deregulated mTOR signalling sustains proliferation by antagonizing these physiological starvation signals, and may contribute to the typical pattern of GBM

pathology, with necrotic cores and aggressive growth at the tumor margins (Carmo *et al.*, 2011). mTOR forms the catalytic core of at least two distinct complexes (mTORC1 and mTORC2) and is one of the Akt downstream effectors.

Several mTOR-PI3K-Akt-PTEN signalling pathway inhibitors have been developed in the past decade, among which the most widely tested are mTOR inhibitors, including rapamycin and its intravenous and oral derivatives temosirolimus and everolimus (Mao *et al.*, 2013). These drugs inhibit mTOR through the formation of a complex with FK-binding protein 12 (FKBP-12), which then binds to mTOR and prevents its activation (Faivre *et al.*, 2006). Multiple studies have been conducted using temosirolimus and everolimus, alone or in combination with other therapies, but results have been limited and there are still numerous clinical trials ongoing to further elucidate the effects of these mTOR inhibitors (Mao *et al.*, 2013).

p53

The *tumor suppressor gene p53*, encoded by the *TP53* gene, regulates cell cycle progression and apoptosis in response to a wide variety of stress signals (Brady & Attardi, 2010). Various roles of p53 that protect against neoplastic transformation include modulation of cell cycle, DNA repair, apoptosis, senescence, angiogenesis and metabolism, resulting in an extremely complex signalling network (England *et al.*, 2013).

p53 function is tightly regulated by phosphorylation: when Ser15 and Ser20 within the p53 N-terminal are phosphorylated, the E3-ligase MDM2 that targets p53 for proteasomal degradation is prevented from interacting with p53, resulting in p53 stabilization. When stabilized, p53 accumulates in the nucleus, where it binds and transcriptionally regulates the promoters of more than 250 potential effectors genes that are involved in cell cycle control and apoptosis (Carmo *et al.*, 2011).

TP53 is the most frequently mutated gene in GBM, and mutations are clustered in the DNA binding domain, a hotspot for p53 mutations in human cancers (TCGA, 2008). In primary GBM, TP53 inactivation is a common event that may occur via amplification or overexpression of the p53 negative regulators MDM2 and MDM4, while in secondary GBM, two thirds of the tumors have loss of TP53 which occur by point mutations or loss of chromosome 17p (Carmo *et al.*, 2011).

Regarding treatment in GBM, p53 targeted-gene therapy and vaccinations have reached phase I clinical trials while therapeutic drugs are still in pre-clinical development (England *et al.*, 2013).

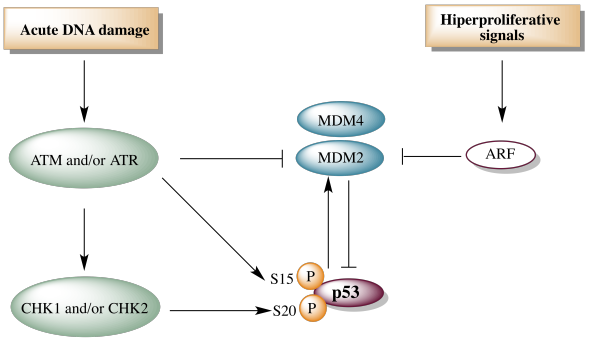

Figure 1.4: p53 induction by acute DNA damage occurs when DNA double-strand breaks trigger activation of ataxia-telangiectasia mutated (ATM) or when collapsed DNA replication forks recruit ataxia telangiectasia and RAD3-related (ATR), which phosphorylates CHK1. p53 is a substrate for both the ATM and ATR kinases, as well as for CHK1 and CHK2, which coordinately phosphorylate p53 to promote its stabilization. Phosphorylation of p53 occurs at several sites and some of the modifications disrupt the interaction between p53 and its negative regulators MDM2 and MDM4. MDM2 and MDM4 bind to the transcriptional activation domains of p53, inhibiting p53 transactivation function, and MDM2 has additional activity as an E3 ubiquitin ligase that causes proteasome-mediated degradation of p53. Hyperproliferative signals activate p53 through perturbation of the MDM2-p53 interaction. ARF activation enhances p53 stability and activity. *Image adapted from Bieging et al. (2014).*

VEGF

Binding of VEGF to its cognate receptors leads to activation of different signalling molecules like PI3K, phospholipase Cg (PLCg), PKC, nitric oxide synthase (NOS), MAPKs and focal adhesion kinases (FAKs) (Carmo *et al.*, 2011). VEGF has been shown to be a dominant driver of angiogenesis, contributing to tumor growth and progression, and angiogenesis is required for GBM growth (Schmidt *et al.*, 1999; Van Meir *et al.*, 2009). Aberrant vascular proliferation, necrosis, and infiltration of surrounding brain tissues are considered hallmarks of GBM (Mao *et al.*, 2013).

The level of VEGF production in a tumor correlates with its degree of malignancy: in a study of surgical glioma specimens, high-grade tumors (III and IV) produced greater than 10-fold more VEGF compared with low-grade tumors (Schmidt *et al.*, 1999).

Bevacizumab was found to be effective for recurrent malignant glioma and to inhibit angiogenesis by blocking VEGF-A; bevacizumab was approved for use in recurrent GBM in 2009 (Cohen *et al.*, 2009).

Antitumor lipids (ATLs)

Short history and current clinical applications

Synthetic antitumor alkylphospholipids are a group of structurally related lipids with similarities to 2-lysophosphatidylcholine (LPC). In the 1960s, it was observed that LPC induced the phagocytic activity of peritoneal macrophages *in vitro* and *in vivo* (Munder *et al.*, 1969; Munder & Modolell, 1973). LPC is not stable and becomes biologically inactivated either by the action of acyltransferase into lecithin (phosphatidylcholine, PC) or by lysophospholipase into glycerophosphocholine (Mulder & Deenen, 1965). In order to achieve a longer activation of macrophages that would help to study the involved signalling pathways, efforts were made to synthesize metabolically stable LPC analogues.

The synthetic alkylphospholipids like edelfosine maintain the same general structure, but instead of the esterified fatty acid of LPC, they present aliphatic side-chains that are ether linked to a glycerol backbone, resulting protected from hydrolysis reactions to which the ester links are susceptible. The hydroxyl group in the sn-2 position has been replaced by a methoxy radical, avoiding the acylation of the hydroxyl group that occurs in LPC (Gajate & Mollinedo, 2002).

Synthetic phospholipid analogues not only worked as effective immune modulators (Munder *et al.*, 1979), but also possessed selective anti-neoplastic activities *in vitro* and *in vivo* (Andreesen *et al.*, 1978, 1979; Tarnowski *et al.*, 1978; Modolell *et al.*, 1979). These studies showed a double anti-tumoral activity: *a)* an indirect one through ALP-dependent macrophage activation and *b)* a direct effect on tumor cells, as observed in *in vitro* studies where macrophages were absent (Andreesen *et al.*, 1978). Since these first studies in the 80s, many more have been performed, demonstrating the anti-tumoral activity of the LPC analogues in hematologic and solid tumor-derived cell lines.

New compounds like miltefosine and perifosine were synthetized to improve antitumoral activity and minimize side-effects. Edelfosine, miltefosine and perifosine have been tested for their anti-tumor activity in clinical phase I and phase II trials for a variety of tumors. Miltefosine was the first anti-tumor lipid to be used clinically and is employed for the topical treatment of cutaneous metastases deriving from mammary carcinomas (Danker *et al.*, 2010). Miltefosine was also proved useful for treating certain cutaneous lymphomas, in which a response of up to 60% has been observed in a preclinical study (Dumontet *et al.*, 2006). However, due to its hemolytic effect, miltefosine could not be administered intravenously but only as an oral or topical formulation (Van Blitterswijk & Verheij, 2013). Unfortunately, gastrointestinal toxicity and lack of activity in patients with advanced soft tissue sarcoma, metastatic colorectal cancer and squamous cell carcinoma of head and neck prevented its development as an oral anti-cancer drug (Van Blitterswijk & Verheij, 2013). Miltefosine shows considerable activity against parasitic infectious diseases, mainly in leishmaniasis, by interfering with the parasite's metabolic pathways that lead to apoptosis-like activation (Sundar *et al.*, 2002, 2006) and was approved by the FDA in 2014 for the treatment of visceral, cutaneous and mucosal leishmaniasis.

Different ATLs - structures and properties

Synthetic antitumor lipids include two major subtypes: ***1)*** **alkyl ether phospholipids** (AEPs), also referred collectively as antitumor ether lipids (AELs) or alkyl-lysophospholipid analogues (ALPs), containing ether bonds in the glycerol backbone of the phospholipid and from which **edelfosine** is the prototype molecule; and ***2)*** **alkylphosphocholines** (APCs), lacking the glycerol backbone and formed by a simple long-chain alcohol esterified into a phosphobase, with the prototypical hexadecylphosphocholine (HPC; **miltefosine**) (Gajate & Mollinedo, 2002; Mollinedo *et al.*, 2004).

The first alkyl-lysophospholipid analog was synthesized as a metabolically stable analog of 2-lysophosphatidylcholine in the late 60s, through the change of a glycerol C1 ester bond in lyso PC to an ether bond, and the addition of other etherlinked methyl group at the C2 position (Gajate & Mollinedo, 2014). Among the distinct compounds synthesized at that time, edelfosine, ET-18-OCH_3, showed the highest antitumor activity (Gajate & Mollinedo, 2002).

Additional synthetic antitumor lipids include: a) **miltefosine** (hexadecylphosphocholine), lacking a glycerol moiety, is the minimal structural requirement for alkylphospholipid antitumor activity, and its structural analogue **oleylphosphocholine** (OlPC) b) **erucylphosphocholine** (ErPC, [13Z]-docos-13-en-1-yl 2-(trimethylammonio)ethyl phosphate), and its homocholine analog **erufosine** (ErPC3,erucylphospho-N,N,N-trimethylpropanolamine) are derivatives with a 22 carbon atom chain and a cis-13,14 double bond, showing distinctive reduced hemolytic activity, thereby allowing intravenous injection; c) **perifosine** (D21266, octadecyl-(1,1-dimethyl-piperidynio-4-yl)-phosphate), identified in 1997 as a promising new orally-active alkylphospholipid compound with potential antineoplastic activity; d) **ilmofosine** (1-hexadecylthio-2-methoxymethyl-rac-glycero-3-phosphocholine) was synthesized as a thio-ether analog but this chemical modification, however, did not alter significantly its metabolic stability or cytotoxic effect, preventing the clinical use of ilmofosine (Mollinedo, 2014).

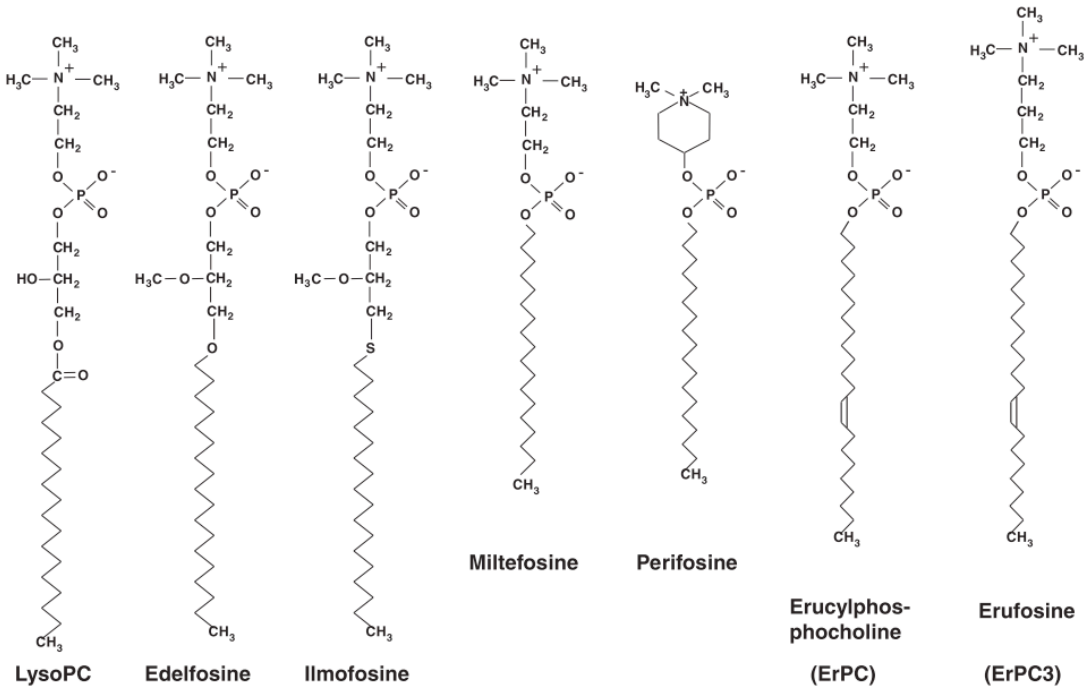

Figure 1.5: Chemical structures and commercial names of synthetic clinically relevant alkyl-phospholipids (ALPs), metabolically stable analogs of natural lysophosphatidylcholine. In the alkyl-lysophospholipid-prototype edelfosine and its thio-ether derivative ilmofosine, the glycerol backbone is maintained. The other ALPs lack the glycerol backbone, the alkyl chain being esterified directly to the phosphate group. Miltefosine (hexadecylphosphocholine) is the prototype of this group of compounds. In perifosine, the choline headgroup is substituted by a heterocyclic methylated piperidyl residue. Erucylphosphocholine (ErPC) differs from miltefosine only by a longer chain length and the introduction of a ω-9 cis-double bond. Erufosine differs from ErPC by one additional methyl group on the choline headgroup. *From Van Blitterswijk & Verheij (2013).*

Edelfosine

Most of the work presented on this thesis was dedicated to study edelfosine effects in GBM cell lines. Although other ATLs were tested and their effect on cellular viability was assessed, edelfosine was the selected ether lipid for deeper evaluation and study. For this reason, the following sections will be descriptive of the current knowledge about edelfosine, although some of the described properties are shared with other ATLs, given their common lipidic nature.

Edelfosine has been widely considered the prototype molecule of ALPs, and much of the current knowledge on the biological activities and mechanisms of action of alkylphospholipids derive from studies on edelfosine (Gajate & Mollinedo, 2014). Its cytotoxic effects have been evaluated in a large variety of leukemic and solid tumors, and also in normal cell types, showing a high degree of selectivity towards tumor cells; however, clinical use of edelfosine has remained limited and its only current application is for bone marrow purging purposes in acute leukemia patients (Gajate & Mollinedo, 2002; Van Blitterswijk & Verheij, 2013).

Mechanism of action

Due to their lipidic nature and similarity with endogenous phospholipids, ALPs tend to interact with biologic membranes. Structurally, ALPs correspond to classical surfactants, amphiphilic molecules, and may cause cell lysis at high concentrations (Pachioni *et al.*, 2013). Cellular lysis involves micellar dissolution and partition into the membrane, phase transition between lamellae and micelles and decrease in the size of micelles (Heerklotz, 2008). Micellar aggregation depends on the space occupied by the hydrophilic and hydrophobic groups of the surfactants (Rangel-Yagui *et al.*, 2005). It is generally accepted that the amount of surfactant required to solubilize a membrane increases with the ease of forming micelles, i.e., with the critical micellar concentration (CMC) (Preté *et al.*, 2002).

Edelfosine is a surface-active lipid with a CMC in the 5-10 μM range, which is a rather low CMC, suggesting higher affinity for its own molecules, hardly accepting a different amphiphile, i.e., the phospholipid, to generate mixed micelles and thus at concentrations similar to its CMC it does not present detergent effect (Busto *et al.*, 2007). LPC and other analogs show similar detergent properties, however edelfosine is the only that shows antitumoral activity, so it does not appear that ATLs antitumoral activity is based on membrane solubilization, which only occurs at high concentrations.

The mechanism of action of ALPs is different from classical chemotherapeutic drugs, since they do not target DNA, but cellular membranes. Because of their chemical structure, ALPs insert into the lipid bilayer of the plasma membrane through their long apolar hydrocarbon chain (Gajate & Mollinedo, 2014), causing a biophysical disturbance of the membrane, affecting the interaction of proteins with other proteins or lipids, interfering with lipid metabolism, lipid-dependent signalling pathways and membrane microdomain formation and behaviour (Van Blitterswijk & Verheij, 2013; Gajate & Mollinedo, 2014).

Although ALPs act mainly through targeting cell membranes, it was shown that edelfosine also affects gene expression. This effect is likely a result of edelfosine action on a number of proteins that act at the membrane level, modulating the expression and activity of transcription factors (Mollinedo *et al.*, 1994, 2004; Gajate *et al.*, 1998). ALPs-induced disturbance often causes cellular stress, deregulation of pro- and/or apoptotic pathways, growth inhibition and cell cycle arrest, and apoptosis (Van Blitterswijk & Verheij, 2013).

Effects on lipid metabolism

Inhibition of phosphatidylcholine biosynthesis and its consequences

Accumulative evidence shows that edelfosine exerts its effect on tumor cells by interfering with cell membrane phospholipid metabolism and with other processes occurring at the cell membrane. There is also evidence that edelfosine may target other subcellular structures at the membrane level: the amphiphilic ALP easily incorporate in the plasma membrane in substantial amounts and then spread among intracellular membrane compartments, including mitochondria and the endoplasmic reticulum (Nieto-Miguel *et al.*, 2007; Mollinedo *et al.*, 2010; Van Blitterswijk & Verheij, 2013). What molecular target is most important for the deleterious action of edelfosine is not entirely clear and seems to depend on the cellular type.

It has been shown that edelfosine has a negative influence on the *de novo* phosphatidylcholine (PC) biosynthesis during the CTP:phosphocholine cytidylyltransferase (CCT) step, which results in cell cycle arrest at different stages (Baburina & Jackowski, 1998; Danker *et al.*, 2010).

CCT, which catalyzes the formation of CDP-choline, is the key enzyme controlling the biosynthesis of phosphatidylcholine, and plays an important role regulating *de novo* phospholipid membrane accumulation. Regulation of CTP:phosphocholine cytidylyltransferase is critical for membrane biogenesis and for the production of new membrane during the S phase of the cell cycle, and inhibition of CCT by either biochemical or genetic methods triggers programmed cell death (Attard *et al.*, 2000). Phosphatidylcholine is essential for cell survival since it is a major structural building block of membranes, it is the precursor of phosphatidylethanolamine and sphingomyelin (other abundant membrane phospholipids) and is also the precursor of important second messengers that interfere in diverse signalling pathways controlling cell functioning, survival and proliferation (Gajate & Mollinedo, 2002). Interfering with these lipid metabolic pathways causes cellular stress and may initiate the apoptotic machinery, leading to cell death. The mechanism by which inhibition of PC biosynthesis initiates apoptosis remains to be fully elucidated, but it was shown that the shortage of PC in the endoplasmic reticulum (ER) causes ER stress and if persistent, ER stress can trigger apoptotic cascades through the activation of the pro-apoptotic transcription factor CHOP/GADD153 (C/EBP homologous protein/growth arrest- and DNA damage-inducible gene 153) or JNK (c-Jun N-terminal kinase) (Nieto-Miguel *et al.*, 2007; Van Blitterswijk & Verheij, 2013). Because PC is the major lipid component in mammalian membranes (accounting for more than 50% of cell membrane phospholipids and

more than 30% of total cellular lipid content) and cells must increase their phospholipid mass to form daughter cells during division, ALP-induced PC biosynthesis inhibition can also be seen as a putative mechanism for the blockade of cell cycle and mitosis inhibition that was observed in different cells following ALPs treatment (Mollinedo *et al.*, 2004).

Another possible consequence of the lack of PC could be the inhibition of the downstream synthesis of sphingomyelin from PC and ceramide, resulting in the accumulation of ceramide (Van Blitterswijk & Verheij, 2013). High levels of ceramide have been implicated in apoptosis induction, but whether it is ceramide itself or the process in which it is generated that induces apoptosis is still discussed (Blitterswijk *et al.*, 2003). The inhibition of PC synthesis is not exclusive of edelfosine, but it was also shown to happen with at least five different ALPs (Blitterswijk & Verheij, 2008) and it was suggested that this interference may be responsible for the biological effects of ATLs.

The finding that the addition of exogenous lysoPC, an alternative precursor for PC production (lysoPC is rapidly taken by cultured mamalian cells and acylated to form PC), prevented apoptosis induced by ALPs but not by other stimuli, strongly suggested that the inhibition of PC synthesis and its interference with the supply of membrane phospholipids could be a direct trigger towards apoptosis induction, rather than a specific role for CCT (Van Blitterswijk & Verheij, 2013). However, exogenous supplementation of lysoPC, although diminished apoptosis induction, was unable to restore cellular proliferation, indicating that edelfosine cytostactic action was independent of its interference with PC biosynthesis (Gajate & Mollinedo, 2002). There are other issues regarding the significance of PC biosynthesis inhibition for the overall effect of edelfosine: e.g., in HL-60 cells, induction of apoptosis following edelfosine treatment occurs long time before any changes in PC metabolism can take place, and several reports indicated a lack of correlation between the interference with phospholipid metabolism and the sensitivity of different cell lines to edelfosine as PC was shown to be inhibited in both sensitive and resistant cells (Gajate & Mollinedo, 2002).

Interference with cholesterol homeostasis

There is considerable evidence showing that the synthesis of PC is coordinately regulated with that of cholesterol; this co-regulation seems to occur via several mechanisms and to depend on the cell type (Marco *et al.*, 2014).

Cholesterol is an essential structural component of cell membranes, ensuring proper membrane permeability and regulating fluidity over a range of physiological temperatures (Marco *et al.*, 2014). Because free cholesterol is one of the major components of membrane lipids, cells must balance the internal and external sources in order to maintain membrane cholesterol homeostasis (Marco *et al.*, 2014). Both the biosynthetic and uptake pathways are well regulated by feedback control. Marco *et al* (Marco *et al.*, 2014), found that miltefosine, edelfosine and perifosine significantly stimulated *de novo* biosynthesis of cholesterol in HepG2 cells, leading to an increase in cholesterogenic activity. All the tested ALPs reduced the

synthesis of cholesteryl esters (CE), showing that all the chemically related drugs disrupted intracellular cholesterol homeostasis. Since cholesterol esterification is a measure of the levels of free cholesterol arriving at the endoplasmic reticulum, the authors suggested that ALP treatment would interfere with CE synthesis due to a reduction in the quantity of plasma-membrane cholesterol flowing to the ER, putting forward a defect in cholesterol transport from the plasma membrane to the ER. This could cause an important deregulation of cholesterol homeostasis, leading to the accumulation of free cholesterol in lipid rafts of the cell membrane (Van Blitterswijk & Verheij, 2013).

The maintenance of a strict free-cholesterol/PC ratio is crucial to optimum cell function and alterations to this ratio may lead to necrosis and/or apoptosis. An increase in cholesterol biosynthesis associated with a concomitant decrease in choline-containing phospholipids synthesis and cholesterol esterification leads to a modification in the free-cholesterol/PC ratio in cells exposed to antitumoral APLs which could have an important role in their cytotoxic activity (Marco *et al.*, 2014). Alteration in the composition of the lipid raft membrane microdomains may affect signalling processes vital to cell survival and growth, as will be discussed next.

Interference with membrane microdomains lipid rafts structure/organization

Current evidence indicates that lipid rafts are plasma membrane microdomains enriched in cholesterol and sphingolipids that have reduced fluidity and serve as foci for recruitment and concentration of signalling molecules (Gajate & Mollinedo, 2015; Mollinedo & Gajate, 2015). Cholesterol is of major importance in raft organization and acts as the dynamic "glue" that holds the raft together (Gajate & Mollinedo (2014)). ALPs could then affect these membrane microdomains as a consequence of the disrupted cholesterol homeostasis they induce. Within this context, it has been demonstrated that the depletion of cholesterol by cyclodextrin results in raft disruption and the subsequent malfunction of numerous signal transduction pathways; interestingly, enrichment of the membrane with cholesterol also destabilizes membrane rafts (Marco *et al.*, 2014).

Fas/CD95 clustering in lipid rafts

Edelfosine was shown to accumulate in lipid rafts, due to its affinity for cholesterol and for cholesterol-enriched membranes (Ausili *et al.*, 2008; Busto *et al.*, 2008). Lipid rafts have been implicated in signal transduction from cell surface receptors, and interestingly, edelfosine was shown to induce a potent aggregation and capping of the death receptor Fas/CD95 (cluster of differentiation 95) that co-localized with the microdomains lipid rafts during the triggering of apoptotic cell death of Jurkat leukemic T-cells and multiple myeloma cells (Gajate & Mollinedo, 2001; Gajate *et al.*, 2004). The adaptor Fas-associated death domain-containing protein (FADD) and procaspase-8, which together with Fas/CD95 form the so-called *death-inducing signalling complex* (DISC), were also recruited in lipid rafts following edelfosine treatment (Gajate *et al.*, 2004, 2009; Gajate & Mollinedo, 2007, 2011).

Physiological activation of Fas/CD95 by its natural ligand FasL/CD95L leads to the assembly of the DISC. The interaction between the elements of the DISC occurs through the death domain (DD) present in Fas and FADD and the death effector domain (DED) present in FADD and procaspase-8. DISC formation leads to procaspase-8 transactivation that releases mature caspase-8, initiating apoptosis through a subsequent caspase activation cascade (Johnson, 2013). Apoptosis is the result of a precise signalling process that is initiated either at the cell surface (death receptor pathway) or intrinsically by intracellular signals such as extensive DNA damage, and that leads to cell termination. This process generally involves the activation of a series of proteins called caspases, which cause the irreversible breakdown of cellular components and ultimately cell death. Caspase-8 activation following DISC formation might also trigger the apoptotic mitochondrial signalling pathway through the cleavage of BH3-interacting domain death agonist (Bid) into truncated Bid (tBid) (Luo *et al.*, 1998).

Edelfosine and perifosine have been shown to translocate Fas/CD95 as well as FADD and procaspase-8 into rafts in hematopoietic cancer cells, facilitating the triggering of apoptosis (Gajate & Mollinedo, 2014). Silencing of Fas/CD95 by RNA interference, transfection with a FADD dominant-negative mutant that blocks Fas/CD95 signalling, and specific inhibition of caspase-8, all prevented the apoptotic response, demonstrating the functional role of Fas/CD95 signalling in edelfosine-induced apoptosis (Gajate *et al.*, 2009; Gajate & Mollinedo, 2014).

Edelfosine was shown to act from within the cell instead of activating Fas from outside the cell membrane like the natural ligand FasL: edelfosine uptake by the cell was necessary to its effects, since cells that were unable to incorporate the drug were spared but became sensitive when microinjected with the drug if they expressed Fas (Gajate *et al.*, 2004). It remains to be elucidated whether edelfosine triggers Fas/CD95 activation by direct interaction with the cytoplasmic part of the death receptor or through an indirect process (Gajate & Mollinedo, 2014).

Disturbances on cholesterol homeostasis and general lipid metabolism induced by edelfosine could affect the plasma membrane fluidity. An hypothesis considered by Segui *et al* (Segui & Legembre, 2010) is that ceramide accumulation resulting from PC inhibition could alter plasma membrane characteristics, facilitating Fas/CD95 capping and oligomerization, in which case ceramide would not act as a second messenger *per se* but would modify the biochemical properties of the plasma membrane, and biophysically enhance CD95 translocation to lipid rafts and DISC formation.

The fact that edelfosine does not activate Fas/CD95 extracellularly, but from inside the cell in a FasL/CD95L-independent manner, and that the ether lipid is taken up preferentially by tumor cells, suggests edelfosine as a promising drug, apparently selective and able to potently trigger apoptosis in cancer cells (Gajate *et al.*, 2004).

Effects on proteins located or acting at the membrane level

Recent data by using different membrane model systems indicate that edelfosine increases fluidity in membrane raft domains, abolishing the fluidity buffering effect of cholesterol (Ausili *et al.*, 2008). Langmuir monolayer studies showed that the fluidizing effect of edelfosine on model membranes is highly cholesterol-dependent (Hac-Wydro *et al.*, 2011). Edelfosine increases the thickness and fluidity of model membranes for lipid rafts, and these actions might affect protein composition and interactions (Ausili *et al.*, 2008).

Protein kinase C

Protein kinase C (PKC) comprises a family of ubiquitously distributed Ser/Thr protein kinases that play a crucial role in several important physiological processes, including cell proliferation and differentiation (Bononi *et al.*, 2011). Many pharmacological inhibitors of PKC induce apoptosis, suggesting that PKC activity could render cells more resistant to apoptotic inducing agents (Gajate & Mollinedo, 2002).

PKC is commonly activated in GBM due to constitutive activation of EGFR and has been pointed as one of the signalling pathways that contribute to the aggressive behavior of glioma cells (Carmo *et al.*, 2013). PKCα exerts a pro-mitotic and pro-survival effect and loss of PKCα was associated with an increased sensitivity to a variety of apoptotic stimuli in glioma cell lines (Carmo *et al.*, 2013), making PKC a potential interesting target for GBM treatment. PKC belongs to a large family of closely related proteins with multiple subtypes that regulate different processes, some of them with opposite effects, which might explain why PKC contribution to the development of GBM is still poorly understood and also why conflicting and contradictory reports have been published concerning the effect of edelfosine on PKC activity.

Despite the diversity of functions, the majority of the isoforms can be activated by diacylglycerol (DAG) (Griner & Kazanietz, 2007), and their stimulation with DAG anologues is known to promote tumor progression (Teicher, 2006). Differences in PKC isozyme protein structure and substrate preferences have allowed the family to be divided into three subgroups, and the activation of the PKC isozyme family is clearly different between them. Conventional PKC isozymes (α, βI, βII, and γ) are calcium-dependent and are phospholipid- and diacylglycerol-activated kinases; novel isozymes (δ, ϵ, μ, and θ) are calcium-insensitive, phospholipid-dependent and diacylglycerol-dependent; the atypical PKC isozymes (η and λ/ι) are both calcium- and diacylglycerol-insensitive enzymes (Teicher, 2006). PKC inhibition was one of the first mechanisms of action described for edelfosine antitumoral effect (Helfman *et al.*, 1983), but most of the investigations on PKC activity after edelfosine treatment have been performed under conditions that were suitable for testing calcium-dependent PKC isoforms, and so the results may not apply to the other isoforms (Gajate & Mollinedo, 2002).

The lipid second messenger diacylglycerol controls the rate, amplitude, duration, and location of protein kinase C activity in the cell and from the three classes of PKC isozymes, the conventional and novel isozymes are acutely controlled by DAG (Gallegos & Newton,

2008). It is known that besides PC biosynthesis inhibition, edelfosine can also under certain signalling conditions prevent its breakdown to phosphatidic acid and further degradation to diacylglycerol (Pachioni *et al.*, 2013). Such deregulation of lipid homeostasis and interference with lipid second messengers is likely to affect PKC activity. However, a functional relationship between PKC level and effect of ET-18-OCH_3 on PKC activity in different sensitive and resistant cell types could not be found and a definitive answer on the effect of edelfosine on PKC remains to be established (Gajate & Mollinedo, 2002).

PI3K-Akt

PI3K is activated by a wide range of tyrosine kinase growth factor receptors, and is the major activator of Akt, having a central role in fundamental biological processes including cell growth, proliferation, migration and survival, through phosphorylation of a plethora of substrates (Reis-Sobreiro *et al.*, 2013). Class I PI3Ks converts phosphatidylinositol-4,5-bisphosphate (PI(4,5)P2) to phosphatidylinositol-3,4,5-trisphosphate at the inner leaflet of the plasma membrane. The production of PI(3,4,5)P3 leads to the binding and recruitment to the inner leaflet of the plasma membrane of enzymes containing pleckstrin homology (PH) domains, such as Akt. Once recruited at the cell surface, Akt is activated through its phosphorylation on Thr308 by another PH-domain-containing serine/threonine kinase named 3-phosphoinositide-dependent protein kinase-1 (PDK1) (Vivanco & Sawyers, 2002). Thr308 phosphorylation is necessary and sufficient for Akt activation, however,maximal activation requires additional phosphorylation at Ser473 by PDK2. Akt then phosphorylates a variety of substrates involved in pleiotropic cell functions, including cell growth, proliferation and survival. Akt is a key regulator of multiple survival routes: it phosphorylates and inactivates the pro-apoptotic Bcl-2 family member Bad, Forkhead and CREB (cAMP response element-binding protein) transcription factors and can contribute to the inactivation of p53 by phosphorylation of Mdm2 (Carmo *et al.*, 2011). Furthermore, Akt phosphorylates and activates mTOR in response to growth factors and oncogenes (Blitterswijk & Verheij, 2008) and suppresses apoptosis by direct phosphorylation of pro-apoptotic proteins such as Bad and pro-caspase-9 (Reis-Sobreiro *et al.*, 2013).

Akt is activated in most human cancers and since its activation contributes to cell growth, proliferation and survival signalling pathways, it has for long been considered an attractive target for anticancer therapy (Pachioni *et al.*, 2013). As mentioned in the previous chapter *"Commonly altered signalling pathways in GBM - possible therapeutic targets?"*, PI3K and Akt are often activated in GBM due to EGFR constitutive activation, c-MET and PDGFR co-activation, or due to mutations in PI3K that amplify or activate its catalytic site; because PTEN is also often mutated, PI3K enzyme can not be directly antagonized through that pathway. Several mTOR-PI3K-Akt-PTEN signalling pathway inhibitors have been developed and tested, but further investigation is needed to understand how they affect glioma cells and why the impact on patient treatment has been so limited.

Not only edelfosine, but other ATLs such as perifosine and miltefosine have been re-

ported to inhibit the PI3K-Akt survival pathway, likely through inhibition of the plasma membrane recruitment of the serine-threonine kinase Akt via its pleckstrin homology domain (Van Blitterswijk & Verheij, 2013). Unlike ATP-competitive inhibitors, perifosine prevented the recruitment of Akt to the plasma membrane by disrupting membrane microdomains essential to growth factor signalling and Akt activation and/or by displacing the natural ligands, PI(4,5)P2 and PI(3,4,5)P3 (generated by PI3K activity) from the PH domain of Akt (Van Blitterswijk & Verheij, 2013), thus Akt cannot adopt the favorable conformation for its activation. Perifosine has been and is currently being tested in combination with other therapies as an orally administered inhibitor of the PI3K/Akt survival pathway (Richardson *et al.*, 2012).

PI3K signalling pathway has been implicated in controlling the lateral mobility of Fas in the plasma membrane (Varadhachary *et al.*, 2001), and Legembre's group decided to investigate whether inhibition of the PI3K activity could account for the redistribution of Fas into lipid rafts observed by Gajate *et al* on human leukemic cells after edelfosine treatment (Gajate & Mollinedo, 2001; Bénéteau *et al.*, 2008). Bénéteau *et al* found that inhibition of PI3K signalling triggered the rapid formation of Fas/CD95 clusters and the redistribution of Fas/CD95 into lipid rafts, linking the molecular target PI3K to the previously well-described redistribution of Fas into the lipid rafts (Gajate & Mollinedo, 2001; Gajate *et al.*, 2004). Similarly to PI3K inhibitors, edelfosine selectively induced cell death in cells expressing high PI3K activity, down-modulated PI3K signalling in T leukemia cell lines and led to the induction of a Fas/CD95-mediated apoptotic signal and the formation of micrometer range clusters of Fas/CD95 into large raft platforms (Bénéteau *et al.*, 2008). In our laboratory, Reis-Sobreiro *et al* also found that edelfosine treatment in mantle cell lymphoma cells displaced survival PI3K/Akt signalling from lipid rafts, whereas Fas/CD95 was recruited into these membrane domains, leading to Akt dephosphorylation and apoptosis (Reis-Sobreiro *et al.*, 2013). Bénéteau *et al* suggested that by virtue of its lipid nature, edelfosine could act directly on PI3K to down-modulate its activity or that its incorporation into the plasma membrane bilayer affects the PI3K substrate, PIP3, modifying its docking activity and thus preventing the downstream recruitment of Akt (Bénéteau *et al.*, 2008).

EGFR, Raf-1, MAPK

The wide range of cancer cells whose growth is inhibited by edelfosine suggests that a common mechanism of action, if it exists, likely involves perturbation of a widely used signal transduction mechanism that initiates proliferation. One such pathway is the Ras-dependent activation of the mitogen-activated protein kinase (MAPK) cascade (Ras/Raf-1/MEK/ERK), which transduces signals from receptor tyrosine kinases, oncogenic tyrosine kinases, and G-protein-coupled receptors (Zhou *et al.*, 1996). Edelfosine has been reported to reduce the number of EGFR sites without affecting the affinity of the receptors in human breast cancer cell lines and this effect was suggested as being responsible for the decreased proliferation of these cancer cells (Gajate & Mollinedo, 2002). EGFR is commonly mutated or amplified in

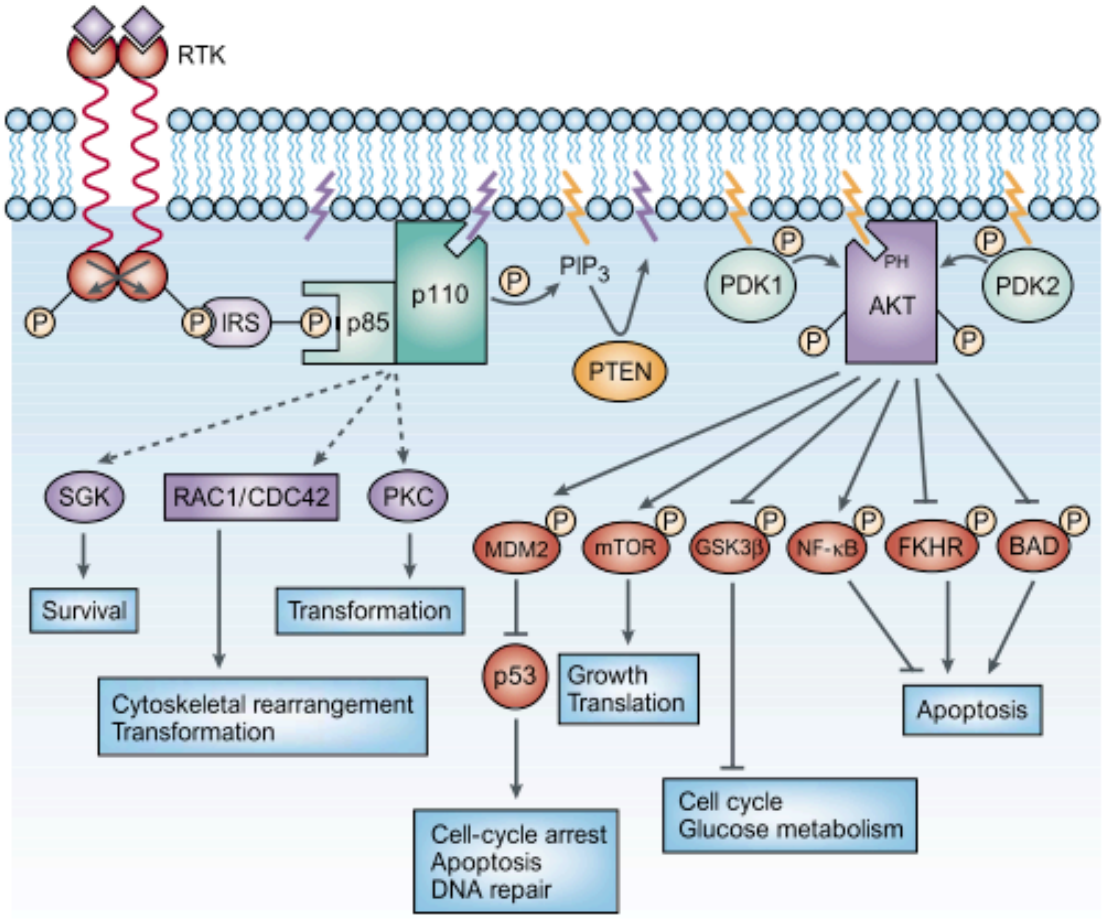

Figure 1.6: Activation of class IA phosphatidylinositol 3-kinases (PI3Ks) occurs through stimulation of receptor tyrosine kinases (RTKs) and the concomitant assembly of receptor-PI3K complexes. PIP3 serves as a second messenger that helps to activate Akt. Through phosphorylation, activated Akt mediates the activation and inhibition of several targets, resulting in cellular growth, survival and proliferation. PI3K has also been shown to regulate the activity of other cellular targets, such as the serum and glucocorticoid-inducible kinase (SGK), the small GTP-binding proteins RAC1 and CDC42, and protein kinase C (PKC), in an Akt-independent manner. The activity of these targets leads to survival, cytoskeletal rearrangement and transformation. *From Vivanco & Sawyers (2002).*

GBM resulting in constitutive activation of the receptor. Although EGFR has been a prime target for therapeutic intervention, the different strategies used had little success and it could be useful to exploit if edelfosine interferes with EGFR signalling in GBM and its potential as a treatment option.

Zhou *et al* (Zhou *et al.*, 1996) found that edelfosine had no effect on the binding of EGF to its receptors, their activation, or p21-Ras activation in MCF-7 cells, but interfered with the association of Raf-1 with membranes, resulting in a decrease in Raf-1 kinase activity. Activation of the mitogen-activated protein kinase pathway subsequent to growth factor stimulation requires the recruitment of Raf-1 from the cytosol to the membrane, a process mediated by the interaction of Raf-1 with activated Ras. Edelfosine has been suggested to associate with Raf-1 in the cytosol interfering in the interaction of Raf-1 with activated Ras, thereby reducing the levels of Raf-1 that are translocated to the membrane for activation (Samadder *et al.*, 2003). However, it is not known whether edelfosine–induced inhibition of Raf-1 activation is due to a direct interaction of the compound with Raf-1, or whether it is achieved indirectly via its effects on unknown intermediary molecules required for the activation and/or attachment of Raf-1 to the membrane (Zhou *et al.*, 1996), or even due to edelfosine-induced biophysical changes in the membrane.

Edelfosine also interferes with the MAPK pathway in another way: by the mentioned effects it exerts on PC biosynthesis. Besides inhibiting PC biosynthesis, edelfosine and other ALPs can also inhibit its breakdown to phosphatidic acid and further degradation to diacylglycerol by inhibiting phospholipase D (Blitterswijk & Verheij, 2008). Phosphatidic acid and diacylglycerol are lipid second messengers involved in the Ras/Raf/MEK/ERK pathway: PA has been implicated in activation of protein kinase C-ζ, c-Raf and mTOR, stimulates type I phosphatidylinositol (PI)-4-phosphate 5 kinase (PIP5K), PIP2 synthesis and membrane vesicular trafficking; DAG binds to and activates protein kinases C and D, and Ras guanine-releasing protein (RasGRP), thus stimulating the MAPK/ERK pathway (Blitterswijk & Verheij, 2008).

It is known that PI3K and MAPK pathways can interact in multiple ways, both in normal and transforming conditions. It was described that Ras interacts with PI3K in a direct manner without involving any other proteins (Rodriguez-Viciana *et al.*, 1994), pointing to PI3K as an effector of Ras. PI3K can activate the Rac GTPase, and this Rho family protein is an important mediator of oncogenic Ras transformation (Castellano & Downward, 2011). The crosstalk between these pathways is made up of a complex network of events, with many feedback loops.

Will *et al* (Will *et al.*, 2014) showed that PI3K is upstream of both Ras and Akt, that inhibition of PI3K downregulates both ERK signalling (transiently) and Akt–mTOR signalling (durably), and that the transient inhibition of ERK was necessary for the potent induction of apoptosis by PI3K inhibitors.

In a large panel of tumor models, PI3K inhibitors were shown to inhibit Akt signalling in

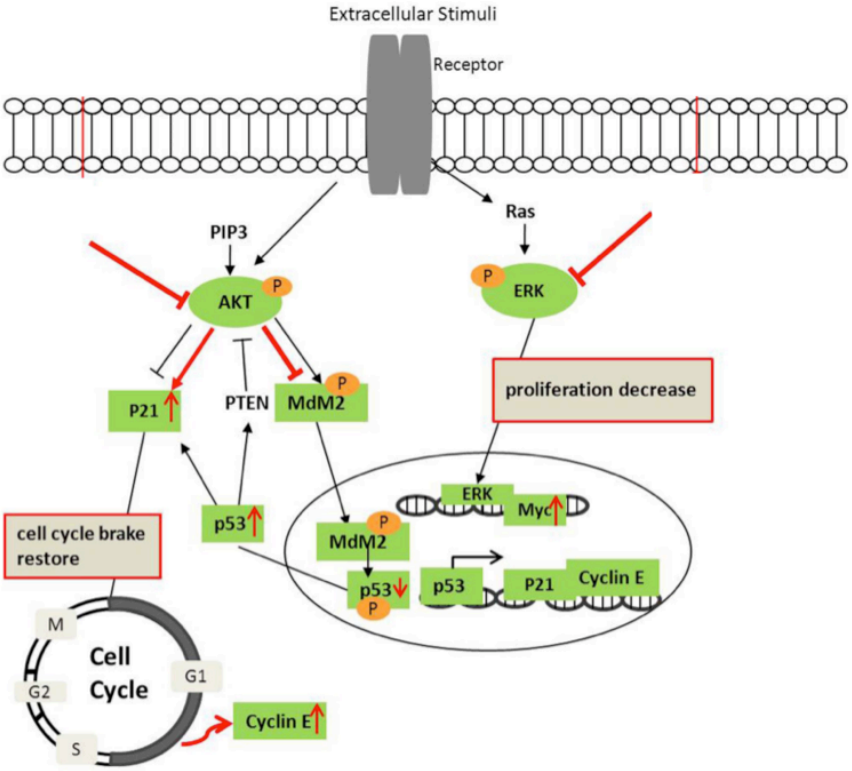

Figure 1.7: Effects that the inhibiton of Akt and ERK could have in GBM, represented with red labels. Akt deactivation decreases MDM2 and p53 phosphorylation and increases stable p53, which trigger its downstream p21 and cyclin E expression. Simultaneously, p53 may increase PTEN to further suppress Akt activation. *Image from Liu et al. (2013).*

all cells and inhibit Ras-ERK signalling in most cells but not those harboring a mutant allele of Ras (Will *et al.*, 2014). Due to the mentioned effect of edelfosine on PI3K, it is likely that it may also have consequences on the MAPK pathway, given the complex crosstalk between the pathways.

As a summary, inhibition of phospholipases, interference with levels of diacylglycerol and phosphatidic acid, effects on the number of EGFR sites and on Raf-1 translocation to the membrane and its consequent activation, and effects on the PI3K pathway could all concur to edelfosine and other ALPs induced attenuation of the MAPK/ERK pathway.

ER stress and SAPK/JNK signalling

Unlike in human hematopoietic cancer cells, where edelfosine induced a rapid apoptotic response, it was observed that in solid tumor cells like HeLa, lung carcinoma A549 and pancreatic adenocarcinoma cell lines, edelfosine promoted a slow and late apoptotic response, preceded by G2/M arrest (Nieto-Miguel *et al.*, 2006; Gajate *et al.*, 2012). Hematopoietic and solid tumor cells incorporated similar amounts of edelfosine but in solid tumors the major accumulation of edelfosine was seen to occur in the ER, instead of in plasma membrane lipid rafts (Nieto-Miguel *et al.*, 2006, 2007; Gajate *et al.*, 2012).

The ER is a complex organelle in terms of both its structure and function, and it is responsible for critical cellular functions, including protein and lipid biosynthesis, post-translational protein modification and cellular calcium storage (Bravo *et al.*, 2013). Disturbance in ER functionality leads to ER stress and aggregation of misfolded proteins, which triggers the unfolded protein response (UPR) to restore normal ER function. If ER stress is persistent, the cytoprotective functions of UPR can turn into a cell death promoting mechanism (Bravo *et al.*, 2013). CTP:phosphocholine cytidylyltransferase must translocate from an inactive nuclear reservoir to a functional state on the ER (Nieto-Miguel *et al.*, 2006), and some have suggested that inhibition of this translocation could itself induce ER stress (Sanden *et al.*, 2003). Edelfosine was found to accumulate in the ER of solid tumor cells and to affect PC biosynthesis in HeLa and A549 cells (Nieto-Miguel *et al.*, 2006), supporting previous reports suggesting a role for the inhibition of PC in the mechanism of action of this drug. Nieto-Miguel *et al* (Nieto-Miguel *et al.*, 2006, 2007) also found a predominant endoplasmic reticulum location for edelfosine in glioblastoma cells.

Three major pathways of ER stress-induced apoptosis are known: the upregulation of the transcription factor CHOP/GADD153, JNK activation, and activation of caspase-12 in murine systems or caspase-4 in human cells (Gajate & Mollinedo, 2014). The JNK pathway is activated by a series of stress signals, and its sustained activation can lead to apoptosis (Davis, 2000). ATLs, including edelfosine, exert numerous effects that could be responsible for JNK activation (Gajate *et al.*, 1998; Van Blitterswijk & Verheij, 2013). Accumulation of edelfosine in the ER of solid tumor cancer cells was seen to induce a potent ER response characterized by inhibition of protein synthesis, CHOP/GADD153 upregulation, eIF2-α (eukaryotic translation initiation factor 2-α) phosphorylation and activation of Bax, caspase-4, and JNK (Gajate & Mollinedo, 2014).

ASK1 (apoptosis signal-regulating kinase 1) is an upstream MAPK kinase kinase (MAP3K) of JNK and its related family member p38. ASK1 is preferentially activated in reponse to various types of stress, including reactive oxygen species (ROS), tumor necrosis factor (TNF-α), lipopolysaccharide, and ER stress (Van Blitterswijk & Verheij, 2013). Inhibition of JNK prevented edelfosine-induced apoptosis, and ASK1 overexpression in HeLa cells enhanced both edelfosine-induced JNK activation and apoptosis, indicating that ASK1/JNK signalling plays an important role in edelfosine-induced apoptosis, at least in these cells (Nieto-Miguel *et al.*, 2007). JNK is able to directly induce the intrinsic pathway of apoptosis, but has also been implicated in the death receptor-induced apoptotic pathway (Van Blitterswijk & Verheij, 2013).

A role for mitochondria

As mentioned in the previous sections, edelfosine can accumulate in either the plasma membrane (lipid rafts) or in the ER, triggering apoptotic-signalling cascades from each subcellular location. Signals derived from plasma membrane rafts or the ER may converge at the level of mitochondria. Interestingly, edelfosine acts on Bid and BAP31, two molecules that link the

extrinsic pathway of apoptosis and the ER with mitochondria (Gajate & Mollinedo, 2014). Active caspase-8 from the extrinsic pathway is known to cleave Bid protein, and the Bid cleavage product (tBid) can migrate to the mitochondria and stimulate cytochrome c release and activation of the intrinsic pathway. BAP31 is an integral membrane protein of the endoplasmic reticulum, regulating ER-mediated apoptosis through its own caspase-8-mediated cleavage into a 20-kDa fragment, which directs pro-apoptotic signals between the ER and mitochondria (Gajate & Mollinedo, 2014). Recent findings correlate ER stress with the control of mitochondrial function and metabolism through mechanisms involving calcium transfer from the ER to mitochondria (Bravo *et al.*, 2013). It is interesting to note that there is physical interaction between ER and mitochondria, and that the transport of phospholipids occurs at specialized fractions of the ER tightly associated with mitochondria (Gajate & Mollinedo, 2014).

Edelfosine and perifosine inhibited mitochondrial respiration and decreased transmembrane electric potential in isolated hepatic mitochondria and edelfosine was also shown to promote a redistribution of lipid rafts from the plasma membrane to mitochondria (Mollinedo *et al.*, 2011). Edelfosine-induced apoptosis in many cells was shown to occur through the loss of mitochondrial transmembrane potential, release of cytochrome c from mitochondria, and activation of caspase-9, while these effects were suppressed by Bcl-2 or Bcl-x_L overexpression (Gajate *et al.*, 2000; Gajate & Mollinedo, 2014).

Edelfosine also increases the levels of reactive oxygen species and stimulates membrane lipid peroxidation in tumor cells. Although the contribution of these effects to edelfosine cytotoxic action is not entirely clear (Gajate & Mollinedo, 2002), those have been described as potentially apoptotic and necroptotic inducers and could be contributors to the ether lipid cytotoxic effects.

ATLs uptake

Regardless of the ATL target and the subsequent molecular pathways that may lead to cell death, incorporation into the cell is known to be a crucial event in the selective action of the ether lipids on tumor cells (Mollinedo *et al.*, 1997; Van Blitterswijk & Verheij, 2013). Unlike tumor cells, normal cells are unable to take up significant amounts of the ether lipid: Mollinedo *et al* showed that a primary culture of normal human fibroblasts did not incorporate significant amounts even after long-term incubations and were unaffected by the presence of the drug, however microinjection of the ether lipid into these normal cells prompted apoptosis (Gajate & Mollinedo, 2002; Gajate *et al.*, 2004).

Although edelfosine uptake is of pivotal importance for its biological action, conflicting data have been reported in order to explain how the ether lipid is incorporated, and no conclusive notion has been reached so far. Direct adsorption onto the plasma membrane followed by passive diffusion, endocytosis, lipid flip-flop, and a specific protein-directed incorporation have been postulated for edelfosine uptake (Gajate *et al.*, 2004). It was recently found that a transmembrane phospholipid flippase P4-ATPase ATP8B1, functioning in com-

plex with CDC50a (TMEM30a) subunit is involved in ALPs taken up by carcinoma cells (Muñoz-Martínez *et al.*, 2010; Chen *et al.*, 2011), but further studies are needed in order to better understand generalities and specificities of the uptake mechanism of edelfosine and other ALPs by tumor cells.

Summary and some important considerations

Different studies have shown strong effects of edelfosine on cellular lipid metabolism, affecting not only the biosynthesis of PC but also that of shingolipids and cholesterol. The complex network of effects that ALPs, including edelfosine, seem to exert upon the metabolism of important molecules involved in cell signalling makes it difficult to pinpoint the mechanism by which these events might participate in anti-proliferative and cytotoxic actions (Marco *et al.*, 2014). Edelfosine actions on lipid metabolism seem to depend largely on the cell type and experimental conditions used, and some compensatory mechanisms that overcome initial lipid metabolism perturbations seem to exist (Mollinedo *et al.*, 2004). In some tumor cells, the reduced incorporation of fatty acids in cellular phospholipids seemed to be a consequence of the inhibition of proliferation by edelfosine rather than its cause. Some authors question if the interference in lipid metabolism is actually the primary and general cause for the inhibition of cell growth and cytotoxic action of edelfosine, but the hypothesis that the ether lipid induces these actions *also* by interfering with the metabolism of cholesterol and/or PC and their related secondary messengers is very plausible since the final effect is a strong imbalance in the metabolism of membrane-lipid components that is vital to cell survival (Marco *et al.*, 2014).

In fact, the lipidic nature of edelfosine can partially explain the variability of its effects. ATLs incorporation into cell membranes interferes with plasma membrane-associated proteins, which in turn interferes with different signalling pathways. The study of the mechanism of action of these drugs is then highly complex, and should distinguish between alterations that directly affect cell survival and those that are rather a consequence of other effects and do not directly contribute to cell death; it should also analyze the role of the first ones in cellular toxicity and explore the relationships between direct and indirect effects.

When comparing different cell lines, and looking for relationships between different sensitivities to compounds and specific characteristics of the cells, it should be taken into account that the unknown factors of the mechanism of action of the drug and the incomplete knowledge about the characteristics of the system under study, when not carefully weighted, can lead to misinterpretation, confounding correlation with causality as thoughtfully mentioned by Marbán (Marbán, 2013).

Cell Death

In their review "A matter of life and death", Green and Evan propose that cancer cells arise and are maintained through the simultaneous acquisition of two cooperating conditions: deregulated cell proliferation and suppressed apoptosis (Green & Evan, 2002). In this section we will be discussing the importance of cell death suppression for the development and maintenance of tumors and its implications for managing therapies and the emerging of resistance.

Over the past few decades, an extraordinary progress has been made in the understanding of cell death, leading to a much deeper knowledge of its mechanisms and underlying molecular features, and consequently to significant changes in the way cell death/survival can be manipulated in order to treat different diseases, including cancer. Decades ago, different types of cell death were defined in purely morphological terms, with limited reference to the underlying biological changes (Golstein & Kroemer, 2005). Since the first descriptions of different cell death modalities, a great amount of work has been made and several new intermediate or mixed cell death types have been reported.

A schematic and very simplified view of the molecular mechanisms underlying the main cell death types in mammalian cells could be the following: **apoptosis**, involving the near-to-obligatory activation of caspases; **autophagic cell death**, with the sequestration of cytoplasmic organelles in autophagosomes followed by their fusion with lysosomes that requires a series of autophagy gene products; **necrosis** that is likely to result, at least in part, from severe ATP depletion (Golstein & Kroemer, 2005).

As reviewed by Golstein in *"Redundant cell death mechanisms as relics and backups"*, in many cases the inactivation of certain cell death-associated effectors will not abolish cell death, but rather suppress a particular cell death mechanism and reveal a different one. E.g., caspase inhibition was shown to lead to a switch from apoptosis to necrosis in thymocytes after DNA damage or from apoptosis to autophagic cell death in growth-factor deprived neurons (Golstein & Kroemer, 2005). In general, cell death pathways may be divided in three distinct stages: the initial **signalling stage**, a subsequent **effector stage** and a final **dismantling phase**. Golstein *et al* suggested that an ancestral cell death mechanism, which may have been similar to necrosis and where mitochondria played a central role, was overlaid with additional mechanisms conferring selective advantage that contributed to the degradation of the cell corpses - apoptosis and autophagy. These "new" mechanisms may have entered cell death pathways at the dismantling stage and lately extended their role to a participation in cell death effector mechanisms, after acquiring autonomy and even exclusivity in some species or types of cells (Golstein & Kroemer, 2005). Autonomy could have been achieved by coupling a lethal signal to the activation of caspases, overriding the phylogenetically ancient mitochondrial checkpoint, as it happens in "type-1" cells, in which Fas/CD95 ligation directly induces massive caspase activation independent of mitochondria (Golstein & Kroemer, 2005).

The explained hypothesis suggests that the number of cell death pathways is probably greater at the dismantling phase than at the effector stage, justifies the widely redundancy of cell death types and alert for the fact that a predominant dismantling mechanism may

be present overlaying a different effector mechanism, which may act as a back-up in case of suppression of the first type of cell death.

Defects in cell death pathways facilitate tumor development and progression, and cause resistance to chemotherapy, radiation and other anticancer treatments, having devastating consequences for the successful treatment of cancer patients. In order to achieve selective and efficient killing of tumor cells, it is essential to understand the molecular mechanisms of cell death, the proteins that act to regulate these pathways and the specific alterations that occur in cancer cells.

In the next sections, it will be made a general description of the main types of cell death, interactions between them and how they can work as "backup" mechanisms, and also a summarized analysis of ways by which cancer cells can avoid their own demise. Due to the extension and complexity of the theme this introduction will be a superficial approach to the field, and deeper development will be made during results description and discussion.

Apoptosis

Historically, three types of cell death have been distinguished in mammalian cells by morphological criteria. Type I cell death, better known as apoptosis, is defined by characteristic changes in the nuclear morphology, including chromatin condensation (pyknosis) and fragmentation (karyorrhexis); minor changes in cytoplasmic organelles; and overall cell shrinkage, blebbing of the plasma membrane and formation of apoptotic bodies that contain nuclear or cytoplasmic material (Golstein & Kroemer, 2007). In vivo, these apoptotic bodies were observed to be engulfed and degraded by macrophages or neighboring cells (Johnson, 2013).

The term "apoptosis" comes from Greek, whose prefix "apo" can be taken as "separation" and the suffix, "ptosis", translated as "falling off" has been generally known as the falling off of leaves from trees in autumn (Duque-Parra, 2005). Apoptosis was initially described by its morphological characteristics, including cell shrinkage, membrane blebbing, chromatin condensation and nuclear fragmentation (Mollinedo *et al.*, 2004). The later realization that apoptosis is a gene-directed program had profound implications for the understanding of developmental biology and tissue homeostasis since the genetic basis for apoptosis implies that cell death, like any other metabolic or developmental program, can be disrupted by mutation (Lowe & Lin, 2000).

The apoptotic machinery is composed of both upstream regulators and downstream effector components. Two pathways of apoptotic execution have been delineated: extrinsic (or death receptor mediated) apoptosis and intrinsic (mitochondrial-mediated) apoptosis as will be presented in the following subsections.

Extrinsic apoptosis

The term *extrinsic apoptosis* has been used to indicate cases of apoptotic cell death induced by extracellular stress signals that are sensed and propagated by specific transmembrane receptors (Galluzzi *et al.*, 2012). Extrinsic apoptosis can be initiated by the binding of the lethal ligands FASL/CD95L, tumor necrosis factor alpha (TNFα) and TRAIL to their respective cell surface death receptor: Fas/CD95, TNFα receptor1 (TNFR1) and TRAIL receptor (TRAILR) 1-2; other transmembrane proteins may also transduce lethal signals, including CD2, CD4, TNFRSF8/CD30, TNFRSF5/CD40, CD45, CXCR4 and class I/II MHC molecules (Galluzzi *et al.*, 2012).

A well described signalling pathway leading to extrinsic apoptosis is the one elicited by Fas mediated signalling (Galluzzi *et al.*, 2012). The binding of Fas ligand results in trimerization of the receptor protein, bringing together the three cytoplasmic regions of Fas (Johnson, 2013). Within the cytoplasmic region of Fas and of other death receptors, there is a domain called the death domain (DD). Trimerization of the Fas DDs results in recruitment of the DD in the adaptor protein FADD (Fas-associated death domain protein), and formation of the death-inducing signalling complex (DISC) (Johnson, 2013). FADD also contains a domain called death-effector domain (DED), which recruits the DED found in the prodomain of the zymogen form of the initiator caspase-8 (or the initiator caspase-10). The recruitment of procaspase-8 to the DISC causes a conformational change that results in modest activation of the enzyme and proximity-induced proteolytic processing of procaspase-8 proteins in the DISC (Johnson, 2013). During this process, the inhibitory prodomain of caspase-8 is removed and large and small caspase-8 subunits are produced. The fully activated caspase is then comprised in an heterotetrameric complex consisting of two large subunits and two small subunits. After being activated, the initiator caspases cleave and activate executioner caspases, including executioner caspase-3, which then cleave specific substrate proteins, resulting in proteolytic destruction of the cell (Johnson, 2013).

Intrinsic apoptosis

The intrinsic apoptosis pathway can be activated by a variety of cellular insults, including withdrawal of essential cytokines or neurotrophic factors and treatment with chemotherapy or radiation (Johnson, 2013). Agents causing cellular damage, such as chemotherapy drugs, prompt a plethora of intracellular stress conditions, including DNA damage, oxidative stress, cytosolic Ca^{2+} overload, accumulation of unfolded proteins in the endoplasmic reticulum, etc., that can relay a signal to mitochondria leading to the release of cytochrome c into the cytosol. The cytosolic cytochrome c associates with the cytoplasmic adapter protein Apaf-1 and the inactive precursor of the initiator caspase-9, forming a complex referred as the apoptosome (Johnson, 2013). Formation of the apoptosome induces a slight conformational change in procaspase-9, sufficient to promote autoprocessing to active caspase-9 which then activates downstream executioner caspases (Johnson, 2013).

The signalling cascades that trigger intrinsic apoptosis can be ignited by a variety of

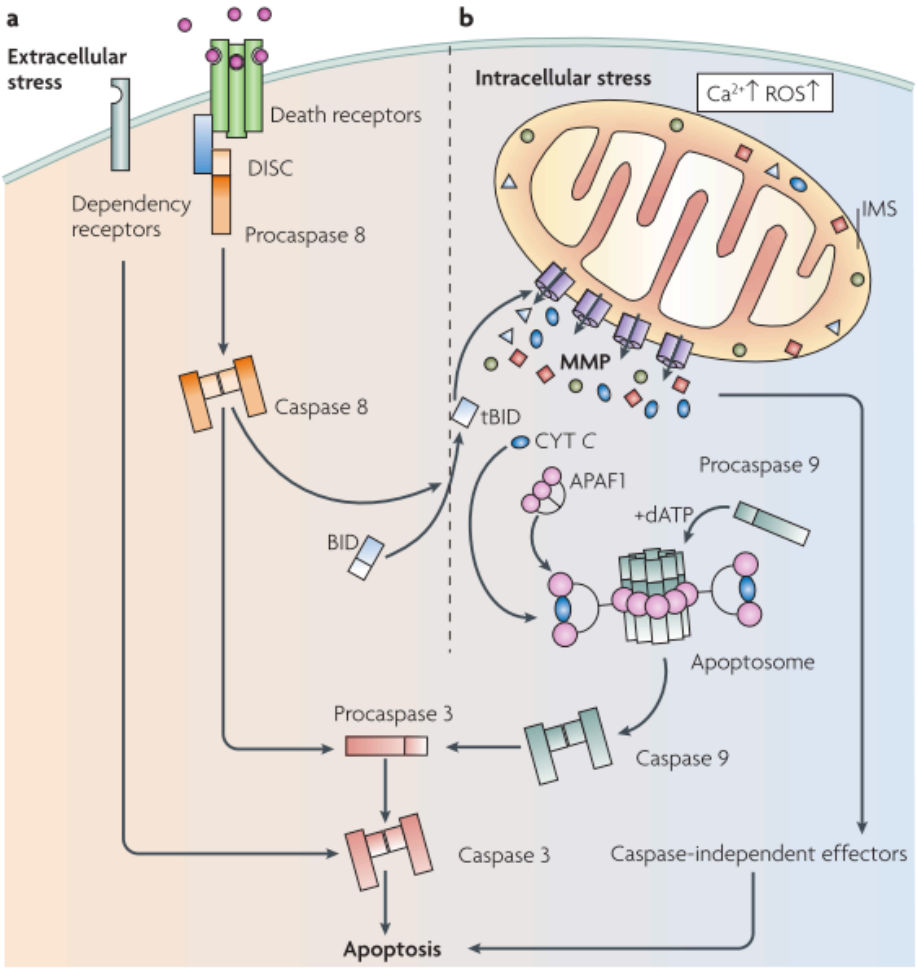

Figure 1.8: Apoptosis can result from the activation of two biochemical cascades, which are known as the extrinsic (part a) and the intrinsic (or mitochondrial, part b) pathways. The extracellular apoptotic pathway is initiated at the plasma membrane by specific transmembrane receptors, whereas mitochondrial apoptosis is triggered by intracellular stimuli. In both pathways, initiator caspases (caspase 8 and 9, respectively) are activated within specific supramolecular platforms and so can catalyse the proteolytic maturation of executioner caspases, such as caspase 3. One of the major links between extrinsic and mitochondrial apoptosis is provided by the protein BID, which can promote MMP following caspase-8-mediated cleavage. Mitochondrial membrane permeabilization (MMP) activates both caspase-dependent and caspase-independent mechanisms that eventually execute cell death. *From Galluzzi et al. (2009).*

stimuli, but they are all connected to a mitochondrion-centered control mechanism (Galluzzi *et al.*, 2012). Mitochondrial membrane permeablization can start due to the Bcl-2 family pro-apoptotic proteins Bak and Bax and their pore-forming activity, or may result from mitochondrial permeability transition (MPT) that occurs at the inner mitochondrial membrane due to the opening of the permeability transition pore complex (PTPC) (Galluzzi *et al.*, 2009).

Irreversible mitochondrial permeabilization affecting the majority of mitochondria in a single cell has multiple lethal consequences; one of them is the release of different proteins such as apoptosis-inducing factor (AIF), endonuclease G (ENDOG), SMAC/DIABLO, HTRA2 (high temperature requirement protein A2), cytochrome c from the mitochondrial intermembrane space. AIF and ENDOG relocate to the nucleus, where they mediate large-scale DNA fragmentation independently of caspases; cytochrome c mediates caspase-9 activation; SMAC/DIABLO and HTRA2 inhibit the antiapoptotic function of several members of the IAP family, thereby derepressing caspase activation; HTRA2 also exerts caspase-independent pro-apoptotic effects (Galluzzi *et al.*, 2012). Generalized and irreversible mitochondrial membrane permeabilization also leads to the dissipation of the $\Delta\psi_{\mathrm{m}}$ and consequent cessation of mitochondrial ATP synthesis and $\Delta\psi_{\mathrm{m}}$-dependent transport activities (Kroemer *et al.*, 2007). Mitochondrial outer membrane permeabilization (MOMP) occurs rapidly upon caspase activation but it can also be caspase independent. The consequent disruption of ATP generation, in the absence of caspase activation, ensures cellular demise, although the mode of cell death may resemble necrosis more than classical apoptosis (Green & Evan, 2002). The breakdown of electron transport also promotes the generation of reactive oxygen species, which may accelerate cell death. The intrinsic apoptotic pathway predominantly leads to the activation of caspase-9 but, al least in certain cells, the intrinsic pathway can proceed in the absence of caspase-9 or APAF1 (Youle & Strasser, 2008). Caspase activation actually seems to have a prominent role in a limited number of instances of stress-induced intrinsic apoptosis *in vitro*, since chemical and/or genetic inhibition of caspases rarely, if ever, confers long-term cytoprotective effects or truly prevents cell death. Usually, in this context, caspase inhibition only delays the execution of cell death, which eventually exhibit morphological features of necrosis (Galluzzi *et al.*, 2012).

Bcl-2 and Bcl-x_{L}, which reside at the outer layer of the mitochondrial membrane, act to negatively regulate the intrinsic apoptosis pathway, preventing mitochondrial permeabilization and the release of cytochrome c, formation of the apoptosome and the activation of caspase-9 (Johnson, 2013). However, Bcl-2 and Bcl-x_{L} appear to control cell survival beyond the APAF1–caspase-9 axis. If caspase activation is inhibited by loss of APAF1 or caspase-9, or even by the combined loss of caspase-9 and caspase-2, the rate of acquisition of apoptotic morphology after stress-induced apoptosis was seen to be significantly delayed in myeloid progenitors and mast cells, but these cells still lose clonogenic potential and die, unlike cells that overexpress Bcl-2 or Bcl-x_{L} (Youle & Strasser, 2008). Thus, the step of apoptosis regulation that is controlled by the Bcl-2 family appears to be the most general final commitment step for the decision between cell life and death. The disruption of mitochondria by BAX and

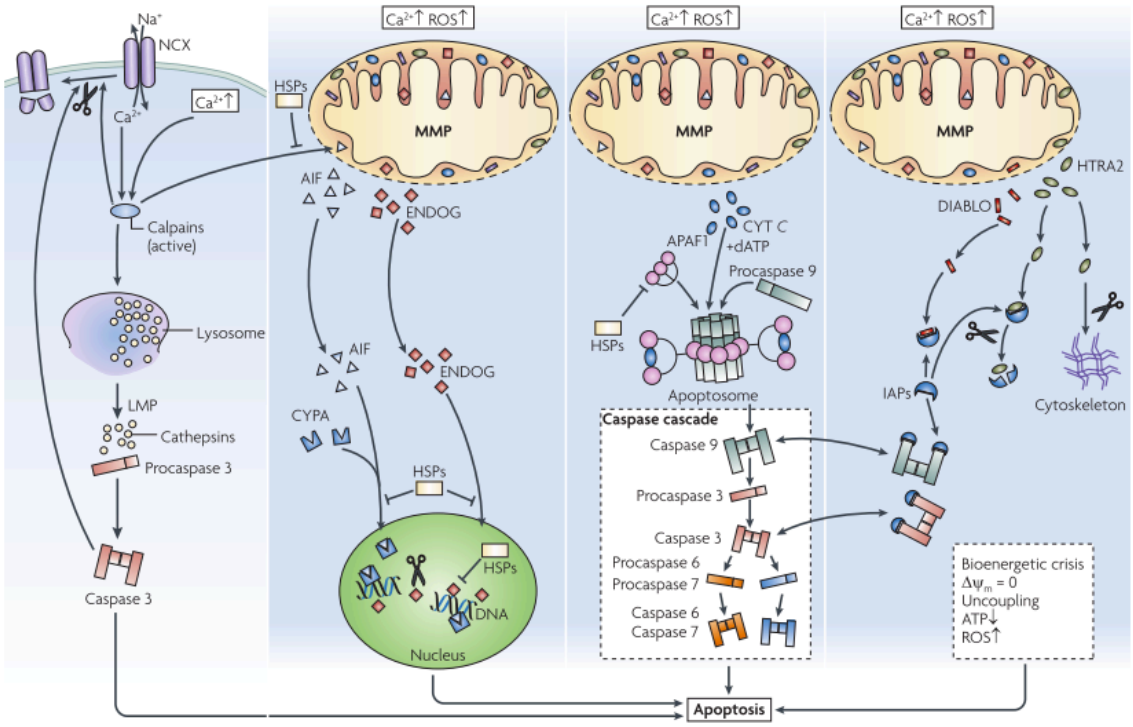

Figure 1.9: Mitochondrial membrane permeabilization (MMP) allows the release of several proteins that are normally confined within the mitochondrial intermembrane space. Cytochrome c (CYT C) recruits the adaptor protein apoptotic peptidase activating factor 1 (APAF1) to assemble the apoptosome, a supramolecular platform that triggers the caspase cascade. DIABLO/SMAC and HTRA2 favour the activation of caspases by relieving the endogenous inhibition that is mediated by the inhibitor of apoptosis proteins (IAPs). Following MMP, endonuclease G (ENDOG) and apoptosis-inducing factor (AIF) can translocate to the nucleus and mediate DNA fragmentation independently of caspases. MMP also causes the dissipation of the mitochondrial transmembrane potential, thereby leading to a bioenergetic crisis that is characterized by respiratory chain uncoupling, ATP synthesis arrest and reactive oxygen species (ROS) overgeneration. Excessive Ca^{2+} triggers MMP and activates calpains, which contribute to cell death in multiple ways; for example by inducing lysosomal membrane permeabilization (LMP), which allows the spillage of harmful hydrolases such as cathepsins into the cytosol. Molecular chaperones from the heat-shock protein (HSP) family exert pro-survival functions by inhibiting both caspase-dependent and caspase-independent executioner mechanisms. *From Galluzzi et al. (2009).*

BAK may be one cause of eventual cell death in the absence of apoptosome activation.

Type-1 and type-2 cells

In the so-called "type I cells", active caspase-8 directly catalyzes the proteolytic maturation of caspase-3, triggering the executioner phase of apoptosis independently of mitochondria, ie, independently of the intrinsic apoptotic pathway. In some instances, early cross-talk between the extrinsic and intrinsic pathways occurs, since active caspase-8 from the extrinsic pathway cleaves Bid protein, and the Bid cleavage product (tBid) can migrate to the mitochondria and stimulate cytochrome c release and activation of the intrinsic pathway. "Type I cells" then may have tBid and mitochondrial outer membrane permeabilization (MOMP) but the mitochondrial involvement is dispensable for the execution of cell death (Galluzzi *et al.*, 2012). "Type II cells" succumb from the activation of death receptors while showing signs of MOMP, including the dissipation of mitochondrial transmembrane potential and the release of proteins that are normally retained within the mitochondrial intermembrane space (IMS) (Galluzzi *et al.*, 2012). Blockage of the intrinsic apoptotic pathway in these cells should prevent apoptotic cell death.

Defective apoptosis signalling in cancer

In view of all the players involved in apoptotic cell death, we can predict that these pathways may be affected at multiple different steps, with different consequences. Tumor cells often acquire resistance to apoptosis by various mechanisms that interfere at different levels of apoptosis signalling; in the following subsections, there will be a brief description of some examples.

1. Mutation or deregulated expression of caspases

Being of critical importance to extrinsic and intrinsic apoptosis, we could expect that genes encoding caspases would be targets for genetic alterations impairing the function or expression of caspases in human tumors, resulting in a great impact over cell death execution. In fact, a great number of studies found mutations or reduced expression of initiator caspases-8 and -10 in different tumors, and a smaller number of publications described the same for caspase-9 and the effector caspases -3 and -7 (Johnson, 2013).

One of the mechanisms responsible for apoptosis resistance in cancer results from silencing of tumor suppressor of pro-apoptotic genes, occurring by hypermethylation of the CpG-rich sites located in the promoter region of the gene (Eramo *et al.*, 2005). Reduced expression or hypermethylation of caspase-8 is a common find in many tumors of the CNS (Johnson, 2013) and the tumorigenic role of methyltransferases is further supported in brain tumors by the repression of caspase-8 expression observed in neuroblastomas and medulloblastomas, where the use of the methyltransferase inhibitor decitabine (5-aza-2-deoxycytidine) results in caspase-8 upregulation and restoration of apoptosis sensitivity (Eramo *et al.*, 2005).

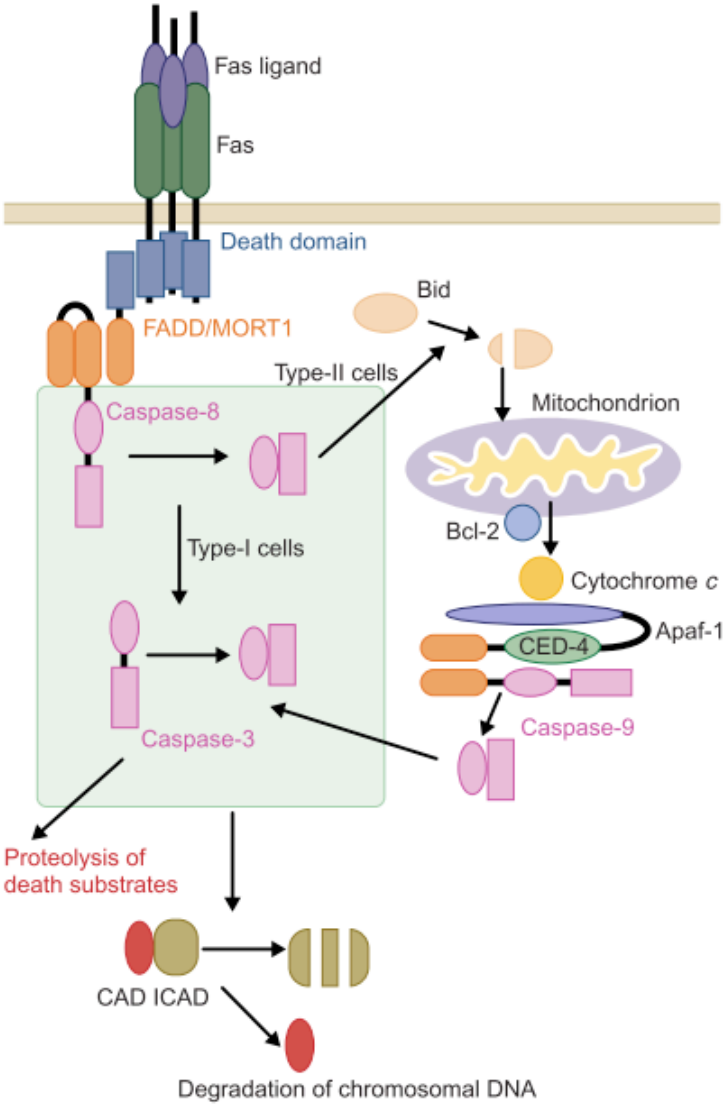

Figure 1.10: Two signalling pathways for Fas ligand (FasL)-induced apoptosis. Binding of FasL to Fas recruits procaspase-8 through the FADD adaptor, which results in processing of procaspase-8 into the active enzyme. In type-I cells, caspase-8 directly cleaves caspase-3. In type-II cells, caspase-8 cleaves Bid and the truncated Bid stimulates the release of cytochrome c from mitochondria. Cytochrome c, together with Apaf-1 and ATP, then activates caspase-9, which in turn activates caspase-3. One of the substrates of caspase-3 is ICAD (inhibitor of caspase-activated DNase (CAD)). Cleavage of ICAD by caspase-3 activates CAD, which causes DNA degradation in nuclei. *Image from Nagata et al (1999).*

Martinez *et al* (Martinez *et al.*, 2007) described that the CpG island promoter hypermethylation of the pro-apoptotic gene caspase-8 was a common hallmark of relapsed glioblastoma multiforme, and that an unmethylated CASP8 CpG island together with another marker in primary GBMs was significantly associated with prolonged time to tumor progression, linking this defect on the extrinsic apoptotic pathway to cell death resistance and tumor progression. Eramo *et al* (Eramo *et al.*, 2005) suggested the combination of TRAIL and demethylating agents to overcome glioblastoma cells resistance to TRAIL-induced apoptosis, by increasing caspase-8 expression, its consequent activation, and cell death execution.

2. Aberrant expression of IAPs

The IAP (inhibitor of apoptosis) family is comprised of eight members: XIAP, cIAP1, cIAP2, NAIP, survivin, MLIAP, BRUCE, and ILP2. XIAP has potent and direct inhibitory activity against caspase-9, caspase-3, and caspase-7, while cIAP1 and cIAP2 can act to indirectly inhibit the activities of these caspases (Johnson, 2013). IAP proteins comprise at least one of the signature baculoviral IAP repeat domains, a protein-protein motif critical to their binding to and inhibition of caspases (Fulda, 2014). In normal healthy cells XIAP will inhibit caspase-9, -3, or -7 activities and prevent the activation of apoptotic cascades. During the activation of intrinsic apoptotic pathways, SMAC is released from the IMS of mitochondria as mentioned in *"Intrinsic apoptosis"*, and the processed SMAC protein containing a sequence that binds to XIAP displaces it from bound caspases, leading to their activation. Many tumors overexpress XIAP, preventing limiting levels of SMAC to overcome XIAP inhibition of the caspase cascade (Johnson, 2013).

cIAP1 and cIAP2 indirectly inhibit caspases via two mechanisms: they may bind and sequester SMAC protein preventing the displacement of XIAP from caspases, or promote ubiquitination of effector caspases-3 and -7, resulting in their degradation via the proteasome (Johnson, 2013). Aberrant overexpression of XIAP and of other IAPs has been observed in multiple solid tumor and hematopoietic malignancies. In several cases, overexpression of XIAP has been shown to correlate with treatment resistance or poor prognosis (Johnson, 2013).

One major antiapoptotic mediator that is overexpressed in gliomas is the transcription factor NF-κB. NF-κB is well known as a mediator of immune and inflammatory processes, but it also activates the transcription of proteins of the IAP family (c-IAP, XIAP, and survivin). IAPs such as XIAP are highly expressed in malignant gliomas, and they have been associated with refractory disease and poor prognosis (Krakstad & Chekenya, 2010). Recently, it has been reported that the infection of malignant glioma cells with adenoviruses encoding antisense RNA to X-linked IAP depletes endogenous XIAP levels and promotes global caspase activation and apoptosis. In intracranial glioma xenografts, the Ad-XIAP gene therapy induced cell death, prolonged survival in nude mice and reduced tumorigenicity, reinforcing their potential as therapeutic target for human gliomas (Naumann *et al.*, 2007).

3. Intrinsic apoptosis pathway defects

The intrinsic apoptosis pathway is tightly regulated by members of the Bcl-2 family, which can be divided into anti-apoptotic proteins and pro-apoptotic proteins. The proteins of the family share homology through conserved domains called Bcl-2 homology, or BH domains (Johnson, 2013).

The anti-apoptotic Bcl-2 family members include Bcl-2, Bcl-x_L, Bcl-w, Mcl-1, A1/Bfl-1, and Bcl-b (Johnson, 2013). These proteins contain multiple BH domains and carboxyl-terminal membrane-anchoring domains, and act to inhibit cytochrome c release from the mitochondria.

The pro-apoptotic Bcl-2 family members can be subdivided into two groups, those containing multiple BH domains (e.g., Bax, Bak and Bok), and those containing only a single BH3 domain (e.g., PUMA, Bik, Noxa, Bid, Bad, etc.), referred to as "BH3 domain-only" proteins. The conserved BH3 domain can bind and regulate the anti-apoptotic Bcl-2 proteins to promote apoptosis (Youle & Strasser, 2008). It appears that the pro-apoptotic family members Bax and Bak are crucial for inducing permeabilization of the outer mitochondrial membrane and the subsequent release of cytochrome c and SMAC, as genetic studies revealed that cells lacking Bax and Bak are highly resistant to stimuli that activate the intrinsic apoptosis pathway (Youle & Strasser, 2008; Johnson, 2013). The anti-apoptotic family members, such as Bcl-2 and Bcl-x_L, inhibit Bax and Bak. Although it is commonly thought that Bax and Bak form pores in membranes, the biochemical nature of such pores and how anti-apoptotic Bcl-2 family proteins regulate them remains a key and controversial issue in the field of cell death (Youle & Strasser, 2008). There are different mechanisms that may account for Bcl-2 overexpression in cancer, such as gene amplification of chromosomal segments encompassing the Bcl-2 gene, gene amplification of Bcl-x_L and Mcl-1 and also hypomethylation of the bcl-2 gene promoter. Recent evidence indicates that expression of Bcl-2 family members can also be controlled via expression of microRNAs, such as microRNAs miR-15a and miR-16-1 that negatively regulate expression of Bcl-2 (Johnson, 2013). The expression level of Bcl-2 proteins is also controlled by transcriptional activation by p53, as will be discussed in the following section *Mutation/deletion of p53*.

Overexpression of anti-apoptotic Bcl-2 has been reported in a wide variety of hematopoietic and solid tumor malignancies, and in many cases overexpression of Bcl-2 and/or Bcl-x_L has been closely related with resistance to chemotherapy or radiation and poor overall survival (Johnson, 2013). Upregulation of the pro-survival proteins Bcl-2 and Bcl-x_L has been described in recurrent GBMs independent of treatment, suggesting that untreated GBMs are subjected to pressure for development of apoptosis resistance and that this might be a natural course of the disease (Krakstad & Chekenya, 2010). In a microarray study of 20 patient GBM biopsies, Ruano *et al* found that negative expression of Bax correlated with an adverse clinical outcome (Ruano *et al.*, 2008). In GBM, overexpression of Bcl-2 or Bcl-x_L not only leads to resistance to apoptosis but has also been linked to increased tumor cell motility (Wick *et al.*, 1998).

Several therapeutic agents that target members of the Bcl-2 family have been developed and many of these have been tested in preclinical or clinical trials but few have been tested on glioblastomas. Only one compound has reached clinical trials with GBM patients and encouraging results are still to be published (Krakstad & Chekenya, 2010).

While anti-apoptotic Bcl-2 family members are frequently overexpressed in human cancers, the pro-apoptotic members are commonly underexpressed or functionally inactivated in human tumors: frameshift and inactivating mutations in the *Bax* gene have been detected in colorectal and hematopoietic malignancies; mutation of noxa gene has been reported in diffuse large B-cell lymphoma, bak gene mutations are present in gastric and colon tumors, homozygous deletion of bim gene has been observed in mantle cell lymphomas and loss of heterozigosity in bik gene occurs in renal cell carcinoma (Johnson, 2013). As in the case of the anti-apoptotic genes, promoter methylation status (in the case of underexpression of the pro-apoptotic genes, hypermethylation of the promoter) is a common alteration, and there is emerging evidence pointing to the role of microRNAs also in the regulation of these Bcl-2 members expression (Johnson, 2013).

Downregulation of Bax has been described in recurrent GBMs, and in the microarray study of Ruano *et al* (Ruano *et al.*, 2008), negative expression of Bax correlated with an adverse clinical outcome, underscoring the importance of different members of the Bcl-2 family for chemotherapy and radiation-induced apoptosis.

4. Mutation/deletion of p53

p53 is often cited as the most commonly mutated protein in human cancers (Johnson, 2013). As mentioned in the previous section *"Commonly altered signalling pathways in GBM – possible therapeutic targets?"*, *TP53* is also the most frequently mutated gene in GBM, with mutations clustered in the DNA binding domain, a hotspot for p53 mutations in human cancers.

p53 actively promotes apoptosis induction via the intrinsic apoptosis pathway, particularly in response to DNA damage, and has a well characterized role as a transcription factor. Direct transcription targets of p53 include pro-apoptotic members of the Bcl-2 family such as Bax and Bim and the BH3-only proteins PUMA and Noxa. As such, the role of p53 is closely related to that of the Bcl-2 proteins (Krakstad & Chekenya, 2010). A role for p53 in the regulation of mitochondrial membrane permeabilization independently of its transcriptional activity was also described (Krakstad & Chekenya, 2010). Mutations in the p53 gene lead to loss of p53 function as a transcription factor or loss of expression of the p53 protein (Johnson, 2013). In both cases, the roles played by p53 in the regulation of cell cycle arrest, DNA repair, apoptosis, and senescence are critically affected. Collectively, the combination of transcription-dependent mechanisms mediated by nuclear p53 and transcription-independent mechanisms mediated by cytosolic/ mitochondrial p53 confers a potent impact on cellular apoptosis (Johnson, 2013). Loss-of-function of TP53 leads to deregulation of apoptosis signalling and increased tumorigenesis. At least two phase I gene therapy trials using adenovirus-

TP53 to reintroduce a functional TP53 gene in patients with recurrent or progressive brain tumors have been completed (NCT00004080 and NCT00004041) but until now no results have been published [Krakstad & Chekenya (2010); *www.clinicaltrials.gov*]

5. Extrinsic apoptosis pathway defects

Multiple defects affecting the extrinsic pathway are also commonly found in tumors. As already mentioned, initiator caspases for the extrinsic apoptotic pathway, caspases -8 and -10 are frequently mutated or underexpressed in human cancers, this way limiting the progression of the cell death signalling pathway. Type II cells, which require mitochondrial involvement for efficient cell killing following activation of death receptors may not be able to fully activate cell death if the intrinsic apoptotic pathway is compromised for some reason, this way impairing killing initiated by the extrinsic pathway.

Loss or mutation of death receptors is commonly detected in different malignant tumors; for example, mutations in Fas, typically leading to an inactive protein, have been detected in both hematologic and solid tumor malignancies and methylation of the Fas gene is also an important mechanism of downregulation of Fas in different human tumors (Johnson, 2013). Apoptosis induced by the death ligand TRAIL is mediated by the death receptors TRAIL-R1 (also called DR4) and TRAIL-R2 (also called DR5), and these receptors were also found to be frequently mutated in many tumors; hypermethylation of the TRAIL-R1 gene was observed in glioma (Johnson, 2013). Again, p53 may have an important role in sensitivity to TRAIL, since genes encoding TRAIL-R1 and TRAIL-R2 were found to be p53 target genes; also genes encoding decoy receptors for TRAIL appear to be p53 target genes, further increasing the complexity of this signalling network. Decoy receptors are closely related to the death receptors but they lack a functional death domain (Igney & Krammer, 2002). Most glioblastoma cell lines express DR5 and DR4 that transduce the apoptotic signal via the death domains, but far fewer express the decoy receptors (Krakstad & Chekenya, 2010). However a majority of glioblastoma cells are resistant to TRAIL despite expressing DR5 and DR4, indicating that the resistance mechanisms might involve defects downstream of the receptor (Krakstad & Chekenya, 2010). FADD mutation is another less commonly found alteration, which may impair transduction of the death signalling initiated through the extrinsic apoptotic pathway.

6. Deregulated c-FLIP expression

The c-FLIP (cellular FLICE-inhibitory protein) proteins are endogenous inhibitors of death receptor-mediated caspase-8/caspase-10 activation. Three major c-FLIP protein isoforms have been reported: c-FLIP(L), c-FLIP(S), and c-FLIP(R).

A large number of publications have shown that high levels of c-FLIP(L), c-FLIP(S), or c-FLIP(R) effectively compete with procaspase-8 and procaspase-10 for binding to FADD or TRADD proteins present in the forming DISC of activated death receptors, limiting the execution of the extrinsic apoptotic pathway. On the other hand, when expressed at only low levels, c-FLIP(L) has been shown to heterodimerize with procaspase-8 and promote

its activation (Johnson, 2013). Overexpression of c-FLIP was detected in a large number of tumors, including glioblastoma, and c-FLIP(L) high levels were found to correlate with tumor progression or poor prognosis in colon, endometrial, liver, ovarian and prostate cancers (Johnson, 2013).

One strategy for sensitizing GBMs to TRAIL is to target the signalling pathway downstream of TRAIL through targeting of c-FLIP, Bcl-2 and XIAP (Krakstad & Chekenya, 2010).

Another way to die

It has often been tacitly assumed that mammalian cell death is mostly mediated by apoptosis; this consensus stemmed in part from the pioneering description of apoptosis as a defined regulated cell death modality (Golstein & Kroemer, 2005). While early studies on *C. elegans* importantly demonstrated genetic control of apoptotic cell death, they may have led researchers to unconsciously apprehend and characterize caspase-dependent apoptosis while neglecting other cell death modalities (Golstein & Kroemer, 2005). This bias may have also been favored by the development of main techniques to identify apoptotic cells such as the TUNEL staining: being used as a general approach to evaluate cell death, it only detects a largely caspase-dependent type of DNA fragmentation, hence ignoring non-apoptotic events (Golstein & Kroemer, 2005).

There are, however, arguments in favor of a relatively high incidence of nonapoptotic cell deaths *in vivo*, especially in conditions in which key apoptotic players are inhibited. As mentioned in the previous section, defective apoptosis is commonly found in cancer cells, stressing the need to consider and study different cell death mechanisms that may be present or can be explored in order to achieve efficient cell killing bypassing an ineffective apoptotic machinery.

Autophagy and autophagic cell death

Autophagy has long been linked with a form of cell death, called autophagic or type II cell death (Ryter *et al.*, 2014). Macroautophagy (hereafter called autophagy) is a lysosome-dependent process that degrades various cargoes varying from molecules to whole organelles. Selective pathways can target distinct cargoes (e.g., mitochondria and proteins) for autophagic degradation (Ryter *et al.*, 2014). Autophagy can be stimulated by different metabolic and therapeutic stresses, including nutrient deprivation, hypoxia, intracellular pathogens, chemotherapy and/or radiotherapy and consists of multiple related vesicular trafficking programs coordinated by a complex interplay between dedicated enzymes, cellular membranes, cytoskeleton, and motor proteins (Johnson, 2013). A complex set of autophagy proteins and autophagy-associated proteins regulate the formation of the autophagosome, its fusion with the lysosome, and the degradation and recycling of cellular components (Johnson, 2013).

On the basis of morphological features, the term 'autophagic cell death' has widely been used to indicate instances of cell death that are accompanied by a massive cytoplasmic vacuolization (Galluzzi *et al.*, 2012). However, it should be noted that the massive cytoplasmic vacuolization observed not always indicates an increased autophagic flux, but may instead result from defects in autophagic pathways. Originally the expression "autophagic cell death" did not imply any functional consideration but scientists quickly adopted the term and used it to imply that autophagy would actually *execute* the cell demise (Galluzzi *et al.*, 2012), maybe beacuse the expression itself is as linguistic invitation to think that cell death is executed by autophagy (Kroemer & Levine, 2008). If persistent, autophagy may indeed result in exhaustion of intracellular resources and terminal starvation (Johnson, 2013); however, in most instances autophagy appears to be associated with, rather than actually causing cell death (Tait *et al.*, 2014). Kroemer and Levine pinpointed that some conditions that kill cells are preceded by extensive autophagy that is visible even in dying cells, leading to the false interpretation that autophagy contributed to the death of the cell (Kroemer & Levine, 2008). Although in some settings autophagy itself is required for cell death (autophagy has been shown to mediate physiological cell death in vivo during the developmental program of *D. melanogaster* and to be responsible for cell death in vitro in some cancers lacking essential apoptotic modulators (Galluzzi *et al.*, 2012)), most often autophagy is primarily a pro-survival stress response. Autophagic catabolism serves a functional role in the stressed cell by producing energy sources that can be used to generate ATP and building blocks to be recycled allowing further growth (Johnson, 2013). Acting as a cytoprotective response activated in dying cells to cope with stress, autophagy inhibition may in fact accelerate cell death rather than prevent it (Galluzzi *et al.*, 2012). Also, autophagy is reversible once initiated, and occurs at a basal level in all eukaryotic cells. In cancer cells autophagy can be induced to even higher levels than in surrounding normal tissue and may serve as a key survival mechanism (Johnson, 2013).

Several methods may be used to determine whether the autophagic pathway is activated in the context of the cellular demise. The Nomenclature Committee on Cell Death (NCCD) recommends using the term "autophagic cell death" only in instances in which cell death is caused by autophagy, that is, in which cell death can be suppressed by the inhibition of the autophagic pathway by chemicals (e.g., agents that target VPS34) and/or genetic means (e.g., gene knockout/mutation or RNAi targeting essential autophagic modulators like AMBRA1, ATG5, ATG12 or beclin 1)(Galluzzi *et al.*, 2012).

When cell death is accompanied by autophagy but its inhibition does not block cell death, then that fact should be described and further biochemical characterization of the cell death phenomenon is required. According to NCCD, all cases of cell death that exhibit markers of autophagy, such as the lipidation of microtubule-associated protein 1 light chain 3 (LC3/Atg8) or an increased degradation of autophagic substrates like sequestosome 1 (SQSTM1), but cannot be blocked by autophagy inhibition should not be classified as autophagic cell death (Galluzzi *et al.*, 2012). Unfortunately, most studies fail to perform kinetic analyses of cell death at serial time points to confirm that cell death (and not just one marker of cell death at

one time point) is truly blocked, and few studies assess the effects of autophagy inhibition on clonogenic survival (Kroemer & Levine, 2008). Autophagy inhibition may affect cell death kinetics, and even commonly used markers to detect other cell death modalities, at least in some circunstances (Qu *et al.*, 2007). On the other hand, if autophagy is clearly inhibited but the cells still die after the same stimulus, one might argue that if apoptosis inhibition may lead to the activation of different cell death modalities after a certain stimulus, autophagy, truly acting as the effector mechanism as a first-line cell death response, could also be replaced by another mechanism following its blockage. It seems reasonable to also consider this possibility, but careful analysis should be done before attributing a role for autophagy in cell killing, evaluating if other cell death modalities, if any, are present after blockage of the autophagic pathway.

Autophagy as a tumor suppressor and as a tumor promoter

Multiple groups demonstrated that autophagy defects could lead to increased DNA damage, genomic instability and tumor progression, suggesting autophagy as a tumor suppressor mechanism. Monoallelic deletion of Beclin 1, a phylogenetically conserved protein essential for autophagy, was found in 40-75% of ovarian, breast, and prostrate cancers, favoring the hypothesis of a tumor suppressor role for autophagy (Johnson, 2013). However, it was also described that autophagy plays a critical role as a stress response in many tumor cells, allowing them to survive in harsh conditions. High levels of autophagy are detected in both metastatic melanoma and pancreas cancer and those elevated levels correlate with metastases and/or poor survival in different tumors (Yang *et al.*, 2011; Lazova *et al.*, 2012).

For the referred monoallelic deletion of beclin 1, initially used as an argument to support a tumor supressor role for autophagy, the retained allele was always wild type, and the beclin 1 "deficient" cells usually had similar levels of autophagy when compared to beclin wild type cells. These beclin+/- mice had lower levels of p53 suggesting that p53 deficiency and not autophagy deficiency could account for the development of malignancies in the beclin-deficient mice. No other mouse model of genetic autophagy deficiency induced spontaneous malignancies, and inactivating somatic mutations that produce cancer have yet to be described for any other autophagy genes; for all these reasons, autophagy may be important for tumorigenesis, and autophagy-deficient tumors are most probably rare (Johnson, 2013). It appears that depending on the cell and cellular environment, autophagy may play the tumor suppressor or the tumor promoter role and those may not be mutually exclusive. Different authors have suggested that autophagy mainly contributes to tumor suppression during the early stage of tumorigenesis and to tumor promotion during the late stage of tumorigenesis (Sun *et al.*, 2013). Some ATG proteins may have autophagy-independent functions and may be converted from pro-autophagy to pro-death proteins by proteolytic cleavage (e.g., ATG5 and ATG6) (Galluzzi *et al.*, 2012). Autophagy is regulated by multiple mechanisms and shares different regulation "points" and signalling nodes with apoptotic and necroptotic pathways. Physiological levels of autophagy, that might be increased in cancer cells, may allow estab-

lished tumors to adapt to nutrient-deprived or hypoxic conditions during cancer progression, while excessive autophagy under especially stressing conditions may lead to cell death. The degree and the duration of autophagy probably are important factors determining the final consequence of its activation.

Autophagy in GBM treatment

The first line treatment for GBM, temozolomide, induces autophagy in glioma cells, and studies demonstrated that clinically relevant doses of TMZ induced autophagy without apoptosis (Ramirez *et al.*, 2013). Time course studies showed that autophagy is detected as much as two days before apoptosis in several glioma lines following TMZ treatment. Inhibition of autophagy in these studies led to an increase in apoptosis and allowed apoptosis to occur at an earlier time point, demonstrating the role of autophagy as a survival mechanism in glioma cells (Knizhnik *et al.*, 2013). Similarly, glioma cells treated with the EGFR tyrosine kinase inhibitor, erlotinib, underwent autophagy with reduced cell death. Co-treatment with the autophagy inhibitor chloroquine (CQ) and erlotinib increased cell death (Ramirez *et al.*, 2013). Inhibiting autophagy in combination with other therapies is then a promising approach to reduce tumor cell survival following chemotherapy and is being tested in the clinic (Ramirez *et al.*, 2013). Because effective autophagy inhibition can be achieved *in vivo* with the anti-malarial drug chloroquine, and there is extensive experience with CQ for the treatment of malaria, rheumatoid arthritis and HIV, multiple trials have been launched in a wide variety of tumor types using chloroquine and its derivative hydroxychloroquine (Johnson, 2013). Chloroquine continues to be evaluated as a treatment for gliomas with clinical data indicating an increase in survival in patients in a phase II trial that added 150 mg daily dose of CQ as part of their adjuvant regimen (Ramirez *et al.*, 2013). Currently, the therapeutic strategy targeting autophagy is by inhibiting it, but further work needs to be pursued concerning pre-identification of sensitive tumor types and recognizing appropriate therapeutic regimens that synergistically act with autophagy inhibition to enhance clinical benefit (Johnson, 2013). Kanzawa *et al* found that inhibition of autophagy in the U373-MG cells following TMZ treatment in different phases (before or after the association of LC3 with the autophagosome membrane) produced distinct results: either rescued cells from cell death or increased apoptosis with activation of caspase-3, respectively (Kanzawa *et al.*, 2004). Because the role of autophagy in resistance to therapy is extremely complex and autophagy may enhance cell death or cell survival, additional studies allowing a better understanding of the regulation of this pathway must be performed in order to determine whether autophagy can be confidently manipulated to enhance cancer therapy.

Necrosis and regulated necrosis / necroptosis

Distinct from apoptosis, necrosis is morphologically characterized by early plasma membrane permeabilization which causes cells to swell and finally rupture, spilling their contents into the extracellular milieu (Long & Ryan, 2012). Unlike apoptotic cells, the nuclei of necrotic cells remain largely intact. For a long time, necrosis has been considered as a merely accidental cell death, and was defined mainly in a negative way, by the absence of morphological traits of apoptosis or autophagy (Galluzzi *et al.*, 2012). A classical positive definition of necrosis was based on morphological criteria such as early plasma membrane rupture and dilatation of cytoplasmic organelles, in particular of mitochondria (Kroemer *et al.*, 2007). In harsh conditions like detergent stress or freeze-thawing, cells can die through a non-regulated, poorly defined, necrotic process (Kroemer *et al.*, 2007). However, it is now clear that necrosis can occur in a regulated manner and that necrotic cell death has a prominent role in multiple physiological and pathological settings (Galluzzi *et al.*, 2012). The following progressively acquired knowledge contributed to the development of this notion: **1.** necrotic cell death of chondrocytes, controlling the longitudinal growth of bones, and also of intestinal epithelial cells can occur physiologically during development and to maintain adult tissue homeostasis; **2.** susceptibility to necrotic death can be regulated by genetic and epigenetic factors; **3.** the inhibition of some enzymes and processes can prevent necrosis; **4.** the same upstream signal that induces apoptosis can cause necrosis when apoptotic signalling is blocked (Kroemer *et al.*, 2007). This necrotic regulated form of cell death has been called "necroptosis" (Degterev *et al.*, 2005). Although morphologically resembling necrosis, necroptosis is a regulated active type of cell death. It was observed that programmed necrosis could be triggered by alkylating DNA damage, excitotoxins and the ligation of death receptors (Galluzzi *et al.*, 2012). The best-characterized inducers of necroptosis are death receptor ligands, in particular, tumor necrosis factor (TNF), although other death receptor ligands, such as Fas, have also been shown to induce necroptosis under conditions of caspase inhibition (Tait *et al.*, 2014). Indeed, it remains highly debated whether necroptosis ever occurs unless caspases are actively inhibited (Tait *et al.*, 2014). Key molecules regulating necroptosis, like RIPK1 and RIPK3 enzymes, have been recently identified, and led to a very active interest in the fundamental biology and the roles that this mechanism may play in different settings. When caspases (particularly caspase-8) are inhibited by genetic manipulations (e.g., by gene knockout or RNA interference) or blocked by pharmacological agents (e.g., chemical caspase inhibitors), RIPK1 and its homolog RIPK3 are not degraded and engage in physical and functional interactions that activate the execution of necrotic cell death (Galluzzi *et al.*, 2012). As stated by the NCCD, the term 'necroptosis' has recently been used as a synonym of regulated necrosis, but it was originally introduced to indicate a specific case or regulated necrosis, which is ignited by TNFR1 ligation and can be inhibited by the RIPK1- targeting chemical necrostatin-1. Like for other types of cell death, NCCD recommends detailed description of the molecules involved in the process: e.g., cases of regulated necrosis that exhibit RIPK1 activation (which can be measured by enzymatic assays or by monitoring RIPK1 phosphorylation on S161) and that

can be suppressed by RIPK1 inhibitors including necrostatin-1, should be labeled 'RIPK1-dependent regulated necrosis'. RIPK3-dependent but RIPK1-independent necrosis has also been described, and although both forms can be considered as necroptosis, the key molecular regulators of each one (RIPK1 – and/or RIPK3- dependent regulated necrosis) should be clearly defined when first using the term necroptosis to describe the process (Galluzzi *et al.*, 2012).

Inducing necroptosis

Current data for the best characterized necroptotic inducer, TNF, supports that during the initiation of necroptosis, TNF receptor-ligand binding through the adaptor protein TRADD leads to an interaction between RIPK1 and RIPK3 (Ofengeim & Yuan, 2013). This interaction that happens through the RIP homotypic interaction motifs (RHIM) present in both proteins, leads to the activation of RIPK1 and RIPK3 and the formation of a complex called the necrosome. The necrosome formation is highly regulated by ubiquitylation: the ubiquitin ligases cIAP-1 and cIAP-2 negatively affect its formation by ubiquitylating RIPK-1, whereas the deubiquitylase CYLD counteracts this and promotes necrosome formation (Tait *et al.*, 2014). RIPK3 is essential for TNF-induced necroptosis but RIPK1 appears to be dispensable, at least in some settings. Other stimuli such as DNA damage can also trigger RIPK3-dependent necroptosis, either directly through adaptors, or indirectly, e.g. through expression of TNF. In this case, activation of RIPK3 occurs at a multi-protein complex, called the ripoptosome, and is dependent upon RIPK1 (Tait *et al.*, 2014).

Executing necroptosis

Following initial activation, the RIPK1–RIPK3 complex propagates a feed-forward mechanism leading to the formation of large filamentous structures dependent upon the RHIM-domain interactions between the two proteins (Li *et al.*, 2012). The generation of these structures and the simultaneously increase in RIPK3 activity strongly engage necroptosis, and modulating the extent of these filamentous structures and RIPK3 activity could possibly dictate the pro-killing functions of RIPK3 versus its roles in inflammation (Tait *et al.*, 2014). Given the stability of these complexes, it is also possible that they can contribute to cellular toxicity in the absence of RIPK3 activity. The pseudokinase mixed-lineage kinase domain-like (MLKL) was identified as a key downstream factor in RIPK3-dependent necroptosis; MLKL does not interfere with the necrosome assembly but is essential for cell death execution following its binding and phosphorylation by RIPK3 since MLKL ablation was found to cause resistance to RIPK3-dependent necroptosis (Murphy *et al.*, 2013). A mutant of MLKL that mimics the active RIPK3-phosphorylated form directly induces cell death, even in the absence of RIPK3, showing that MLKL is the key RIPK3 substrate in necroptosis (Murphy *et al.*, 2013).

Necrotic dying cells often display signs of mitochondrial dysfunction such as production of reactive oxygen species and swelling of mitochondria, ATP depletion, failure of Ca^{2+} home-

ostasis and perinuclear clustering of organelles, activation of proteases such as calpains and cathepsins, lysosomal rupture, and plasma membrane rupture (Golstein & Kroemer, 2007). The chronological and molecular order of these events remains elusive besides intensive studies on that matter. Most of the these events are not specific to necrosis (indeed some are shared with apoptosis) but "it is the possible accumulation of these events in an organized and programmed cascade of self-destruction that might define necrosis" (Golstein & Kroemer, 2007). Various studies proposed a role for either ROS or rapid depletion of cellular ATP in the execution of necroptosis, while others have implicated mitochondrial dysfunction as a key event in the necroptotic execution (Tait *et al.*, 2014). Lysosomal membrane permeabilization, apoptosis inducing factor and PARP have also been implicated (Long & Ryan, 2012). Supporting a role for mitochondria in necroptotic induction, it was found that following the necrosome formation, it translocates to mitochondrially associated ER membranes and two mitochondrial proteins were suggested to be downstream components of necroptotic signalling, leading to extensive mitochondrial fission and ROS production (Wang *et al.*, 2012). The relationships among Ca^{2+}, ATP and ROS can be complex, presumably because of the existence of self-destructive feed-forward loops (Golstein & Kroemer, 2007). Recently, it was found that MLKL can translocate to and permeabilize the plasma membrane following RIPK3 phosphorylation (Cai *et al.*, 2013). Necroptosis is an open field for intense research. Key remaining questions are whether the general mechanism of necroptosis execution is conserved between different cell types and/or following different stimuli and if ROS impacts on how the immune system reacts to a necroptotic cell, as has been observed in apoptotic cells (Tait *et al.*, 2014).

Necroptosis in cancer and GBM

Little has been reported about the role of necroptosis in cancer but several studies have advocated a possible link between necroptosis and tumor suppression. RIPK3- and caspase-8-double knockout mice exhibit enlarged spleens and lymph nodes and an abnormal accumulation of T cells in secondary lymphoid tissues, and a marked increase in T-cell numbers was also observed in RIPK1- and FADD-double knockout chimaeras, suggesting that a hyperproliferative disorder can occur when components of necroptosis signalling are altered (Long & Ryan, 2012). The truncated splice variant of RIPK3, RIPK3g, was reported to be upregulated in cancer tissues. *In vitro*, RIPK3g acts in a dominant negative manner to attenuate full-length RIPK3-mediated cell death, again implying that defective necroptosis may account for cancer progression (Long & Ryan, 2012).

Necrosis arising from chemotherapy treatment is not uncommon and could be further explored as an alternative pathway to eliminate apoptosis-defective cancer cells. Necrosis is correlated with RIPK3 protein level in multiple human and murine cancer cell lines, including a GBM cell line, T98G, whereas RIPK1 was expressed to similar levels in all cell types (Jiang *et al.*, 2011).

Crosstalk between different cell death subroutines

Cell death subroutines are neither isolated nor mutually exclusive and cell death comprises, in the vast majority of settings, a complex interplay between apoptosis, necrosis/necroptosis and autophagy. These types of cell death may all occur independent of, or simultaneously with each other: in some situations, a specific stimulus evokes only one of the processes while in other situations a combined cell death phenotype is observed (Long & Ryan, 2012). Stress conditions can result in the activation of multiple lethal mechanisms with different degrees of overlap, or a particular pathway may predominate over others which are only activated if the dominant pathway is attenuated (Long & Ryan, 2012). It is also important to note that a cell death-associated biochemical process can develop at a sublethal or transient level and do not always lead to the cellular demise (Galluzzi *et al.*, 2012); the severity of the damage and the stress suffered by the cells also determines if the cell dies, and by which cell death modality. In the following sections it will be made reference to some of the already known interactions between different cell death pathways.

Also, most often, pro-survival pathways are engaged along with the propagation of lethal signs, as will be discussed in *"Survival signalling and cell death resistance"*. The crosstalk between pro-survival and pro-death pathways determines if and by which subroutine the cell will eventually die.

It is important to keep in mind that the different cell death processes modulate each other by mutual inhibitory mechanisms but, being controlled by multiple feedback loops, may also serve as alternative backup death routes upon defect in the 'first-line cell death response' (Berghe *et al.*, 2015).

Interconnections between apoptosis and necroptosis

Apoptosis and necroptosis are deeply intertwined. Some apoptosis-inducing stimuli (the best-known example is TNF) can also initiate necroptosis, as mentioned in a previous section. The decision between apoptosis and necroptosis is dictated by caspase-8 activity: active caspase-8 suppresses necroptosis by cleaving substrates that include RIPK1, RIPK3 and CYLD. CYLD-mediated deubiquitylation of RIPK1 was reported to facilitate RIPK1 kinase activation and subsequent necroptosis induction (Berghe *et al.*, 2015). The pro-apoptotic/anti-necroptotic function of caspase-8 is regulated by specific interactions with c-FLIP. Caspase-8/caspase-8 homodimers engage apoptosis, while caspase-8/c-FLIP(L) heterodimers suppress both apoptosis and necroptosis. c-FLIP(L) binding to caspase-8 sufficiently limits caspase-8 activity to prevent apoptosis, but the remaining low levels of enzymatic activity are enough to cleave and inactivate RIPK1 and RIPK3. On the other hand, caspase-8 heterodimerization with an alternative form of c-FLIP, c-FLIP(S), prevents caspase-8 activity but favors necroptosis induction. From the available information, it appears that the amount of c-FLIP in cells protects them from extrinsic apoptosis and that the ratio c-FLIP(L) and c-FLIP(S) isoforms determines the sensitivity to necroptosis (Berghe *et al.*, 2015).

In vivo, necrotic cell death was found to replace apoptotic cell death for the loss of

interdigital cells in the mouse embryo when caspase activity was inhibited. Although delayed, digit separation was complete in surviving neonates in which apoptosis had been inhibited by drugs or prevented genetically (Chautan *et al.*, 1999).

Despite the recently revealed important roles for necroptosis in different settings, many questions remain to be answered: why is necroptosis so interconnected with apoptosis? Does necroptosis occur without caspase activity being inhibited? Are there other key regulatory steps/checkpoints?

As mentioned in the beginning of the *"Cell death"* chapter, some authors proposed necrosis/necroptosis as an ancestral cell death mechanism, with autophagy and apoptosis being added as dismantling mechanisms to facilitate the disposal of cell death corpses, and latter gaining autonomy and even exclusivity. This theory could help to explain the intricate connections between these cell death pathways, and why the inhibition of a certain type of cell death can result in the manifestation of another (Golstein & Kroemer, 2005).

Interplay between autophagy and other cell death pathways

Autophagy has been associated with stress adaptation and increased survival, but increased autophagosome formation is often coincident in cells that are dying. Excess activation of autophagy may represent a failed adaptative mechanism contributing to cell death. Numerous interconnections between autophagy and other cell death processes are already known, but how they interact for the determination of cell fate is far from being completely understood. Recent studies suggest that factors well known to regulate apoptosis also exert regulatory activity on factors that regulate autophagy and vice-versa. E.g., it has been shown that oligomerized caspase-8 may bind to the autophagosome leading to its activation, connecting apoptosis and autophagy; antiapoptotic Bcl-2 family members such as Bcl-2 and Bcl-x_L inhibit autophagy by binding to the BH3 domain of Beclin-1 and preventing its association with the class III PI3K complex; BNIP3, which can trigger apoptosis by sequestering antiapoptotic Bcl-2 proteins and promoting mitochondrial release of pro-apoptotic mediators may also stimulate mitophagy (Wu *et al.*, 2014). Once activated, apoptosis might suppress autophagy, since caspases may cleave and inactivate Beclin-1. Some ATG proteins may have autophagy-independent functions and may be converted from pro-autophagy to pro-death proteins by proteolytic cleavage; e.g., Atg5 is transformed in a pro-apoptotic truncation product (tAtg5) following calpain-dependent cleavage. tAtg5 promotes apoptosis by binding to and inhibiting antiapoptotic proteins such as Bcl-x_L; Atg5 may also affect extrinsic apoptosis pathways through interactions with the Fas-associated death domain (FADD) protein (Ryter *et al.*, 2014).

Recent data suggest that the oncogenic effect of Bcl-2 arises from its ability to inhibit autophagy but not apoptosis (Tekedereli *et al.*, 2013). Inhibition of Bcl-2 leads to autophagic cell death in MCF7 breast cancer cells. Since molecules that regulate apoptotic pathways seem to be able to either facilitate or block autophagy induction, it remains unclear whether autophagy and apoptosis are co-regulated or mutually exclusive processes (Ryter *et al.*, 2014).

The antiapoptotic protein c-FLIP, an endogenous inhibitor of caspase-8, can also negatively regulate autophagy by preventing the binding of Atg3 to LC3, which impairs LC3 processing (Ryter *et al.*, 2014).

Autophagy may then precede apoptosis or be simultaneously induced. Autophagy may also be induced upon inhibition of apoptosis, either to counteract necrosis/necroptosis or to coordinate with necrosis/necroptosis to promote cell death (Long & Ryan, 2012). Autophagy is commonly activated during necroptotic cell death but it remains unclear whether the process of autophagy acts as an effector or bystander of necroptosis (Ryter *et al.*, 2014). Some authors showed that autophagy is induced by necroptosis, raising the possibility that cellular stress during cell death may lead to the induction of autophagy. Limited autophagy may provide the cells with metabolic substrates to meet their energetic demands under stressful conditions and act as a pro-survival mechanism limiting cell death through apoptosis or necroptosis. For example, enhanced autophagy by spermidine inhibits loss of membrane integrity and release of chromatin protein high mobility group B1 (HMGB1), a biomarker of necrosis (Eisenberg *et al.*, 2009), but the molecular mechanism underlying this relationships remains elusive and controversial.

As a summary, apoptosis has been shown to regulate autophagy through Bcl-2-mediated sequestration or caspase-dependent cleavage of Beclin 1 but autophagy was also reported to impede apoptosis by degrading caspase-8. The causal relationship between autophagy and various forms of regulated or nonregulated cell death remains unclear. Autophagy can occur in association with necrosis-like cell death triggered by caspase inhibition. Autophagy and apoptosis have been shown to be coincident or antagonistic, depending on experimental context, and share cross-talk between signal transduction elements (Ryter *et al.*, 2014). Interrelationship between apoptosis, necrosis/necroptosis and autophagy is then likely to be extremely complex and the choice of route may vary under different circumstances.

Survival signalling and cell death resistance

Survival signalling allows the cell to overcome stressful or deleterious environments by inducing expression or availability of survival factors (Krakstad & Chekenya, 2010). Survival signalling is different from apoptosis resistance and may rescue cancer cells from death following otherwise lethal insults. Both apoptosis (and other cell death modalities) resistance and increased survival signalling are major regulators of cancer cell survival and both should be targeted to obtain therapeutic effects (Krakstad & Chekenya, 2010).

Many tumors bypass the requirement for survival factors signalling by engaging the PI3K/Akt pathway. PI3Ks are activated by receptor tyrosine kinases (RTKs) and are highly implicated in cancer cell survival (Masui *et al.*, 2013). As already discussed, PTEN, the cellular antagonist of PI3K, is frequently deleted in advanced tumors and the lost of functional PTEN, the phosphatase that dephosphorylates PIP3 to shut down Akt, implies that Akt remains active in those cells. Moreover, Akt, a serine/threonine kinase that mediates survival signals, is overexpressed in several malignancies, including GBM. All these alterations lead to

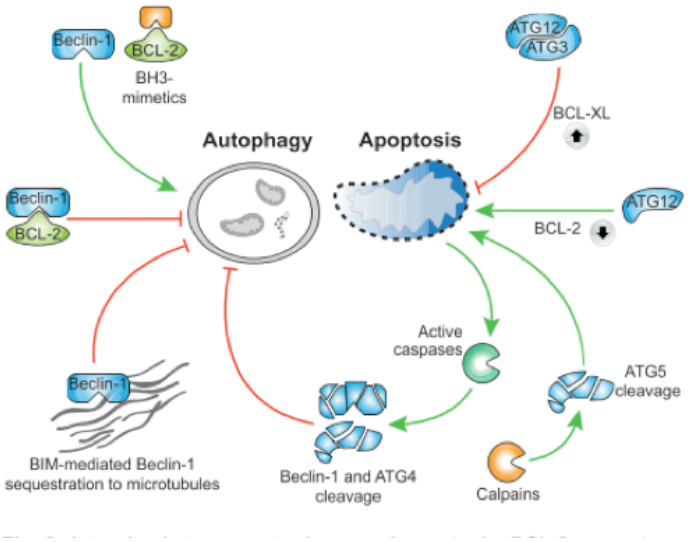

Figure 1.11: The figure represents the interplay between autophagy and apoptosis. Bcl-2 sequesters Beclin-1, thereby inhibiting autophagy that can be reversed by BH3 mimetics. Bim can sequester Beclin-1 onto microtubules, also inhibiting autophagy. In contrast, Atg12 conjugation to Atg3 enhances Bcl-x_L expression, thereby inhibiting apoptosis. Unconjugated Atg12 can act in a manner like BH3-only proteins and induce mitochondrial-dependent apoptosis. Calpain-mediated cleavage of Atg5 results in the liberation of a pro-apoptotic fragment of Atg5 that leads to mitochondrial outer membrane permeabilisation and cell death. Caspase-mediated cleavage of autophagy proteins inhibits autophagy. *From Tait et al. (2014).*

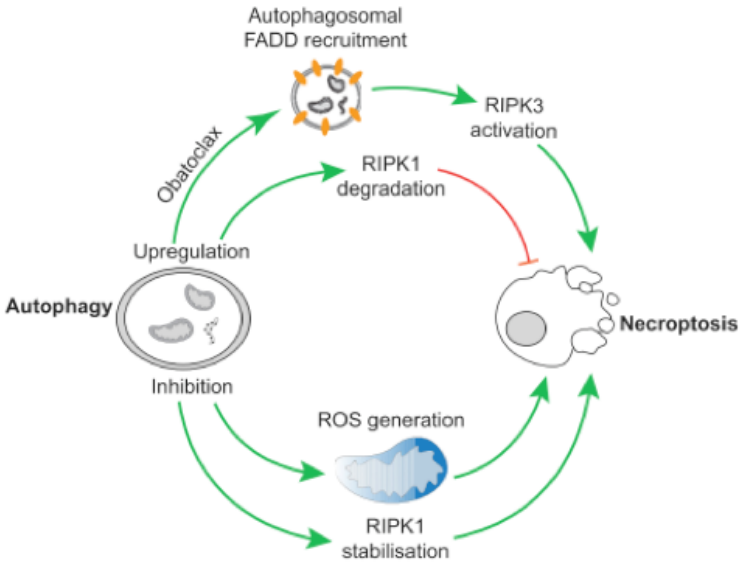

Figure 1.12: Upregulation of autophagy by Obatoclax can lead to FADD recruitment to autophagosomal membranes and RIPK3 activation resulting in necroptosis. Upregulation of autophagy can also lead to RIPK1 degradation and inhibition of necroptosis. Stimulation of autophagy, but inhibiting its completion, leads to RIPK1 stabilisation and ROS production,contributing to the induction of necroptosis. *From Tait et al. (2014).*

a 'constitutively active' survival signalling pathway that enhances the insensitivity of tumor cells to apoptosis induction (Igney & Krammer, 2002).

p65RelA-p50 transcription factor, NF-κB, is another important regulator of cell survival. NF-κB promotes cell survival by antagonizing the apoptotic pathway triggered by death receptors, at least in part through induction of expression of IAP proteins (Green & Evan, 2002). NF-κB can also induce the expression of anti-apoptotic members of the Bcl-2 family and repress expression of Bax. Like most potentially oncogenic signalling molecules, however, NF-κB also has a paradoxical ability to promote cell death in some instances (Green & Evan, 2002). An immunohistochemistry study of 70 GBMs on a tissue micro-array reported that 91.3% of the GBMs samples possessed activated NFκB that highly correlated with activated Akt levels (Krakstad & Chekenya, 2010). EGFRs and PDGFRs are the most common RTKs with intrinsic tyrosine kinase activity that are aberrantly expressed in GBMs. The Ras/Raf/MEK/ERK and PI3K/Akt/mTOR cascades are often activated by genetic alterations, either by mutations in upstream signalling molecules or by mutations in intrinsic pathway components. This has profound effects on proliferative, apoptotic and differentiation pathways, and deregulation of their components can contribute to malignant transformation, resistance to other pathway inhibitors, and chemotherapeutic drug resistance (McCubrey *et al.*, 2012).

The median survival of GBM patients with activated PI3K (n = 42/56) and Akt (37/56) was 11 months compared to 40 months in patients with lower activation levels of PI3K and Akt. Despite receiving only partial surgical resection and adjuvant radiotherapy, the patients with diminished PI3K and Akt activation had an extraordinarily high median survival of 40 months (Krakstad & Chekenya, 2010).

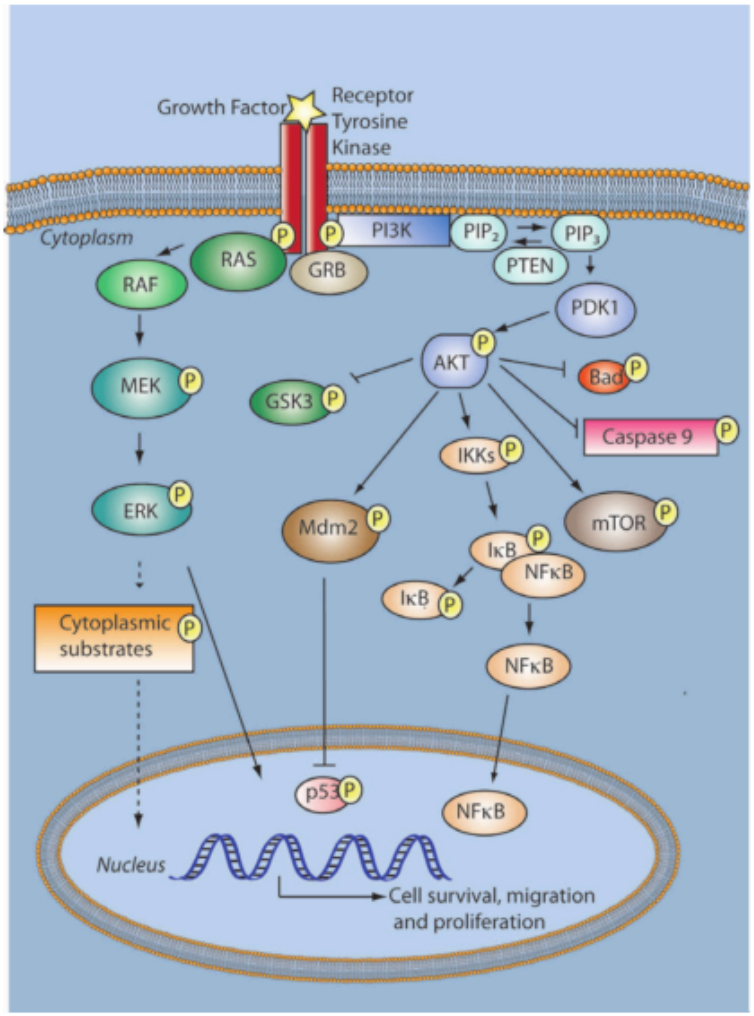

Figure 1.13: Hyperactive receptor tyrosine kinases in GBMs, e.g., EGFR, PDGFR, signal upon ligand binding or constitutive activation via Ras-MEK-ERK to mediate cell growth and angiogenesis and via PI3K/AKT to mediate survival. AKT phosphorylates multiple substrates that lead to release of survival factors or interference with the execution of apoptosis. These pathways are highly deregulated in GBMs. *From Krakstad & Chekenya (2010).*

The importance of understanding survival signalling and cell death: a matter of life and death

In *"A matter of life and death"*, Green and Evan propose that cancer cells arise and are maintained through the rare simultaneous acquisition of two cooperating conditions: deregulated cell proliferation and suppressed apoptosis (Green & Evan, 2002).

Normal somatic cell proliferation and tissue homeostasis are sustained by an absolute need for external mitogens and sensitivity to inhibition by growth-suppressive signals. Frequently, oncogenes mimic normal growth signalling, allowing tumor cells to generate their own growth signals, being then liberated from dependence on exogenous signals and on stimulation from their normal tissue microenvironment (Hanahan & Weinberg, 2000). However, deregulation of cell proliferation also requires acquisition of refractoriness to normal growth inhibitory signals. In their landmark review "The Hallmarks of Cancer," Hanahan and Weinberg reviewed the main mechanisms limiting effectiveness of anti-growth signals that must be acquired by incipient cancer cells in order for them to thrive, many of these mechanisms relying on the pRb signalling circuit. Disruption of the pRB pathway liberates transcription factors allowing cell proliferation and renders cells insensitive to antigrowth signals (Hanahan & Weinberg, 2000).

But even after having acquired independence from external mitogens and not being responsive to inhibitory growth signals, "pre-cancer cells" still have another difficulty to bypass. Excessive growth-stimulating signals emanating from growth factor receptors or overexpressed oncogenes are sensed by the cell and will trigger a safeguard response that results in cell death through apoptosis in normal situations (Van Meir *et al.*, 2009). Many, perhaps all, mechanisms that drive cell proliferation have the potential to trigger, or sensitize a cell to apoptosis (Evan & Littlewood, 1998). Examples include activation of the Ras/Raf pathway, deregulated expression of c-Jun and promiscuous activity of the E2F G1 progression transcription factors (Green & Evan, 2002). Activated Raf and Ras oncoproteins can trigger permanent growth arrest and the apoptosis suppressor Bcl-2 has a growth inhibitory action (Green & Evan, 2002).

Apoptosis is now widely accepted as a prominent tumor-suppression mechanism. Elimination of cells bearing activated oncogenes by apoptosis may represent the primary means by which such mutant cells are continually removed from the body's tissues (Hanahan & Weinberg, 2000). Mutations in the *myc* oncogene resulting in the activation of cell proliferation, require a second mutation to inhibit the apoptosis machinery so that tumor promotion can proceed efficiently (Youle & Strasser, 2008). In order to overcome limitations in their growth, tumor cells will then have typically genetically inactivated pro-apoptotic pathways or/and activated the overexpression of genes that can promote cell survival (Van Meir *et al.*, 2009).

Suppression of apoptosis also brings the catastrophic potential of promoting mutation and genome instability since apoptosis is the major avenue for disposal of mutated or damaged cells (Green & Evan, 2002). Blocking that disposal will have consequences in genome plasticity and contribute to tumor progression as shifting selective pressures shape the evolu-

tion of the tumor and an increased heteregenity and adaptability are progressively selected. It is likely that different cells within the tumor acquire different mechanisms of apoptosis resistance, and even multiple resistance mechanisms may develop in a single tumor cell (Igney & Krammer, 2002).

Since there are other mechanisms besides apoptosis for cell death execution, and with which apoptosis is intertwined, we suggest extending the expression "need of suppressed apoptosis" as a requisite for tumors to thrive, to "suppressed/deregulated cell death". However some questions arise from this assumption: do tumors develop resistance to other cell death modalities? Are there common events that cause apoptosis inhibition that also lead to inhibition of other cell death mechanisms? Or, on the other hand, does apoptosis inhibition leave the door open for other cell death modalities to take place, and these could be exploited as potential therapeutic targets? Would apoptosis inhibition make cells potentially more vulnerable to the execution of other cell death mechanisms? Or all these things perhaps may happen during the natural evolution of tumors?

As most, if not all of the tumors, GBM display aberrant proliferation and apoptosis signalling. As already discussed, growth factor pathways that stimulate cell proliferation are constitutively activated in malignant gliomas, due to overexpression/ genetic amplification of growth factor receptor genes or gene mutations that send constitutive growth signals. Also, the PI3K pathway can be constitutively activated when the positive signalling molecules are mutated and signal constitutively, or when the negative regulators are lost through gene loss or mutation, like PTEN. Another contributor to cell proliferation in gliomas is c-Myc, a transcription factor that drives the expression of cell cycle promoters and blocks the transcription of cell cycle inhibitors (Van Meir *et al.*, 2009).

Despite pursuing aggressive treatment, GBM patients still have dismal prognosis; GBMs resistance to radiation and chemotherapy invariably leads to disease relapse. Contrasting with other types of cancers like some types of leukemia or gastrointestinal tumors, therapeutic changes in the treatment of GBM (with only one new therapy to be approved in more than a decade - bevacizumab) had little impact on overall survival and produced a very modest benefit. The development of new efficacious therapies for GBM is delayed by the complex and heterogeneous nature of the disease, with the set back of having to pass the blood brain barrier. The employed therapies fail to achieve cell death of all tumoral cells, and face the emergence of resistant cells. Although there is a deeper knowledge of the genetic alterations involved in GBM and multiple attractive molecular targets were identified, this knowledge has not yet been transformed into an useful tool for patients; many of these were not successfully targeted or did not yield the expected result or benefit when translated into the clinic. Green and Evan point out the following in their paper *"A matter of life and death"*: "Arguably the greatest problem with the conventional therapeutic approach is that it fails to correct the tumor's specific anti-apoptotic lesion(s) and instead employs a cruder strategy of simply loading up the pro-apoptotic side of the equation in the hope of exceeding the apoptotic threshold in the tumor cells before it happens in too many normal ones" (Green & Evan, 2002).

Deregulated cell proliferation and suppressed apoptosis/cell death may be the common ancestry/base of all the tumors, including GBM, and it is essential to overcome these two problems as early as possible in the course of tumor evolution in order to achieve effective therapy. The disruption of apoptosis during tumor evolution promote drug resistance and consequent therapy failure. All forms of cancer therapy risk selecting for resistance, a problem compounded by the plasticity of the tumor cell genome and the most effective therapeutic strategy is likely to consist of a coordinate attack on several targets, potentiating cell death execution (Green & Evan, 2002). By the very nature of the cancer platform, a cancer cell would be most sensitive to the restoration of the apoptotic pathways that it has specifically suppressed. Although there could be an enormous variety of ways to restrict apoptosis due to the genetic plasticity of cancer cells and variety of selective pressures that challenge them, different data do indicate that tumor evolution favors adoption of specific and restricted pathways of apoptosis suppression. E.g., Bcl-x_L level correlated with resistance to cell death in a panel of 60 cell lines challenged with different chemotherapeutics (Green & Evan, 2002). Unfortunately, we have little idea of the repertoire of anti-apoptotic mechanisms in human cancer, including GBM. This ignorance has been preventing us from achieving more effective therapies as "it may be only by targeting the specific anti-apoptotic lesion(s) in any tumor cell that we will be able to ensure its rapid and specific demise" (Green & Evan, 2002). It is urgent to explore the anti-apoptotic mechanisms used/developed by cancer cells and the connections between different cell death mechanisms, in order to be able to manipulate them and prompt the execution of cell death either by apoptosis or through an alternative mechanism that compensates for apoptosis resistance. We need to understand how altered survival signalling interferes with cell death execution in order to counteract survival signalling and favor cell death. Survival signalling and cell death blockage both contribute to tumor progression and deregulated cell proliferation; we should find the links and common points where to interfere: eliminating these two conditions should shut down cancer cells! However, the complex network and intricate interplay between survival/cell proliferation/cell death alert us for the difficulty of this task, underscoring the importance of achieving a comprehensive understanding of this complexity in order to confidently (and efficiently) manipulate cell death mechanisms for the benefit of patients.

Parallel to clinical trials and development of new drugs with specific targets, basic research is needed to address too many unanswered questions. Shared information and organized databases for this basic research with common goals could not only help to improve GBM treatment but also favor important discoveries that would ultimately translate into progression in the treatment of different cancers. The way cell death is controlled is central to understand cancer itself: to better understand cancer will arm us with important knowledge to therapeutically explore its weaknesses. Due to tumor's complex nature and redundancy of mechanisms facilitating cell survival/ inhibition of cell death, combinatorial approaches targeting several molecular pathways will likely yield the most effective treatments.

Why edelfosine and other ATLs

Edelfosine and other ATLs may prove effective against GBM. In fact, there are already some reports that showed significant tumor remissions in experimental rat gliomas treated with erucylphosphocholine and erufosine at relatively low doses (these two drugs having advantage over other ALPs because of their superiority in crossing the BBB and accumulate in the brain tissue) (Van Blitterswijk & Verheij, 2013). In glioma cells both compounds enhanced radiation induced apoptosis and eradication of clonogenic tumor cells through Akt inhibition (Handrick *et al.*, 2006; Rübel *et al.*, 2006). However there is no clinical data available yet for these compounds. Peña and coworkers found that subcutaneous gliomas did not show enhanced response to radiation after treatment with perifosine despite inhibition of Akt (Peña *et al.*, 2006). Because only one dose schedule was used in this study, it remains uncertain whether an increased radiation response by perifosine might be obtained at optimal (i.e. clinically relevant) dose scheduling (Van Blitterswijk & Verheij, 2013).

One of the best-characterized APL targets is Akt, a serine/threonine kinase that regulates multiple cellular processes, including apoptosis, proliferation, differentiation and metabolism. The PI3K-Akt signalling cascade promotes cell survival by phosphorylating and inactivating pro-apoptotic proteins as already described. However, few clinical studies of combination of perifosine and radiotherapy are available. Perifosine in combination with mTOR inhibitors effectively killed platelet-derived growth factor driven mouse glioblastomas and clinical trials for this combination in neuroblastoma are underway (Van Blitterswijk & Verheij, 2013). The combination of perifosine with the mTOR inhibitor temsirolimus is also ongoing (NCI, 2015); phase I trial data demonstrated that perifosine combined with temsirolimus was well tolerated and showing relatively favorable results (Zentaris, 2012). There is also a report showing miltefosine as a sensitizer of paclitaxel therapy in glioblastoma (Thakur *et al.*, 2013).

ErPC and ErPC3 compounds would be in theory more attractive for GBM treatment since besides their effects at relatively low dosis and reduced toxicity they can cross the BBB; however perifosine and miltefosine may also be able to penetrate the brain to some extent under certain conditions (Van Blitterswijk & Verheij, 2013). After the advent of ALPs as candidate drugs for this type of cancer, technical advances were made in drug formulation, e.g., lipidic nanovesicles have been developed and tested by different groups with success in the delivery of the drugs and achieving the necessary concentration in the brain tissue (Estella-Hermoso De Mendoza *et al.*, 2011; Thakur *et al.*, 2013).

Different ATLs, and in particular edelfosine, have been shown to selectively induce apoptosis in tumor cells. Although there is a high number of publications investigating the effects of these compounds on multiple systems, frequently the results could not be reproduced by different groups or even produced conflicting data; the reason(s) for the discrepancy might be the variety of the systems that were employed, the use of different methodologies, or may even be correlated with the lipidic nature of the compounds. As already discussed, ether lipids are able to affect many different cellular processes since they interfere with plasma membrane-associated proteins thus altering many signalling pathways. They exert complex

effects on lipid metabolism and lipid-dependent signal transduction pathways and may not only affect the composition and signalling pathways at the plasma membrane level, but also at different organelles. The produced results are likely to vary greatly depending on specific characteristics of the cells and how they deal with the imposed effects. On a more positive note, it is also worth to note the commonly reported effects induced by edelfosine and other ether lipids about their potent antitumoral effect in many systems and ability to directly activate the apoptotic machinery in some cancer cells, while sparing normal ones.

Based on the above background, it would be beneficial to further study edelfosine (and other ATLs) mechanism of action. Which effects are common to all affected cells, the role of those effects in the killing action of the drug and which are the death triggers induced by edelfosine that force the cell to commit suicide are points that need further investigation. It is important to understand which are the cell death triggers and executioners activated by edelfosine; to find if cell death triggers are absent or how they have been blocked/avoided in cells that are not affected by the drug, or if the triggers can be pulled but execution of cell death is blocked/ avoided by defects in cell death pathways, or counteracted by survival signalling. Understanding differences in the incorporation levels of the drug could help us to gain insight into its mechanism of incorporation. Incorporation of the drug was shown to be essential for its deleterious effects but how it occurs is far from being understood. Besides the mechanism(s) of incorporation, it could be useful to compare sensitive and resistant cells. However, a too general approach comparing groups of sensitive *versus* resistant cells, although appealing, brings the danger of not going into enough detail to consider all the specific factors for each cell; the reason why a particular cell is resistant to edelfosine may be completely different from the reason another one is also resistant. Besides their similarities, we must not forget the differences and specificities of each system. Some characteristics may have a relation with the sensitivity or resistance, because they are paralleled selected or developed, while not being its cause.

Many questions are there to be answered: which triggers is edelfosine pulling? Are they present or not in both sensitive and resistant cells? And the executioners: are they present and can work in both cells? Due to the dynamic nature of tumoral evolution and the complex network and redundancy of pathways, we may find that certain triggers are blocked, that executioners are blocked, that both are blocked, or that their effects are completely counteracted by survival signalling, and most likely these findings will differ from one cell type to another. The aim is to find the common reasons for resistance and the common reasons for sensitivity, and learn how to manipulate them. Lipid rafts/death receptors, endoplasmic reticulum, and mitochondria have all been shown to participate in edelfosine-induced cell death in different cell systems. Edelfosine and its pleiotropic effects offer a canvas of interactions to explore, and works as a model of different pressures exerted on tumor cells. The diversity of its effects is acting on the diversity of GBM cells: what can we learn from that? This basic research model brings the chance to find out how different mechanisms work and are controlled, by modulating critical signal transduction pathways involved in phospholipid metabolism, proliferation, cell death and survival.

2
Objectives

A better understanding of the mechanism of action of the drug, the distinct underlying signalling pathways and the cross-talk between them, as well as of how resistance mechanisms develop, will help us to design new approaches to trigger and modulate cell death processes of critical importance in the treatment of GBM and other tumors.

With this hope in mind and the genuine desire to contribute to this field of research, building knowledge for the rational development of improved therapies, the project of this thesis involves the next three major goals:

A) Analysis of the action of edelfosine and other antitumor lipids (ATLs) on the induction of cell death in glioblastoma cells

B) Analysis of signalling pathways leading to cell death and cell survival following edelfosine treatment and their interactions

C) Analysis of putative mechanisms of resistance to edelfosine

In order to accomplish these goals, the following more detailed objectives have been pursued:

1) Detailed characterization of the type of cell death (apoptosis, necrosis, autophagy) induced by edelfosine in the U118 glioblastoma cell line

The putative involvement of mitochondria will be evaluated as a major underlying mechanism in the anticancer action of ATLs against solid tumors.

2) Relative role of cell death versus survival signalling routes in the U118 cell line

Particular attention will be paid to the expression and function of a number of survival signaling routes, including ERK and NF-κB, in comparison to apoptosis signaling routes (death receptor downstream signalling, mitochondrial related apoptotic promoting molecules).

3) Analysis of the impact of the executed cell death modality in overall survival, and possible implications for development of resistance in the U118 cell line

4) Development of a resistant cell line, from the U118 cell line, through repeated exposure to edelfosine.
Comparative analysis of some characteristics such as drug incorporation and expression of proteins involved in cell death and cell survival pathways in order to gain insight into possible mechanisms of resistance to edelfosine.

5) Effect of ATLs in the induction of cell death and cell cycle arrest in different glioblastoma cell lines

The effect of distinct ATLs (including edelfosine, perifosine, miltefosine, erufosine, erucylphosphocholine and oleylphosphocholine) on a number of human glioblastoma cell lines (A172, T98G, SF268 and GOS-3), will be tested by measuring apoptotic DNA degradation and other changes in the cell cycle through cell cycle analysis by flow cytometry. MTT tests to assess overall cellular viability will also be performed.
Distinct ATL analogues (including edelfosine, perifosine, miltefosine, erufosine, erucylphosphocholine and oleylphosphocholine) will be assayed to determine the most active compound against GBM cell lines.
The expression and activation status of proteins involved in a number of survival and cell death signalling routes will be compared between different cell lines.

6) Potentiation of edelfosine action - interfering with cell death execution and survival signalling in different glioblastoma cell lines

The action of edelfosine will be potentiated by inhibiting prominent survival signalling routes characterized in the above sections as well as by potentiating cell death signalling processes.

Modulation of Fas/CD95-mediated apoptosis through increased expression of the death receptor Fas/CD95 in the T98G cell line and Bcl-x_L inhibition in the SF268 and GOS-3 cell lines will be strategies used to increase edelfosine-induced cell death.

3

Effect of edelfosine in the induction of cell death in the U118 glioblastoma cell line

Cell proliferation and viability were assessed by the MTT (3-(4,5-dimethylthiazol-2-yl)-2,5-diphenyltetrazolium bromide) assay, which is based on the conversion of this tetrazolium salt to a purple colored product - formazan - by metabolically active cells. The precipitated formazan is dissolved using acidic isopropanol and the absorbance values are read using a spectrophotometer. The more metabolically active cells, the more formazan is formed and higher absorbance values are obtained. This constitutes a rapid, simple and affordable assay to evaluate cellular proliferation (Sylvester, 2011).

In some cases the MTT assay might also allow to evaluate cellular viability. If the absorbance values obtained after drug exposure are lower than the values of the control at the beginning of the experiment (all the conditions having the same number of seeded cells), that means there are less metabolically active cells after the treatment, either because they died, or because the drug is affecting cellular metabolic activity (MTT and other tetrazolium dyes depends on the cellular metabolic activity due to NADPH flux).

After testing cellular proliferation and/or viability with MTT assays for edelfosine, perifosine, miltefosine, erucylphosphocoline (ErPC), erufosine (ErPC3) and oleoylphosphocholine (OlPC), we found that edelfosine was the ether lipid that had a stronger effect in the U118 cell line, drastically reducing MTT metabolism. Although all the ether lipids tested diminished cellular proliferation, since all of them have lower absorbance values than the control after 48 hours, edelfosine did it more potently at a lower concentration.

Besides affecting cellular proliferation, edelfosine also reduced cellular viability, since the absorbance levels of the treated cells were lower then the levels of the untreated cells at the beginning of the experiment, meaning that not also the cells did not proliferate, but that there

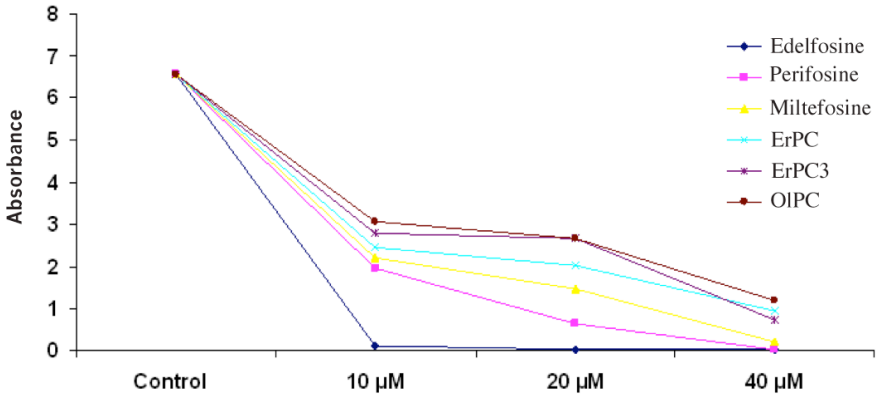

Figure 3.1: A representative MTT assay performed 48 hours after treatment for each compound at the indicated concentrations in the U118 cell line. Control absorbance values were read in untreated cells at time zero of the experiment.

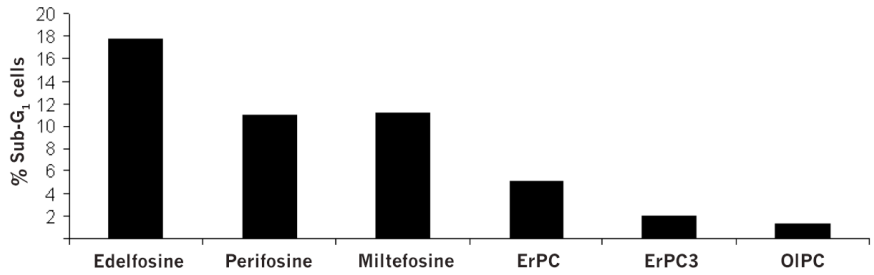

Figure 3.2: U118 cells were treated with 20 μM of the indicated ATL for 24 h. Apoptosis (% Sub-G_1 cells) was evaluated using flow cytometry cell cycle analysis. Data are expressed as means of experimental triplicates and are representative of two independent experiments.

were less viable cells after the treatment, or that alive cells had lower ability to metabolize MTT. Perifosine was the second most effective drug affecting cellular proliferation, followed by miltefosine (Figure 3.1). Although none of the ether lipids induced a strong apoptotic response in U118 cells, as assessed by measuring DNA degradation using flow cytometry, we found that edelfosine also induced the highest DNA degradation at a lower dose among the ATLs tested (Figure 3.2).

Based on the strong inhibition of metabolism and induced cell death observed by flow cytometry and under the microscope, we decided to further analize the effects of the ether lipid edelfosine in the U118 cell line.

Edelfosine promotes rapid cell death in U118 human glioma cells

We found that incubation of the U118 human glioblastoma cell line with 10 μM edelfosine induced a rapid cell death response. Concentration-dependent assays showed that 10 μM was the optimum drug concentration for the inhibition of cell proliferation and induction of cell death (Figure 3.3), but interestingly edelfosine at <1 μM rather promoted cell proliferation (Figure 3.4).

Cells rapidly lost their ability to metabolize MTT following incubation with 10 μM edelfosine. There was a reduction of about 50% in the ability of U118 to metabolize MTT within 3 h of drug treatment, and ~80% of the cells were unable to metabolize MTT after 24 h incubation (Figure 3.5).

This rapid cell death was easily visualized by phase contrast microscopy, revealing dramatic morphological changes in U118 cells following edelfosine treatment. These changes started as early as 150 min-3 h upon drug addition and included rounding-up of the cells and loss of cell adhesion. Using a time-lapse videomicroscopy analysis we could follow the temporal morphological changes during the drug treatment, including cell swelling and apparently necrotic death (Figure 3.6, lower; and Supplementary Video U118).

A mixture of swelled cells, cells showing membrane bubbling, and cells lacking plasma membrane integrity could be observed, these latter being the majority of the cells after 9 h of treatment (Supplementary Video U118).

The loss of nuclear membrane integrity was also detected by DAPI staining (Figure 3.7), and confirmed by sytox green staining directly applied into the culture medium after 24 hours of edelfosine treatment (Figure 3.8). The release of DNA in the culture medium following membranes rupture was evident and these "balls of thread", that could be seen with the naked eye, quickly disappeared after the addition of DNase to the culture medium (not shown).

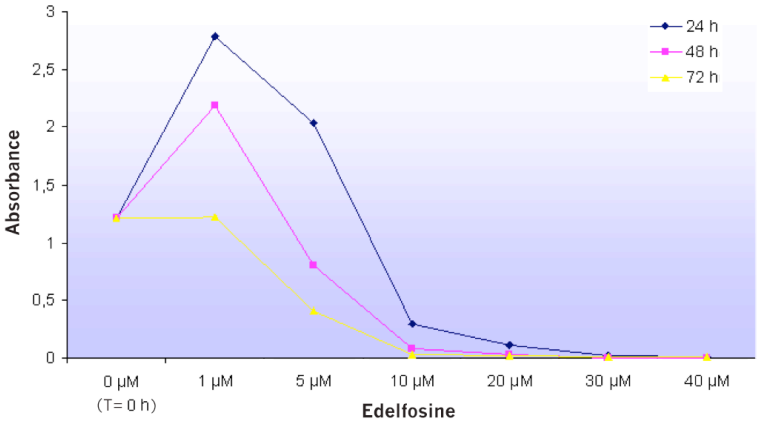

Figure 3.3: U118 cells were treated with the indicated concentrations of edelfosine for 24, 48, and 72 h. Absorbance values after MTT assay were registered and compared to values obtained for untreated cells at time 0 of the experiment (T= 0 h). Data are expressed as means of experimental triplicates.

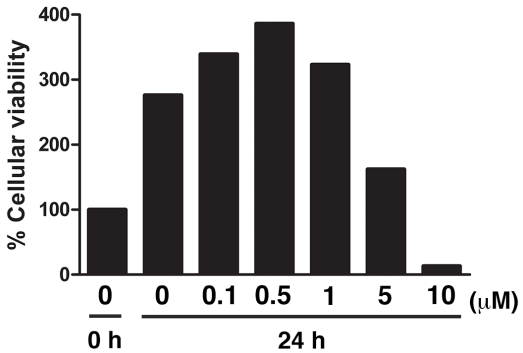

Figure 3.4: U118 cells were incubated in the absence or presence of the indicated concentrations of edelfosine for 24 h, and then analyzed by MTT assay. Cells at time 0 were also measured by MTT assay. Data are expressed as means of experimental triplicates and are representative of two independent experiments.

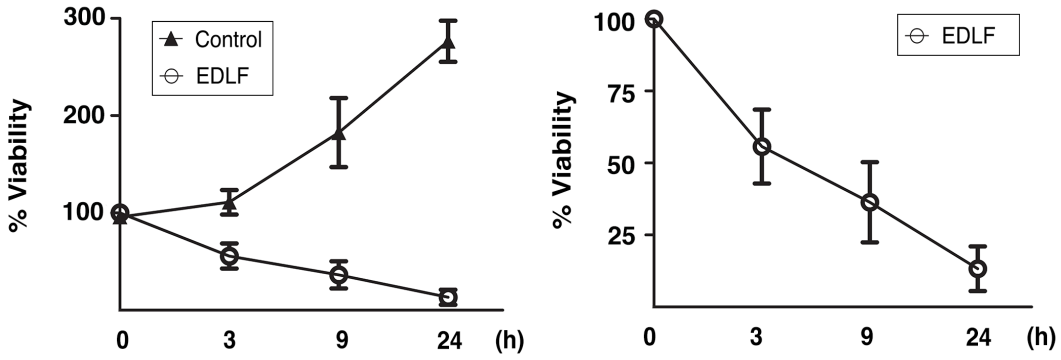

(a) (b)

Figure 3.5: (a) U118 cells were incubated in the absence (Control) or presence of 10 μM edelfosine (EDLF) for the indicated time points and then analyzed by MTT assay. Data are expressed as mean ± SD of at least three independent experiments, each one performed in triplicate. (b) The plot on the right shows only the measurements for edelfosine (EDLF) for an easier appreciation of changes.

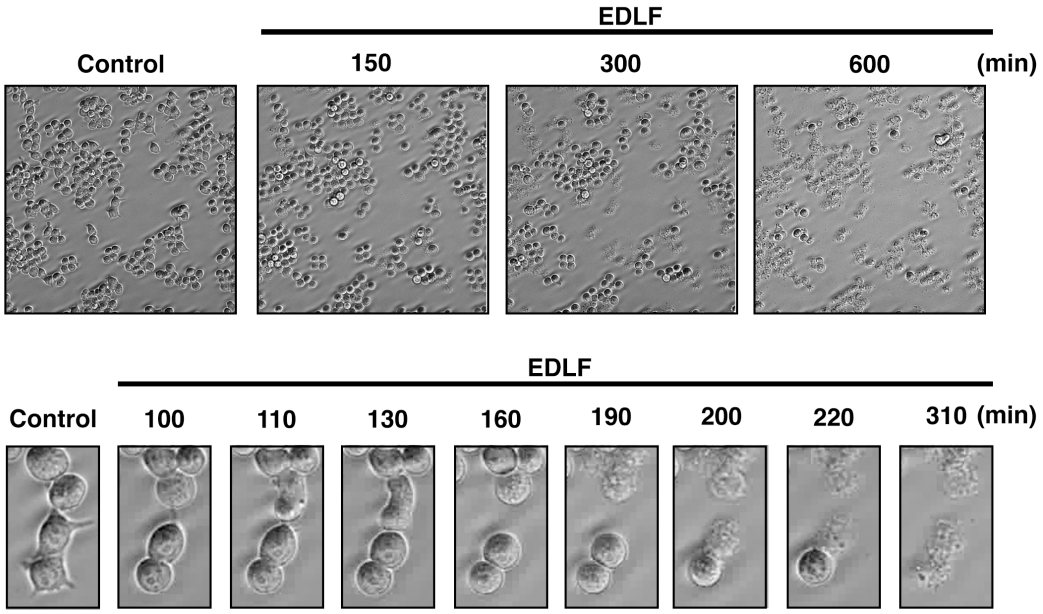

Figure 3.6: Selected phase-contrast time-lapse videomicroscopy frames (magnification, 10x) from U118 cells untreated (Control) or treated with 10 μM edelfosine (EDLF) at the indicated times. Lower panels show cells undergoing explosive death. The elapsed time in minutes are indicated on top of each frame.

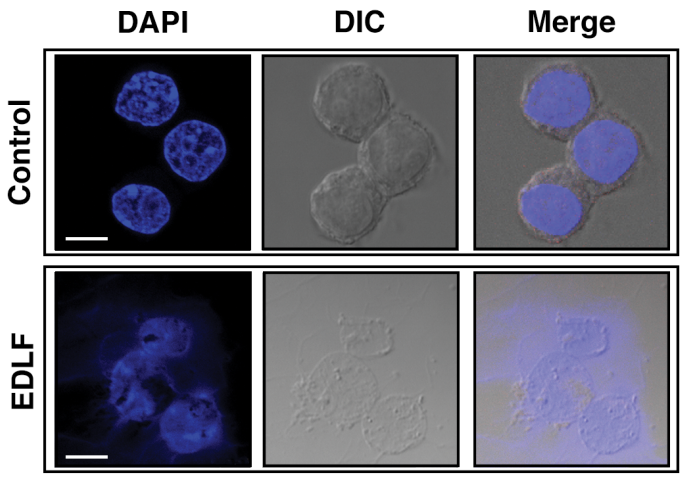

Figure 3.7: Cell morphology of U118 cells untreated (Control) and treated with 10 μM edelfosine (EDLF) for 24 h. Differential interference contrast microscopy (DIC) and DAPI staining shows loss of plasma and nuclear membrane integrity after 24 h treatment. Bar, 10 μm.

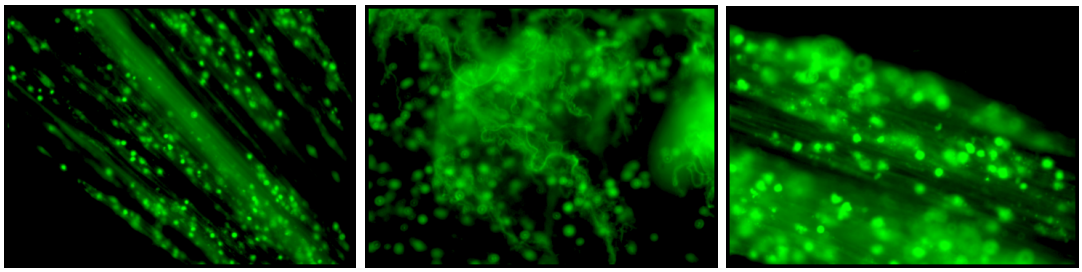

Figure 3.8: Sytox green staining of U118 cells treated with 10 μM edelfosine for 24 h, evidencing plasma and nuclear membrane rupture of cells, leading to DNA dispersion in the culture medium.

Induction of apoptosis in edelfosine-treated U118 cells

Because edelfosine has been reported to promote a potent and typical apoptosis response in a wide number of tumor cells, we analyzed whether the killing activity of the ether lipid on U118 cells was mediated through apoptosis. Following cell cycle analysis, we found that ~20% of the U118 cells treated with 10 μM edelfosine for 24 h displayed DNA degradation, as assessed by the percentage of cells in the Sub-G_1 region of cell cycle (Figure 3.9).

Edelfosine treatment led to the typical DNA laddering pattern by agarose gel electrophoresis, a hallmark of apoptosis, indicating internucleosomal DNA degradation (Figure 3.10a). In addition, edelfosine induced caspase-3 activation, as assessed by the appearance of the activated cleaved caspase-3 form, and the cleavage of poly(ADP-ribose) polymerase (PARP), a major caspase-3 substrate (Figure 3.10b).

Furthermore, preincubation with the pan-caspase inhibitor z-VAD-fmk completely blocked the edelfosine-induced apoptosis response (Figure 3.11a), but was unable to inhibit the overall cell death response exerted by edelfosine in U118 cells (Figure 3.11b) as well as the changes in cell morphology. These results indicate that edelfosine is able to promote a caspase-dependent apoptosis response in U118 glioma cells, but this apoptosis response is a rather minor cell death response that cannot account for the massive cell death detected by microscopy and MTT assays.

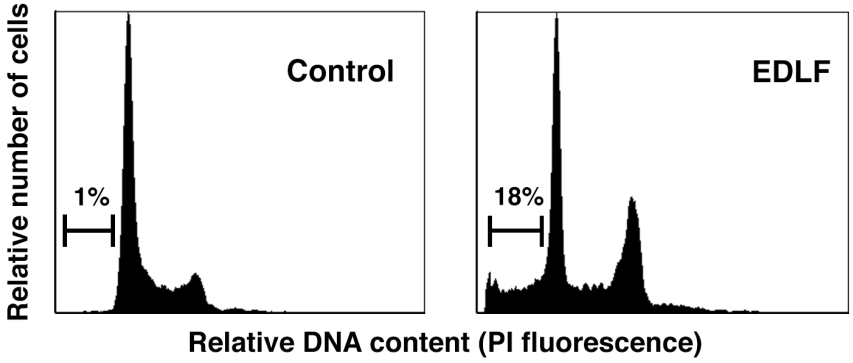

Figure 3.9: Representative cell cycle analysis histograms of untreated U118 cells (Control) and U118 cells treated with 10 μM edelfosine (EDLF) for 24 h. The percentage of apoptotic cells, identified as the Sub-G_1 population by flow cytometry, is indicated in each histogram.

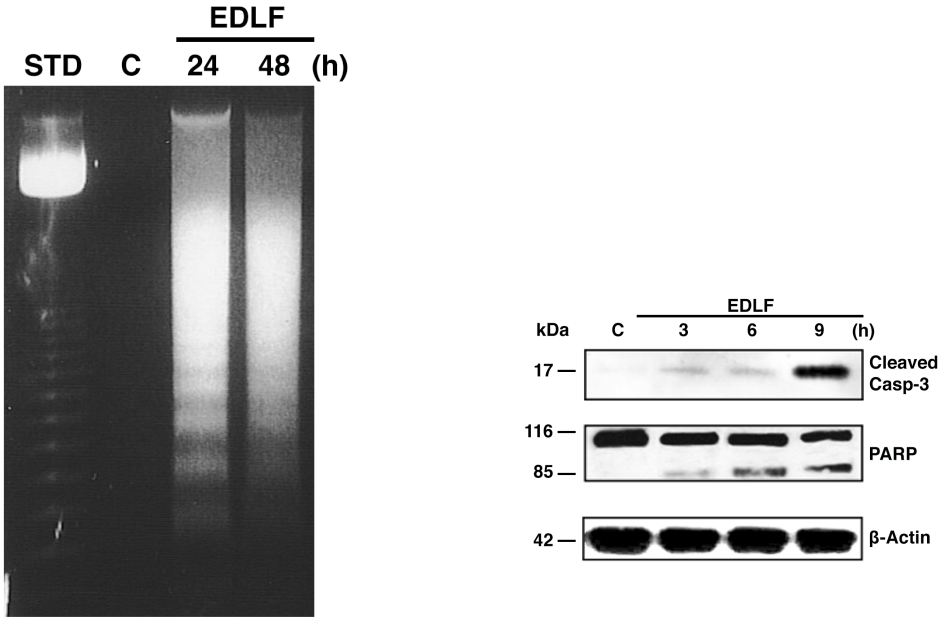

(a) (b)

Figure 3.10: (a) U118 cells treated with 10 μM edelfosine (EDLF) for 24 and 48 h were assayed for DNA fragmentation in agarose gels. Control untreated cells (C) were run in parallel in the same gels. A 123-bp DNA ladder was used as standard (Std). (b) Cells were untreated (Control, C) or treated with 10 μM edelfosine (EDLF) for the indicated times, and then analyzed by immunoblotting using specific antibodies against cleaved caspase-3 and PARP. Immunoblotting for β-actin was used as an internal control for equal protein loading in each lane.

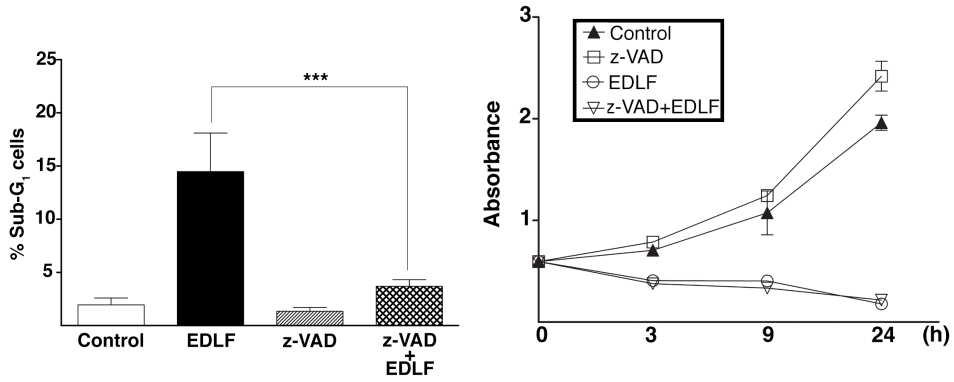

(a) (b)

Figure 3.11: (a) Cells were preincubated without or with 100 μM pan-caspase inhibitor z-VAD-fmk (z-VAD) for 1 h, and then incubated in the absence (Control) or presence of 10 μM edelfosine (EDLF) for 24 h. Cells were analyzed by flow cytometry to evaluate apoptosis as the percentage of Sub-G_1 population in cell cycle analysis. Data shown are means $\pm$ SD of three independent experiments. $***$ P<0.001 EDLF vs. z-VAD+EDLF, Student's t test. (b) MTT assays were conducted after culturing U118 cells without or with 100 μM pan-caspase inhibitor z-VAD-fmk (z-VAD) for 1 h, and then incubated in the absence (Control) or presence of 10 μM edelfosine (EDLF) at the indicated time points. Data are expressed as means $\pm$ SD of three independent experiments, each one performed in triplicate.

Induction of autophagy in edelfosine-treated U118 cells

In order to verify if another type of cell death could be involved in the execution of U118 cells after edelfosine treatment, and because some anticancer drugs, including temozolomide, induce autophagy in glioblastoma, we examined the ability of edelfosine to elicit an autophagic response in U118 cells. First, by using the acidotropic agent acridine orange, which has been employed as an early stain to monitor the development of acidic vesicular organelles (AVOs) during autophagy (Paglin *et al.*, 2001; Lefranc & Kiss, 2006), we found an intense vital red fluorescence staining of U118 cells after edelfosine treatment (Figure 3.12a).

The lysosomotropic agent acridine orange is used to detect acidic compartments because it moves freely across biological membranes as a weak base when uncharged, but its protonated form accumulates in acidic compartments, forming aggregates that fluoresce bright red (Traganos & Darzynkiewicz, 1994). Thus, these data show that edelfosine promotes the generation of acidic vacuoles in U118 cells. A major hallmark of autophagy lies in the conversion of microtubule-associated protein 1 light chain-3B (LC3B) from free form cytosolic LC3B-I (approximately 16 kDa) to the LC3B-II phosphatidylethanolamine conjugated form (approximately 14 kDa), which is tightly bound to the membrane of the autophagosome (Klionsky, 2014), a critical step in autophagosome formation. We found that edelfosine treatment led to the rapid conversion of LC3B-I to LC3B-II after a 3-h treatment, reaching its maximum following 24-h treatment (Figure 3.12b).

The formation of LC3B-II, and thereby of autophagosomes, was evidenced by both Western blot (Figure 3.12b) and confocal microscopy (Figure 3.13), this latter approach showing

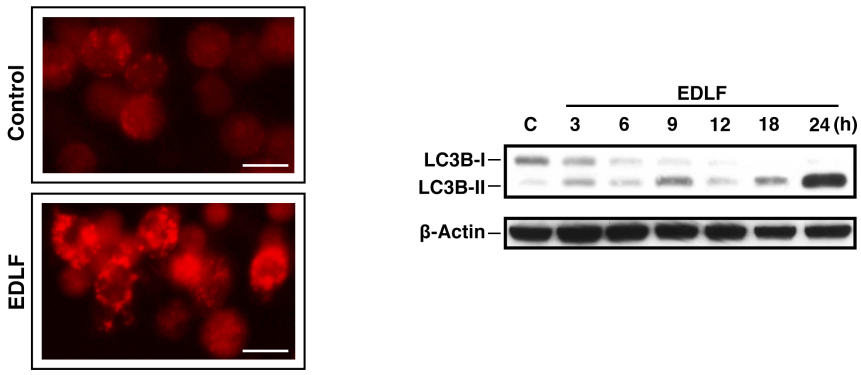

(a) (b)

Figure 3.12: (a) Cells untreated (Control) and treated with 10 μM edelfosine (EDLF) for 24 h were stained with acridine orange and analyzed by fluorescence microscopy (bar, 10 μm). (b) Western blot analysis of LC3B-I/II in cells untreated (Control, C) or treated with 10 μM edelfosine (EDLF) for the indicated times. Immunoblotting for β-actin was used as an internal control for equal protein loading in each lane.

the fluorescent punctuate pattern of LC3B-II associated with autophagosomal membranes.

To confirm that edelfosine was indeed increasing the autophagic flux (autophagic vesicle formation and clearance by fusion with lysosomes), and not only interfering with organelles clearance, we used bafilomycin A1, which blocks fusion between lysosomes and autophagosomes and therefore leads to an accumulation of autophagosomes. We observed an increase in the level of the LC3B-II form in cells treated with bafilomycin A1 in comparison with untreated control cells as well as with those treated with edelfosine alone (Figure 3.14), indicating ongoing autophagic flux and the blockade of the fusion between autophagosomes and lysosomes.

However this inhibition of the late stages of autophagy hardly affected the apoptotic response (Figure 3.15), with a weak increase in apoptosis that was not statistically significant. In addition, pretreatment of U118 cells with bafilomycin A1 did not increase overall viability upon edelfosine incubation, with no significant change in MTT reduction (Figure 3.16) or propidium iodide (PI) incorporation. The scarce protective effect on MTT assays (Figure 3.16) could be due to the weak increase in apoptosis response.

In addition, we also found that pretreatment of U118 cells with additional autophagy inhibitors, including 20 nM chloroquine or 200 nM wortmannin, did not affect edelfosine-induced cell death response as assessed by examining cell morphology under the microscope and flow cytometry (results not shown).

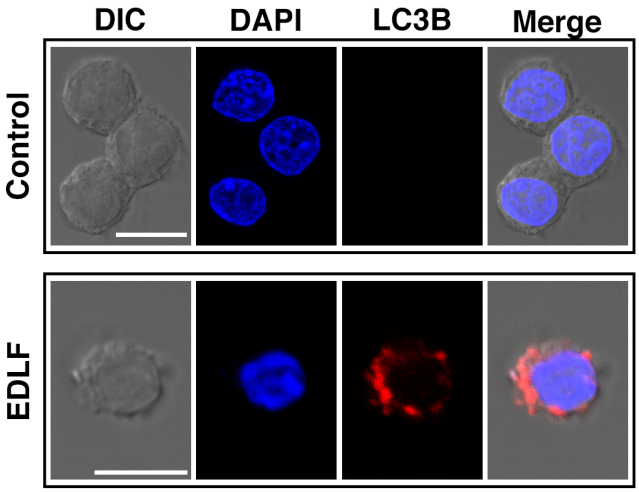

Figure 3.13: Confocal immunofluorescence microscopy of LC3B punctae (red fluorescence) in U118 cells following treatment with 10 μM edelfosine (EDLF) for 3 h. Nuclei were labeled with DAPI (blue fluorescence). Bar, 10 μm.

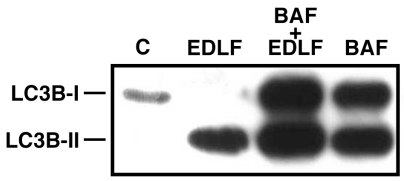

Figure 3.14: Western blot analysis of LC3B-I/II in U118 cells treated with 10 μM edelfosine (EDLF), 25 nM bafilomycin A1 (BAF), or both (BAF+EDLF) for 24 h. β-Actin was used as a control for protein loading.

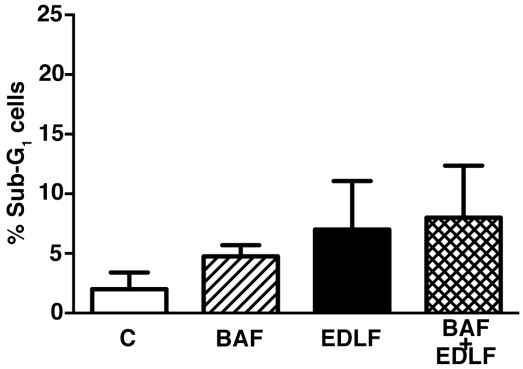

Figure 3.15: Cells were preincubated without or with 25 nM bafilomycin A1 (BAF) for 1 h, followed by incubation in the absence (Control, C) or presence of 10 μM edelfosine (EDLF) for 6 h, and then analyzed by flow cytometry to evaluate apoptosis. Data shown are means $\pm$ SD of three independent experiments.

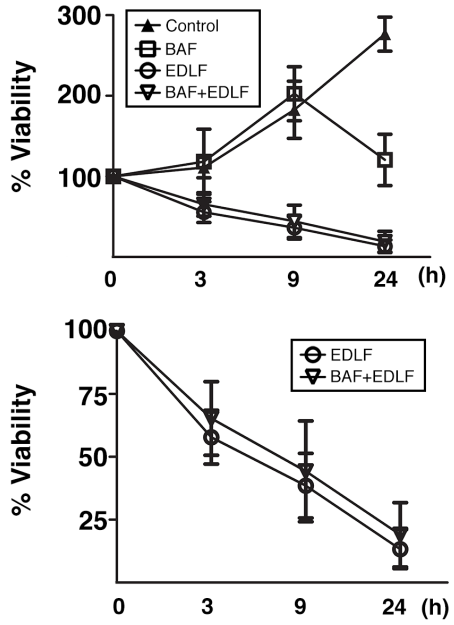

Figure 3.16: MTT assay of U118 cells untreated (Control) or treated with 25 nM bafilomycin A1 (BAF) for 1 h, and then incubated in the absence or presence of 10 μM edelfosine (EDLF) at the indicated time points. Data are expressed as means ± SD of at least three independent experiments, each one performed in triplicate. The lower plot shows only the measurements for edelfosine and bafilomycin A1+edelfosine-treated cells for an easier appreciation of changes.

Edelfosine induces mainly a necrotic type of cell death in U118 cells

The above results showed that the cell death induced by edelfosine in U118 cells was not primarily mediated by apoptosis or autophagy. In contrast, the morphological changes observed in Figure 3.6, 3.7 and 3.8 apparently corresponded to a necrotic cell death. This was further assessed by the high presence of non-viable cells measured by trypan blue staining and PI exclusion assay in non-permeabilized cells following edelfosine treatment, whereas only a minor proportion of these cells corresponded to cells with a Sub-G_1 DNA content (Figure 3.17).

These data indicated that most of the drug-treated cells became rapidly permeable to PI and unable to metabolize MTT, but did not show apoptotic features. Thus, edelfosine treatment induced a quick loss of cellular membrane integrity, a hallmark of necrotic cell death, and the percentage of cells that lost membrane integrity after 24-h treatment, detected by Trypan blue exclusion method, was similar to the percentage of non-viable cells detected by the MTT assay (Figure 3.17).

To further analyze the contribution of apoptosis and necrosis to cell death, and to exclude the hypothesis that a secondary necrosis was occurring, we carried out time-course experiments using an annexin V/PI assay, including staurosporine as a positive control for

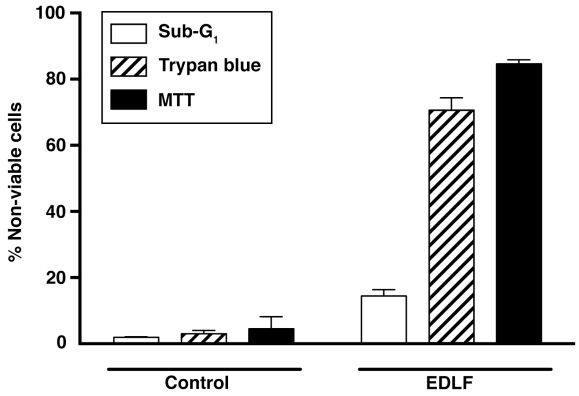

Figure 3.17: Percentage of non-viable cells in cells untreated (Control) or treated with 10 μM edelfosine (EDLF) for 24 h, as determined by three different methods: cell cycle analysis (Sub-G_1 population measured by flow cytometry), Trypan blue method, and MTT assay (cells unable to metabolize MTT).

induction of apoptosis and phosphatidylserine exposure. An increasing percentage of cells stained positive for both annexin V and PI following edelfosine treatment (Figure 3.18), whereas the apoptosis-inducer staurosporine prompted a high percentage of annexin V^+/PI^- cells (Figure 3.18). After a 24-h treatment, most of the edelfosine-treated cells were annexin V^+/PI^+ (Figure 3.19).

In contrast to edelfosine, which hardly induced apoptosis at early incubation times (Figure 3.20A), staurosporine induced a high apoptotic response, as assessed by an increase in the annexin V^+/PI^- cell population (Figure 3.20A) and by an increase in the hypodiploid Sub-G_1 cell population by cell cycle analysis (Figure 3.21). Plasma membrane permeability was also confirmed by the release of soluble cytosolic LDH into the culture medium at early incubation times following edelfosine addition, although LDH release showed a slower kinetics than that of PI incorporation in non-permeabilized cells (Figure 3.20B). A weak increase in hypodiploid Sub-G_1 phase (apoptosis) was detected at a slower rate, after 6-9 h of treatment (Figure 3.20B). Taking together, these data indicate a loss of cellular membrane integrity, a hallmark of necrotic cell death, and the onset of this type of cell death was detected long before the onset of apoptosis in edelfosine-treated cells. Thus, the necrotic response induced by edelfosine in U118 cells was a rapid and direct one, and not a consequence of secondary necrosis that usually takes place in the late phases of apoptosis.

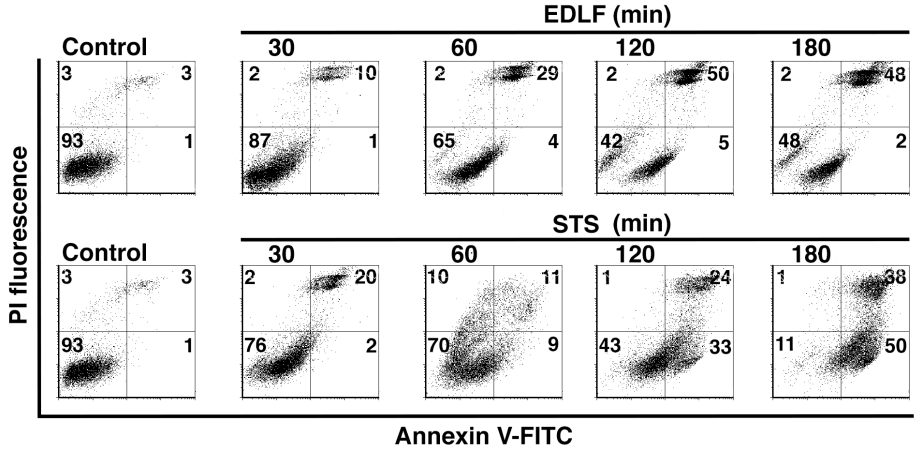

Figure 3.18: Annexin V/PI staining was analyzed from cells untreated (Control) and treated with 10 μM edelfosine (EDLF) or with 0.5 μM staurosporine (STS) at the indicated time points. Lower right quadrant shows annexin V^+/PI^- cells (early apoptotic cells). Upper right quadrant represents annexin V^+/PI^+ cells (necrotic or late apoptotic cells). Percentages of cells in each quadrant are indicated. Results are representative of three independent experiments.

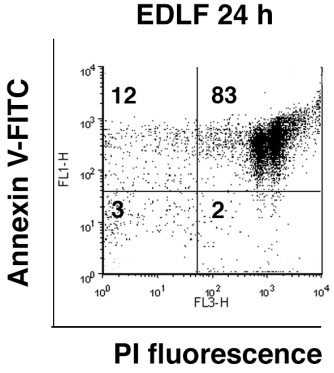

Figure 3.19: Annexin V/PI staining was analyzed from cells treated with 10 μM edelfosine (EDLF) for 24 h. Upper right quadrant represents annexin V^+/PI^+ cells (necrotic or late apoptotic cells). Results are representative of three independent experiments.

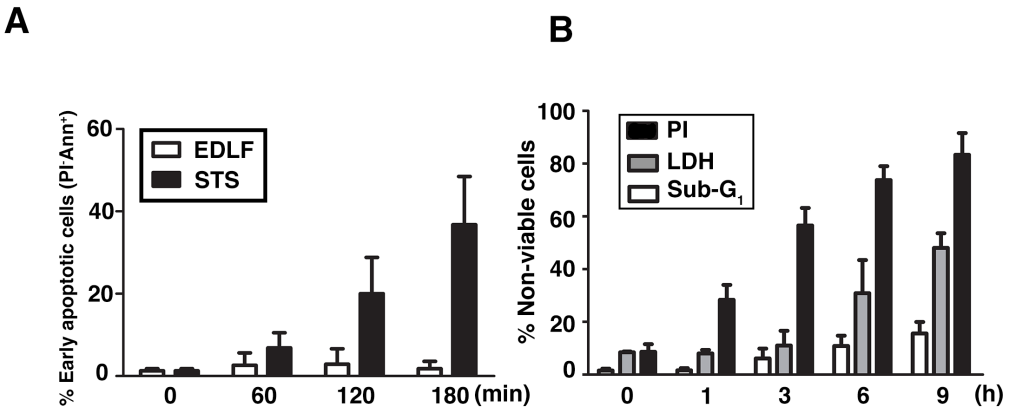

Figure 3.20: (A) Quantification of early apoptotic cells (annexin V^+/PI^- cells) at the indicated time points, following 10 μM edelfosine (EDLF) and 0.5 μM staurosporine (STS) treatments. (B) Cells were incubated with 10 μM edelfosine (EDLF) for the indicated periods of time, and then non-viable cells were measured using PI incorporation in non-permeabilized cells (necrosis), LDH release assays, and cell cycle analysis (quantification of apoptotic/Sub-G_1 population). Data shown are means ± SD of three independent experiments.

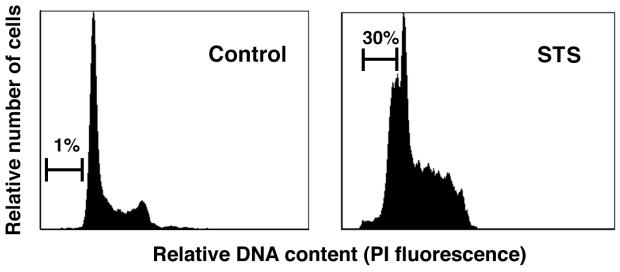

Figure 3.21: Representative cell cycle analysis histograms of untreated U118 cells (Control) and U118 cells treated with 0.5 μM staurosporine (STS) for 4 h. The percentage of apoptotic cells, identified as the Sub-G_1 population by flow cytometry, is indicated in each histogram.

ROS and $\Delta\Psi_m$ in apoptosis and necrosis

Opening of the mitochondrial permeability transition pore has been demonstrated to induce depolarization of the transmembrane potential ($\Delta\Psi_m$), release of apoptogenic factors and loss of oxidative phosphorylation (Ly *et al.*, 2003). It has been seen that in some models, loss of $\Delta\Psi_m$ may be an early event in the apoptotic process, while in other cases it may not be an early requirement for apoptosis but rather a consequence of the apoptotic signalling pathway (Ly *et al.*, 2003).

The apoptotic response triggered by edelfosine has been found to require the participation of mitochondrial-mediated signalling, this latter acting as the critical event that leads eventually to the demise of the tumor cell. Edelfosine-induced apoptosis involves disruption of the mitochondrial transmembrane potential and release of mitochondrial cytochrome c to the cytosol in a number of hematological cancer cells (Gajate *et al.*, 2000; Gajate & Mollinedo, 2007). Edelfosine induced swelling in isolated mitochondria, indicating an increase in mitochondrial membrane permeability, and it has been shown to accumulate in mitochondria in different tumor cells in a cell-type dependent way. Edelfosine has also been found to accumulate in the endoplasmic reticulum of solid tumor cells, promoting an endoplasmic reticulum stress response (Nieto-Miguel *et al.*, 2007; Gajate *et al.*, 2012; Bonilla *et al.*, 2015). *In vitro* and *in vivo* evidences suggest that edelfosine-induced apoptosis in solid tumor cells is mediated through the ER stress response and that its pro-apoptotic effect requires a mitochondrial-related step to eventually promote cell death (Nieto-Miguel *et al.*, 2007; Gajate *et al.*, 2012; Bonilla *et al.*, 2015).

Considering that apoptosis is an ATP-dependent process, depletion of ATP by a massive mitochondrial dysfunction would favor necrosis. Although the permeability transition pore would eventually cause the rupture of the mitochondrial outer membrane and release of apoptotic death effectors, these events could also be a downstream consequence of the onset of necrosis (Li *et al.*, 2007).

ROS is a well described mediator of necrosis, involved in the propagation and execution phases of necrotic cell death, directly or indirectly provoking damage to proteins, lipids and DNA, which culminates in disruption of organelle and cell integrity (Festjens *et al.*, 2006). It has been well documented that besides activating caspase-9, ROS could induce necrosis although in other context, intracellular ROS elevation was a downstream consequence of the opening of the permeability transition pore (Li *et al.*, 2007). A recent study has demonstrated that the kinase RIPK, which is essential for TNF-induced necrosis, can inhibit ATP/ADP exchange on mitochondrial membranes by a direct interaction with the adenine nucleotide translocase (ANT), thereby causing mitochondrial dysfunction and cell death (Temkin *et al.*, 2006). Thus mitochondrial alterations may constitute a rate-limiting step of necrotic cell death, at least in some instances.

We studied whether these actions were involved in U118 edelfosine-induced cell death by double staining experiments, using HE (non-fluorescent) that becomes ethidium (Eth, red fluorescent) after its oxidation via ROS, and $DiOC_6(3)$(green fluorescent), a cationic probe

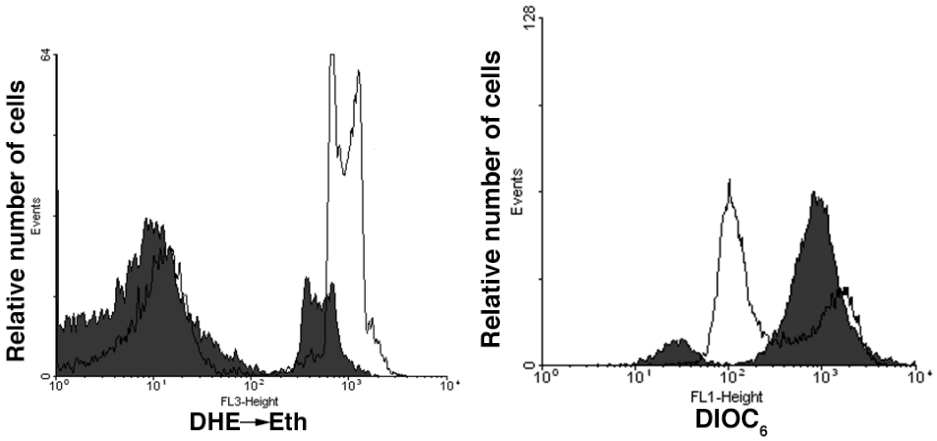

(a) (b)

Figure 3.22: (a) U118 cells treated with 10 μM edelfosine for 24 h were analyzed for ROS generation (DHE -> Eth^{high}) by flow cytometry (clear histogram). Control untreated cells were run in parallel (thick histogram). (b) U118 cells treated with 10 μM edelfosine for 24 h were analyzed for $\Delta\Psi_m$ disruption ($DiOC_6(3)^{low}$) by flow cytometry (clear histogram). Control untreated cells were run in parallel (thick histogram).

that accumulates into mitochondria as a function of its potential. We could observe a very significant increase in ROS starting shortly after edelfosine treatment, and its levels were even increased during longer periods of exposure to edelfosine, as shown in Figure 3.22a, after 24 h of exposure to edelfosine. We also found loss of mitochondrial transmembrane potential following edelfosine treatment (Figure 3.22b), which has been described as a requirement for the killing effect of this ether lipid in some solid tumors.

In this case, we found cytochrome c and AIF were released from mitochondria and that caspase-9 and caspase-3 activation occurred at a similar pace, starting after 3 hours of exposure to edelfosine (Figure 3.23) and showing maximum activation at 9 h.

However, the majority of the cells with high levels of ROS also lost mitochondrial membrane potential shortly after edelfosine treatment (Figure 3.24); and the clear increase in the population of cells with $\Delta\Psi_m$ disruption that can be seen using flow cytometry analysis occurs following the detection of released mitochondrial proteins (AIF and cytochrome c), making it difficult to evaluate which event started earlier, and if in this case loss of $\Delta\Psi_m$ is required for apoptosis or if it is rather a consequence of the already started process. On the other hand, as already mentioned, it is possible that the activation of the intrinsic apoptotic pathway may be consequence of a necrotic process, as ROS are clearly increased after a short period of exposure to edelfosine and they may be responsible for damage to mitochondria. In that case, damage of mitochondria by ROS could lead to rupture of the mitochondrial outer membrane and release of the apoptotic death effectors. Oxidative damage affects replication and transcription of mtDNA and results in a decline in mitochondrial function which in turn leads to enhanced ROS production. Mitochondria are the major producer of ROS in cells and the bulk of mitochondrial ROS is generated at the electron transport chain, but in addition to being generated during cellular metabolism in mitochondria, ROS can be produced

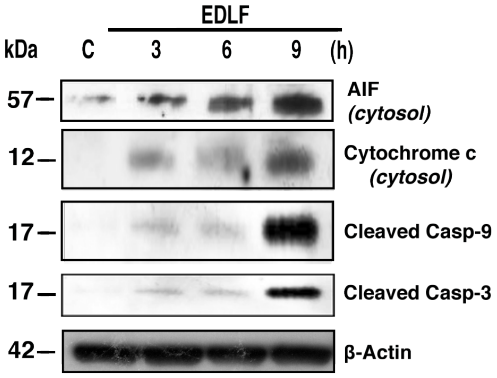

Figure 3.23: U118 untreated cells (C), and cells treated with 10 μM edelfosine for the indicated times, were analyzed by immunoblotting using specific antibodies against cleaved caspase-3, and cleaved caspase-9. Cytosolic extracts, excluding the mitochondrial fraction, were analyzed using specific antibodies against AIF and cytochrome c. Immunoblotting for β-actin was used as an internal control for equal protein loading.

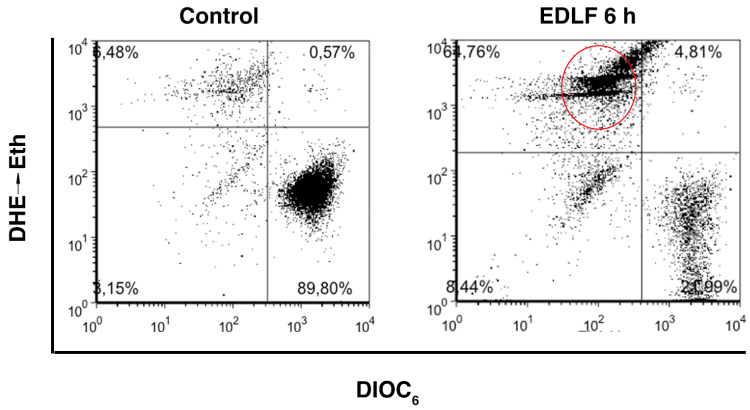

Figure 3.24: U118 cells treated with 10 μM edelfosine for 6 h were analyzed for ROS generation ((DHE -> Eth)^{high}) and $\Delta\Psi_m$ disruption ($DiOC_6(3)^{low}$) by flow cytometry. Control untreated cells were run in parallel. Treated cells with $\Delta\Psi_m$ disruption and ROS generation are indicated in the upper left quadrant.

in response to different environmental stimuli by a number of cytosolic enzymes (Cui *et al.*, 2012). Once they are produced, ROS react with lipids, proteins, and nucleic acids causing oxidative damage to these macromolecules.

We can infer an early mitochondrial disfunction is taking place after edelfosine treatment, since MTT reduction is strongly affected shortly after exposure to edelfosine (Figure 3.5). Depletion of ATP by this massive mitochondrial dysfunction could be favoring necrosis in U118 cells, and making apoptosis a rather secondary effect, resulting from the release of apoptogenic factors from the already damaged mitochondria. Colocalization of the ether lipid with mitochondria within one hour of exposure to edelfosine was also observed in the U118 cells (Figure 3.25).

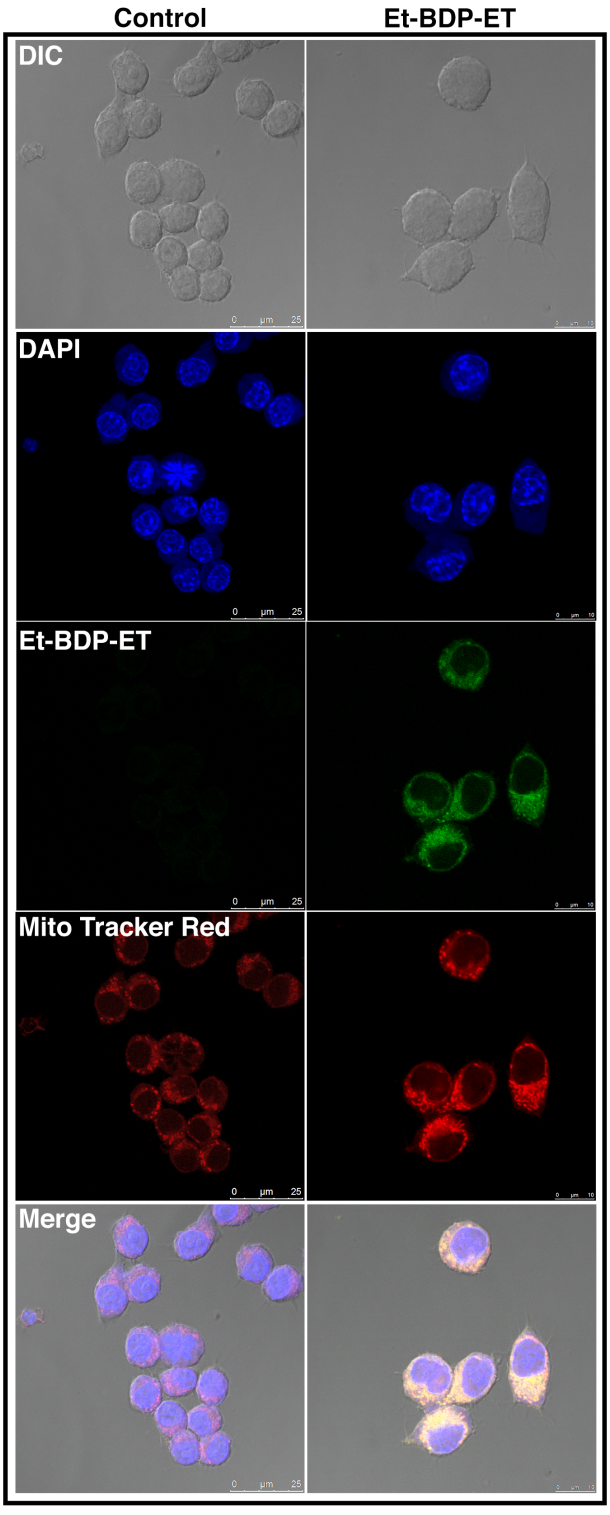

Figure 3.25: Control untreated cells or U118 cells treated with 10 μM edelfosine analogue conjugated with the fluorophore BODIPY for 1 h were stained with DAPI and 100 nM Mito Tracker red. Areas of colocalization between mitochondria and Et-BDP-ET are shown in yellow in the merge panels. Images are representative of two independent experiments.

Lysosomal membrane permeabilization

Lysosomal membrane permeabilization (LMP) is induced by a plethora of distinct stimuli including reactive oxygen species, lysosomotropic compounds with detergent activity, as well as some endogenous cell death effectors such as Bax (Boya & Kroemer, 2008). We wanted to assess lysosomal permeabilization in U118 cells, since massive LMP was shown to often result in cell death with a necrotic appearance. Also, hexadecylphosphocholine (miltefosine) was described as an agent capable of inducing cell death through a lysosomal pathway characterized by partial lysosomal rupture and cathepsin B relocation (Paris *et al.*, 2007). Using Lysotracker dye, a lysosomotropic fluorochrome, we found weaker fluorescence shortly after edelfosine treatment, when analyzing the cells by flow cytometry (Figure 3.26).

Decreased lysotracker fluorescence may reflect LMP and/or an increase in lysosomal pH, meaning that this method is not absolutely specific for LMP (Boya & Kroemer, 2008). Acridine orange (AO), as mentioned before, is a lysosomotropic metachromatic fluorochrome that can also be used to assess the functional state of lysosomes. When excited with blue light, AO emits red fluorescence at high concentrations (when present in acidic compartments, such as lysosomes) and green fluorescence at low concentrations (when present in the cytosol and the nucleus) (Boya & Kroemer, 2008). This pattern can be clearly seen in Figure 3.27, where untreated U118 cells were stained with acridine orange.

AO-loaded cells manifest reduced red fluorescence and increased green fluorescence after LMP (Antunes *et al.*, 2001). We found reduced red fluorescence (Figure 3.28, pale orange shade in the histograms) and increased green fluorescence (not shown), as soon as one hour after exposure to edelfosine, with AO staining, corroborating the results obtained with lysotracker. Time-course analysis of changes in the red fluorescence are represented in Figure 3.28.

The increase in acridine orange red fluorescence started a few hours later, in a subpopulation of the analyzed cells (bright red shade in the histograms, starting to increase in the 3-h treatment histogram), accompanying the beginning of autophagy as determined by other techniques and referred to in a previous section (*Induction of autophagy in edelfosine-treated U118 cells*).

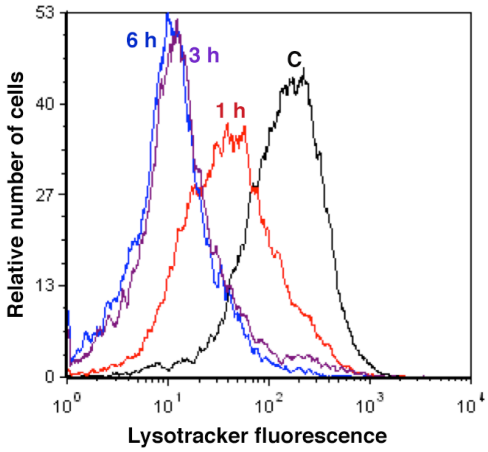

Figure 3.26: Control untreated cells (C, black curve) or U118 cells treated with 10 μM edelfosine for 1, 3, or 6 h (red, purple, and blue curves, respectively) were analyzed by flow cytometry following incubation with lysotracker; treated cells had decreased fluorescence intensity.

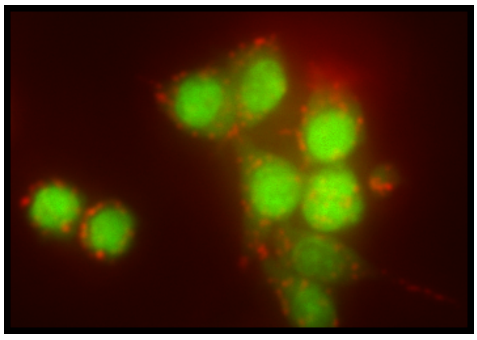

Figure 3.27: U118 untreated cells stained with acridine orange. The image results from merging the microscopy photographs obtained for red and green fluorescence.

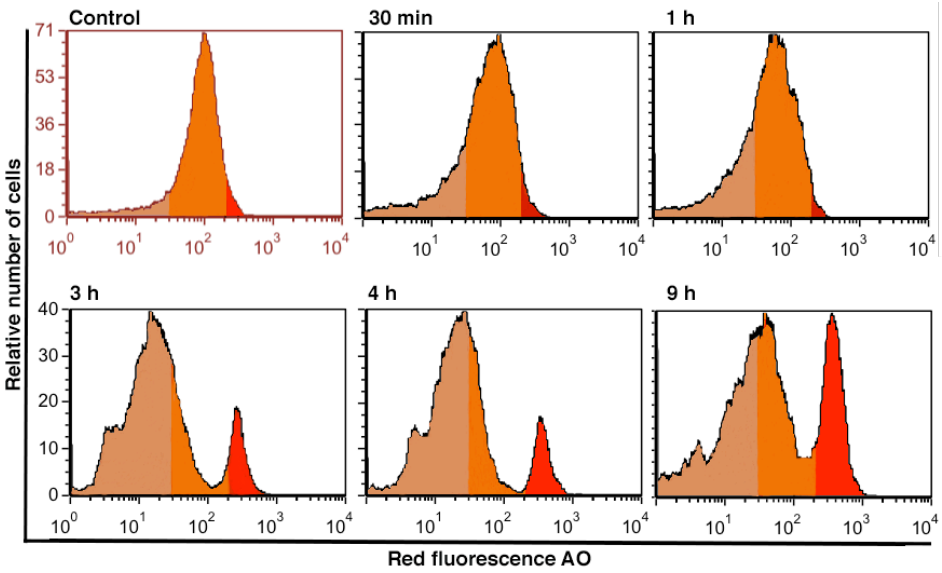

Figure 3.28: Control untreated cells (Control), or U118 cells treated with 10 μM edelfosine for the indicated times, were incubated with acridine orange and red fluorescence was analyzed by flow cytometry.

Calcium

Because a connection between Ca^{2+} homeostasis and necrosis has been suggested, and an increase in intracellular calcium concentration was found to be a trigger of lysosomal exocytosis in some cells (Rodríguez *et al.*, 1997; Ono *et al.*, 2001) we next examined whether calcium was involved in edelfosine-induced cell death by measuring intracellular calcium levels using the calcium indicator dye Fluo-4 AM. Incubation of U118 cells with edelfosine led to a prompt and persistent increase in the free intracellular calcium concentration (Figures 3.29 and 3.30a).

Following 24-h drug incubation, swollen dying cells still displayed bright green fluorescence, indicative of a high intracellular calcium concentration (data not shown). To further analyze the role of intracellular calcium on the distinct cell death processes triggered by edel-

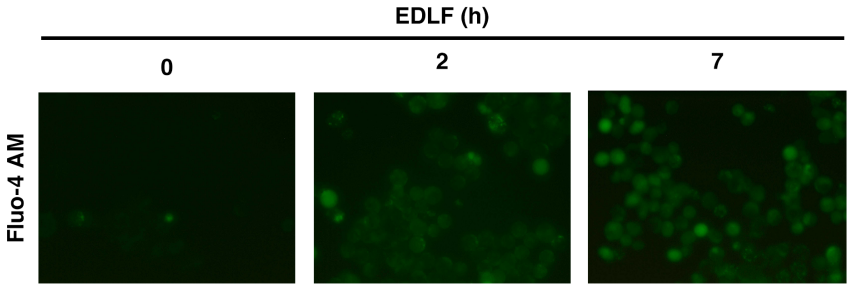

Figure 3.29: Cells were treated with 10 μM edelfosine (EDLF) for the indicated times followed by incubation with Fluo-4-AM for 30 min at 37ºC, before being analyzed by fluorescence microscopy.

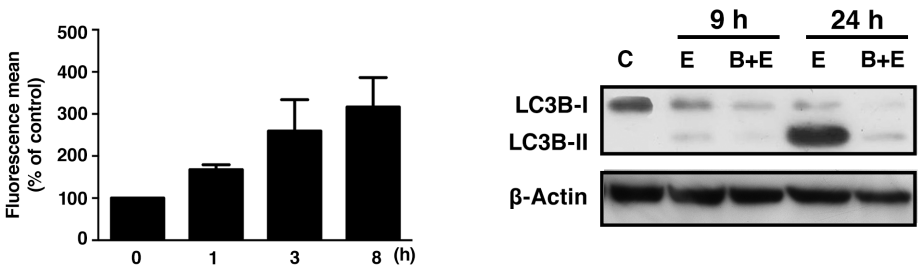

(a) (b)

Figure 3.30: (a) Cells were treated with 10 μM edelfosine (EDLF) for the indicated times, then incubated with Fluo-4-AM dye for 30 min and fluorescence intensity was measured by flow cytometry. (b) Untreated control cells (C), cells treated with 10 μM edelfosine (E) for the indicated times, or cells incubated with 4 μM BAPTA for 1 h and then treated with 10 μM edelfosine (B+E) for the indicated times, were analyzed by immunoblotting using a specific antibody for LC3B-I/II.

fosine, we used the membrane permeable calcium chelator BAPTA-AM, that inhibited ~55% the increase in free calcium concentration induced by edelfosine treatment. BAPTA-AM strongly diminished edelfosine-induced autophagy as assessed by a lower number of AVOs and a reduced conversion of LC3B-I to LC3B-II in drug-treated cells (Figure 3.30b).

However, BAPTA-AM preincubation did not affect the overall cell survival measured by MTT assay (Figure 3.31), but slightly increased the apoptotic response, although the difference was only statistically significant at 9-h treatment (Figure 3.32a). Preincubation with the extracellular calcium chelator EGTA diminished the level of intracellular calcium (Figure 3.32b) and slightly potentiated edelfosine-induced apoptosis (Figure 3.33), this increased apoptotic response being blocked by the inhibitor of inositol 1,4,5-trisphosphate-mediated Ca^{2+} release 2-APB (2-aminoethoxydiphenyl borate) (Figure 3.33).

Taken together, these data suggest that the increase in intracellular free calcium concentration induced by edelfosine is prompted mainly through an inward flux of extracellular calcium ions, a process that could be rather independent of, but concomitant with, the onset of necrosis, and that is suggested to promote a rather antiapoptotic and proautophagic response. However, when the influx of extracellular free calcium is blocked, the previously reported release of intracellular free calcium from internal stores elicited by edelfosine in solid tumor cells seems to play a role in the triggering of the minor apoptotic cell death response in U118 cells since the observed increase in apoptosis levels is blunted when 2-APB is used, blocking calcium release from internal stores.

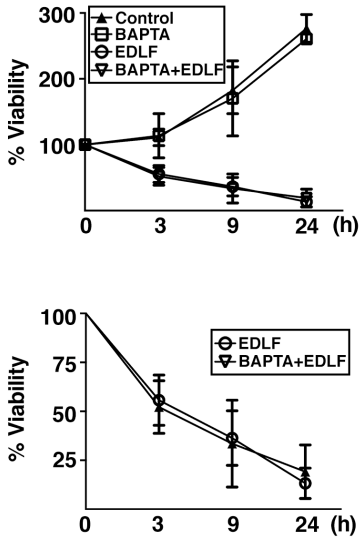

Figure 3.31: MTT assays were conducted after culturing U118 cells without or with 4 μM BAPTA-AM for 1 h, and then incubated in the absence or presence of 10 μM edelfosine (EDLF) at the indicated time points. Untreated control cells were run in parallel. Data shown are means $\pm$ SD of three independent experiments, each one performed in triplicate. The lower plot shows only the measurements for edelfosine- and BAPTA-AM+edelfosine-treated cells for an easier appreciation of changes.

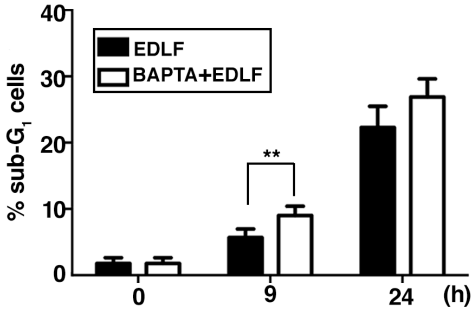

(a)

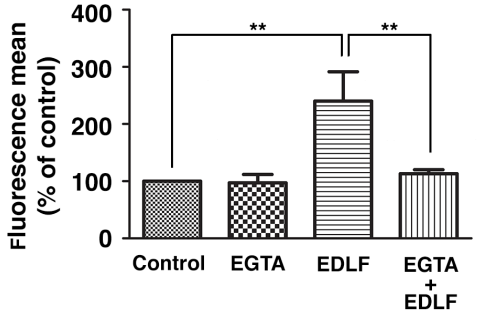

(b)

Figure 3.32: (a) Cells were preincubated without or with 4 μM BAPTA-AM for 1 h, and then treated with 10 μM edelfosine (EDLF) for the indicated time points and analyzed by flow cytometry to evaluate apoptosis. $**$, P<0.01 EDLF vs. BAPTA+EDLF, Student's t test. (b) Cells incubated for 1 h without or with 10 mM EGTA, and then in the absence or presence of 10 μM edelfosine (EDLF) for 4 h, were incubated with Fluo-4-AM for 30 min and fluorescence was measured by flow cytometry. Untreated control cells were run in parallel. Data are expressed as means ± SD of three independent experiments. $**$, P<0.01, Student's t test.

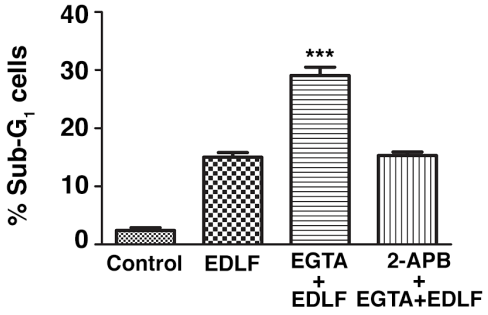

Figure 3.33: Cells were pretreated with EGTA (10 mM) or 2-APB (60 μM) + EGTA (10 mM) for 1 h, and then incubated in the absence or presence of 10 μM edelfosine (EDLF) for 24 h, and analyzed by flow cytometry to evaluate apoptosis. Untreated control cells were run in parallel. Data are expressed as means ± SD of three independent experiments. ***, P<0.001 EGTA+EDLF vs. EDLF or 2-APB+EGTA+EDLF, Student's t test.

Necroptosis - RIPK1 and RIPK3 involvement

Because our data indicated that necrosis was the major process involved in the cell death response induced by edelfosine in U118 cells, we next examined whether this necrotic type of cell death was a controlled mechanism for cellular demise. Necroptosis is a mechanism of regulated necrosis that is dependent of receptor-interacting protein 1 kinase (RIPK1) (Vanlangenakker *et al.*, 2012; Wu *et al.*, 2012; Vanden Berghe *et al.*, 2014). Here, we found that necrostatin-1 (Nec-1), a specific inhibitor of RIPK1 (Degterev *et al.*, 2005, 2008), was able to improve overall viability of edelfosine-treated U118 cells, as assessed by protecting MTT metabolism (Figure 3.34), reducing the incorporation of PI in non-permeabilized cells (Figure 3.35), and preventing the necrotic morphology of the dying cells (Figure 3.36). Necrotic morphology was readily detected by either bright-field microscopy (Figure 3.36, upper-panel) or SSC/FSC flow cytometry analysis (Figure 3.36, lower-panel), where dead cells turned up with a lower size (low FSC values).

In contrast, preincubation of Nec-1 induced a slight, but significant, increase in apoptosis in edelfosine-treated cells, which was assessed by an increase in the level of cells with a Sub-G_1 DNA content following cell cycle analysis (Figure 3.37a) and an increase in caspase-3 activation (Figure 3.37b). In addition, we found that Nec-1 preincubation inhibited the autophagic response induced by edelfosine in U118 cells (Figure 3.37b). Furthermore, inhibition of necroptosis by Nec-1 prior to edelfosine treatment led to a slower decrease in the intracellular level of calcium, but this effect was not statistically significant (Figure 3.38).

Because Nec-1 is also known to inhibit indoleamine-2,3-dioxygenase (IDO) (Muller *et al.*, 2005; Takahashi *et al.*, 2012; Degterev *et al.*, 2013), we tested the effect of Nec-1s, a more specific RIPK1 inhibitor lacking the IDO-targeting effect (Degterev *et al.*, 2008; Takahashi *et al.*, 2012). Nec-1s showed a similar protective effect to that observed with Nec-1, highly reducing PI incorporation in edelfosine-treated U118 cells (Figure 3.35), and thereby the effect of Nec-1 on PI uptake was not due to suppression of IDO activity.

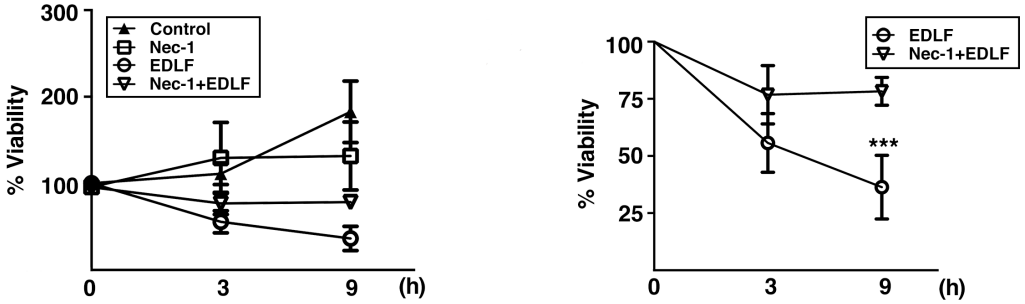

Figure 3.34: Cell proliferation was measured by MTT assay at the indicated time points, after culturing U118 cells without or with 200 μM Nec-1 (Nec-1) for 2 h, and then incubated in the absence or presence of 10 μM edelfosine (EDLF). Untreated control cells were run in parallel. Data are expressed as means ± SD of at least three independent experiments, each one performed in triplicate. The right plot shows only the measurements for edelfosine- and Nec-1+edelfosine-treated cells for an easier appreciation of changes. ***, P<0.001 EDLF vs. Nec-1+EDLF, Student's t test.

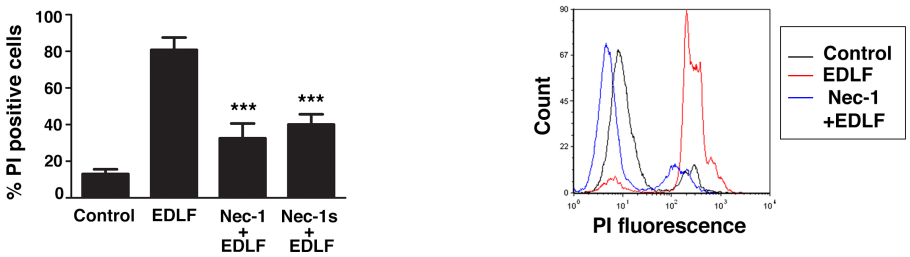

(a) (b)

Figure 3.35: (a) Quantification of U118 cells stained with PI after treatment with 10 μM edelfosine (EDLF) for 4 h without and with a pretreatment of 200 μM Nec-1 (Nec-1+EDLF) or 200 μM Nec-1s (Nec-1s+EDLF). Data shown are means ± SD of three independent experiments. ***, P<0.001 Nec- 1+EDLF vs. EDLF; ***, P<0.001 Nec-1s+EDLF vs. EDLF, Student's t test. (b) Representative flow cytometry analysis histograms of PI incorporation showing untretated control cells (Control), 10 μM edelfosine-treated cells (EDLF), and cells treated with Nec-1 (200 μM, 2 h pretreatment) + EDLF 10 μM (Nec-1+EDLF) for 4 h.

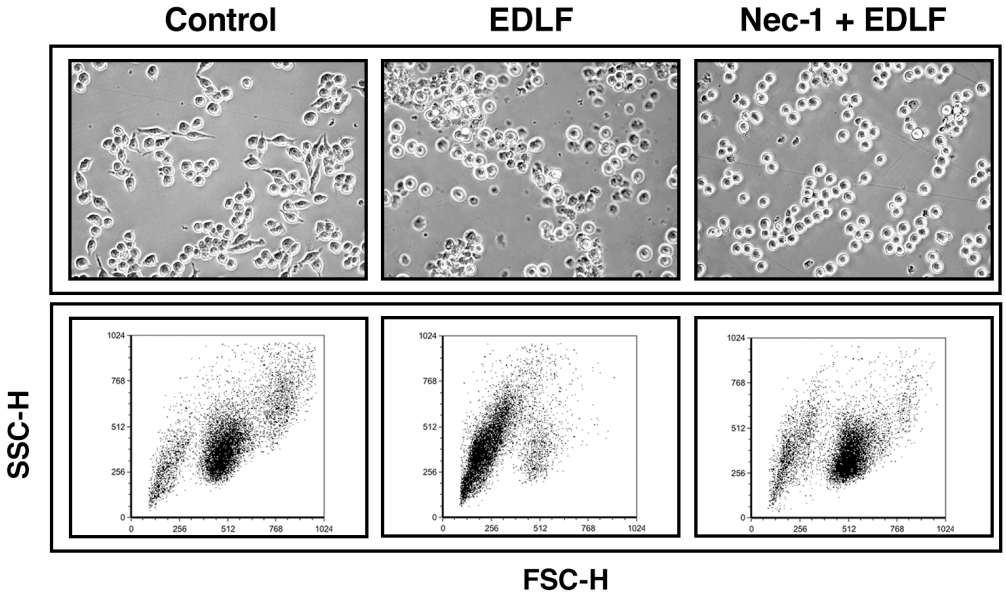

Figure 3.36: Upper pannel: Bright-field microscopy of untreated control cells, 10 μM edelfosine treated cells for 4 h (EDLF), and cells preincubated with 200 μM Nec-1 for 2 h and then treated for additional 4 h with 10 μM edelfosine (Nec-1+EDLF). Magnification, 20x. Lower pannel: FSC/SSC histograms of the cells treated as in the upper panels, showing cellular size (FSC-H) and granularity (SSC-H). Dead cells show lower FSC than living cells.

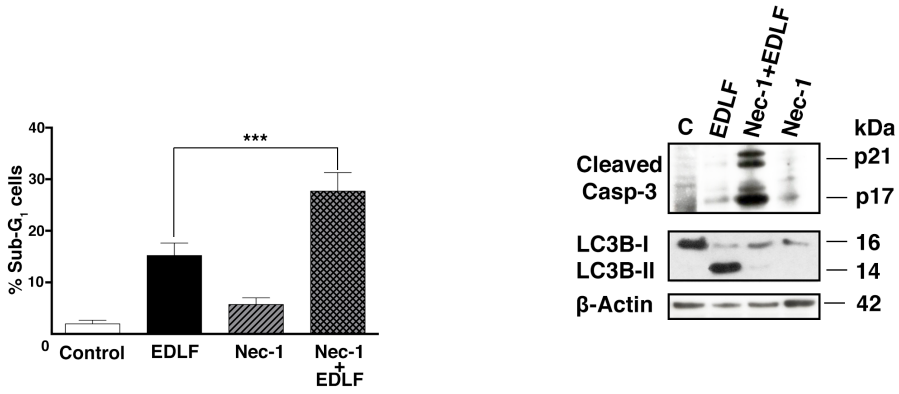

(a) (b)

Figure 3.37: (a) Cells were preincubated without or with 200 μM Nec-1 (Nec-1) for 2 h, then incubated in the absence or presence of 10 μM edelfosine (EDLF) for 24 h, and analyzed by flow cytometry to evaluate apoptosis. Untreated control cells were run in parallel. Data shown are means ± SD of three independent experiments. ***, P<0.001 EDLF vs. Nec-1+EDLF, Student's t test.(b) Cells were untreated (Control, C), treated with 10 μM edelfosine for 24 h (EDLF), pretreated with 200 μM Nec-1 for 2 h and then incubated with edelfosine for 24 h (Nec-1+EDLF), or treated with 200 μM Nec-1 for 26 h (2 h + 24 h). Cells were then analyzed by immunoblotting using specific antibodies against cleaved caspase-3 and LC3B-I/II. Immunoblotting for β-actin was used as an internal control for equal protein loading in each lane. Data shown are representative of three independent experiments.

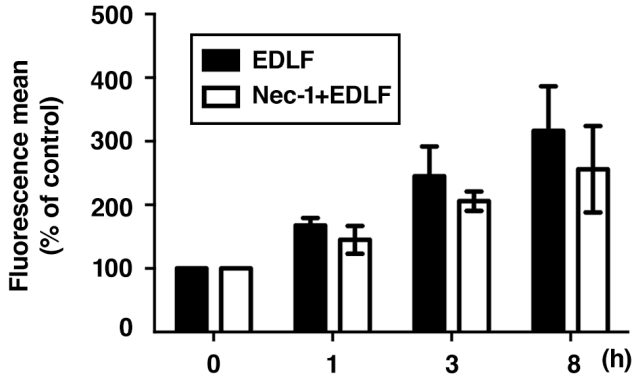

Figure 3.38: Cells treated with 10 μM edelfosine for the indicated times without (EDLF) or with Nec-1 pretreatment (Nec-1+EDLF) were incubated with Fluo-4-AM for 30 min at 37^{o}C, and fluorescence was measured by flow cytomtery.

U118 cells express RIPK1 and have low levels of extrinsic apoptotic molecules

Edelfosine has been reported as a potent apoptosis inducer in cancer cells (Mollinedo *et al.*, 1997; Gajate & Mollinedo, 2007; Nieto-Miguel *et al.*, 2007; Gajate *et al.*, 2012). Induction of apoptosis by edelfosine in a variety of hematological cancer cells involves the recruitment into lipid rafts of extrinsic apoptotic molecules forming clusters of Fas/CD95 death receptor and downstream signalling molecules, such as FADD and caspase-8 (Gajate & Mollinedo, 2007; Nieto-Miguel *et al.*, 2007; Gajate *et al.*, 2009). Here we found that U118 expressed RIPK1, a critical protein in necroptosis, but very low levels of Fas/CD95, FADD and 57 kDa procaspase-8, critical proteins involved in apoptosis via the extrinsic pathway, as compared to HeLa (human cervical carcinoma) and Jurkat (human acute T-lymphocytic leukemia) cells (Figure 3.39), two cancer cell lines that readily undergo apoptosis following edelfosine treatment (Nieto-Miguel *et al.*, 2006; Gajate & Mollinedo, 2007). In addition, as shown in Figure 3.39b, a high level of caspase-8 activation, assessed by the generation of its 43/41 kDa cleaved form, was detected in both HeLa and Jurkat cells upon edelfosine treatment, but not in U118 cells. This drastic difference in the ratio of RIPK1:procaspase-8 levels between the above cell lines suggests that U118 cells, unlike HeLa and Jurkat cells, may be prone to undergo necroptosis rather than apoptosis following incubation with the ether lipid.

A number of studies have shown that several stimuli that in certain experimental conditions trigger apoptosis can also induce necroptosis following caspase inhibition (Green *et al.*, 2011). Inhibition of caspases by the pan-caspase inhibitor z-VAD-fmk inhibited the apoptotic response (Sub-G_1 cell population) induced by edelfosine in Jurkat cells (Figure 3.40a), but did not promote a change to a necrotic type of cell death, as evaluated by PI incorporation assays (Figure 3.40a) or morphology FSC/SSC studies by flow cytometry (Figure 3.40b). In fact, preincubation with z-VAD-fmk decreased PI uptake (Figure 3.40a), likely due to a decrease in apoptosis and subsequent secondary necrosis, and also diminished the number of cells undergoing changes in FSC/SSC values (Figure 3.40b). These data suggest that apop-

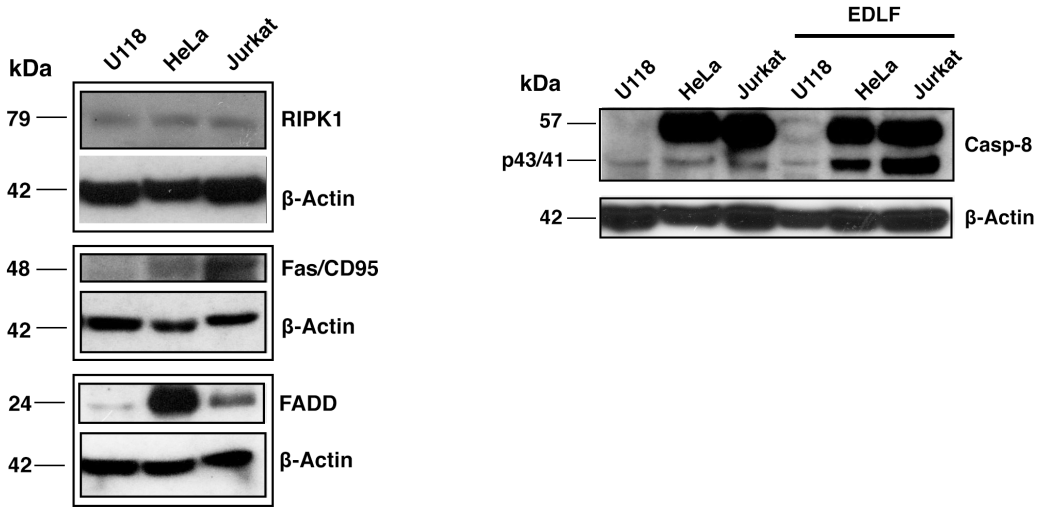

(a) (b)

Figure 3.39: (a)U118, HeLa and Jurkat cell lines were analyzed by immunoblotting using specific antibodies against RIPK1, Fas/CD95 and FADD. Immunoblotting for β-actin was used as an internal control for equal protein loading in each lane. (b) U118, HeLa and Jurkat cells untread and treated with 10 μM edelfosine (EDLF) for 24 h were analyzed by immunoblotting using a specific antibody that recognizes full-length 57-kDa procaspase-8 and p43/41 cleaved active caspase-8 fragments. The molecular weight of each immunodetected band is indicated. Data shown are representative of three experiments.

totic response is not switched to necrosis in edelfosine-treated leukemic Jurkat cells after caspase inhibition.

Using the Ewing´s sarcoma cell line CADO-ES1, that showed a higher expression of caspase-8 protein expression than U118 cells, but much lower than that of Jurkat cells (Figure 3.41a), we found that edelfosine induced apoptosis in this cell line that was totally prevented by z-VAD-fmk preincubation, but not by Nec-1 (Figure 3.41b). Nec-1 slightly reduced PI incorporation following edelfosine treatment in CADO-ES1 cells (Figure 3.41b), and z-VAD-fmk pretreatment did not decrease PI uptake (Figure 3.41b), suggesting that Nec-1 could prevent the rather small portion of necrotic response that was not due to a secondary necrosis following apoptosis. Thus, it could be envisaged that these cells could die by necrosis/necroptosis when apoptosis is blocked. Taken together, these data support the notion that low levels of procaspase-8 or lack of caspase-8 activation might favor the induction of necroptotic cell death.

To further analyze the role of RIPK1 in edelfosine-induced necroptosis in U118 cells, we silenced RIPK1 by using small interfering RNA (siRNA), leading to a 80% reduction in protein level (Figure 3.42, upper immunoblot).

However, surprisingly RIPK1 silencing did not render the same protection offered by Nec-1 against necrosis, as assessed by PI incorporation (Figure 3.43) or by morphologic changes (data not shown) after edelfosine treatment. However, Nec- 1 totally prevented PI uptake in RIPK1-silenced cells upon edelfosine incubation (Figure 3.43). Because we were not able to achieve a complete RIPK1 knockdown, we cannot rule out the possibility that the remaining RIPK1 may still mediate necroptosis or that Nec-1 has other effects besides RIPK1 and IDO inhibition. In this regard, it has been reported (Cho *et al.*, 2011) that Nec-1 inhibited necrosis induced by tumor necrosis factor (TNF) in murine fibrosarcoma cell line L929 cells, however siRNA-mediated silencing of RIPK1 did not inhibit TNF-induced necrosis in these cells, suggesting the presence of a RIPK1- independent necrosis, yet inhibitable by Nec-1.

Necroptosis has been shown to depend on the activation of RIPK1 and RIPK3, which associate forming complexes that are referred to as necrosomes (Li *et al.*, 2012). RIPK3 has been identified as a crucial regulator of necroptosis (He *et al.*, 2009; Zhang *et al.*, 2009), and recent evidence indicate that oligomerization of RIPK3 is sufficient to induce necroptosis, independent of TNF stimulation or RIPK1 activity (Orozco *et al.*, 2014). We found that U118 cells expressed RIPK3, and we were able to knockdown RIPK3 by using siRNA, which reduced RIPK3 protein level by 65% (Figure 3.42 lower immunoblot). RIPK3 silencing had a different effect from RIPK1 silencing in edelfosine-treated U118 cells. We found that RIPK3-silenced cells still died very quickly, but the predominant necrotic cell population was replaced by an apoptotic one following edelfosine treatment, as assessed by an increase in Sub-G_1 cell population through cell cycle analysis (Figures 3.44a and 3.44b), and this apoptotic population was not futher increased following silencing of both RIPK3 and RIPK1 (Figure 3.44a). Cells transfected with a non-targeting sequence behaved as untreated control cells (Figure 3.44a). Morphologic characteristics of apoptosis, including cell surface blebbing and chromatin condensation were prevalent in RIPK3-silenced cells upon edelfosine treatment,

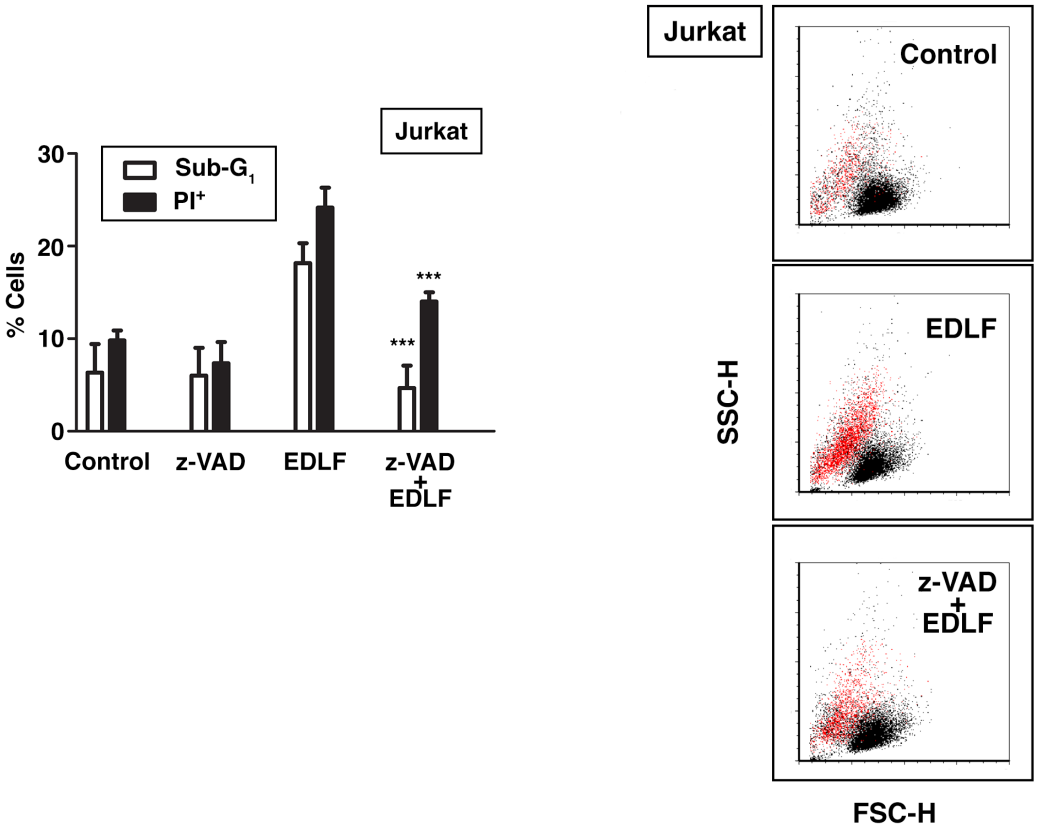

(a) (b)

Figure 3.40: (a)Jurkat cells were preincubated without or with 50 μM pan-caspase inhibitor z-VAD-fmk (z-VAD) for 1 h and then incubated in the absence (Control) or presence of 10 μM edelfosine (EDLF) for 18 h. Cells were analyzed by flow cytometry to evaluate apoptosis (as the percentage of Sub-G_1 population in cell cycle analysis) and necrosis (PI incorporation without previous permeabilization). Z-VAD-fmk significantly reduces both Sub-G_1 population and PI incorporation. Data shown are means $\pm$ SD of three independent experiments. ***, P<0.001 z-VAD+EDLF vs. EDLF, Student's t test. (b) Representative FSC/SSC histograms of Jurkat cells treated as in (a), showing cellular size (FSC-H) and granularity (SSC-H). Edelfosine-treated cells (EDLF) show an increase in cells with lower FSC-H values and z-VAD-fmk ameliorates this increase.

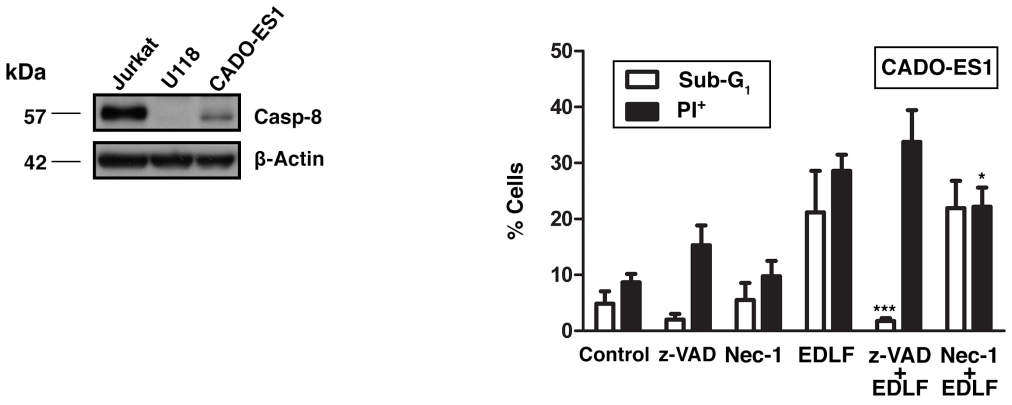

(a) (b)

Figure 3.41: (a) Immunoblot comparing 57-kDa procaspase-8 expression levels in Jurkat, U118 and CADO-ES1 cells by using a specific antibody. β-actin was used as an internal control for equal protein loading in each lane. (b) CADO-ES1 cells were untreated or preincubated for 1 h with z-VAD-fmk (50 μM) or Nec-1 (100 μM), followed by incubation in the absence or presence of 10 μM edelfosine for 24 h. Cells were then analyzed by flow cytometry to evaluate apoptosis (Sub-G_1 population) and necrosis (PI^+ cells). z-VAD-fmk significantly reduced the Sub-G_1 population, but induced a non-significant increase in PI incorporation. Nec-1 very slightly reduced PI incorporation in edelfosine treated cells. Data shown are means $\pm$ SD of three independent experiments. $***$, $P<0.001$ z-VAD+EDLF vs. EDLF; *, $P<0.05$ Nec-1+EDLF vs. EDLF, Student's t test.

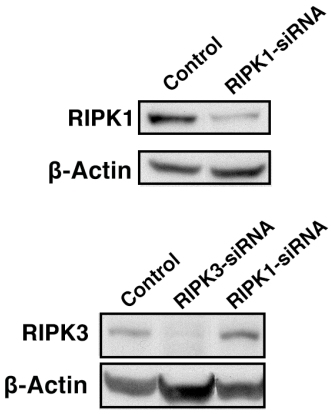

Figure 3.42: Immunoblottings to assess knockdown of RIPK1 and RIPK3 proteins using specific antibodies following transfection with the corresponding RIPK1-siRNA (200 nM) and RIPK3-siRNA (100 nM). β-actin was used as a control for protein loading. Protein expression was evaluated 5 days after transfection.

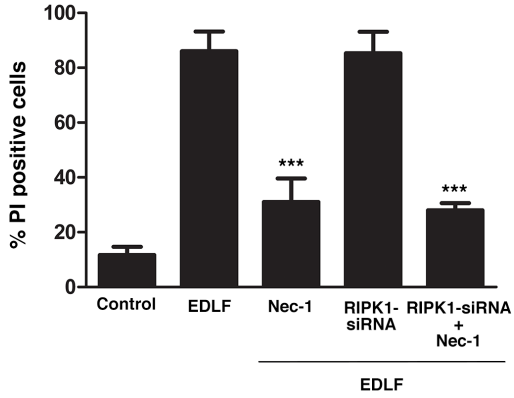

Figure 3.43: PI incorporation in untreated control cells or RIPK1-siRNA-transfected cells after 4-h edelfosine (10 μM) treatment with or without 200 μM Nec-1 preincubation. Control cells or RIPK1-siRNA transfected cells significantly incorporated much less PI following edelfosine treatment when preincubated with Nec-1, but RIPK1 knockdown (RIPK1-siRNA) did not affect PI incorporation induced by edelfosine treatment. Data shown are means $\pm$ SD of three independent experiments. ***, P<0.001 Nec-1+EDLF vs. EDLF; ***, P<0.001 RIPK1-siRNA+Nec-1+EDLF vs. EDLF, Student's t test.

instead of the darkened cells lacking plasma membrane integrity in control edelfosine-treated non-targeting-siRNA cells (Figure 3.44b), and the percentage of cells showing a necrotic phenotype was dramatically reduced (~80%).

A stronger apoptosis induction following RIPK3 silencing was further confirmed by DAPI staining, showing apoptotic nuclei with chromatin condensation (Figure 3.44b) and caspase-3 and caspase-8 activation (Figure 3.45). Cells transfected with RIPK3-siRNA showed a high increase in the level of active caspase-3 forms, and a decrease in procaspase-8 protein level with a concomitant increase in the p18 active fragment (Figure 3.45).

Because we found a similar increase in apoptosis when silencing RIPK3 alone or RIPK1 and RIPK3 together (Figures 3.44a and 3.45), which was completely inhibited by the pan-caspase inhibitor z-VAD-fmk (~90% inhibition, Figure 3.46), it might be envisaged that RIPK3 acts a molecular switch from necrosis to apoptosis induction. The mixed lineage kinase domain-like protein (MLKL) has been identified as a key mediator of necrosis signalling downstream of RIPK3 and the small molecule called (E)-N-(4-(N-(3-methoxypyrazin-2- yl)sulfamoyl)phenyl)-3-(5-nitrothiophene-2-yl)acrylamide, usually referred to as necrosulfonamide, blocks necrosis downstream of RIPK3 by covalently modified MLKL (Sun *et al.*, 2012). Here, we also found that necrosulfonamide increased in a similar way to RIPK3-siRNA the induction of apoptosis in edelfosine-treated U118 cells (Figure 3.47). These results further support the key role of RIPK3 in modulating edelfosine-induced necroptosis in U118 cells and in the switch from necrosis to apoptosis in these cells.

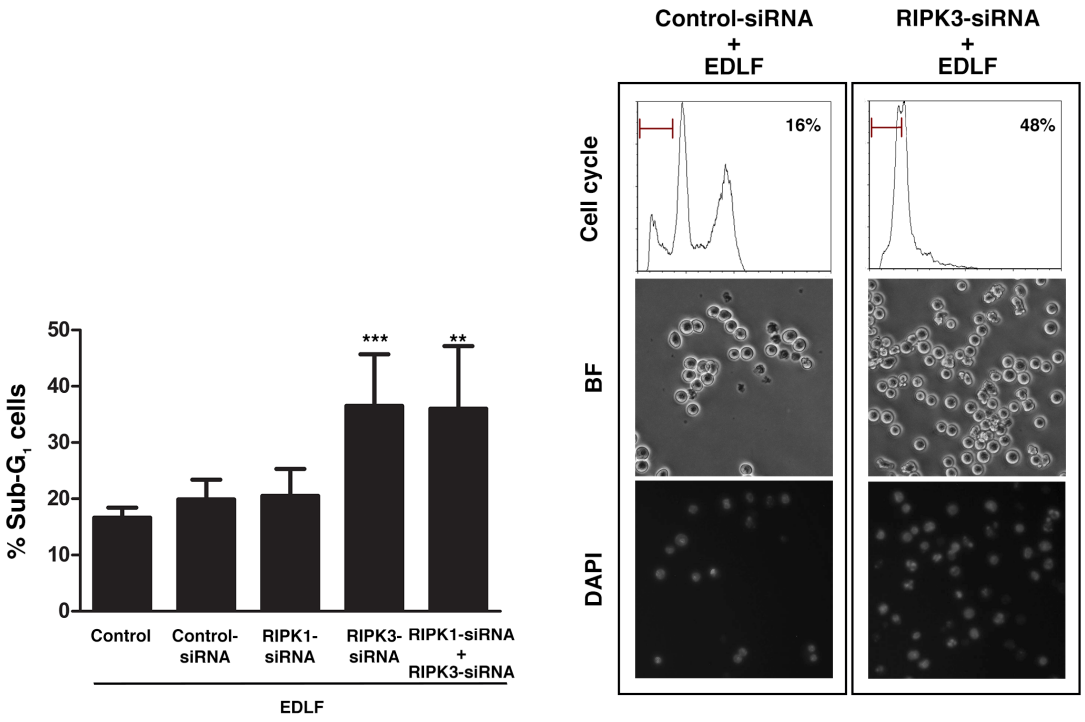

(a) (b)

Figure 3.44: (a) U118 untreated control cells, cells transfected with a non-targeting sequence (siRNA Control), and cells transfected with 200 nM RIPK1-siRNA, 100 nM RIPK3-siRNA, or both RIPK1-siRNA and RIPK3-siRNA, were incubated with 10 μM edelfosine for 20 h and apoptosis was evaluated by flow cytometry analysis of the cell cycle (Sub-G_1 cell population). Data shown are means ± SD of three independent experiments. ∗∗∗, P<0.001 RIPK3-siRNA+EDLF vs. Control- siRNA+EDLF; ∗∗, P<0.01 RIPK1-siRNA+RIPK3-siRNA+EDLF vs. Control-siRNA+EDLF, Student's t test. (b) Non-targeting siRNA (control)- and RIPK3-siRNA-transfected cells treated with 10 μM edelfosine were analyzed by cell cycle flow cytometry (Sub-G_1 fractions and percentages of Sub-G_1 cells are indicated in each histogram) after 20-h drug treatment (upper panel); bright-field microscopy to visualize cell morphology after 4-h edelfosine treatment (middle panel), and DAPI staining of nuclei following 20-h drug treatment (lower panel).

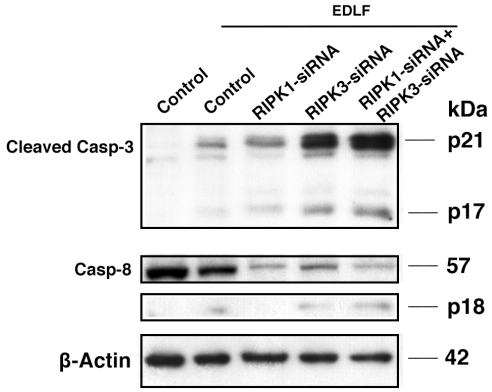

Figure 3.45: Immunoblotting for cleaved caspase-3 forms and caspase-8 (procaspase-8 and cleaved p18 fragment) in untreated cells (Control), and in control cells, RIPK1-siRNA-, RIPK3-siRNA-, and RIPK1-siRNA+RIPK3-siRNA-transfected cells treated with edelfosine 10 μM for 9 h. β-actin was used as a control for protein loading.

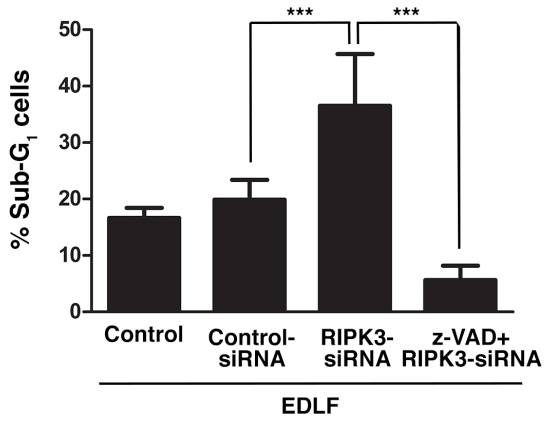

Figure 3.46: U118 untreated control cells, cells transfected with a non-targeting sequence (siRNA Control), and cells transfected with 100 nM RIPK3-siRNA were incubated with 10 μM edelfosine for 20 h in the absence or presence of z-VAD-fmk, and apoptosis was evaluated by flow cytometry analysis of the cell cycle (Sub-G_1 cell population). Data shown are means $\pm$ SD of three independent experiments. $***$ $P<0.001$ RIPK3-siRNA+EDLF vs. Control-siRNA+EDLF; $***$, $P<0.001$ z-VAD+RIPK3-siRNA+EDLF vs. RIPK3-siRNA+EDLF, Student's t test.

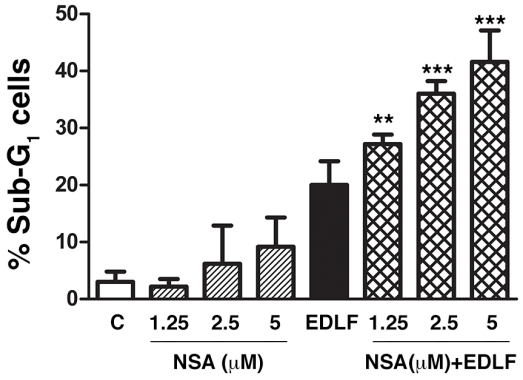

Figure 3.47: U118 cells were untreated (C) or treated with necrosulfonamide (NSA) at the indicated concentrations for 21 h, treated with 10 μM edelfosine for 20 h, and pre-treated with NSA for 1 h and then treated with edelfosine for 20 h. Then apoptosis was evaluated by flow cytometry analysis of the cell cycle (Sub-G_1 cell population). Data shown are means $\pm$ SD of three independent experiments. $**$, $P<0.01$ and $***$, $P<0.001$ NSA+EDLF vs. EDLF, Student's t test.

4

Inhibition of ERK1/2 phosphorylation by MEK1/2 inhibitor U0126 shifts the predominantly necrotic response induced by edelfosine to an apoptotic type of cell death in U118 cells

We found that 10 μM edelfosine induced a rapid and massive cell death in U118 glioblastoma cell line. Although only ~18% of the cells displayed DNA degradation (corresponding to apoptotic cells), as assessed by the percentage of cells in the Sub-G_1 region of cell cycle, most of the cells (~80%) had already lost plasma membrane integrity after 24-h treatment, being permeable to propidium iodide (PI^+ cells). This necrotic response was inhibited by 200 μM necrostatin-1 (~72% inhibition) and necrostatin-1s (~61% inhibition), suggesting that edelfosine-induced cell death in U118 cells is mainly through necroptosis.

Interestingly, pre-incubation for 2 h with 10 μM of the selective MEK1/2 inhibitor U0126 led to a dramatic change in the type of cell death induced by edelfosine in U118 cells. The predominant necrotic morphology observed after 4-h treatment with edelfosine alone (dark cells, lacking plasma membrane integrity) turned to a typical apoptotic morphology (bright cytoplasm and characteristic cell surface blebbing) when cells were pre-incubated with U0126 before edelfosine addition, while U0126 alone did not induced any visible change after the same period of time (Figure 4.1a). Furthermore, cell cycle analyses showed a dramatic increase in the percentage of apoptotic cells, as assessed by an increase in the Sub-G_1 region, in edelfosine-treated U118 cells that were pre-treated with U0126 (Figure 4.1b).

SYTOX-Green nucleic acid staining showed that most of the edelfosine-treated cells were permeable to the stain and had an intact nuclei (Figure 4.2a, upper panel), whereas the nuclei of the cells that were pre-incubated with U0126 exhibited apoptotic morphological changes, including chromatin condensation (Figure 4.2a, lower panel). The increased Sub-G_1 popula-

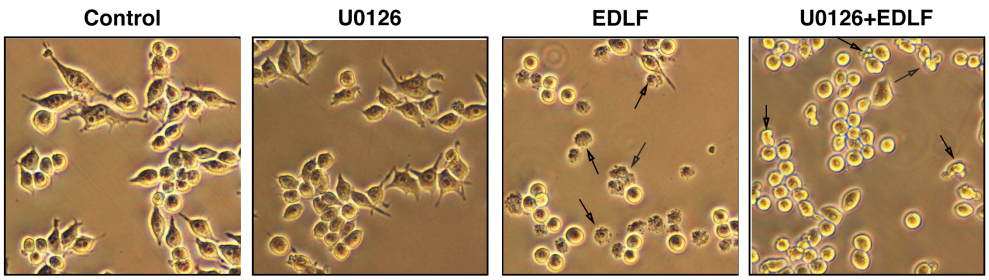

(a)

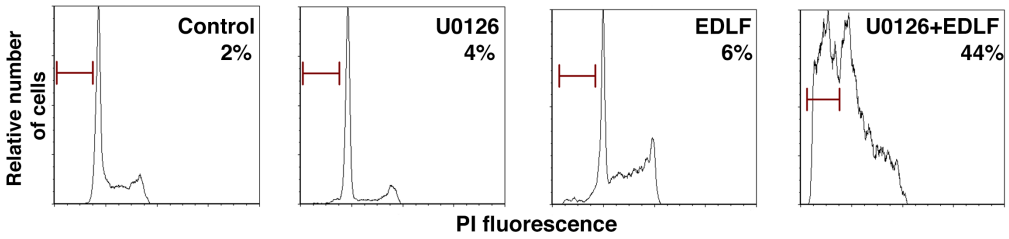

(b)

Figure 4.1: (a) Representative bright-field microscopy images of U118 untreated control cells, U118 cells treated with 10 μM U0126 for 6 h (U0126), 10 μM edelfosine-treated cells for 4 h (EDLF), and cells pre-incubated with 10 μM U0126 for 2 h and then treated with edelfosine for additional 4 h (U0126 + EDLF). Arrows indicate cells with necrotic morphology in the EDLF panel and with apoptotic morphology in the U0126 + EDLF panel. Magnification, 20×. (b) Representative cell cycle analyses of untreated U118 cells (Control), cells treated with 10 μM U0126 for 9 h (U0126), cells treated with 10 μM edelfosine for 7 h (EDLF), and cells pre-incubated for 2 h with 10 μM U0126 and then treated with 10 μM edelfosine for 7 h (U0126 + EDLF). The apoptotic fraction, identified as the Sub-G_1 population, is indicated in each histogram.

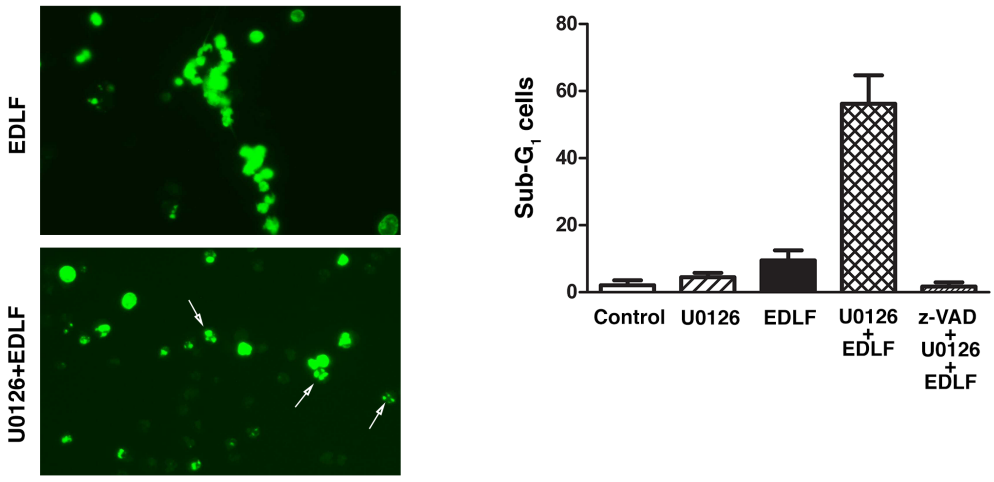

(a) (b)

Figure 4.2: (a)Representative fluorescence microscopy images for SYTOX-Green nucleic acid staining of 10 μM edelfosine-treated cells for 24 h (EDLF) and cells pre-incubated with 10 μM U0126 for 2 h and then treated with 10 μM edelfosine for additional 24 h (U0126 + EDLF). Arrows indicate cells with pyknotic nuclei in the U0126 + EDLF panel. Magnification, 20×.(b) U118 cells were pre-incubated without or with 100 μM z-VAD-fmk for 1 h, incubated in the absence or presence of 10 μM U0126 for 2 h, and finally treated with 10 μM edelfosine for 7 h. Untreated control cells were run in parallel. Apoptosis was evaluated using flow cytometry cell cycle analysis. Data shown are means ± SD or representative experiments of three performed.

tion detected in the cell cycle analysis, as a result of DNA fragmentation, following edelfosine treatment in U0126-pretreated cells was totally blocked by the pan-caspase inhibitor z-VAD-fmk (Figure 4.2b). These data support the notion that U0126 pre-treatment turns the necrotic cell death triggered by edelfosine in U118 cells into a caspase-dependent apoptotic response.

Inhibition of ERK1/2 phosphorylation promotes a dramatic increase in apoptosis biochemical markers and leads to RIPK1 downregulation

Pre-treatment of U118 cells with U0126 followed by edelfosine incubation led to a drastic inhibition of ERK1/2 phosphorylation that was complete after 9 h incubation (Figure 4.3). The time-dependent progressive inhibition of ERK1/2 phosphorylation was concomitant with a high activation of caspase-3 and caspase-8 (Figure 4.3).

U118 cells showed constitutively a potent ERK phosphorylation by themselves that was even increased at early times of incubation with edelfosine (Figure 4.4a). Incubation with U0126 alone led to a decrease in ERK phosphorylation (Figure 4.4a), but this inhibition

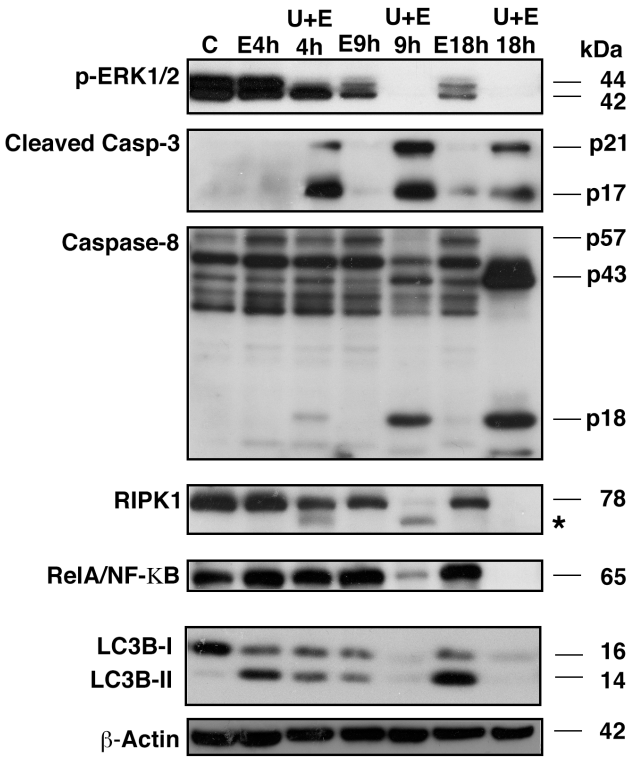

Figure 4.3: U118 untreated cells (C), cells treated with 10 μM edelfosine for the indicated times (Exh), and cells pre-incubated for 2 h with 10 μM U0126 and then with 10 μM edelfosine for the corresponding indicated times (U + Exh), were analyzed by immunoblotting using specific antibodies against p-ERK1/2, cleaved caspase-3, caspase-8, RIPK1, RelA/NF-κB p65 and LC3B-I/II. Immunoblotting for β-actin was used as an internal control for equal protein loading. The molecular weights of the immunodetected bands are indicated. * indicates cleaved RIPK1.

was not accompanied by a significant induction of apoptosis (Figure 4.1a and Figure 4.1b). However, pre-incubation with U0126 followed by treatment with edelfosine abrogated completely ERK phosphorylation (Figure 4.3 and Figure 4.4a) and led to the potent activation of caspases (Figure 4.3) and induction of apoptosis (Figure 4.1b and Figure 4.2b). Edelfosine by itself did not trigger a strong activation of caspases 3 and 8 (Figure 4.3 and Figure 4.4a) or major apoptosis (Figure 4.1b), but pre-incubation with U0126 completely abolished ERK phosphorylation and triggered an extremely potent activation of caspases 3 and 8 (Figure 4.3 and Figure 4.4a). We also found that 78-kDa full-length RIPK1 resulted degraded upon incubation with U0126 plus edelfosine (Figure 4.3 and Figure 4.4b). Degradation of RIPK1 was concomitant with caspase activation (Figure 4.3). It is known that caspase-8 cleaves RIPK1 in TNF-induced apoptosis (Lin *et al.*, 1999a), and we found a perfect correlation between caspase-8 activation and RIPK1 cleavage in U0126+edelfosine-treated samples (Figure 4.3). Using an antibody that recognizes the carboxy-terminal fragment of RIPK1 (45 kDa) produced by caspase-8-dependent cleavage, we found that this cleavage was inhibited by the pan-caspase inhibitor z-VAD-fmk (Figure 4.4b), suggesting that RIPK1 cleavage was caspase mediated. Edelfosine induced a slight increase in the protein level of Rel/NF-κB p65 transcription factor in U118 cells, but the treatment of U0126 with edelfosine led to a complete degradation of NF-κB. Degradation of both RIPK1 and NF-κB, regulating necrosis and survival responses, respectively, might prompt apoptosis in U118 cells.

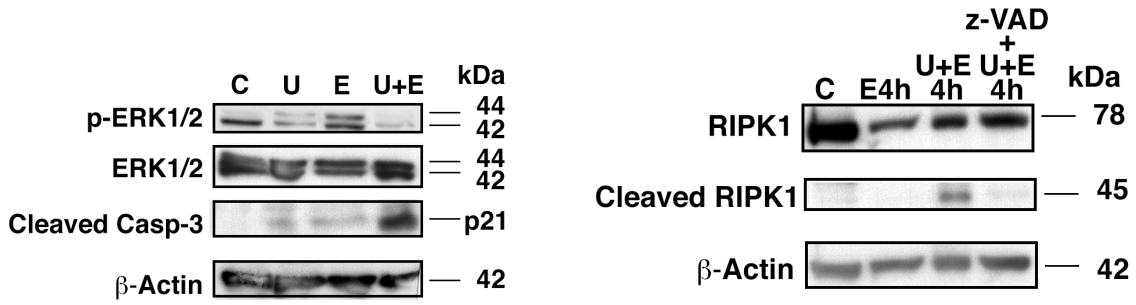

(a) (b)

Figure 4.4: (a) U118 untreated cells (C), cells treated with 10 μM U0126 for 5 h (U), cells treated with 10 μM edelfosine for 3 h (E), and cells pre-incubated for 2 h with 10 μM U0126 and then with 10 μM edelfosine for 3 h (U + E) were analyzed by immunoblotting using specific antibodies against p-ERK1/2, ERK1/2 and cleaved caspase-3. Immunoblotting for β-actin was used as an internal control for equal protein loading. (b) U118 untreated cells (C), cells treated with 10 μM edelfosine for 4 h (E), cells pre-incubated for 2 h with 10 μM U0126 and then with edelfosine for 4 h (U + E), and cells pre-incubated with 100 μM z-VAD-fmk for 1 h, 10 μM U0126 for 2 h and then with 10 μM edelfosine for 4 h (z-VAD + U + E) were analyzed by immunoblotting using a specific antibody against RIPK1 that recognizes full length RIPK1 protein and the carboxy-terminal fragment of RIPK1 (45 kDa) generated by caspase-8 dependent cleavage. The appearance of this fragment is inhibited by z-VAD-fmk. Immunoblotting for β-actin was used as an internal control for equal protein loading. Data shown are representative experiments of three performed.

Activation of the mitochondrial intrinsic pathway of apoptosis in U118 cells treated with U0126 and edelfosine

Incubation of U118 cells with edelfosine led to disruption of the mitochondrial transmembrane potential ($\Delta\Psi_m$) and an increase in reactive oxygen species (ROS) (Figure 4.5). However, some cells (~20%) remained intact regarding $\Delta\Psi_m$ (Figure 4.5). When cells were treated with U0126 and edelfosine, practically all the cells underwent a total $\Delta\Psi_m$ loss (~95%), whereas the percentage of cells showing increased ROS generation was lower than that observed in cells treated with edelfosine alone (Figure 4.5).

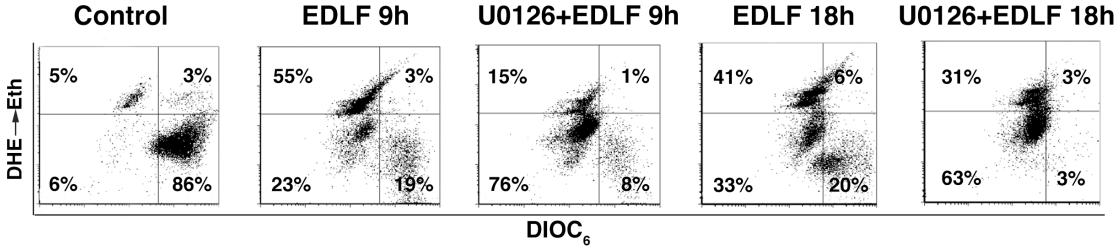

Figure 4.5: U118 cells, pre-incubated for 2 h in the absence or presence of 10 μM U0126 and then with 10 μM edelfosine for the indicated periods of time, were analyzed for $\Delta\Psi_m$ disruption ($DiOC_6(3)^{low}$) and ROS generation (DHE -> Eth^{high}) by flow cytometry. Control untreated cells were run in parallel. The corresponding percentage of cells in each quadrant is indicated.

This massive $\Delta\Psi_m$ dissipation was concomitant with a dramatic decrease in the protein level of Bcl-x_L, a potent activation of caspase-9, and a high induction of apoptosis, as assessed as the percentage of cells in the Sub-G_1 region of cell cycle analysis (Figure 4.6). These data suggest that ERK inhibition largely potentiated mitochondrial-mediated apoptosis. Treatment with edelfosine alone induced a potent necrotic response accompanied by a rapid and very high increase in ROS generation and $\Delta\Psi_m$ dissipation, but a certain percentage of cells remained viable (Figure 4.5). However, U0126 pre-incubation made U118 cells extremely sensitive to edelfosine, and practically all the cells underwent $\Delta\Psi_m$ loss (Figure 4.5), undergoing apoptosis (Figure 4.2b).

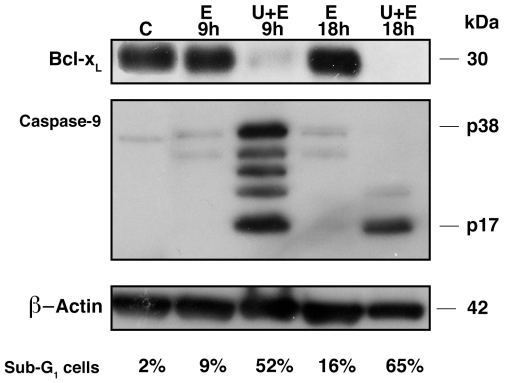

Figure 4.6: Immunoblotting of U118 control cells (C), cells treated with 10 μM edelfosine (E) and cells pre-incubated with 10 μM U0126 and then with edelfosine (U + E) for the indicated times, using specific antibodies against Bcl-x_L and caspase-9. Immunoblotting for β-actin was used as an internal control for equal protein loading on each lane. The percentage of cells in the Sub-G_1 phase of the cell cycle (a measure of apoptosis) is indicated under each corresponding lane of treatment. Data are representative experiments of three performed.

Autophagy is inhibited when necroptosis is switched to apoptosis in U118 cells

We found that edelfosine treatment led to the rapid conversion of LC3B-I to LC3B-II after a 3-h treatment, reaching its maximum following 24-h treatment (Figure 3.12). With U0126, we observed an important reduction of this autophagic marker, especially after 9 hours treatment; interestingly, there was a reduction not only in the LC3B-II form, but also in the LC3B-I (Figure 4.3). In this case, the shift from a necrotic/necroptotic type of cell death to an apoptotic type seems to inactivate the autophagic response. This is in agreement with our previous finding that necroptosis inhibition by Nec-1 also reduced the autophagic response in U118 edelfosine-treated cells (Figure 3.37b). Autophagy has been described as a side effect of the stress imposed to cells undergoing necrosis and many studies associated ERK activity with autophagy in different models, in response to different stresses (Cagnol & Chambard, 2010). Moreover, direct ERK activation by overexpression of constitutively active MEK can promote autophagy without any other stimulus (Corcelle *et al.*, 2006).

Geldanamycin promotes edelfosine-induced apoptosis together with ERK2 and RIPK1 downregulation in U118 cells

The above data suggest that ERK phosphorylation allows cell death by necrosis, but blocks edelfosine-induced apoptosis. ERK inhibition leads to RIPK1 degradation and to the switch of a necrotic to an apoptotic cell death. Because Hsp90 inhibition has been reported to lead to inhibition of ERK signalling (Hostein *et al.*, 2001; Zhang & Burrows, 2004; Georgakis *et al.*, 2006; Moser *et al.*, 2009), as well as to proteosomal degradation of RIPK1 (Lewis *et*

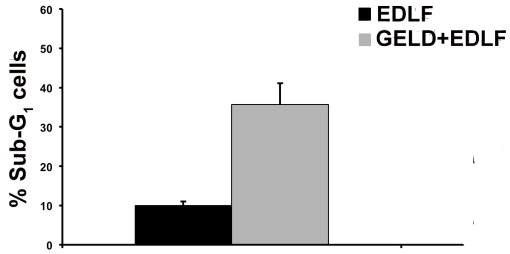

Figure 4.7: U118 cells were treated with 10 μM edelfosine for 12 h (EDLF) or pre-incubated with 2 μM geldanamycin for 14 h and then treated with edelfosine for additional 12 h (GELD + EDLF). Apoptosis was evaluated using flow cytometry cell cycle analysis. Data shown are means ± SD of three independent experiments.

al., 2000; Fearns *et al.*, 2006; Palacios *et al.*, 2010; Chen *et al.*, 2012), we analyzed how the Hsp90 inhibitor geldanamycin affected edelfosine-induced cell death. The combined treatment of geldanamycin plus edelfosine in U118 cells largely increased by 4-fold the apoptotic response induced by edelfosine treatment alone, following 12 hours of incubation, as assessed by quantitation of the percentages of Sub-G_1 cell population (Figure 4.7). This increase in apoptosis was also readily detected by morphological changes, leading to a high percentage of cells showing apoptotic morphology under the combined treatment of geldanamycin plus edelfosine (Figure 4.8), whereas apoptotic cell death was scarcely detected in cells treated either with edelfosine or geldanamycin alone (Figure 4.8).

This increase in apoptotic cell death was further supported by the dramatic activation of caspases 3, 8 and 9 following the combined treatment of geldanamycin and edelfosine (Figure 4.9), that was concomitant with ERK downregulation and inhibition and RIPK1 degradation (Figure 4.9). These data further support that ERK inhibition potentiates edelfosine-induced apoptosis in glioblastoma U118 cells. Hsp90 inhibition has been reported to induce tumor regression in glioblastoma (Zhu *et al.*, 2010), and thereby the combined use of Hsp90 inhibitors and edelfosine could be an interesting approach in the induction of apoptotic cell death in glioblastoma.

Interestingly, we also observed an important decrease in ERK1/2 phosphorylation when combining geldanamycin with edelfosine. Others have previously found that geldanamycin or its analogues could downregulate phosphorylation of ERK1/2 and increase cell death (Georgakis *et al.*, 2006). It has also been described that Hsp90 could mediate oxidative stress-stimulated, late-phase activation of ERK1/2 (Liu *et al.*, 2007). We found that pre-incubation with geldanamycin favored a fast cell death, mainly, but not totally, apoptotic as observed by morphological changes, increase in Sub-G_1 population by cell cycle analysis, and caspases activation. We could also detect caspase-8 activation after a short period of incubation, not detectable with edelfosine treatment. Again, ERK phosphorylation decrease might favor the activation of the apoptotic machinery instead of the necroptotic one and RIPK1 degradation/cleavage might block the necroptotic pathway. The complete change

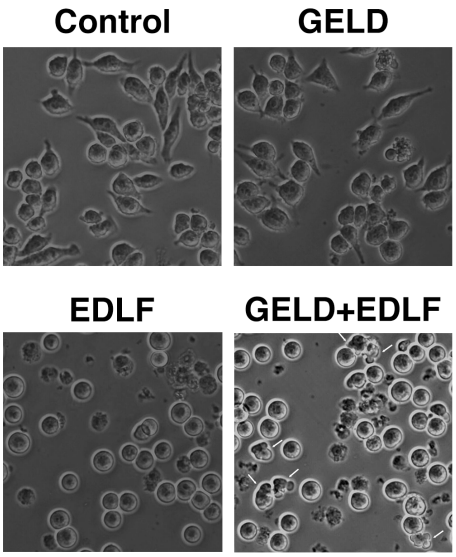

Figure 4.8: Representative bright-field microscopy images of U118 untreated control cells, U118 cells treated with 2 μM geldanamycin for 20 h (GELD), treated with 10 μM edelfosine for 6 h (EDLF), and pre-incubated with 2 μM geldanamycin for 14 h and then treated with edelfosine for additional 6 h (GELD + EDLF). Arrows indicate cells with apoptotic morphology in the GELD + EDLF treatment. Magnification 20x.

from a necroptotic type of cell death to an apoptotic one is not as sharp as in the case of U0126 combination with edelfosine; this could be due to a smaller decrease in ERK phosphorylation with the use of geldanamycin, and/or because Hsp90 function could interfere with many other proteins that could act as regulators of distinct cell death/survival signalling pathways, thus influencing cellular fate outcome.

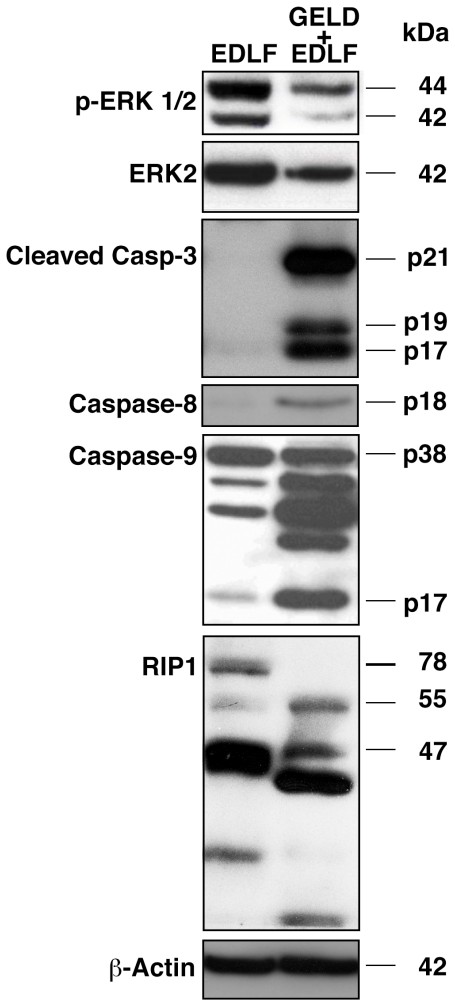

Figure 4.9: Western-blot analysis of U118 cells treated with 10 μM edelfosine for 4 h (EDLF), and cells pre-incubated for 14 h with 2 μM geldanamycin and then treated with 10 μM edelfosine for 4 h (GELD+EDLF). Immunoblotting was performed using specific antibodies against p-ERK 1/2, ERK2, cleaved caspase-3, caspase-8, caspase-9 and RIPK1. β-actin was used as an internal control for equal protein loading. Data shown are representative experiments of three performed.

Distinct cellular outcomes induced by edelfosine depending on drug concentration and ERK phosphorylation.

We found that different concentrations of edelfosine promoted different cellular outcomes in U118 cells. Incubation of U118 cells with low concentrations of edelfosine (between 0.1-1 μM) increased cell proliferation, whereas the ether lipid diminished cell proliferation when used at 5 μM, and promoted cell death at 10 μM (Figure 4.10a). By carrying out time-course experiments with 1-10 μM edelfosine treatments, we found that edelfosine induced a rapid and transient activation of ERK phosphorylation (Figure 4.10b), followed by a weak activation of caspase-3 when the level of ERK phosphorylation was decreasing (Figure 4.10b).

Duration of ERK phosphorylation was dependent of drug concentration. Thus, 10 μM edelfosine induced a more prolonged ERK phosphorylation than 1 μM (Figure 4.10b and Figure 4.11a). No cell death responses were observed at low drug concentrations (1-5 μM), whereas 10 μM edelfosine treatment led to a potent necrotic cell death with little apoptosis (Figure 4.11a). ERK phosphorylation did not prevent edelfosine-induced necrosis because, after a 9-h treatment, ERK phosphorylation was still high with high levels of necrosis (Figure 4.11a). Thus, edelfosine was able to promote either cell proliferation or necrotic cell death in U118 cells depending on the drug concentration used, but the apoptotic response was largely blocked. Interestingly, combining U0126 with edelfosine resulted in a dramatic increase in apoptosis, even when edelfosine was used at low concentrations (Figure 4.11b), suggesting that ERK phosphorylation restricts apoptosis following edelfosine treatment. These data suggest that ERK phosphorylation could act as a protective antiapoptotic response following edelfosine incubation, thus allowing the onset of additional cell responses, either survival or necrotic cell death. Once apoptosis is inhibited, low concentrations ($\leq$ 1 μM) of edelfosine would only be able to lead to survival, but when edelfosine concentration is high enough (10 μM) would lead to the generation of sufficient pro-cell death signals that lead to necrosis provided ERK is still activated (Figure 4.11a). However, the fact that pre-treatment of U118 cells with U0128 highly potentiates apoptosis in detriment of the other survival or necrotic responses suggests that inhibition of ERK phosphorylation leads to permissive conditions for the induction of apoptosis by edelfosine as the major cellular outcome (Figure 4.11b).

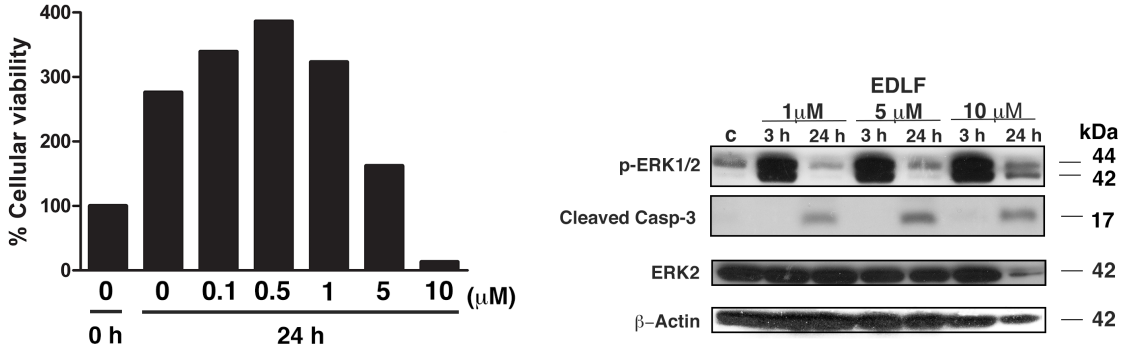

(a) (b)

Figure 4.10: (a) U118 cells were incubated in the absence or presence of the indicated concentrations of edelfosine for 24 h, and then analyzed by MTT assay. Cells at time 0 were also measured by MTT assay. Data are expressed as means of experimental triplicates and are representative of two independent experiments. (b) U118 cells were untreated (C) or treated with 1 μM, 5 μM, or 10 μM edelfosine (EDLF) for the indicated times, and then analyzed by immunoblotting, using specific antibodies against p-ERK1/2, cleaved caspase-3 and ERK2. β-actin was used as an internal control for equal protein loading.

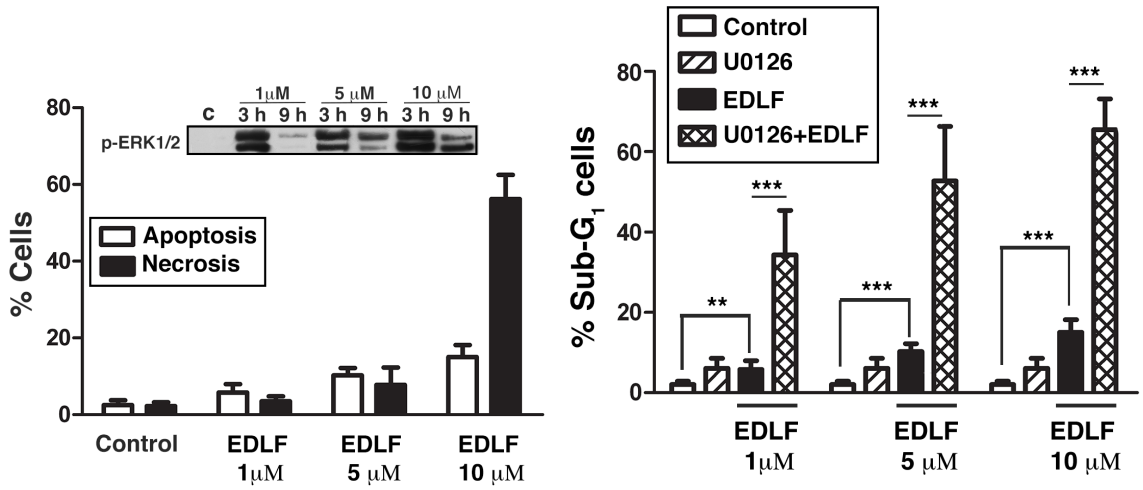

(a) (b)

Figure 4.11: (a) U118 cells were untreated (Control) or treated with 1 μM, 5 μM, or 10 μM edelfosine (EDLF) for 9 h. Apoptosis was evaluated as the percentage of cells in the Sub-G_1 phase of the cell cycle, and necrosis was determined following examination of cellular morphology under the microscope. Data shown are means ± SD of three independent experiments. ((a), inset) Representative western blot for p-ERK1/2 showing longer activation of ERK with higher doses of edelfosine. (b) U118 cells were pre-incubated in the absence (Control) or presence of 10 μM U0126, and then treated with 1 μM, 5 μM, or 10 μM edelfosine for 9 h, and analyzed by flow cytometry to evaluate apoptosis. Data shown are means ± SD of three independent experiments. $**$, $P < 0.01$; $***$, $P < 0.001$, Student's t-test.

5

Identification of a subpopulation of edelfosine-resistant U118 cells

We observed that following edelfosine treatment, the majority of the cells died through a necrotic process in a short period of time, but a small proportion of the cells (~10-20%) was resistant to the drug and did not die through apoptosis or necrosis. These surviving cells could be identified by examining cell morphology under the microscope (showing refringent cytoplasm as opposed to dark cells or fragments of dead cells, in which membrane rupture was evident in bright-field images) (Figure 5.1a); by using confocal microscopy and DIC images (Figure 5.1b); and by flow cytometry evaluation of different parameters, such as: cells that did not lose $\Delta\Psi_m$ (~26% after 18 h treatment (Figure 5.1c); cells that did not incorporate PI (~ 15% of the cells after 24 h treatment, although 12% of them are labeled with Annexin V, which might suggest an apoptotic response (Figure 5.1d), or cells that remained with normal FSC and SSC values (not shown). Although each of these parameters individually can not ascertain if a cell is alive or executing a cell death program, these data, in conjunction with the fact that these cells were able to proliferate again following drug removal, as will be described next, indicate that part of the treated cells were in fact resistant to edelfosine at this concentration that neverthless was enough to kill the majority of the U118 cells.

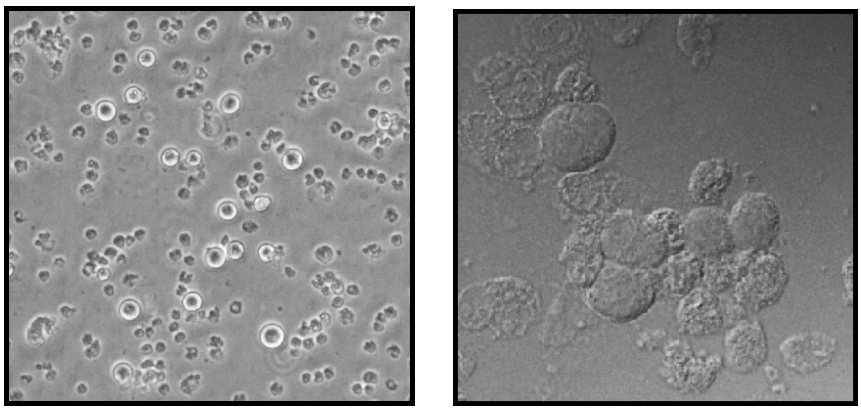

(a) (b)

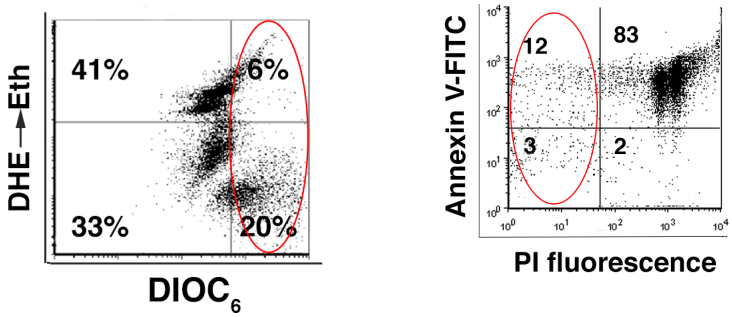

(c) (d)

Figure 5.1: (a) Bright-field image shows U118 cells treated with 10 μM edelfosine for 24 h. The majority of the cells are dead, but few cells remain with refringent cytoplasm. Magnification, 10x. (b) Differential interference contrast microscopy (DIC) shows that some of the cells did not lose plasma membrane integrity even after 24 h treatment with 10 μM edelfosine. Magnification, 63x. (c) U118 cells treated with 10 μM edelfosine for 18 h were analyzed for ROS generation (DHE -> Eth^{high}) and $\Delta\Psi_m$ disruption ($DiOC_6(3)^{low}$) by flow cytometry. ~26% of the cells did not lose $\Delta\Psi_m$ (upper+lower right quadrants). (d) Annexin V/ PI staining was analyzed in U118 cells treated with 10 μM edelfosine for 24 hours. ~15% of the cells do not show PI incorporation (left quadrants), although 12% of them are Annexin V^+ (upper left quadrant), which might suggest an apoptotic response. Percentages of cells in each quadrant are indicated.

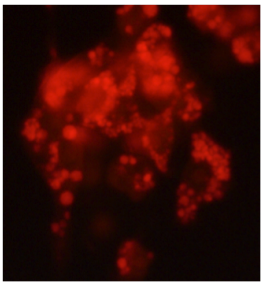

Figure 5.2: U118 cells were treated for 24 h with edelfosine 10 μM. The cell culture medium containing edelfosine was removed and replaced with fresh cell culture medium without the drug. Acridine orange stain reveals that edelfosine-treated-surviving cells display strong autophagy 96 h after edelfosine withdrawal. Magnification, 40x.

Edelfosine wash-off after 6-h treatment increases apoptosis/autophagy ratio in the U118 cells

After incubating the cells with 10 μM edelfosine for 24 hours and drug removal following that period of time, we observed that the few cells that survived displayed strong autophagy (Figure 5.2) and were able to proliferate again after a few days.

We next decided to investigate what would be the outcome if the cells were incubated with edelfosine for a shorter period of time (6 hours). At 6 hours, there was an arrest in the G_2 phase of the cell cycle as assessed by flow cytometry cell cycle analysis (Figure 5.3b), and many necrotic cells and few apoptotic cells could be observed, as previously described. However, follow-up of these treated cells after edelfosine wash-off, revealed a reduced proportion of cells dying with a necrotic morphology, and an increased percentage of apoptotic dying cells, as compared to cells that were mantained in the presence of the drug for more time. This suggests that edelfosine stimulus for 6 hours is enough to trigger cell death mechanisms, and possibly, the removal of the drug and reduced pressure of the stimulus allows for the apoptotic response to occur, preferably over the necroptotic one. Through cell cycle analysis, we found that the G_2 arrest following the 6-h edelfosine treatment was maintained up to 4-5 days with a progressive increase in the apoptotic fraction (Sub-G_1 cells) (Figure 5.3b). The increase in the apoptotic fraction in the following days after drug withdrawal is shown by strong caspase-3 activation (Figure 5.3a, immunoblot panel), higher percentage of cells in the Sub-G_1 fraction of the cell cycle (Figure 5.3b), and DAPI staining (Figure 5.3a, upper pannel).

The majority of the edelfosine treated cells, as mentioned before, displayed increased autophagy by 6 h of treatment (starting after ~3 hours). Removal of the drug resulted in an increased apoptosis rate and also in strong persistent activation of autophagy, as shown by LC3B immunoblotting (Figure 5.3a, immunoblot panel), increased monodansylcadaverine staining and acridine orange staining (Figure 5.4, upper and lower panels, respectively), that was maintained for up to 96 hours.

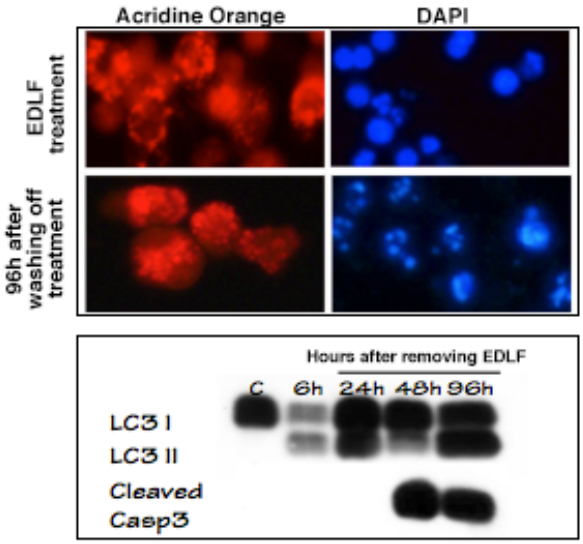

(a) Upper panel: U118 cells treated with 10 μM edelfosine for 24 h (EDLF treatment) and U118 cells 96 h after edelfosine 6-h treatment wash-off, display bright red fluorescence with acridine orange staining (magnification, 40x), and 96 h after drug removal pyknotic nuclei are evident following DAPI staining (magnification, 20x). Lower pannel: U118 untreated cells (C), U118 cells treated for 6 hours with 10 μM edelfosine (6 h), or treated for 6 h and then mantained without edelfosine for the indicated times, were analyzed by immunoblotting, using specific antibodies against LC3B-I/II and cleaved caspase-3.

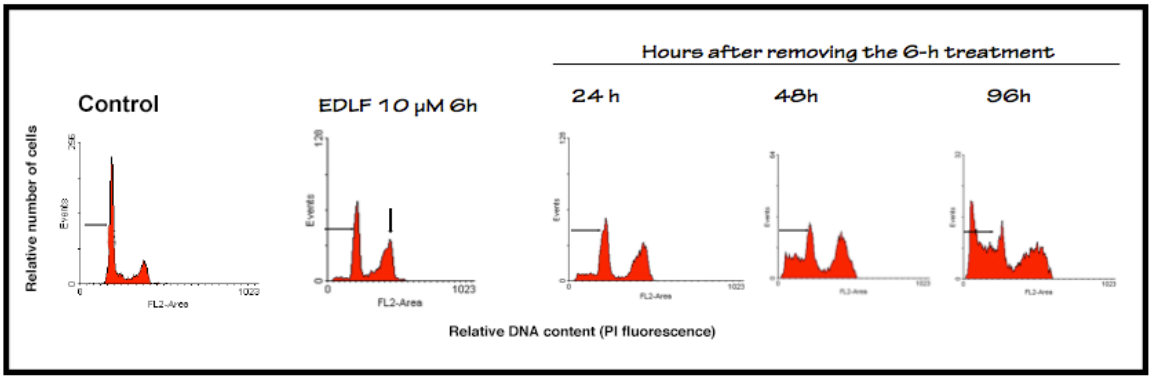

(b) Representative cell cycle analysis of U118 cells treated with edelfosine 10 μM for 6 hours and for the indicated times following removal of the 6-h treatment, firstly show cell cycle arrest in G_2 (indicated with a vertical arrow) and then a subsequent increase in Sub-G_1 phase (indicated in each histogram).

Figure 5.3

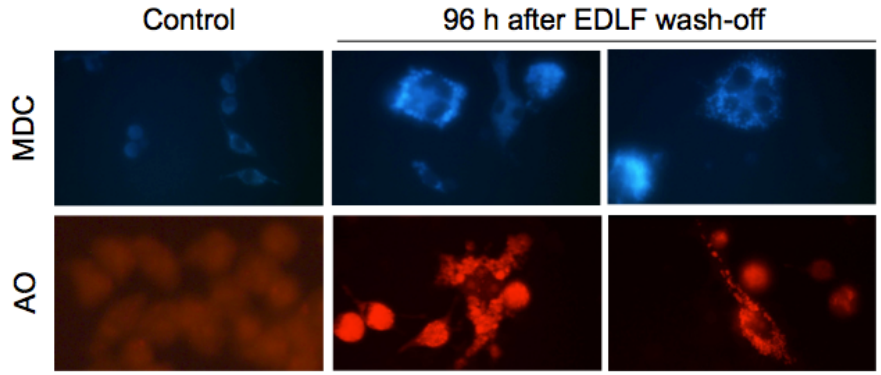

Figure 5.4: Untreated U118 cells (Control) or U118 cells treated with 10 μM edelfosine for 6 h, and then incubated for 96 hours in the absence of the drug, reveal strong autophagy by both acridine orange and monodansylcadaverine staining. 96 h after EDLF wash-off treatment magnification, 40x.

Surviving U118 cells undergo extensive multinucleation following edelfosine wash-off

Exposure to edelfosine resulted in changes in the size, appearance and growth of the cells. Over time, following edelfosine withdrawal, surviving cells increased their size and underwent extensive multinucleation (Figure 5.5). This fact was more prominent the longer the incubation period with edelfosine. Thus, after a 24-h treatment followed by drug wash-off, the surviving cells became bigger and contained a higher number of nuclei as compared to surviving cells after a 6-h drug treatment. Staining with Hoechst 3342 dye indicated that the giant cells were multi-nucleated, with up to 14 nuclei. Figure 5.6 shows a giant cell with 6 nuclei; the upper pannel depicts control cells for better appreciation of changes.

This finding was consistent with the flow cytometric data that is represented in Figure 5.7, assessed as the percentage of cells with more than 4n DNA content (PI fluorescence higher than that of the cells in the G_2 peak), although the flow cell sorting may underestimate the level of ploidy given that a proportion of the giant cells may have been sheared during the analysis; in fact, we would have expected a higher proportion of hiperploidy, since ~55% of the cells presented at least two nuclei as shown in a representative field of one of three experiments performed (Figure 5.8a). Figure 5.8b shows the multinucleated cells with increased magnification. Flow cytometry analysis also showed increased cellular granularity as detected by side-scatter counts (Figure 5.10a), and FSC was also increased, suggesting augmentation in cell size (Figure 5.10b). The strong reduction in those values 48 h after edelfosine wash-off may reflect better the increase in cell death than the minor population of surviving cells that keep increasing their size and number of nuclei, as sensitive cells continue dying by necrosis and apoptosis (Figure 5.3b).

The origin of these large multinucleated cells is uncertain, but because of the fact that the dying cells seem to be attached to the plasma membrane of the giant cells (Figures 5.11 and

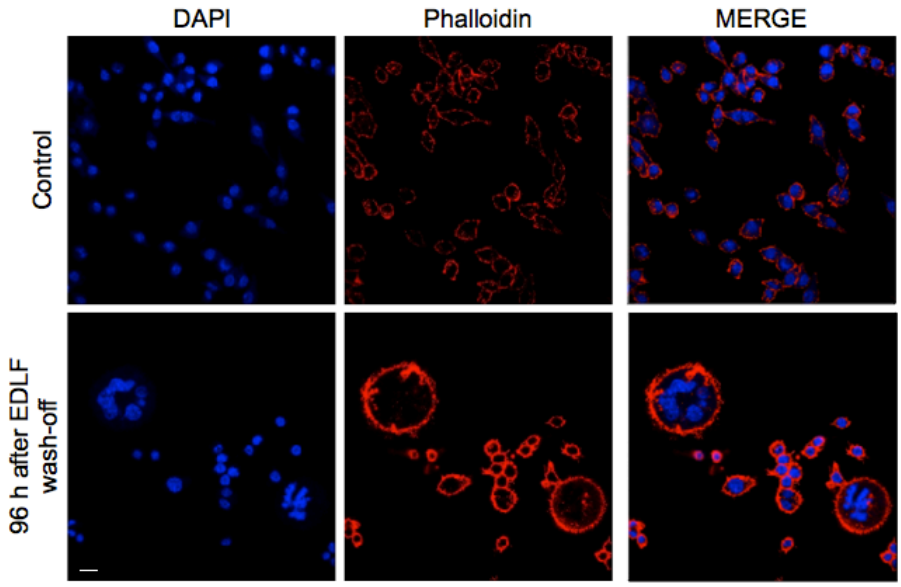

Figure 5.5: Control cells and U118 cells treated with edelfosine for 24 h, and then incubated in the absence of the drug for 96 h, were stained with DAPI and Alexa Fluor 594 phalloidin. Previously treated cells have increased size, with the presence of giant cells that are multinucleated. Magnification, 40x. Bar, 10 μm.

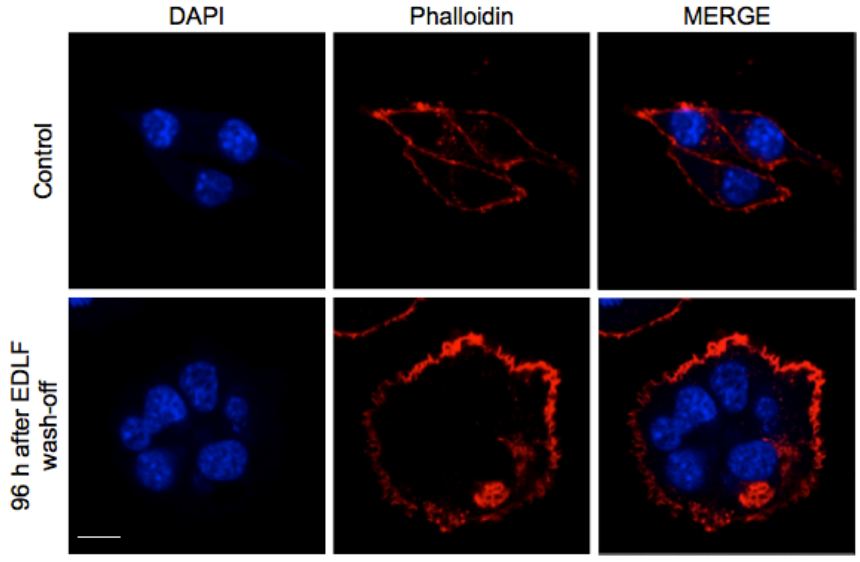

Figure 5.6: Control cells and U118 cells treated with edlefosine for 24 h, and then incubated in the absence of the drug for 96 h, were stained with DAPI and phalloidin. This figure shows control cells and one of the giant multinucleated cells for better appreciation of changes. Bar, 10 μm.

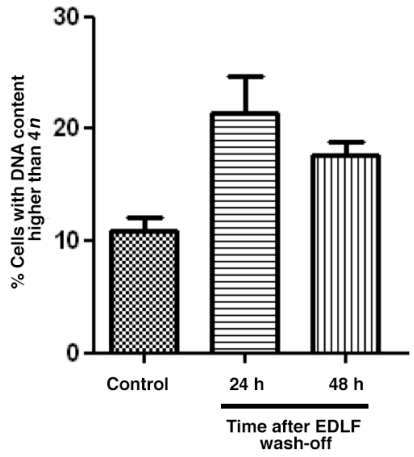

Figure 5.7: Untreated control cells and U118 cells that were treated with 10 μM edelfosine and then mantained without edelfosine for 24 h ou 48 h, were analyzed by flow cytometry and the percentage of multinucleated cells is represented (assessed as the percentage of cells with more than 4n DNA content, thus showing a PI fluorescence higher than that of the cells in the G_2 peak.

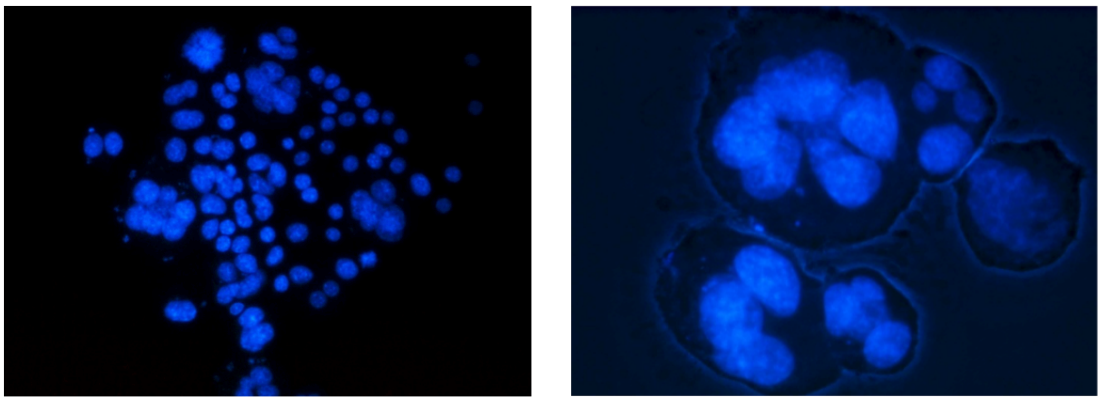

(a) (b)

Figure 5.8: (a) U118 cells treated with edelfosine 10 μM for 24 h were stained with DAPI, 96 h after edelfosine wash-off. One microscope field representative of the large number of multinucleated cells generated days after edelfosine removal, and representative of the heterogenity in the number, size and shape of the nuclei. Magnification, 20x. (b) U118 cells treated with edelfosine 10 μM for 24 h were stained with DAPI, 96 h after edelfosine wash-off. This is a zoomed-in image of the field in (a), observed with greater magnification, 40x.

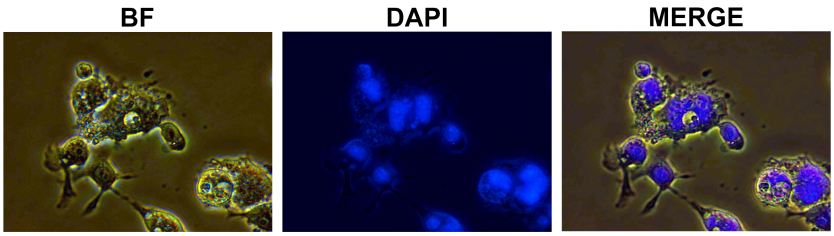

Figure 5.9: U118 cells treated with edelfosine 10 μM for 24 h were stained with DAPI, 96 h after edelfosine wash-off. Merging images of bright-field microscopy to visualize cell morphology and DAPI staining shows irregular size and shape of the nuclei.

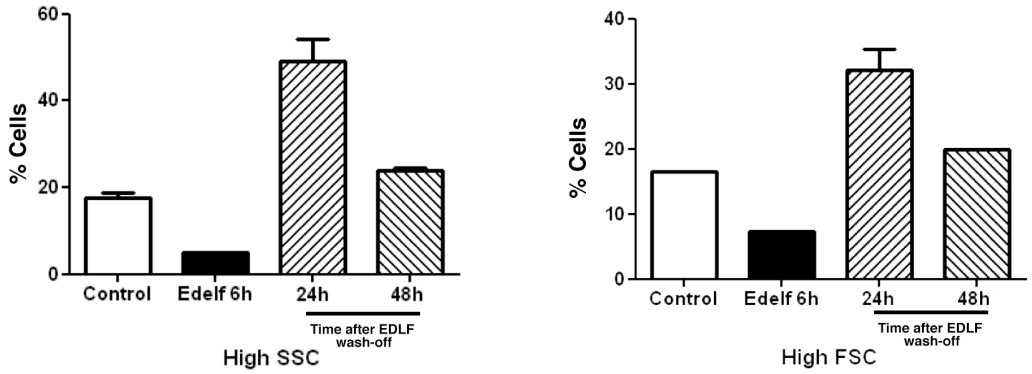

(a) (b)

Figure 5.10: (a) Flow cytometry analysis of untreated U118 cells (Control), cells treated with edelfosine 10 μM for 6 hours, and for the indicated times following removal of the 6-h treatment. There is a marked increase in cellular granularity as detected by side-scatter counts (SSC). (b) Flow cytometry analysis of cells treated as in (a) shows that there is an increase in forward scatter counts (FSC), reflecting increased cell size.

5.12) and the presence of distinct compartments within the cells (Figure 5.13), it is tempting to suggest the possibility that cell fusion between dying/dead cells and surviving cells may occur. The presence of different nuclei with degraded DNA, displaying bright green fluorescence inside a larger cell, could be detected using acridine orange staining (Figure 5.13). With phase contrast or differential interference contrast, margins of intracellular compartments could also be clearly marked off (Figure 5.13). The nuclei of the giant cells presented different sizes and shapes (Figures 5.14). External genetic material could be incorporated by the surviving cells, following complete engulfment of the cell or of cellular components of the dying cells containing DNA, as dead cells surrounding the bigger cells (Figures 5.11 and 5.12) progressively disappear, while bigger cells continuosly increased their size and number of nuclei. However, at least three mechanisms could account for multinucleated cell formation, namely: endomitosis, cell engulfment and/or cell fusion. Re-fusion, a process similar to acytokinetic mitosis, in which the two daughter cells from the mitosis remain connected by a cytoplasmic bridge and soon re-unite is preceded by incomplete cytokinesis (Rengstl *et al.*, 2013). Edelfosine has previously been shown to affect cytokinesis. We found abnormal microtubule patterns in surviving cells (Figure 5.15b), where we could not identify normal mitotic images (Figure 5.15b) as in control cells (Figure 5.15a).

Mitotic catastrophe is a cell death mode occurring during or shortly after a dysregulated/failed mitosis and can be accompanied by morphological alterations including micronucleation (which often results from chromosomes and/or chromosome fragments that have not been distributed evenly between daughter nuclei) and multinucleation (the presence of two or more nuclei with similar or heterogeneous sizes, derived from a deficient separation during cytokinesis). Mitotic catastrophe could also be responsible for the death of some of the U118 cells in the first days after edelfosine withdrawal, leading eventually either to apoptosis or necrosis.

The mitotic apparatus of the few proliferating giant cells was highly irregular and complex, with congested chromossomes and multifocal spindle forming microtubules (Figure 5.16). The polarity of spindles was disordered, and there was no evidence of cytoplasm division. Repetitive endomitosis with defective cytokinesis could also contribute to multinucleation in the surviving cells.

Using Ki-67 staining, we found a strong reduction in the number of cells cycling following edelfosine treatment (Figure 5.17b). During interphase, the Ki-67 antigen can be exclusively detected within the cell nucleus, whereas in mitosis most of the protein is relocated to the surface of the chromosomes. Ki-67 protein is present during all active phases of the cell cycle (G_1, S, G_2, and mitosis), but is absent from resting cells (G_0). The fact that few cells are in a proliferative state following edelfosine removal favours the hypothesis that at least part of the extra nuclear material may came from the dying cells.

Multinucleation was progressively reduced with the restoration of normal cellular proliferation. The number of large cells tended to decrease by the addition of fresh medium to the cell culture and with the ability of cells to proliferate normally, this fact supporting the notion that multinucleation could be a consequence of blocked cell cycle progression or

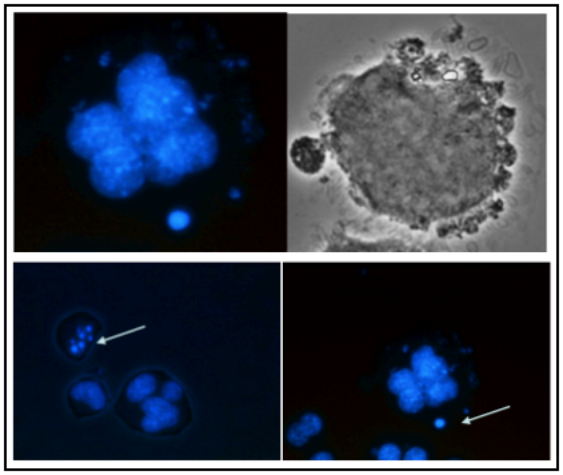

Figure 5.11: Bright-field and fluorescence microscopy images of a U118 cell that survived edelfosine treatment, 96 h following drug wash-off. DAPI staining reveals that the giant cell is multinucleated, and that there is DNA in the periphery of the cell.

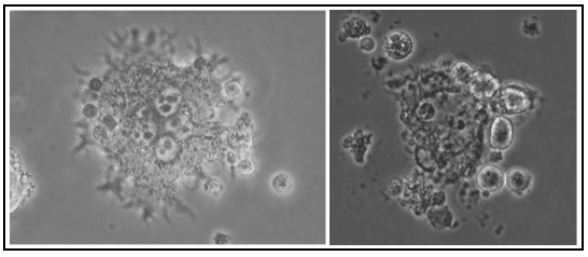

Figure 5.12: Bright-field microscopy image of a giant multinucleated U118 cell that survived 10 μM edelfosine treatment, 96 h after edelfosine wash-off. Dying or dead cells surround the giant cell, and seem attached to its plasma membrane. Magnification, 40x.

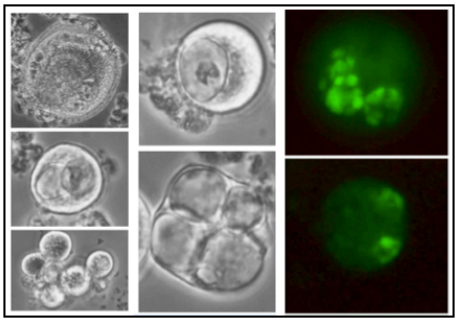

Figure 5.13: Bright-field microscopy and acridine orange stain fluorescence images of surviving cells, few days after efelfosine wash-off. The presence of distinct compartments within the cells might suggest the possibility that cell fusion between dying/dead cells and surviving cells may occur. The presence of different nuclei with degraded DNA, displaying bright green fluorescence inside a larger cell can be seen with acridine orange staining.

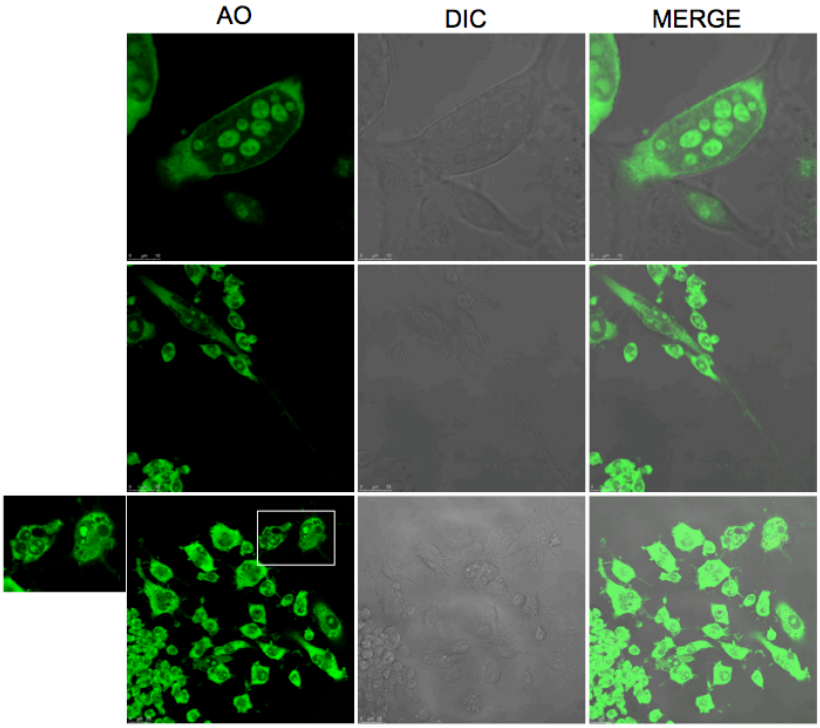

Figure 5.14: Confocal microscopy images of U118 cells, 4 days after 6-h 10 μM edelfosine treatment was removed. Following acridine orange (AO) staining, strong green fluorescence is visible in nuclear structures. Giant cells are multinucleated and nuclei show different sizes and shapes.

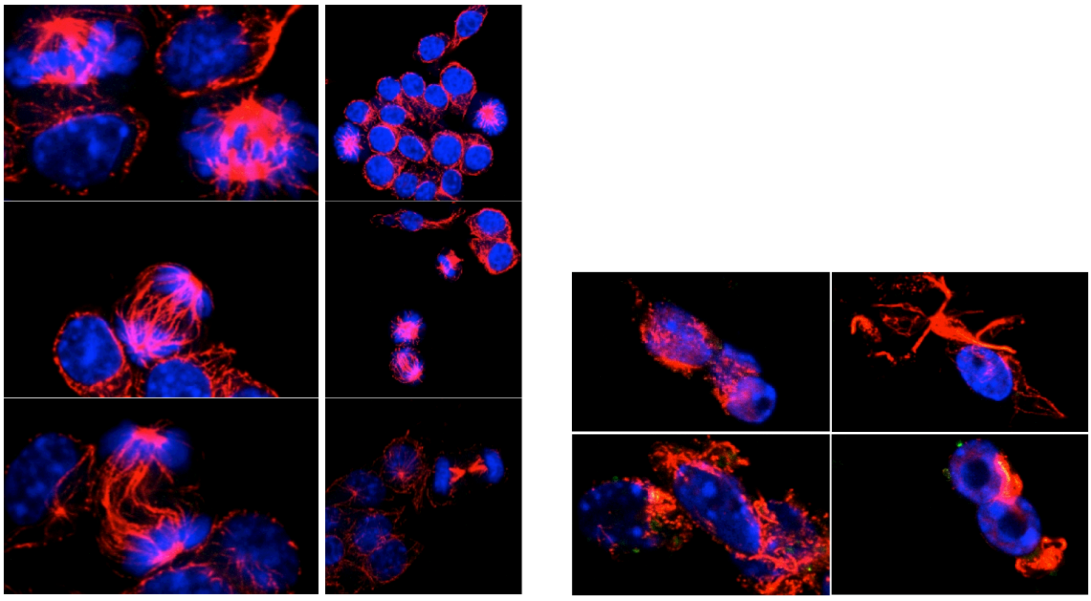

(a) (b)

Figure 5.15: (a) Confocal immunofluorescence microscopy of α-tubulin (red fluorescence) of untreated U118 cells shows cells undergoing mitosis. Nuclei were labeled with DAPI (blue fluorescence). (b) U118 cells that survived the 10 μM edelfosine treatment, 4 days after edelfosine removal. There are no cells undergoing normal mitosis and the α-tubulin shows an abnormal pattern of staining.

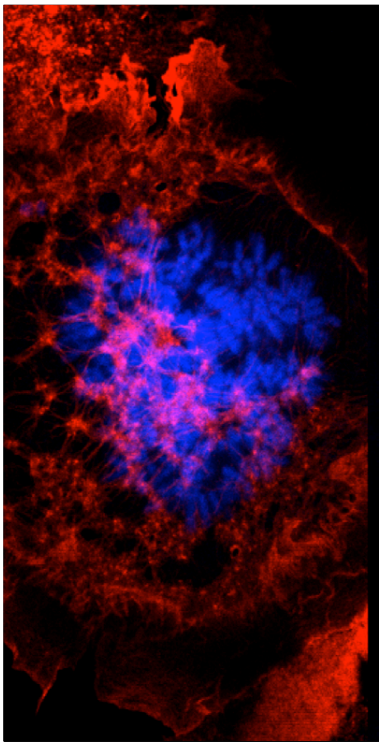

Figure 5.16: Confocal microscopy image of a giant cells showing highly irregular and complex mitotic apparatus, with congested chromossomes and multifocal spindle forming microtubules.

defects in cytokinesis, this way limiting the increase of the cell population. However, dead detached cells were also progressively removed, either by engulfment by the surviving cells or by the regular change of the culture medium, making it difficult to evaluate which of the processes (cell engulfment, blocked cell division) or even if both of them, are relevant to the formation of the large multinucleated cells.

With time, normal-sized cells started to grow at a normal pace for the U118 cell line, and giant cells became diluted in this new quickly growing population. After ~10 days, atypical pleomorphic cells with very long extensions could be seen, and the development of small "tumors", with cells growing on top of each other instead of the typical monolayer of cultured cells, together with the pseudopalisading appearance surrounding these areas of intense cell proliferation, were striking findings after edelfosine removal (Figure 5.19).

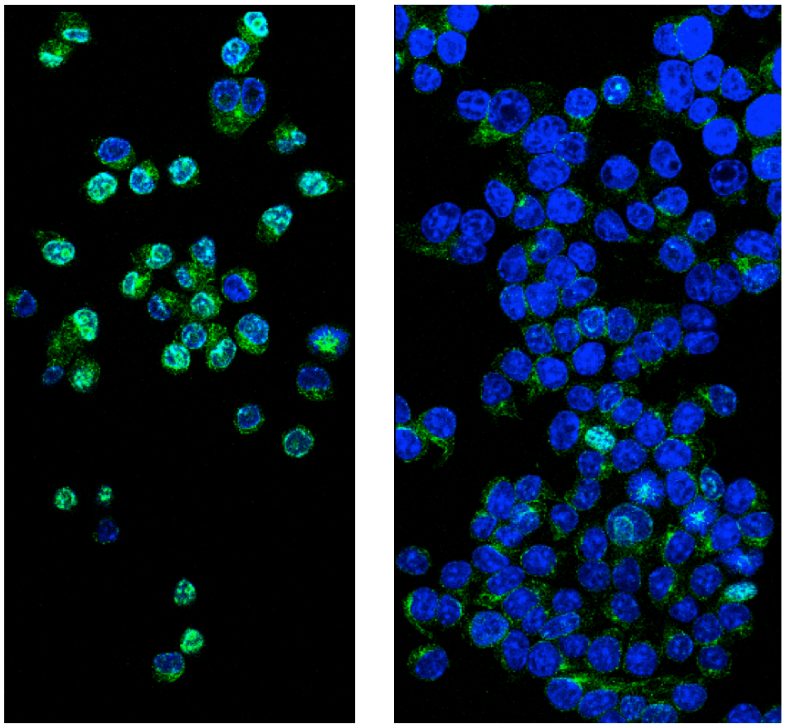

(a) (b)

Figure 5.17: (a) U118 untreated cells were fixed and stained with DAPI and a specific antibody against Ki-67-FITC conjugated. This is a representative confocal microscopy photograph (fluorescences merged), showing that ~77% of the cells were cycling (Ki-67+). Magnification, 40x. (b) U118 cells that survived the 10 μM edelfosine treatment, 4 days after edelfosine removal, were fixed and stained with DAPI and a specific antibody against Ki-67-FITC conjugated. There is a strong reduction in the number of cells that stain positive for Ki-67. Magnification, 40x.

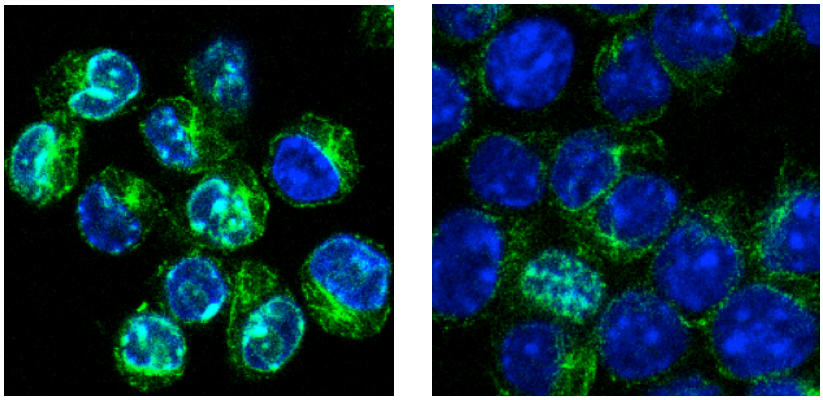

(a) (b)

Figure 5.18: (a) Greater magnification (63x) of U118 untreated cells stained with DAPI and a specific anti Ki-67 antibody, showing strong Ki-67 nuclear fluorescence, reflecting the presence of cells in a proliferative state. (b) Greater magnification (63x) of a field of U118 cells that survived the 10 μM edelfosine treatment, 4 days after edelfosine removal, stained with DAPI and a specific anti Ki-67 antibody; only one of the cells showed Ki-67 positive staining.

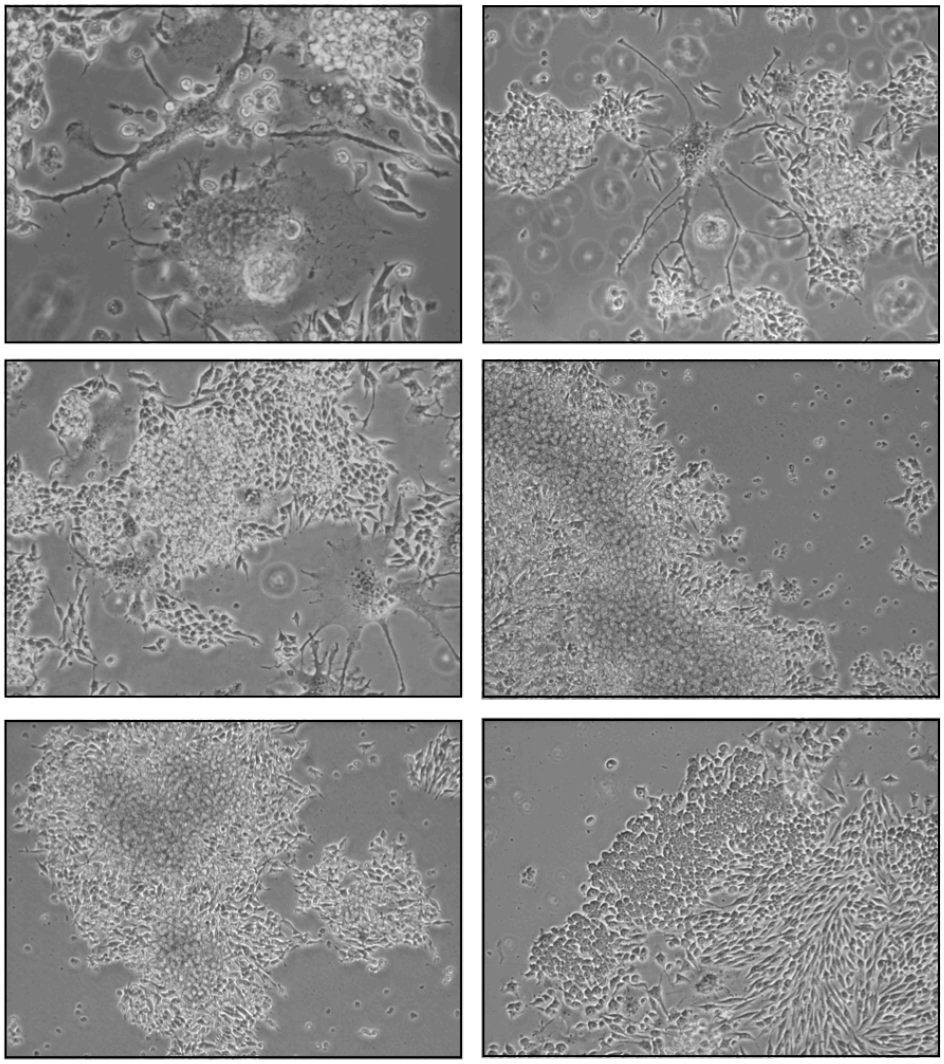

Figure 5.19: Bright-field microscopy images of U118 cells that survived edelfosine treatment, 10 days after edelfosine wash-off. Giant multinucleated cells are still visible but smaller cells have now recovered their normal proliferative state. The images show atypical pleomorphic cells with very long extensions, the development of small "tumors" in the cell culture plates, with cells growing on top of each other instead of in the typical monolayer and the pseudopalisading appearance surrounding areas of intense cellular proliferation.

The BH-3 mimetic ABT-737 inhibitor reduces cell survival and the number of giant multinucleated cells

We found that U118 cells overexpressed Bcl-x_L after 10 μM edelfosine treatment for 24 hours (Figure 5.20). Bcl-x_L has been shown to protect cells from apoptosis and also from necrotic types of cell death, and since the expression of Bcl-x_L increases with treatment time in the U118 cell line, being strongly expressed at 24 h, we decided to evaluate if it could be responsible for extended survival. Bcl-2 and Bcl-x_L have also been implicated in multinucleation and cellular fusion events (Minn *et al.*, 1996; Nuydens *et al.*, 2000).

With that hypothesis in mind, and since we have observed a very important reduction in Bcl-x_L expression when we pre-treated cells with U0126 (Figure 5.20) together with a reduced number of cells surviving to this combined treatment, we decided to evaluate the effect of Bcl-x_L inhibition in the surviving cells.

We first treated U118 cells with 10 μM edelfosine for 6 hours, washed-off the drug and then added ABT-737. This resulted in increased cell death compared to cells not treated with ABT-737, as shown by less cells with refringent cytoplasm and more cells with increased necrotic and apoptotic morphology under the microscope (Figure 5.21, upper pannel), and by flow cytometer analysis, where an increase in the Sub-G_1 population of the cell cycle together with a higher number of cells with decreased FSC and SSC values could be seen (Figures 5.22a; 5.22b), indicating the presence of a higher number of dead cells.

Incubation with ABT-737, following 10 μM edelfosine removal led to an increased loss of mitochondrial membrane potential (Figure 5.23) and a stronger activation of caspase-9 (Figure 5.24), resulting in increased cell death through apoptosis (Figure 5.22a).

Besides the reduction in the number of the surviving cells, we also found a very significant decrease in the number of multinucleated cells, and among these, in the number of nuclei per cell. We found that the effect on the formation of multinucleated cells was stronger if we let the cells recover for 24 hours after edelfosine removal, and then add ABT-737, as opposed to adding ABT-737 immediately after edelfosine withdrawal, suggesting that Bcl-x_L is important for both the survival and the multinucleation process at that stage, and that maybe these two processes are connected and interdependent. The clear reduction in the total number of

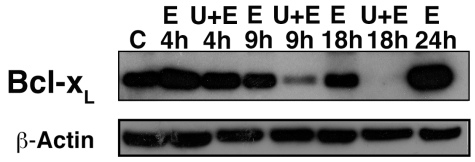

Figure 5.20: U118 untreated cells (C), cells treated with 10 μM edelfosine for the indicated times (E x h), and cells pre-incubated for 2 h with 10 μM U0126 and then with 10 μM edelfosine for the corresponding indicated times (U + E x h), were analyzed by immunoblotting using a specific antibody against Bcl-x_L. β-actin was used as an internal control for equal protein loading in each lane.

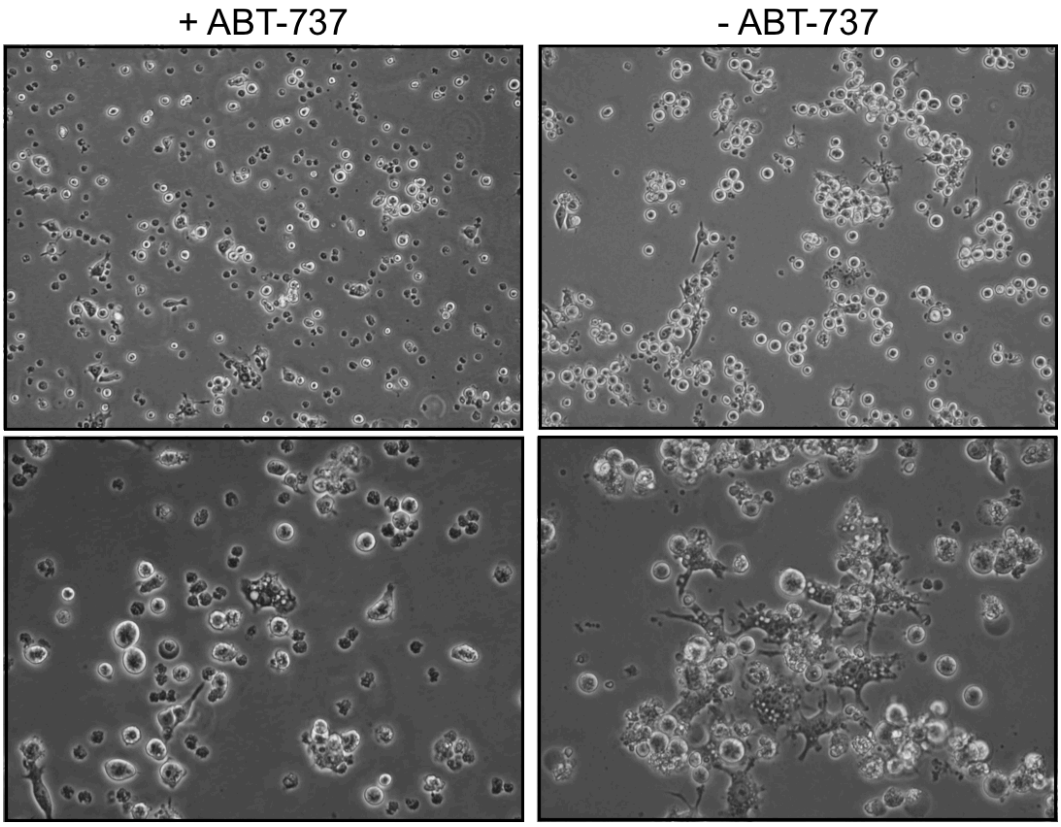

Figure 5.21: Representative bright-field microscopy images of U118 cells 24 h after removal of the 6-h 10 μM edelfosine treatment (-ABT-737), and of U118 cells that following the 6-h treatment wash-off were incubated with ABT-737 for 24 h (+ABT-737). Upper pannels with 10x amplification and lower pannels with 20x amplification.

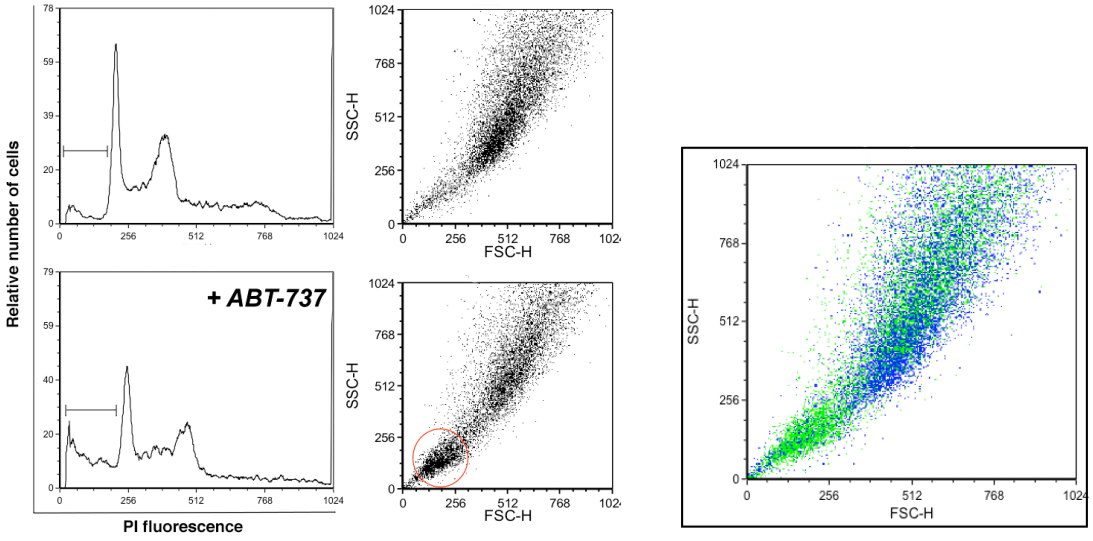

Figure 5.22: (a) Cell cycle flow cytometry analysis (histograms) and respective FSC/SSC plots of U118 cells 24 h after removal of the 6-h 10 μM edelfosine treatment (upper histogram and plot) and of U118 cells that after edelfosine wash-off were incubated with ABT-737 for 24 h (lower histogram and plot), showing an increased Sub-G_1 population in the cells that were treated with the BH-3 mimetic inhibitor. (b) Overlay of the FSC/SSC plots of both treatments, showing in green the cells that were treated with ABT-737 and show lower values of FSC and SSC as compared to cells that were not treated with ABT-737, shown in blue, and mostly survived.

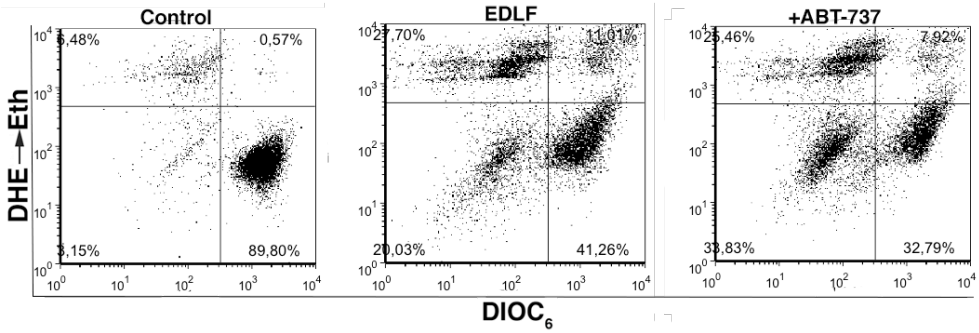

Figure 5.23: U118 cells 24 h after removal of the 6-h 10 μM edelfosine treatment and U118 cells that were incubated with ABT-737 for 24 h after 10 μM 6-h edelfosine treatment wash-off, were analyzed for ROS generation ((DHE -> Eth)^{high}) and $\Delta\Psi_m$ disruption ($DiOC_6(3)^{low}$) by flow cytometry. Control untreated cells were run in parallel. ABT-737 cells show an increased loss of $\Delta\Psi_m$ (lower left quadrants).

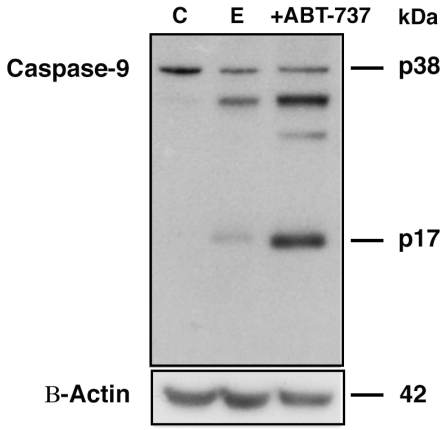

Figure 5.24: U118 untreated cells (Control, C), cells treated for 6 h with 10 μM edelfosine, 24 h after drug removal (E) and U118 cells incubated with ABT-737 for 24 h following 10 μM edelfosine 6-h treatment wash-off (+ ABT-737), were analyzed by immunoblotting using a specific antibody for caspase-9. β-actin was used as an internal control for equal protein loading in each lane.

cells, and on the multinucleated cells, can be seen in Figure 5.25. There were much more cells in the edelfosine only-treated plates, and a high proportion of them were multinucleated cells, while in ABT-737 treated plates there were few surviving cells and those were mono or binucleated (Figure 5.25). PI fluorescence also indicated a lower percentage of cells with hiperploidy after using ABT-737 (Figure 5.26).

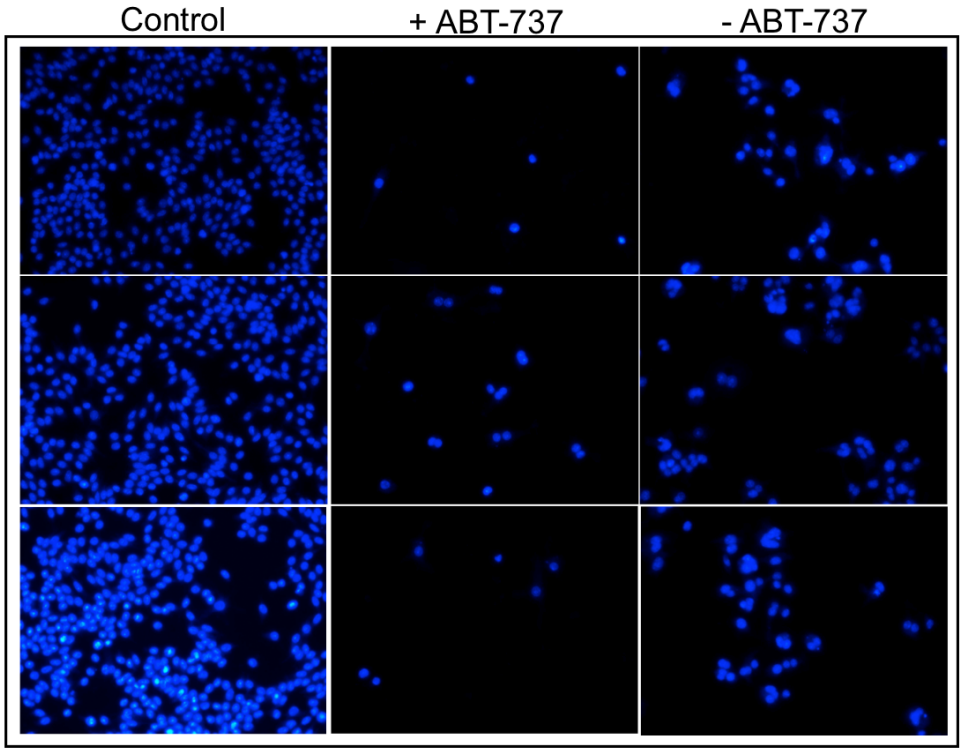

Figure 5.25: U118 untreated cells (Control), cells treated with 10 μM edelfosine for 6 h and then incubated with ABT-737 24 h after edelfosine removal for another 24 hours (+ABT-737) or incubated in the absence of ABT-737 for 48 h following the 6-h treatment edelfosine wash-off (-ABT-737), were stained with DAPI. Detached cells were removed before staining. Representative fields of ABT-737 treatments show much less cells alive and that the few resistant ones are mono or binucleated.

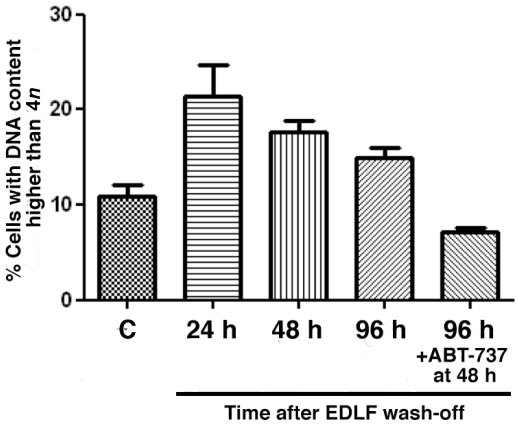

Figure 5.26: Flow cytometry analysis of the DNA content of U118 cells (measured by PI fluorescence) treated with 10 μM edelfosine for 6 h, after the indicated times following edelfosine wash-off, or with the addition of ABT-737 at 48 h of edelfosine wash-off, for 24 h (+ABT-737 at 48 h). Histogram represents the percentage of cells for each treatment with DNA content higher than 4n.

Bcl-x_L mediates cell survival following edelfosine treatment

When U118 cells were incubated with 10 μM edelfosine, most of them lost mitochondrial membrane potential after few hours of treatment, but some cells (~20%) remained intact regarding $\Delta\Psi$m (Figure 4.5) at 18 h after treatment. Bcl-x_L was downregulated by pre-treatment with U0126 and in that case practically all the cells underwent a total $\Delta\Psi$m loss (~95%). We could detect a stronger activation of caspases-9 and -3, more apoptotic cell death and less surviving cells. When we used ABT-737 to inhibit overexpressed Bcl-x_L in the surviving cells, we obtained again an increase in $\Delta\Psi$m loss, higher activation of caspase-9 and apoptosis, and less cells were able to survive. These results suggest an important role for Bcl-x_L in mediating cell resistance to edelfosine and in blocking cell death, either by apoptosis or/and necroptosis. Also, activation of apoptosis instead of necroptosis appears to favor cell death and reduce the percentage of resistant surviving cells.

These results suggest that although the necroptotic pathway is a very fast and highly efficient form of cellular demise after edelfosine treatment in the U118 cell line, the activation of this program instead of the apoptotic one is also allowing the survival of some cells that seem not to be resistant to the apoptotic cell death program, but that are resistant to necroptosis and are allowed to survive since apoptosis is blocked. The MEK inhibitor U0126, geldanamycin, or direct Bcl-x_L inhibition seem to re-direct the execution of cell death to the apoptotic program, which ends up in all cases with less surviving cells.

Generating a resistant cell line - U118-R

Observing that a subpopulation of U118 cells was resistant to edelfosine treatment, we decided to select this population and further increase its tolerance to the drug, in order to compare it with the general/normal population of U118 cells and thus gain insight into possible mechanisms of resistance.

Incubation of U118 cells with increasing concentrations and increased time of exposure to edelfosine (allowing the cells to recover and proliferate normally before repeating the treatment) led to the generation of super-resistant cells, which were able to tolerate ~10 times higher doses of edelfosine than the original U118 cell line. This new cell line was named U118-R, and resulted from the selection of the cells that survived edelfosine treatment and that, as already mentioned, presented strong autophagy following drug removal and were often multinucleated giant cells. In each step of the resistance generation process, we allowed normal proliferation and morphology to be restored before repeating the treatment with edelfosine, either at the same concentration for a longer period of time, or at an increased dose. The time taken to restore normal proliferation varied, and seemed to be dependent on the confluence of the cells that remained viable after treatment, and also on the number of culture medium changes performed. In general, cells recovered 10 to 12 days after drug removal, as observed by a normal rate of proliferation, normal cell cycle, normal morphology with reduction in the number of multinucleated/giant cells, and also normal expression level

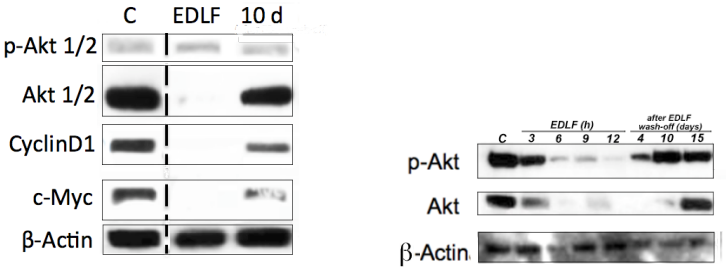

(a) (b)

Figure 5.27: (a) Immunoblot analysis of U118 untreated cells (C), U118 cells treated with 10 μM edelfosine for 24 h (EDLF), and U118 cells that survived 10 μM edelfosine 24-h treatment, 10 days after drug removal (10d). Cells were analyzed using specific antibodies against p-Akt 1/2, Akt 1/2, cyclin D1 and c-Myc. Immunoblotting for β-actin was used as an internal control for equal protein loading in each lane. Data shown are representative of three independent experiments. (b) U118 untreated cells (C), cells treated with 10 μM edelfosine for increased times (3, 6, 9 and 12 h), and cells that survived edelfosine treatment incubated in the absence of the drug for 4, 10 and 15 days were analyzed using specific antibodies against p-Akt 1/2 and Akt 1/2. Immunoblotting for β-actin was used as an internal control for equal protein loading in each lane.

of proteins such as Akt, cyclin D1 and c-Myc, all found to be strongly downregulated at 24h treatment, but having their levels of expression restored 10 days after edelfosine removal, as seen in figure 5.27a. Decrease in the total level of Akt1/2, and p-Akt upon edelfosine treatment, followed by an increase in those protein bands after edelfosine withdrawal, can be seen in Figure 5.27b.

U118 cells tolerated an extended time of exposure to the same concentration they had experienced before better than an increase in drug concentration. However, after selecting cells that were able to survive to ~40 μM of edelfosine, these cells could tolerate more easily progressive increases in drug concentration, even a 20 μM increase in one step, and if then the drug was removed within 24 hours they started to proliferate more quickly than their precedent cells did, after their correspondent lower dose had been removed.

We obtained a very high level of resistance to edelfosine after following the stepwise scheme of drug incubation, allowing the referred recovery phases between each step, as follows:

Generating intermediate level of resistance:

10 μM 48 h; 10 μM 90 h; 20 μM 70 h; 60 μM 24 h; 60 μM 48 h; 90 μM 48 h

Generating super-resistant U118-R:

10 μM 48 h; 10 μM 90 h; 20 μM 70 h; 60 μM 48 h; 90 μM 48 h; 100 μM 24 h; 120 μM 24 h

The results that will be presented next were obtained using this super-resistant cell line, that will be labeled only as U118-R from now on.

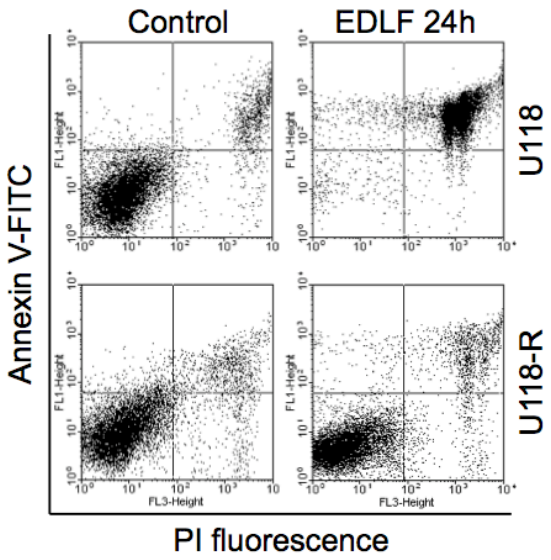

Figure 5.28: U118 cells and U118-R cells treated with 10 μM edelfosine for 24 h were analyzed for Annexin V/PI staining. Control cells were run in parallel for each cell line. At 24 h the majority of the U118 cells are Annexin V^+/PI^+, while U118-R cells remain Annexin V^-/PI^-.

When treating U118-R cells with the same drug concentration that killed U118 cells, 10 μM, we could not detect necrosis, increase in ROS production or loss of mitochondrial membrane potential. There was no significant increase in PI incorporation or Annexin-V staining even after 24 hours of edelfosine treatment (Figure 5.28), and no major morphological changes could be identified at 20 μM or even 50 μM (Figure 5.29).

Confirming that no major changes were occuring at these drug doses, we found that expression levels of JNK1, ERK2 and cyclin D1 were not affected by 10 μM or 50 μM edelfosine in U118-R cells, as opposed to the strong changes observed in the expression of these proteins for the U118 cell line at 10 μM edelfosine (Figure 5.30).

Figure 5.31a depicts LC3B, p-ERK and p-Akt pattern of expression for the U118 cell line (C), the U118 cell line treated with 10 μM edelfosine for 24 h (T), and for the untreated resistant cell line U118-R (R). Autophagy is strongly activated during treatment and also in the first days following edelfosine wash-off, however U118 and U118-R cells show similar basal levels of autophagy. p-ERK is first strongly activated in edelfosine-treated U118 cells, however the amount of phosphorylated protein progressively diminishes during treatment, probably as a consequence of strong total ERK protein downregulation (Figure 5.30). Resistant cell line U118-R shows higher levels of basal ERK phosphorylation. p-Akt and Akt are dramatically reduced after 24 hours of edelfosine treatment, but again are expressed and phosphorylated in the resistant cell line (Figure 5.31a).

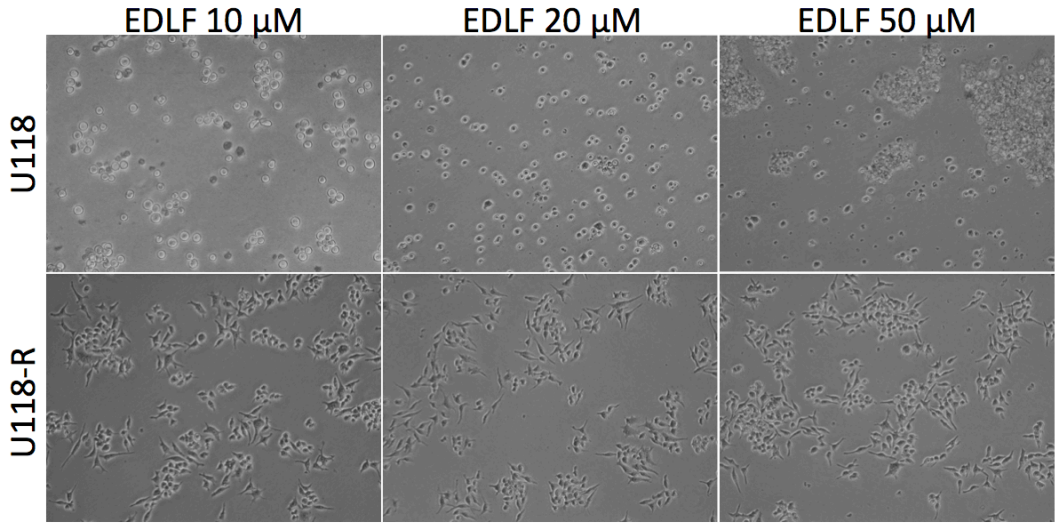

Figure 5.29: Bright-field microscopy images of U118 and U118-R cells treated with 10, 20 and 50 μM edelfosine, showing that the resitant cell line does not undergo morphological changes even when incubated at the higher concentration.

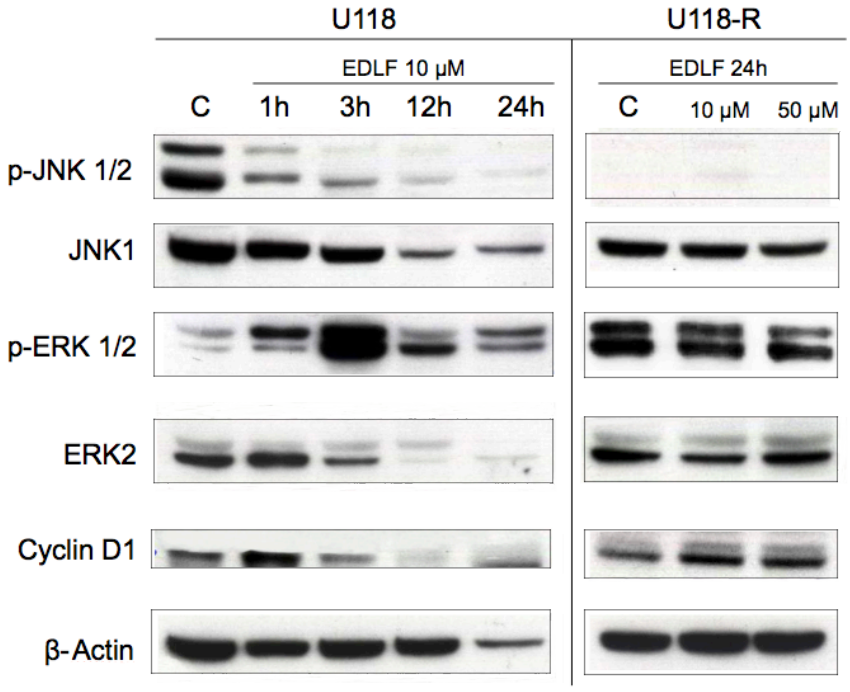

Figure 5.30: U118 untreated cells (C, U118), U118 cells treated with edelfosine 10 μM for the indicated times, U118-R cells (C, U118-R), and U118-R cells treated with 10 μM or 50 μM edelfosine for 24 h were analyzed by immunoblotting using specific antibodies against p-JNK1/2, JNK1, p-ERK1/2, ERK1/2 and cyclin D1. Immunoblotting for β-actin was used as an internal control for equal protein loading in each lane.

U118-R cells show higher basal phosphorylation of ERK1/2

Basal levels of ERK phosphorylation were higher in the U118-R than in U118 cell line (Figures 5.30 and 5.31a), however, following 10 μM edelfosine treatment there was no further increase in ERK phosphorylation in the resistant cell line at the observed 24 h time point (Figure 5.30). ERK2 levels were stable in U118-R treated cells, while a strong decrease was observed in the U118 cell line (Figure 5.30). As observed for other proteins, including β-actin, total ERK2 could be reduced due to generalized protein degradation as a consequence of autophagic and necroptotic processes following edelfosine admnistration in the U118 cell line, this possibility being supported by the finding that strong protein ubiquitination occurs in edelfosine treated cells (results not shown). Since these processes are not activated in the U118-R cells until a very high concentration of the drug is used, this could be the reason for the maintenance of stable levels of proteins, including ERK, following edelfosine treatments of 10-50 μM. However, challenging U118-R cells with higher doses, we observed the same phenotype of cell death as in U118 cells, but at a concentration ~10 times higher: at 100 μM almost all the cells died with necrotic morphology, also displaying autophagy and a reduced proportion of apoptotic cell death. Autophagy was activated when a 50 μM concentration was used, and was also strongly activated during cell death of the U118-R cells at 90 μM (Figure 5.31b). In the U118-R cells, even 90 μM edelfosine could not totally abolish Akt expression, although it was strongly reduced (Figure 5.31b).

Cells that do not execute apoptosis, possibly due to p-ERK mediated blockade of this pathway, and that are also resistant to necrosis, are selected during the treatments as the surviving fraction, resulting in a final population of cells with higher levels of p-ERK. ERK phosphorylation, while avoiding apoptosis, does not block necroptosis, and in the presence of p-ERK, U118 cells activate survival signalling, mainly through the activation of NF-κB. We found NF-κB to be degraded only in the presence of the MEK1/2 inhibitor U0126, or p-ERK inhibition and apoptosis activation.

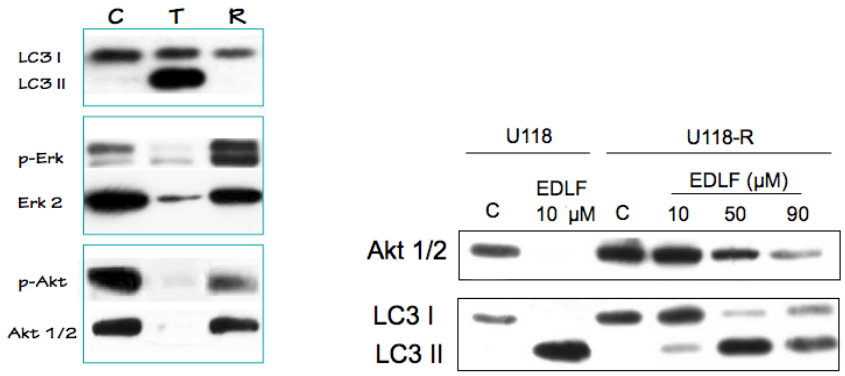

(a) (b)

Figure 5.31: (a) U118 untreated cells (C), U118 cells treated with 10 μM edelfosine for 24 h (T) and U118-R untreated cells (R), were analyzed by immunoblotting using specific antibodies against LC3B-I/II, p-ERK1/2, ERK2 and p-Akt/Akt1/2. (b) U118 untreated cells (C, U118), U118 cells treated with 10 μM edelfosine for 24 h (U118, EDLF 10 μM), U118-R untreated cells (C, U118-R), and U118-R cells treated with the indicated concentrations for 24 h were analyzed by immunoblotting using specific antibodies against Akt 1/2 and LC3B-I/II.

Edelfosine incorporation is strongly reduced in U118-R cells

We next evaluated if edelfosine incorporation was affected in the resistant cell line. By using an edelfosine fluorescent analogue, Et-BDP-ET (1-*O*-(11′-(6″-ethyl-1″,3″,5″,7″-tetramethyl-4″,4″-difluoro-4″-bora-3a″,4a″-diaza-*s*-indacen-2″-yl)undecyl)-2-*O*-metil-*rac*-glycero-3-phosphocholine, we saw that edelfosine incorporation was strongly reduced in the resistant cell line, comparing to the U118 cells. We confirmed this by flow cytometry analysis (Figure 5.32) and confocal microscopy (Figure 5.33). Flow cytometry analysis showed that the level of drug incorporation was rather heterogeneous among U118 cells, and that a small subset of them had markedly reduced incorporation (blue circle in the histogram (Figure 5.32)); these cells could be more resistant to the drug and be selected in the survival fraction, resulting in a progressive enrichment in these cells, ultimately leading to the extremely homogeneous edelfosine-low incorporating U118-R cell line (red peak in the histogram (Figure 5.32).

We found that edelfosine incorporation was reduced when incubating the cells at 4ºC, but even at that temperature, U118 cells incorporated more edelfosine that U118-R at 37ºC (Figure 5.34).

Reduced incorporation of the drug could be an explanation, at least in part, for the fact that the dose used to kill the normal cell line (10 μM) was insufficient to cause cell death in the resistant cell line, and this could be due to various reasons: decreased expression of proteins involved in edelfosine uptake; increase in expression and/or activity of edelfosine extrusion pumps and also to changes in the fluidity/compositon of the cell membrane that would affect edelfosine incorporation. The fact that temperature affects the incorporation of the drug makes it reasonable to assume that some kind of energy-dependent mechanism is used to

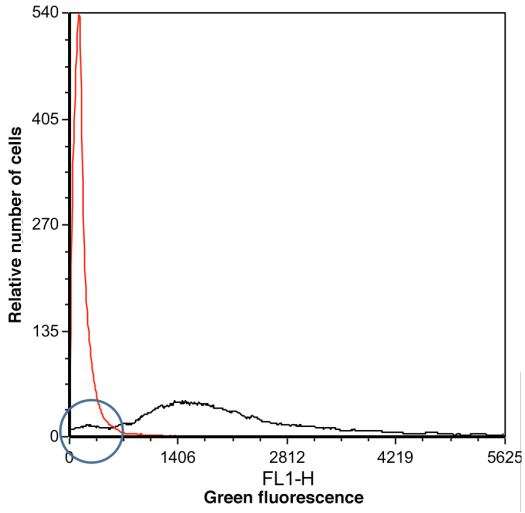

Figure 5.32: U118 cells and U118-R cells were incubated with 10 μM edelfosine analogue conjugated with the fluorophore BODIPY (Et-BDP-ET) for 4 h and fluorescence was analyzed by flow cytometry.

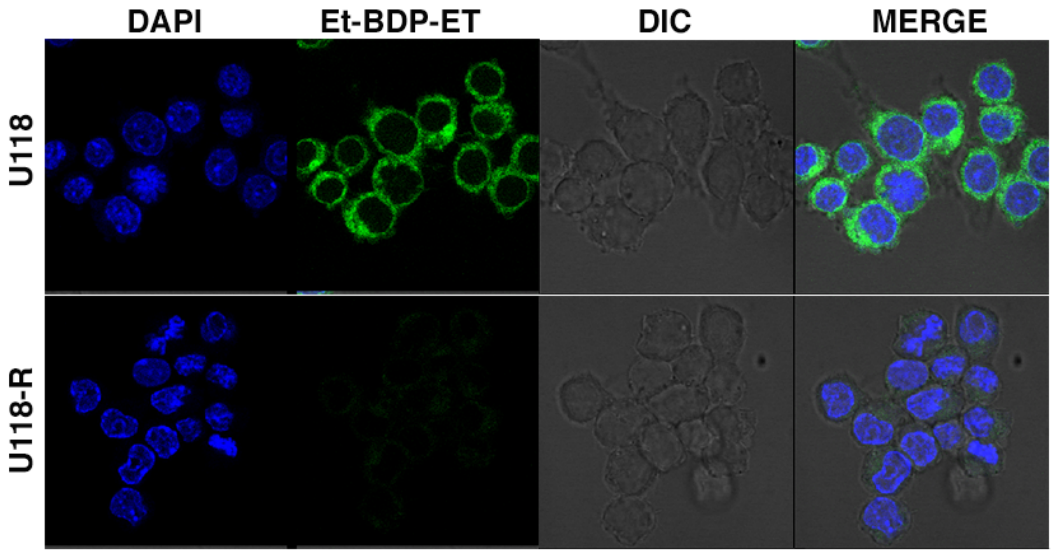

Figure 5.33: U118 and U118-R cells were incubated with the fluorescent analogue Et-BDP-ET for 1 h and nuclei were stained with Hoechst. Confocal microscopy images show reduced fluorescence and incorporation of edelfosine in U118-R cells.

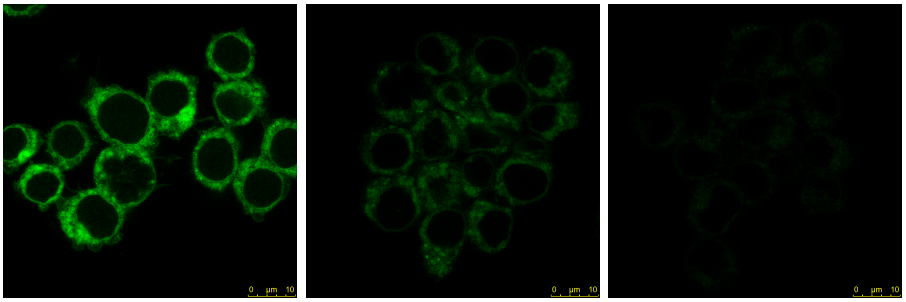

(a) (b) (c)

Figure 5.34: Incorporation of Et-BDP-ET in U118 cells, incubated with the fluorescent analogue at 37ºC (a); reduced incorporation of the drug when U118 cells were incubated with Et-BDP-ET at 4ºC (b) and U118-R cells show even more reduced incorporation, even when incubated at 37ºC (c).

transport edelfosine and that it is slowed down at lower temperatures; it is also possible that temperature affects membrane fluidity consequently affecting edelfosine incorporation into the plasma membrane.

6

Types of cell death induced by edelfosine in other glioblastoma cell lines and possible ways to increase cell death - where to interfere in order to maximize cell death and avoid drug resistance

Effect of edelfosine in the induction of cell death in SF268 cells

SF268 cell line was quite resistant to all the ether lipids evaluated, even when tested at a 30 μM concentration. ErPC, ErPC3 and OlPC did not induce visible changes or cell death, even at 50 μM, and cells continued to proliferate normally. Perifosine and miltefosine caused cellular detachment from the culture plate, and a temporary cytostatic effect. Few cells died when treated with miltefosine, and many continued to proliferate normally. Perifosine-treated cells detached from the culture plate and cell death increased by raising the drug concentration used. Analyzing cell cycle, however, less then 10% corresponded to cells with a Sub-G_1 DNA content, for all the ether lipids evaluated, as shown for a representative experiment in Figure 6.1. Since edelfosine was the ether lipid that mostly impacted cell morphology and proliferation, and also caused the highest apoptosis induction (although very modest), we again decided to only further evaluate edelfosine effects on the SF268 cell line.

Concentration-dependent assays showed that 20 μM of edelfosine was the optimum drug concentration for the inhibition of cell proliferation, as assessed by MTT assays (Figure 6.2). We found that 10 μM edelfosine caused an important reduction in cell proliferation but did not completely prevent cell growth, since after 24 hours of drug incubation MTT absorbance values were higher than those at the beginning of the experiment (Figure 6.2). 20 μM and 30 μM edelfosine had a similar effect on inhibiting cellular proliferation but caused limited cell

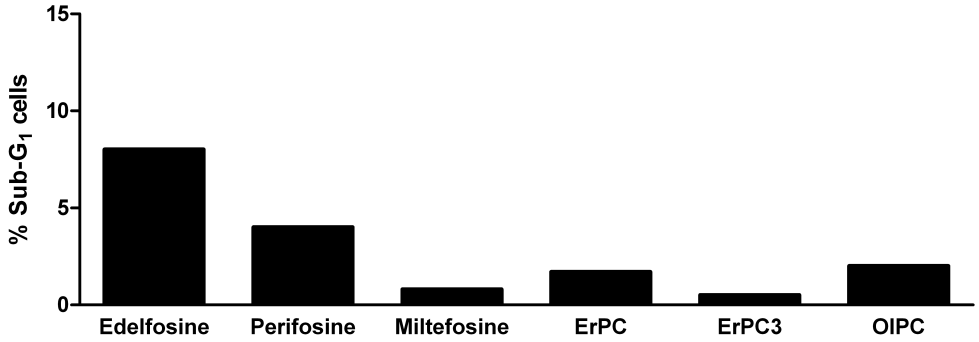

Figure 6.1: Representative experiment showing the percentage of SF268 apoptotic cells (as a measure of Sub-G_1 after flow cytometry analysis), following incubation with edelfosine and other ether lipids at 30 μM for 48 h. Data are expressed as means of experimental triplicates and are representative of two independent experiments.

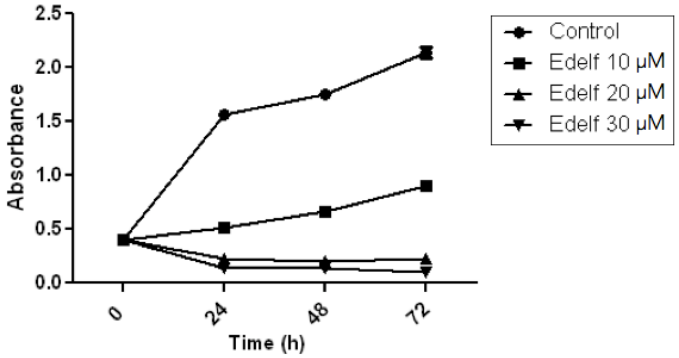

Figure 6.2: SF268 cells were incubated in the absence or presence of the indicated concentrations of edelfosine for 24 h, 48 h and 72 h, and then analyzed by MTT assay. Cells at time 0 were also measured by MTT assay. Data are expressed as means of experimental triplicates and are representative of two independent experiments.

death (Figure 6.2), so we selected the lowest effective drug concentration - 20 μM - to better analyze its effects on SF268 cells.

Time-lapse videomicroscopy analysis showed, confirming MTT assays, that SF268 cells incubated with 20 μM edelfosine did not proliferate normally, and that some cells died during the 72 hours treatment. The occurring type of cell death, however, could not be clearly identified, although some apoptotic features and what seemed the release of apoptotic vesicles were seen (Figure 6.3, Supplementary Video SF268). Cell death might be associated with the release of microparticles in different circunstances. As currently defined, microparticles (MPs) are small membrane-bound vesicles that are released from cells during cell activation and cell death, ranging in size from 0.1 to 1.0 μm and contain an assemblage of nuclear and cytoplasmic components, with extracellular release occurring by a blebbing process (Pisetsky, 2014). Blebs are small bubblelike structures that occur both during early as well as late apoptosis and while their function is not known, the formation of these structures may regulate surface-to-volume changes during apoptotic cell shrinkage and facilitate phagocytic uptake of cellular debris

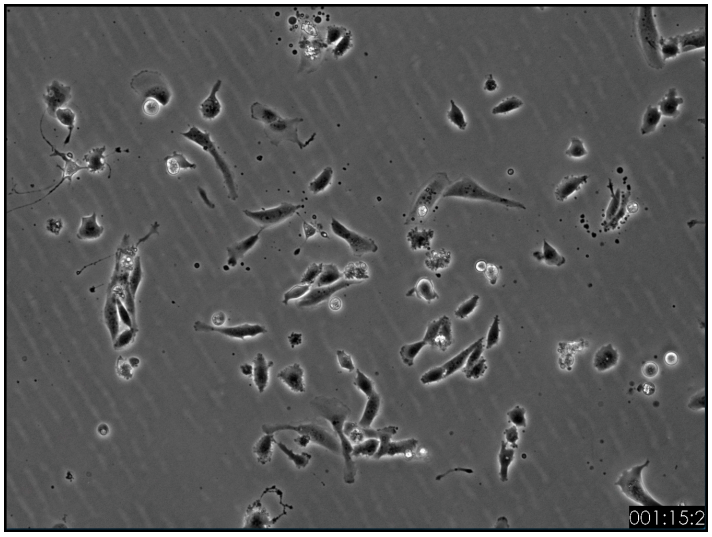

Figure 6.3: Phase-contrast time-lapse videomicroscopy frame (at elapsed time 1 day and 15 hours (001:15:2)) of SF268 cells treated with 20 μM edelfosine, showing the release of microparticles.

(Pisetsky, 2014). In contrast to blebs, apoptotic bodies are larger structures and the collapsed remains or remnants of dying cells, but given the similarity in the origin and composition of microparticles and apoptotic bodies, these structures may represent a continuum both morphologically and biochemically.

We next decided to evaluate DNA degradation, as a consequence of the activation of apoptotic cell death, by flow cytometry analysis. We found that less than 10% of the cells exhibited DNA degradation after 72 hours of incubation with 20 μM edelfosine (Figure 6.4). However, a significant cell cycle arrest, with accumulation of cells in the G_2 phase of the cell cycle (from ~20 % in the control to ~36 %) could be detected already at 24 hours (Figure 6.5, brown bars); but these cells, even with longer periods of incubation did not activate apoptosis (Figure 6.5, red bars) and were able to recover from edelfosine treatment and proliferate again.

These results are in perfect agreement with the data obtained by the MTT assay, in which we found that cell proliferation was strongly affected, but that there was not an important change in cellular viability (Figure 6.2). In order to better understand the mechanism of cell death of the dying cells and the mechanism of resistance presented by the majority of the cells, we decided to perform immunoblot assays to study proteins involved in cell death and cell proliferation/cell survival.

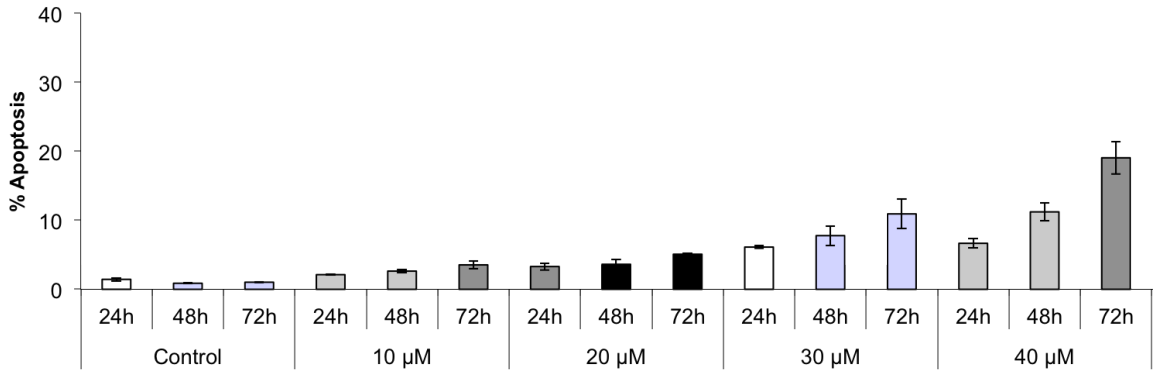

Figure 6.4: Apoptosis was evaluated as the percentage of cells in the Sub-G_1 phase of the cell cycle following flow cytometry analysis and is shown for control untreated SF268 cells, and for SF268 cells treated with the indicated concentrations of edelfosine for 24, 48 and 72 hours. Data are expressed as means ± SD of three independent experiments, each one performed in triplicate.

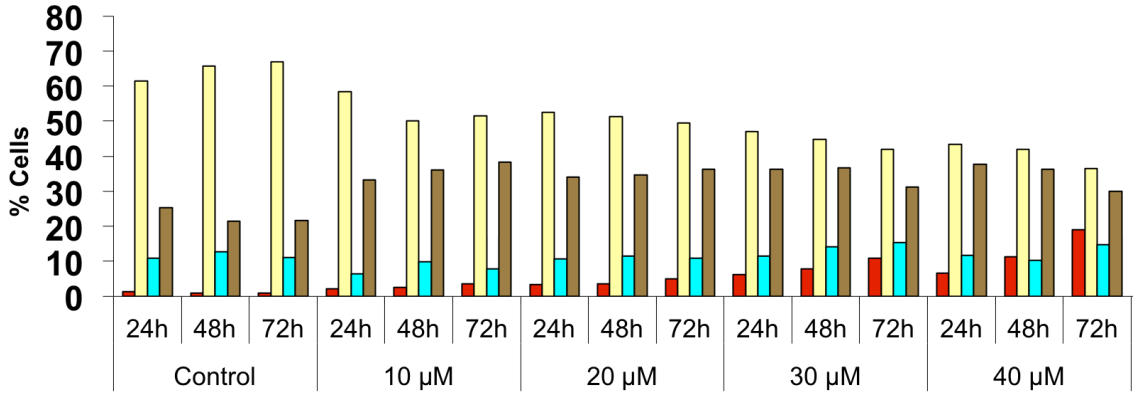

Figure 6.5: Edelfosine-induced changes in the cell cycle phases (red-Sub-G_1; yellow-G_1; blue-S phase; brown-G_2) of SF268 cells treated with edelfosine for the indicated times with the indicated concentrations. Control cells were run in parallel. Data are expressed as means of experimental triplicates and are representative of two independent experiments.

The BH-3 mimetic ABT-737 inhibitor increases apoptosis via the instrisic apoptotic pathway in SF268 cells

A marked reduction in proforms of caspases -8, -9 and -3 was observed, but we could only detect extremely weak bands, or not any band at all, in the molecular weight range corresponding to the cleaved active caspase fragments, at 24, 48 and 72 h of incubation with 20 μM edelfosine (Figure 6.6). Although p-ERK and Akt phosphorylation on Ser347 were drastically reduced at 24 h drug treatment, the phosphorylation of these proteins was only temporarily decreased (Figure 6.7), and the majority of the cells did not activate a cell death process. We decided to evaluate Bcl-x_L expression, since we found it played an important role in U118 cells survival following edelfosine treatment (see chapter *Bcl-x_L mediates cell survival following edelfosine treatment*). Overexpression of Bcl-x_L protects cells from CD-95-induced apoptosis and blocks most of the associated features such as cell detachment, DNA fragmentation, loss of mitochondrial membrane potential and release of cytochrome c (Stegh *et al.*, 2002). Interestingly, Bcl-x_L expression was increasingly upregulated in edelfosine-treated SF268 cells (Figure 6.7). In order to evaluate the importance of Bcl-x_L in limiting edelfosine-induced cell death in SF268 cells, we used the Bcl-2 family inhibitor ABT-737. Pre-incubating the cells for 2 hours with 5 μM ABT-737 before the 20 μM edelfosine treatment, resulted in a very significant increase in the percentage of cells that lost mitochondrial membrane potential after only a short period (~7 hours) of incubation with edelfosine (Figure 6.9), accompanied by a much stronger activation of caspase-9 and effector caspase-3, comparing to edelfosine treatment alone (Figure 6.10). Increase in cytochrome c release from mitochondria following $\Delta\Psi_m$ disruption was also verified by immunoblot assay in ABT-737 pre-treated SF268 cells (Figure 6.8), confirming an increased activation of the intrinsic apoptotic pathway, leading to cell death execution with DNA degradation as assessed by flow cytometry analysis of the cell cycle (Figure 6.12). At 24 h, not only the cells lost $\Delta\Psi_m$ but also had an increment in the production of ROS, as compared to edelfosine-treated cells (Figure 6.9), and there was strong caspase-3 activation and PARP degradation (Figure 6.11). The extrinsic apoptotic pathway apparently was not affected by the ABT-737 inhibitor and not activated, since caspase-8 activation remained undetectable (results not shown). ABT-737 reduced cellular viability, even for longer periods of incubation. At 72 h, cells treated with edelfosine revealed a tendency to increase MTT values, probably meaning that SF268 cells overpassed edelfosine cytostatic effect, while ABT-737 pre-treated cells showed continued reduction in their ability to metabolize MTT (Figure 6.13).

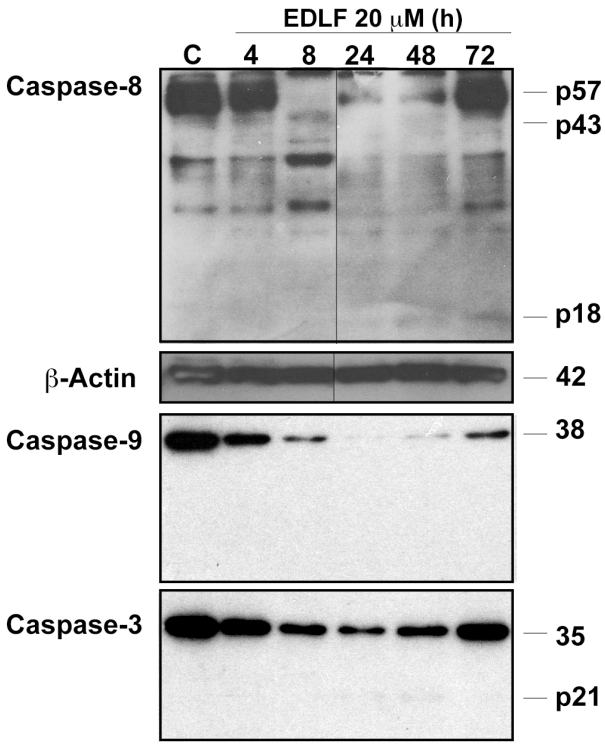

Figure 6.6: Immunoblot analysis of SF268 untreated cells (C) and SF268 cells treated with 20 μM edelfosine for the indicated times, using specific antibodies against caspases -8, -9 and -3. β-actin was used as an internal control for equal protein loading.

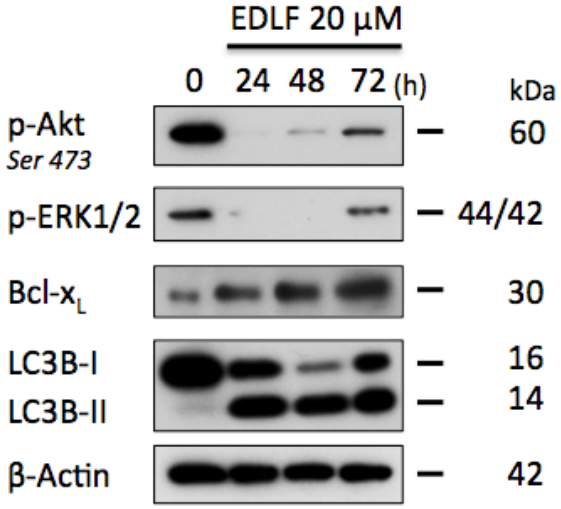

Figure 6.7: Immunoblot analysis of SF268 cells treated with 20 μM edelfosine for the indicated times, using specific antibodies against p-Akt, p-ERK1/2, Bcl-x_L and LC3B-I/II. β-actin was used as an internal control for equal protein loading. Immunoblotting representative of three independent experiments.

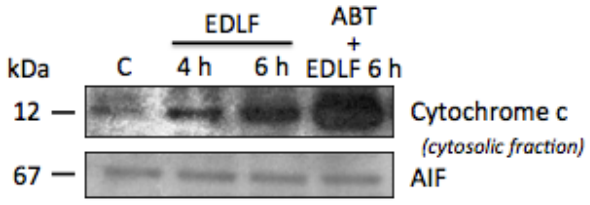

Figure 6.8: SF268 untreated control cells (C), 20 μM edelfosine-treated cells for 4 h and 6 h (EDLF), and cells pre-incubated with 10 μM ABT-737 for 2 h and then treated with edelfosine for additional 6 h (ABT+EDLF) were analyzed by immunoblot using specific antibodies against cytochrome c and AIF in cytosolic fractionated extracts. Cells that were pre-incubated with the BH3-mimetic inhibitor show increased release of cytochrome c into the cytosol.

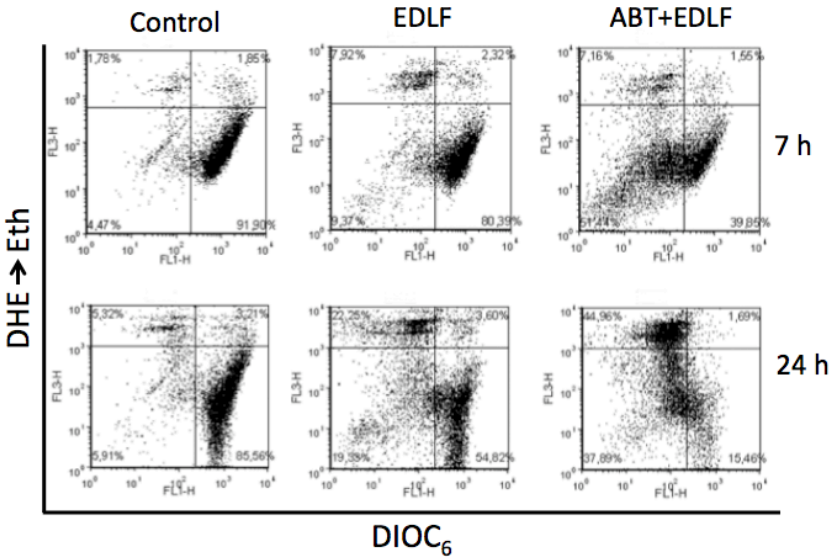

Figure 6.9: SF268 untreated cells (Control), SF268 cells treated with 20 μM edelfosine for 7 h or 24 h, and SF268 cells pre-incubated with 5 μM ABT-737 for 2 h, and then treated with 20 μM edelfosine for 7 or 24 h, were analyzed for ROS generation ((DHE -> Eth)^{high}) and $\Delta\Psi_m$ disruption (DiOC$_6$(3)^{low}) by flow cytometry. ABT-737-preincubated cells show increased $\Delta\Psi_m$ disruption (left quadrants) when compared to the same time treatment with edelfosine alone. The percentages of cells in each quadrant are shown.

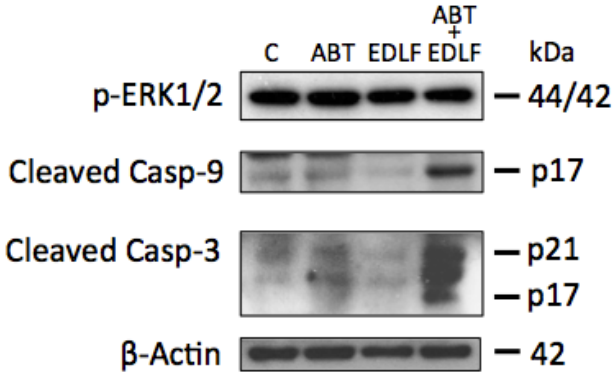

Figure 6.10: SF268 untreated control cells (C), SF268 cells treated with 10 μM ABT-737 for 2 h (ABT), 20 μM edelfosine-treated cells for 7 h (EDLF), and cells pre-incubated with 10 μM ABT-737 for 2 h and then treated with edelfosine for additional 7 h (ABT+EDLF) were analyzed by immunoblot using specific antibodies against p-ERK1/2, cleaved caspase-9 and cleaved caspase-3. Cells that were pre-incubated with the BH3-mimetic inhibitor show no changes in p-ERK levels but increased activation of caspases -9 and-3.

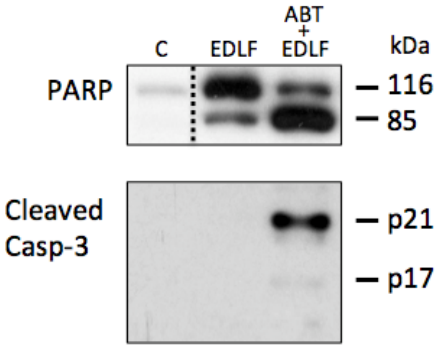

Figure 6.11: SF268 untreated control cells (C), SF268 cells treated with 20 μM edelfosine (EDLF) for 24 h, or pre-incubated with 5 μM ABT-737 for 2 h and then treated with 20 μM edelfosine for 24 h (ABT+EDLF), were analyzed by immunoblot using specific antibodies against PARP and cleaved caspase-3.

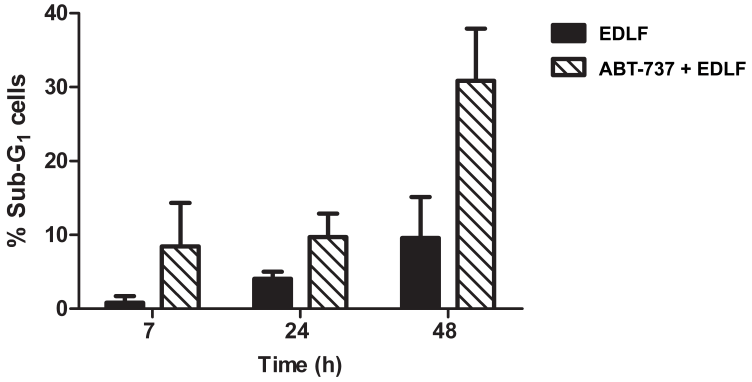

Figure 6.12: Apoptosis was evaluated in SF268 cells treated with edelfosine 20 μM (EDLF) or pre-incubated with 5 μM ABT-737 for 2 h and then treated with edelfosine 20 μM (ABT+EDLF) for the indicated times using flow cytometry cell cycle analysis. Data shown are means ± SD of three independent experiments performed.

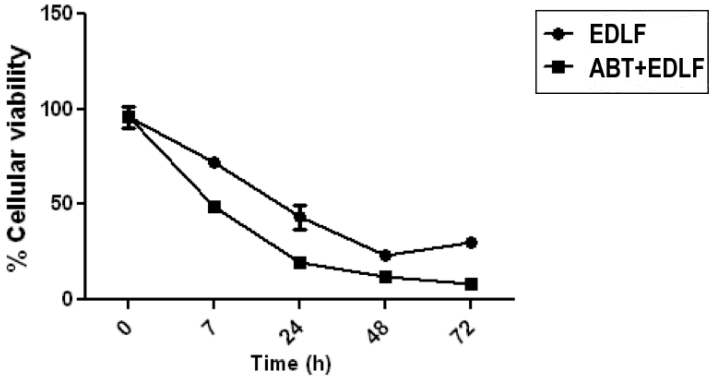

Figure 6.13: SF268 cells were treated with 20 μM edelfosine (EDLF) or pre-incubated with ABT-737 (5 μM for 2 h) and then treated with 20 μM edelfosine (ABT+EDLF) and analyzed by MTT assay at the indicated time points. Cells at time 0 were also measured by MTT assay. Data are expressed as means of experimental triplicates and are representative of two independent experiments.

PARP and AIF mediate SF268 cell line response to edelfosine

Strikingly, in edelfosine-treated SF268 cells, there was an important increase in 116 kDa PARP protein, especially after long incubation periods (Figure 6.11, 24 h), but specific caspase-cleavage produced fragment of 85 kDa was weakly detected, particularly between 8 and 24 hours of treatment (Figures 6.11 and 6.14). The increase in the 116 kDa band was accompanied by the transient increase in immunodetected bands of higher molecular weight in edelfosine-treated cells; in ABT-737-pretreated cells however, there was no increase in the 116 kDa form of PARP or of any other higher molecular weight forms at short incubation times (2 h or 6 h) (Figure 6.14), but cleavage of PARP and the resulting fragment of 85 kDa could be clearly observed at 24 h (Figure 6.11), probably due to the stronger activation of caspase-3 that occurs in the ABT-737-pretreated cells (Figure 6.11).

Besides PARP overexpression, we also found AIF expression to be importantly increased shortly after edelfosine exposure (starting at ~2 h)(Figure 6.14). AIF has a dual mission in the cell. Normally, it resides in the mitochondrial membrane, helps to maintain optimal mitochondrial respiratory function and protects cells against the undesirable and eventually deadly consequences of oxidative damage. Under conditions of excessive stress leading to mitochondrial dysfunction and culminating in apoptosis, AIF translocates from the mitochondria to the cell nucleus, resulting in large-scale DNA fragmentation (Stambolsky *et al.*, 2006). Here, we found an important increase in the 67 kDa form of AIF induced by the edelfosine treatment, in total cell extracts (Figure 6.14). However, when cytosolic and mitochondrial extracts were separated, we did not detect increased AIF levels in the cytosolic fraction (Figure 6.8). Possibly, AIF protein is localized in the mitochondrial membrane, where it has been shown to play an important role in the maintenance of mitochondrial morphology and energy metabolism. The redox activity of AIF is essential for optimal oxidative phosphorylation (Sevrioukova, 2011). AIF was shown to be released after the loss of mitochondrial membrane potential, and this release may be inhibited by overexpression of Bcl-2, which preserves the mitochondrial integrity (Susin *et al.*, 1996). We suggest that AIF expression is upregulated by edelfosine, but its release from the mitochondria and relocation to the nucleus is blocked, possibly by a BH3-protein. When SF268 cells were pre-treated with ABT-737, there was no increase in AIF expression following edelfosine treatment (Figure 6.14). AIF translocation to the nucleus has been show to induce large-scale DNA fragmentation, and a necroptotic type of cell death associated with PARP, calpains and Bax. We also observed overexpression of PARP in the SF268 edelfosine-treated cells, and the induction of cell death, not fully characterized, in a small proportion of the cells. The use of ABT-737 unblocks the activation of the intrinsic apoptotic pathway, as observed by mitochondrial membrane potential loss and activation of caspase-9 and -3, and interestingly, also seems to have an impact in PARP and AIF expression, suggesting that the activation of the intrinsic pathway may block/reduce the activation of a first-response cell death mechanism; or that, on the other hand, if AIF overexpression constituted a pro-survival mechanism, it would not be activated when the BH3-mimetic inhibitor was used. In general, ABT-737 was able to, in part, reduce the follow-

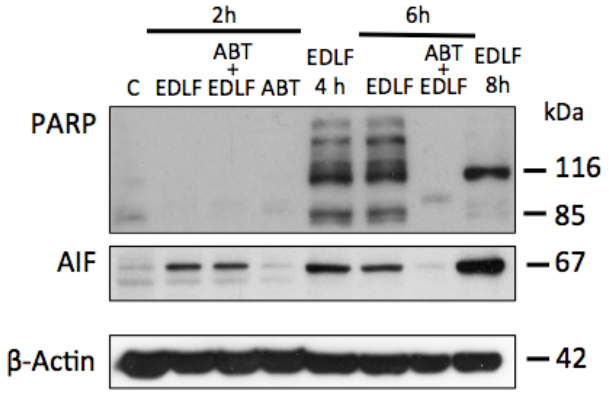

Figure 6.14: Untreated control SF268 cells (C), cells treated with the BH3-mimetic inhibitor ABT-737 (ABT), treated with 20 μM edelfosine (EDLF) or pre-treated with ABT-737 for 2 h and then treated with edelfosine (ABT+EDLF) were analyzed by immunoblot at the indicated time points using specific antibodies against PARP and AIF. β-actin was used as an internal control for equal protein loading in each lane.

ing effects that prevented further execution of edelfosine-induced cell death in SF268 cells: arrest in G2/M, resistance to apoptosis due to increased Bcl-x_L and attenuated cytochrome c release in cytosol.

Edelfosine induces apoptosis via the extrinsic apoptotic pathway in T98G cells

In the T98G cell line, edelfosine induced a detectable apoptotic response following a relatively low dose of 10 μM. Edelfosine at this concentration quickly and potently induced cell cycle arrest in the G_2 phase of the cell cycle (Figures 6.15 and 6.16), followed by an increase in the Sub-G_1 population (Figures 6.15 and 6.17). Again, edelfosine was the ether lipid that induced a higher level of cell death and apoptotic cell death in this cell line (Figure 6.18). Perifosine and ErPC3 had a similar effect in the induction of apoptosis in T98G cells (Figure 6.18), but we only further analyzed edelfosine and compared its effects on T98G cells with those effects in other glioblastoma cell lines.

Confirming that the DNA degradation detected as the Sub-G_1 population resulted from a caspase-dependent apoptotic program, we found that caspases -8 , -9 and -3 were strongly activated and their levels were mantained elevated through the analyzed treatments (up to 72 hours)(Figure 6.19), resulting in increased cell death with incubation time. Edelfosine induced effector caspase-3 activation, as assessed by the appearance of the activated cleaved caspase-3 form and the cleavage of poly(ADP-ribose) polymerase (PARP), a major caspase-3 substrate (Figure 6.19). In this cell line we did not detect activation of autophay as assessed by microtubule-associated protein 1 light chain-3B (LC3B) immunoblot, there was no con-

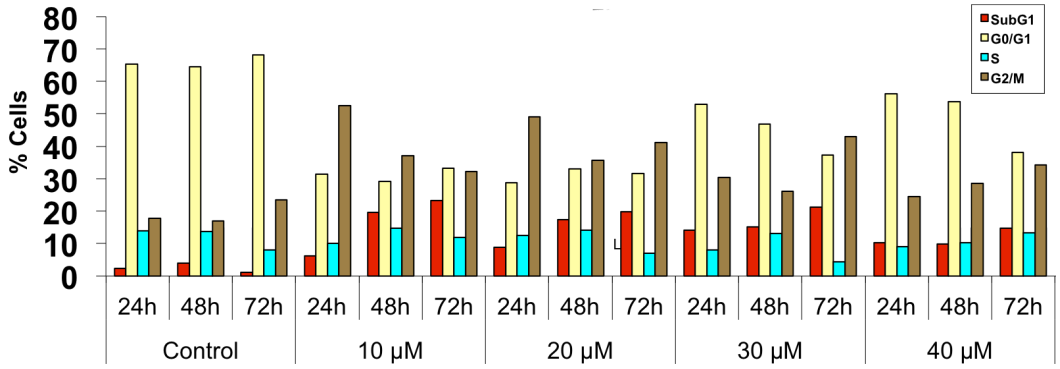

Figure 6.15: Edelfosine-induced changes in the cell cycle phases of T98G cells (red-Sub-G_1; yellow-G_1; blue-S phase; brown-G_2) treated with edelfosine for the indicated times at with the indicated concentrations. Control cells were run in parallel. Data are expressed as means of experimental triplicates and are representative of two independent experiments.

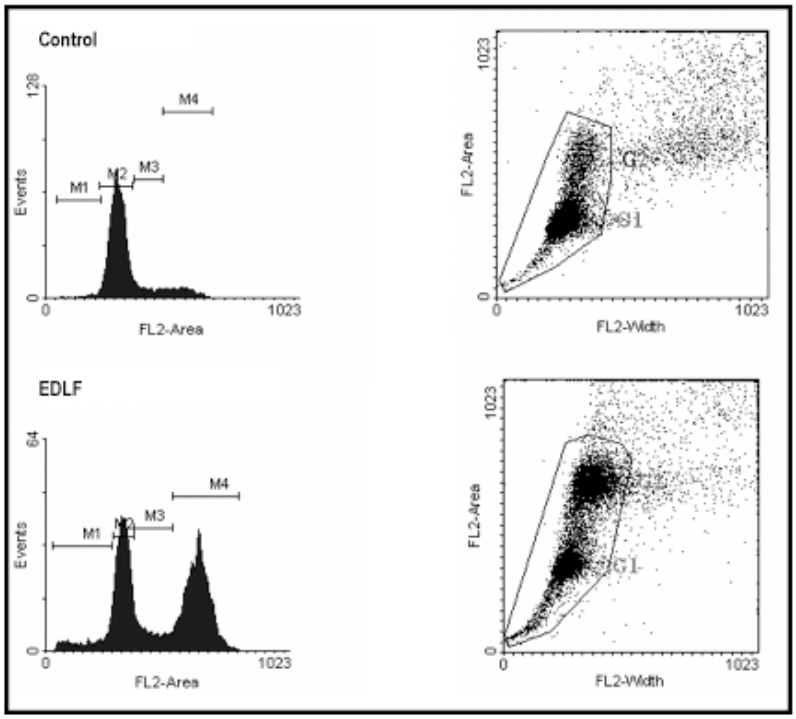

Figure 6.16: Representative histogram and dot plot cell cycle analysis of T98G untreated cells (Control) and T98G cells treated with 10 μM edelfosine for 24 h (EDLF) showing dramatic arrest at the G_2 phase of the cell cycle induced by edelfosine treatment.

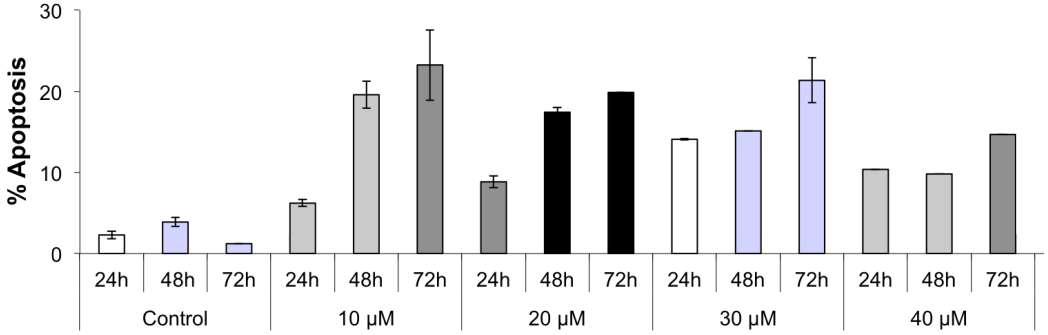

Figure 6.17: Apoptosis was evaluated as the percentage of cells in the Sub-G_1 phase of the cell cycle following flow cytometry analysis and is shown for control untreated T98G cells and for T98G cells treated with the indicated concentrations of edelfosine for 24, 48, and 72 hours. Data are expressed as means ± SD of three independent experiments, each one performed in triplicate.

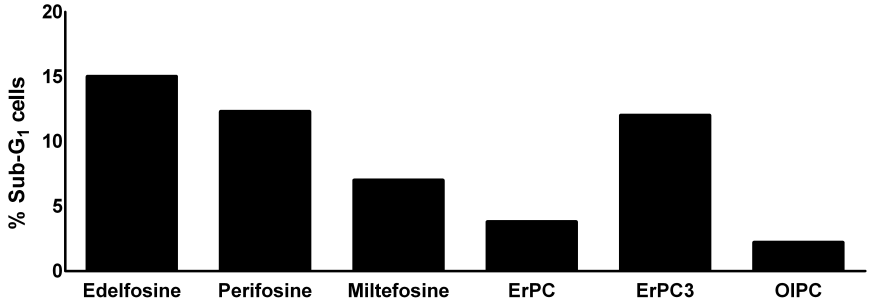

Figure 6.18: Representative experiment showing the percentage of T98G apoptotic cells (as a measure of Sub-G_1 after flow cytometry analysis) following incubation with edelfosine and other ether lipids at 30 μM for 48 h. Data are expressed as means of experimental triplicates and are representative of two independent experiments.

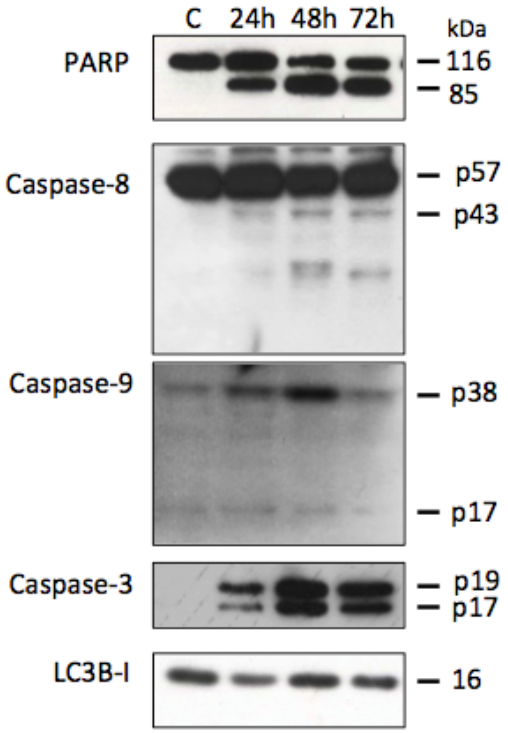

Figure 6.19: T98G untreated cells (C) or cells treated with 10 μM edelfosine for the indicated time were analyzed by immunoblot using specific antibodies against PARP, caspase-8, caspase-9, caspase-3 and LC3B-I/II.

version of LC3B from free form cytosolic LC3B-I (approximately 16 kDa) to the LC3B-II phosphatidylethanolamine conjugated form (approximately 14 kDa)(Figure 6.19). Comparing with the other cell lines, in which the apoptotic response was weaker, we found that T98G cells had comparatively stronger activation of caspase-8, and lower activation of caspase-9. The extrinsic apoptotic pathway is suggested to be activated in this cell line, while we could not detect this activation in other cell lines. This led to a much stronger activation of the effector caspase-3, and PARP degradation. We then decided to compare the expression of different proteins and compare their activation/degradation after edelfosine treatment.

Contrary to the U118 cell line, there was not a reduction in the total level of the protein Akt after edelfosine treatment, but a strong dephosphorylation of Akt in Ser473 was detected in T98G cells (Figure 6.21). ERK appeared to be transiently activated, but then p-ERK levels were subsequently reduced to lower levels than those of control cells (Figure 6.20). The initial activation of ERK was followed by the induction of caspase-8 and -3 activation as well as apoptosis by the time ERK phosphorylation level was decreased (Figure 6.20), thus suggesting again a regulatory role of ERK in edelfosine-induced apoptosis in glioblastoma, and that inhibition of ERK phosphorylation leads to permissive conditions for the induction of apoptosis by edelfosine, particularly through caspase-8 activation and the extrinsic apoptotic pathway.

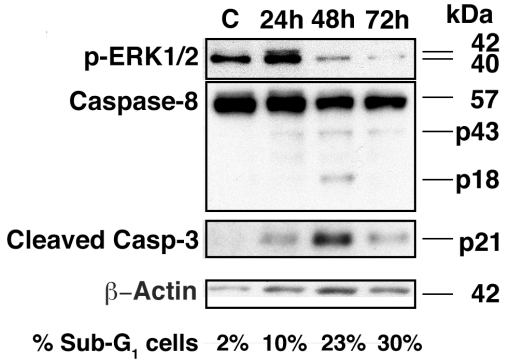

Figure 6.20: Western blot analysis of untreated T98G cells (C) and T98G cells treated with 10 μM edelfosine for the indicated times. Immunoblotting was performed using specific antibodies against p-ERK1/2, caspase-8, and cleaved caspase-3. β-actin was used as an internal control for equal protein loading. The mean percentage of the Sub-G_1 cell population, determined by flow cytometry analysis of three independent experiments, is indicated under each corresponding lane of treatment. Western blots are representative experiments of three performed.

There was no marked activation of the intrinsic apoptotic pathway in the T98G cell line, evaluated as caspase-9 activation and loss of $\Delta\Psi_m$ (~18% at 24 h). Furthermore, since we found that Bcl-x_L overexpression strongly reduced cell death and favored cell survival in different cell lines, during the treatment and following edelfosine removal, we decided to assess the expression levels of Bcl-x_L following edelfosine treatment in the T98G cell line. We found that Bcl-x_L was transiently upregulated, but following this increase its levels returned to lower than control levels at 72 h (Figure 6.22). In order to evaluate if Bcl-x_L overexpression at 48 hours and its antiapoptotic effects could be counteracted somehow, to allow execution of the apoptotic pathway to proceed, we analyzed Bad expression. Pro-apoptotic Bad expression was increased, but not Bad phosphorylation (Figure 6.22) (possibly due to the mentioned Akt dephosphorylation (Figure 6.21)). Phosphorylation on serine 136 inhibits the pro-apoptotic function of Bad, disrupting the binding of Bad to prosurvival Bcl-2 proteins thereby promoting cell survival. Increased expression of Bad, without increased phosphorylation, could possibly block increased Bcl-x_L levels, favoring apoptotic execution in the T98G cells. Dephosphorylated Bad forms a heterodimer with Bcl-2 and Bcl-xL, inactivating them and thus allowing Bax/Bak-triggered apoptosis. When Bad is phosphorylated by Akt/protein kinase B (triggered by PIP3), it forms the Bad-(14-3-3)protein homodimer. This leaves Bcl-2 free to inhibit Bax-triggered apoptosis. Bad phosphorylation is thus anti-apoptotic, and Bad dephosphorylation (e.g., by Ca^{2+}-stimulated calcineurin) is pro-apoptotic. Furthermore, if caspase-8 is efficiently activated in this cell line, and T98G cells are "type I cells", then mitochondrial involvement could be dispensable for cell death execution, and as it is suggested,

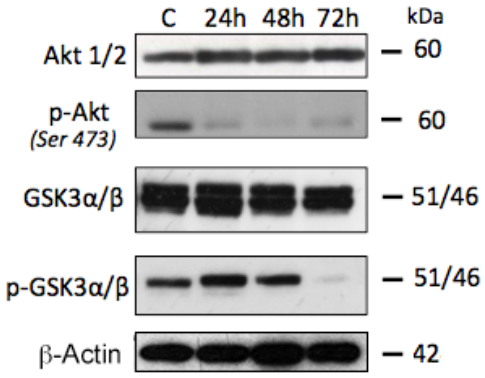

Figure 6.21: T98G untreated cells (C) or treated with 10 μM edelfosine for the indicated time points were analyzed by immunoblot using specific antibodies against Akt 1/2, p-Akt, GSK3α/β and p-GSK3α/β. β-actin was used as an internal control for equal protein loading.

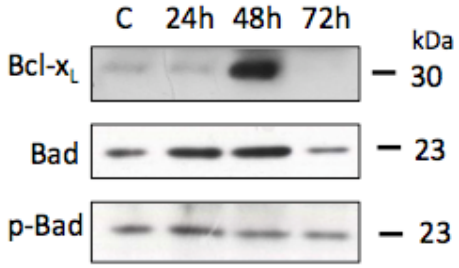

Figure 6.22: T98G untreated cells (C) or treated with 10 μM edelfosine for the indicated time points were analyzed by immunoblot using specific antibodies against Bcl-x_L, Bad and p-Bad (Ser 136).

caspase-8 activation could directly catalyze the proteolytic maturation of caspase-3, resulting in potent activation of effector casapases and apoptotic cell death execution (Figures 6.19 and 6.20).

Interferon-γ treatment increases Fas/CD95 expression in T98G cells

Since edelfosine activates the extrinsic apoptotic pathway in the T98G cell line, possiby through the death receptor Fas/CD95, we tested if this apoptotic effect could be further potentiated by increasing Fas expression in this cell line. Using interferon-γ, which effect in the upregulation of Fas expression in tumor cell lines and sensitization to apoptosis has been previously described (Zheng *et al.*, 2002), we were able to increase Fas expression as assessed by flow cytometry analysis and western-blot (Figures 6.23 and 6.24). Interestingly, we also found that it upregulated p57 caspase-8 proform (Figure 6.24), which has been previously described (Li *et al.*, 2002). In this regard, it is worth to note that results from a phase I clinical trial in neuroblastoma have shown that treatment with interferon-γ within an immunotherapeutic regimen resulted in upregulation of caspase-8 protein levels in tumor cells *in vivo* (Reid *et al.*, 2009).

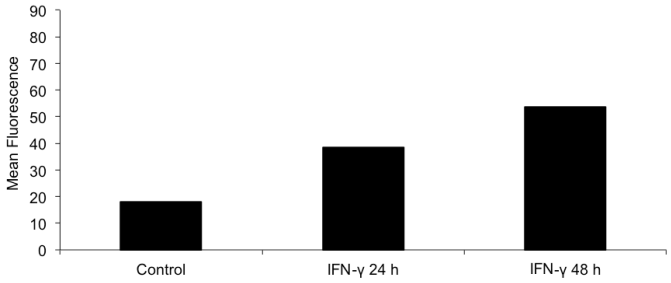

Figure 6.23: Cell surface expression of Fas/CD95 was determined by immunofluorescence flow cytometry as mean fluorescence intensity values in T98G cells untreated (Control) and treated with 50 ng/ml IFN-γ for 24 h and 48 h. Data are expressed as means of experimental duplicates and are representative of two independent experiments.

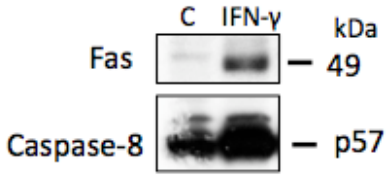

Figure 6.24: T98G untreated cells (C) and cells treated with 50 ng/ml IFN-γ for 48 h (IFN-γ) were analyzed by immunoblot using specific antibodies against Fas and caspase-8.

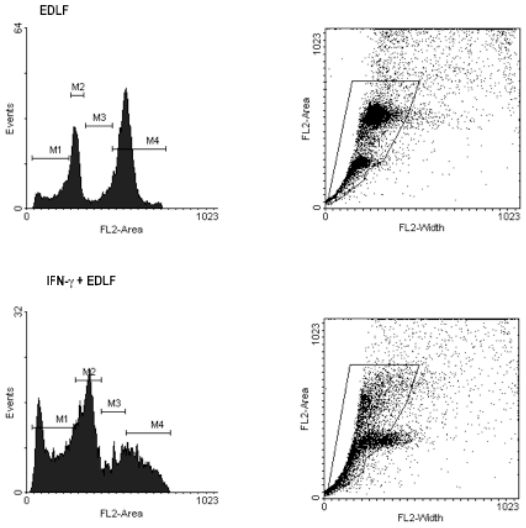

Figure 6.25: T98G cells treated with 20 μM edelfosine for 48 h (ELDF) or treated with 50 ng/ml IFN-γ and 20 μM edelfosine for 48 h (IFN-γ+EDLF) were analyzed by flow cytometry. Marker M1 indicates apoptosis. Data are representative of three independent experiments performed.

Coadministration of interferon-γ and edelfosine increases apoptosis in T98G cells

We next evaluated the effect of treating T98G cells with edelfosine concomitantly with interferon-γ. We found that coadministration of IFN-γ with edelfosine resulted in earlier and increased apoptosis, as assessed by earlier cell-cycle arrest in G_2 and Sub-G_1 accumulation of cells (Figure 6.25). Edelfosine treatment for 24 h and 48 h caused a sharp increase in the number of cells in the G_2 phase of the cell cycle, from ~15% in the control to ~50% in edelfosine-treated cells (Figure 6.15). This increase was less pronounced in IFN-γ-treated cells, in which the percentage of Sub-G_1 cells was already ~28% at 24 hours. Representative cell cycles for 48 h treatments in the presence or absence of IFN-γ are shown in Figure 6.25. At 72 h, ~50% of IFN-γ-treated cells were in the Sub-G_1 phase of the cell cycle, while in edelfosine only treated cells there was still a high accumulation of cells in the G_2 phase of the cell cycle (~47%) and ~25% shown DNA degradation. Complementing microscopic observation and flow cytometry analysis, western-blot also revealed higher activation of the extrinsic apoptotic pathway and of the effector caspase-3 (Figure 6.26). In this case,T98G cells were pre-incubated with IFN-γ for 48 h, in order to achieve maximum expression of Fas and caspase-8 before adding edelfosine treatment. Besides strong activation of caspases -8 and -3, we also found stronger cleavage of Bid in IFN-γ pre-treated cells (Figure 6.26), linking the extrinsic and intrinsic apoptotic pathways; Bid-mediated Bax activation may favor MMP and cytochrome c-dependent caspase-3 activation, thus favoring apoptosis execution.

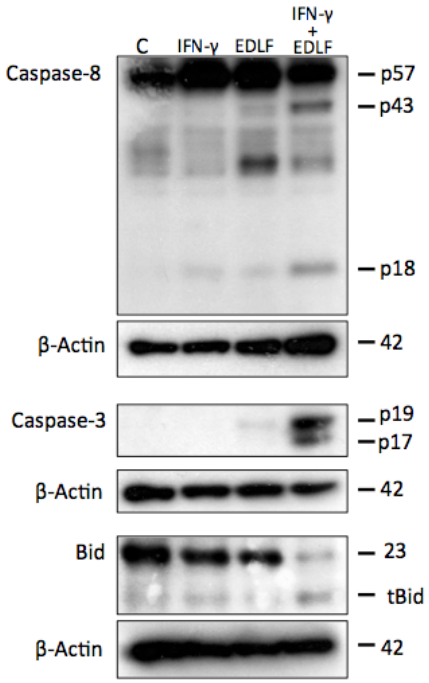

Figure 6.26: T98G untreated cells (C), cells treated with 50 ng/ml IFN-γ for 48 h (IFN-γ), treated with 10 μM edelfosine for 24 h (EDLF), and pre-treated with IFN-γ for 48 h and then 10 μM edelfosine for 24 h (IFN-γ+EDLF) were analyzed by immunoblot using specific antibodies against caspase-8, caspase-3 and Bid. Immunoblotting for β-actin was used as an internal control for equal protein loading in each lane.

Effect of edelfosine in the induction of cell death in GOS-3 cells

In order to induce cell death in the GOS-3 cell line, a concentration of 30 μM edelfosine was required. Time-lapse videomiscroscopy showed that a significant proportion of the cells quickly activated an apparently apoptotic response, as cell detachment, contraction and typical blebbing was readily vizualized in this cells (Figure 6.27; Supplementary Video GOS3). However, as seen in Figure 6.28, the amout of cells in the Sub-G_1 phase of the cell cycle was rather low, reaching ~ 25% after 72 h drug treatment.

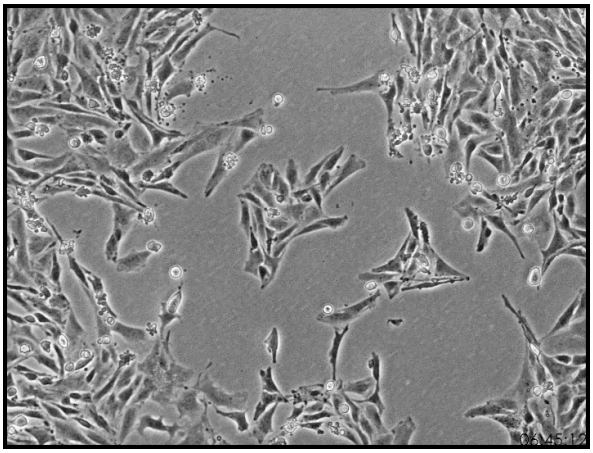

Figure 6.27: Phase-contrast time-lapse videomicroscopy frame (elapsed time 7 hours) of GOS-3 cells treated with 30 μM edelfosine, showing typical apoptotic blebbing in dying cells.

Caspases -8 and -3 activation, could be hardly detected even at that time point (Figure 6.29), suggesting that the observed DNA degradation could be not mediated by caspases. The PARP specific caspase-cleavage produced fragment of 85 kDa was also only weakly detected at 24 h treatment (Figure 6.29). Caspase-8 was expressed, its expression was not altered during the treatment (up to 72 hours), but its activation could be barely detected only at 24 h treatment (Figure 6.29). Akt phosphorylation in the Ser473 was reduced at 24 hours, as well as ERK phosphorylation, but the levels of both phosphorylated proteins increased again at 48 hours (Figure 6.29). The fact that we can only detect slight changes in apoptosis-related proteins at 24 hours, may reflect the fact that sensitive cells that activate apoptosis do so during the first 24 hours of treatment, and the cells that do not detach in this time frame remain attached and do not show blebbing (Supplementary Video GOS3).

Besides typical apoptotic blebbing in some of the dying cells, we could also observe necrotic phenotypes (Figure 6.30a) that could represent late phases of previously apoptotic execution but also other types of cell death. In this regard, extensive cell vacuolization could also be observed (Figure 6.30b), pointing to the possibility that other types of cell death besides apoptosis may be occurring in GOS-3 treated cells.

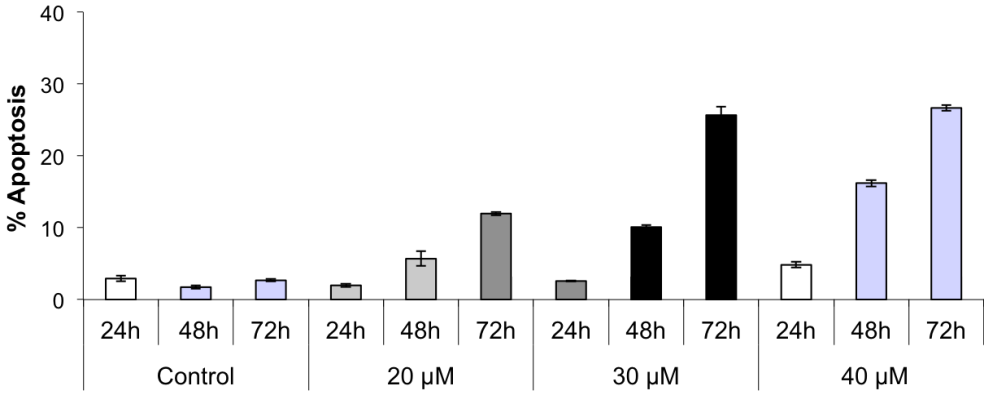

Figure 6.28: Apoptosis was evaluated as the percentage of cells in the Sub-G_1 phase of the cell cycle following flow cytometry analysis and is shown for control untreated GOS-3 cells and for GOS-3 cells treated with the indicated concentrations of edelfosine for 24, 48, and 72 hours. Data are expressed as means ± SD of three independent experiments, each one performed in triplicate.

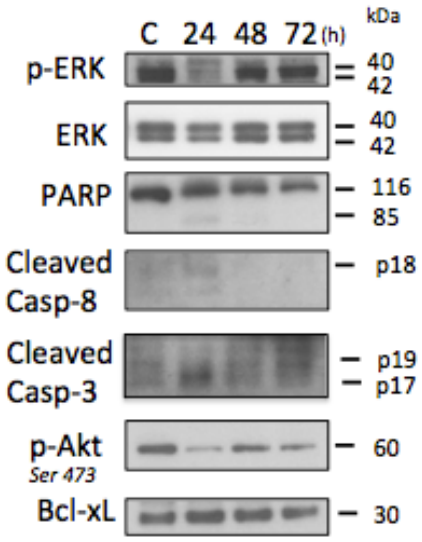

Figure 6.29: GOS-3 untreated cells (C) or treated with 30 μM edelfosine for the indicated time points, were analyzed by immunoblot using specific antibodies against p-ERK, ERK, PARP, cleaved caspase-8, cleaved caspase-3, p-Akt and Bcl-x_L.

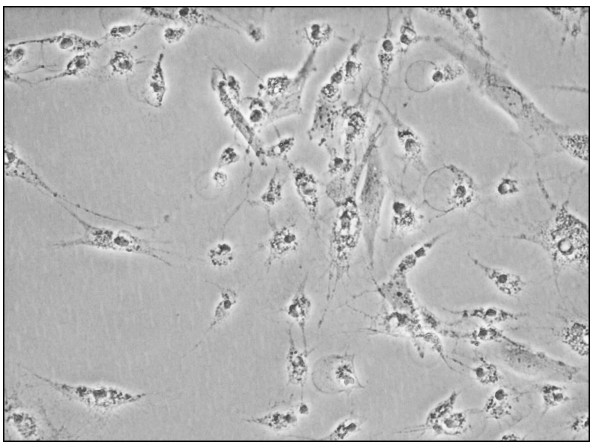

(a)

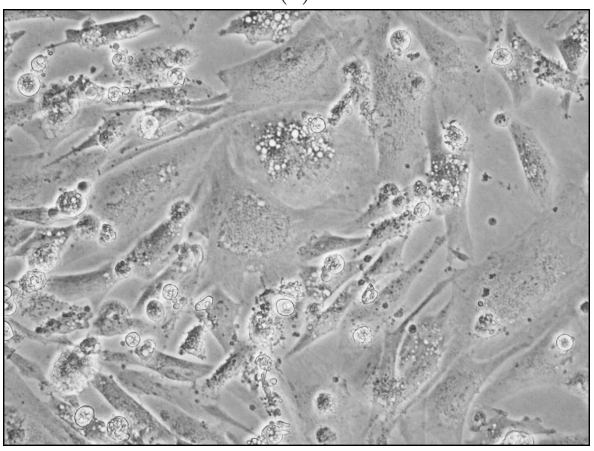

(b)

Figure 6.30: (a) Bright-field image of GOS-3 cells treated with 30 μM edelfosine for 24 h, showing a field with numerous necrotic cells. (b) Bright-field image of GOS-3 cells treated with 30 μM edelfosine for 24 h, showing a field with larger cells displaying strong vacuolization.

The BH-3 mimetic ABT-737 inhibitor increases apoptosis via the instrisic apoptotic pathway in GOS-3 cells

GOS-3 cells expressed Bcl-x_L, and its levels did not suffer considerable changes during the treatments (Figure 6.29), so we decided to evaluate the effect of pre-incubating the cells with ABT-737 inhibitor on the induction of cell death in GOS-3 cells. We found that ABT-737 led to an increase in DNA degradation, as assessed by an increase in the Sub-G_1 phase of the cell cycle analysis and decrease in the G_2 (Figure 6.32) and increased morphological changes in dying cells: there was an increased number of rounded-up cells detached from the culture plate, and the reduced number of attached cells exhibited extensive vacuolization (Figure 6.31).

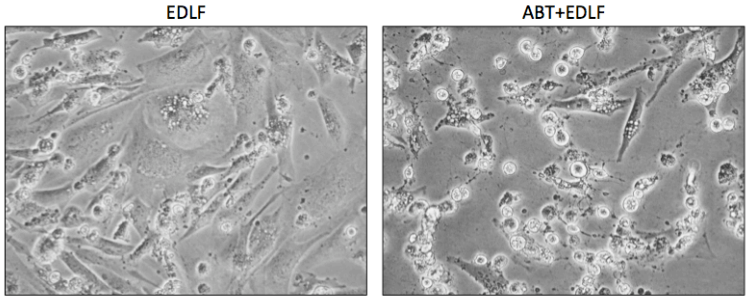

Figure 6.31: Representative bright-field images of GOS-3 cells treated with 30 μM edelfosine for 24 h and of GOS-3 cells incubated with 5 μM ABT-737 for 2 h before edelfosine treatment, showing increased cell death in ABT-737 pre-treated cells.

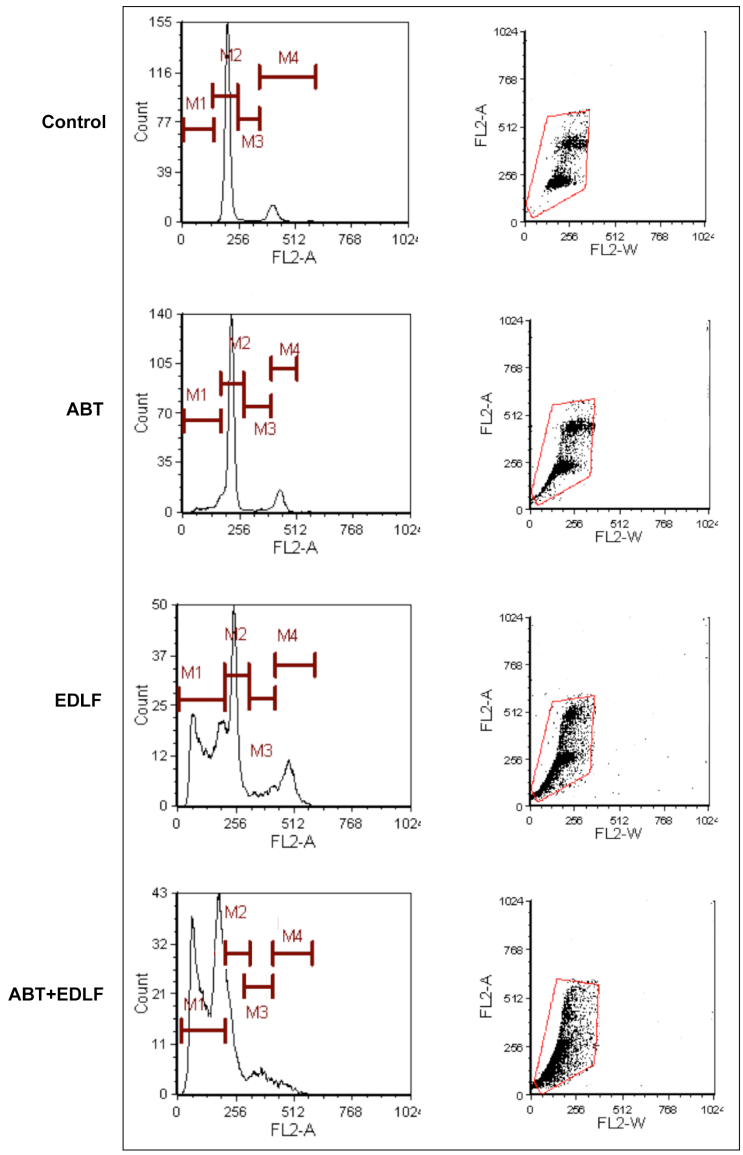

Figure 6.32: Representative flow cytometry analysis cell cycle histograms and dot plots of untreated GOS-3 cells (Control), cells treated with 5 μM ABT-737 for 48 h (ABT), cells treated with 30 μM edelfosine for 48 h (EDLF) and cells pre-incubated with 5 μM ABT-737 and then treated with 30 μM edelfosine for 48 h (ABT+EDLF), showing less cells in the G_2 phase of the cell cycle and more cells in the Sub-G_1 phase in ABT-737 pre-treated cells.

Effect of edelfosine in the induction of cell death in A172 cells

After evaluating apoptosis induction by all the ether lipids, we again found that edelfosine was the drug that more potently induced apoptotic cell death in the A172 cell line (Figure 6.33). We found that in this cell line, increase in the time of treatment led to progressive increase in cell death, as observed following time-lapse videomicroscopy of 10 μM edelfosine-treated A172 cells (Supplementary Video A172); contrary to what occurs in the GOS-3 cell line, in which the majority of the cell death is induced within the first 24 hours of treatment. In A172 cells, even 10 μM edelfosine was able to induce DNA degradation in a very high proportion of the treated cells after 48-72 h of treatment. Although not clearly constituted a Sub-G_1 population, we found that both populations G_1 and G_2 lost DNA content, resulting in an increase in the theoretically Sub-G_1 and S populations (Figure 6.34). To further support that this observation actually represented DNA degradation resulting from the activation of caspases, we performed western blot analysis and found caspase-8 and -3 activation, and also PARP cleavage, starting at 24 hours, but being more strongly activated at 72 hours of treatment (Figure 6.35a). We found no changes in total ERK levels and a reduction in ERK phosphorylation, which we have seen in all the analyzed cases to favor apoptotic execution, and also a reduction in the phosphorylation of Akt (Ser 473) (Figure 6.36). Pro-apoptotic Bad expression was strongly increased at 72 hours, while p-Bad phosphorylation was reduced (Figure 6.35b), probably facilitating apoptosis induction, although there was only a slight reduction in the expression of Bcl-x_L (Figure 6.35a).

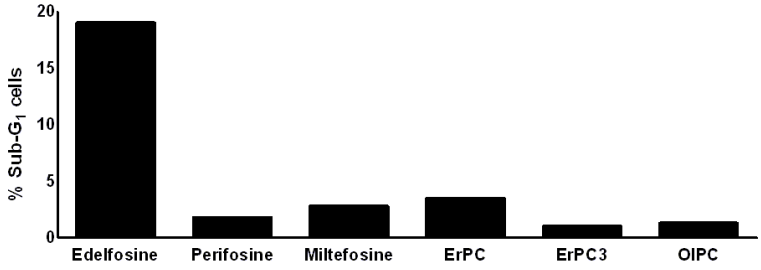

Figure 6.33: Representative experiment showing the percentage of A172 apoptotic cells (as a measure of Sub-G_1 after flow cytometry analysis) following incubation with edelfosine and other ether lipids at 30 μM for 48 h. Data are expressed as means of experimental triplicates and are representative of two independent experiments.

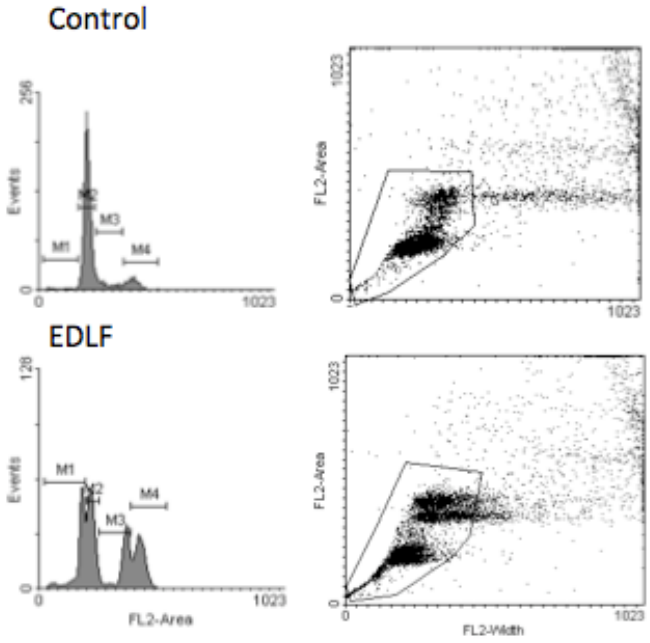

Figure 6.34: Representative cell cycle analysis histograms of untreated A172 cells (Control) and A172 cells treated with 10 μM edelfosine for 48 h. DNA degradation in edelfosine treated G_2 cells is reflected in the increase in the S phase (marker M3) and DNA degradation of G_1 cells in an increase in the Sub-G_1 phase (subpeak in the lower histogram, M1 marker).

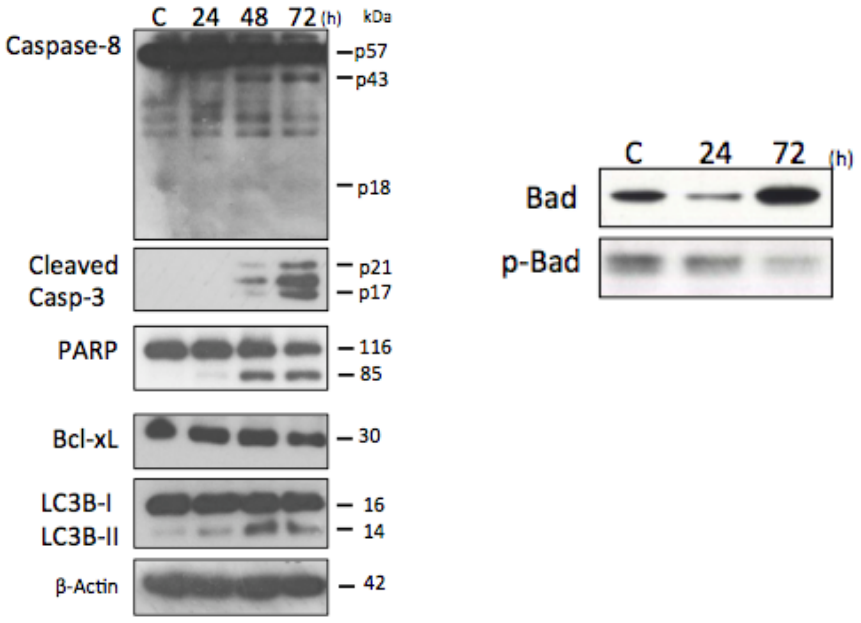

(a) (b)

Figure 6.35: (a) A172 untreated cells (C) or treated with 10 μM edelfosine for the indicated time points were analyzed by immunoblot using specific antibodies against caspase-8, cleaved caspase-3, PARP, Bcl-x_L and LC3B-I/II. β-actin was used as an internal control for equal protein loading in each lane. (b) A172 untreated cells (C) or treated with 10 μM edelfosine for 24 h or 72 h were analyzed by immunoblot using specific antibodies against Bad and p-Bad.

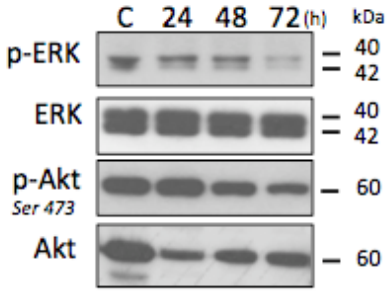

Figure 6.36: A172 untreated cells (C) or treated with 10 μM edelfosine for the indicated time points were analyzed by immunoblot using specific antibodies against p-ERK1/2, ERK1/2, p-Akt, and Akt.

Autophagy inhibition favors apoptosis in A172 edelfosine-treated cells

Since there was increased conversion of LC3B-I to LC3B-II in A172 edelfosine-treated cells (Figure 6.35a), we decided to evaluate the impact of inhibiting autophagy. We found that incubating the cells with the autophagy inhibitors bafilomycin and chloroquine at the same time of edelfosine resulted in accelerated cell death with increased percentages of DNA degradation being reached at earlier time points and resulting in increased total cell death (Figure 6.37, results shown for bafilomycin-treated cells), revealing that in the A172 cell line the activation of autophagy probably constitutes a protective scenario from apoptosis, and that its inhibition accelerates cell death execution and potentiates cellular demise.

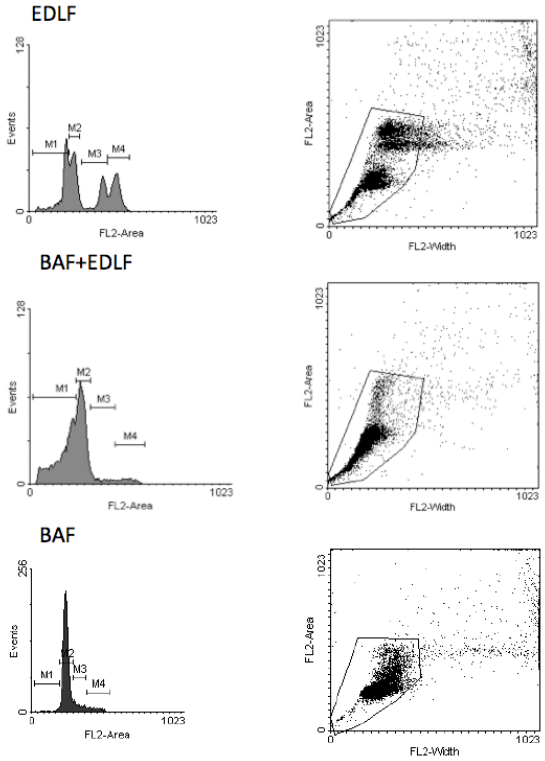

Figure 6.37: Representative cell cycle analysis of A172 cells treated with 10 μM edelfosine for 72 h (EDLF), cells treated with 25 nM bafilomycin + EDLF (BAF+EDLF), and cells treated with 25 nM bafilomycin alone (BAF), showing increased cell death in cells that were simultaneously treated with the autophagy inhibitor.

7
Discussion

Results I

The results reported in chapter 3 - *Effect of edelfosine in the induction of cell death in the U118 glioblastoma cell line*- show for the first time that an APL molecule, edelfosine, is able to induce necroptosis in a tumor cell. The ether phospholipid edelfosine induces a rapid necrotic cell death in human U118 glioblastoma cells, which is inhibited by the specific RIPK1 inhibitors Nec-1 and Nec-1s as well as by RIPK3 silencing, but not by caspase inhibition, and accounts for most of the cell death (~80%) occurring in edelfosine-treated U118 cells, thus involving both RIPK1 and RIPK3 in the cell death process. Our data also indicate that edelfosine elicits a minor caspase-dependent apoptotic response (~18%) in U118 cells. Time-lapse videomicroscopy assays indicated that the onset of the necrotic process took place after only 150 min of edelfosine addition. The data reported here indicate a concomitant and fast reduction in the metabolic activity of the cells, as assessed by a dramatic decrease in the capacity to metabolize MTT, and the loss of cellular membrane integrity in a short period of time (~3-4 h), turning the cells permeable to PI.

Necroptosis is a programmed and regulated necrosis process that is dependent on RIPK1 and RIPK3 (Vanlangenakker *et al.*, 2012; Berghe *et al.*, 2014), and has been linked to death receptor activation, including Fas/CD95 (Vercammen *et al.*, 1998; Berghe *et al.*, 2014 Holler *et al.* (2000)) and tumor necrosis factor receptor (Chan *et al.*, 2003; Vanden Berghe *et al.*, 2014). In this regard, edelfosine has been found to promote apoptosis in a wide number of cancer cells through the involvement of Fas/CD95 death receptor (Gajate & Mollinedo, 2001, 2007; Gajate *et al.*, 2004; Mollinedo & Gajate, 2006a, 2006b).

However, the results reported here indicate that edelfosine induces a major necroptotic response in U118 glioma cells, while the triggering of apoptosis was a minor response. This readiness for necroptosis might suggest that this U118 glioma cell line comprises some molec-

ular features that make the cell prone to undergo necroptosis. In this regard, U118 cells hardly express procaspase-8 as compared to HeLa (human cervical carcinoma) and Jurkat (human acute T-lymphocytic leukemia) cells, two cancer cell lines that readily undergo apoptosis following edelfosine treatment (Gajate *et al.*, 2004; Nieto-Miguel *et al.*, 2006), whereas RIPK1 levels were rather similar in the above three cell lines. Thus, the relative ratio of RIPK1:procaspase-8 level was much higher in U118 than in HeLa and Jurkat cells, and might predispose U118 cells to undergo necroptosis upon edelfosine treatment.

The RIPK1 inhibitor Nec-1 also inhibits IDO activity (Muller *et al.*, 2005; Takahashi *et al.*, 2012; Degterev *et al.*, 2013), raising some doubts on the role of RIPK1 in the edelfosine-induced necrotic process. However, we have found that Nec-1s, a more specific RIPK1 inhibitor lacking the IDO-targeting effect (Degterev *et al.*, 2008; Takahashi *et al.*, 2012), shows the same inhibitory effect on necrosis as that observed with Nec-1 in edelfosine-treated U118 cells, indicating that edelfosine-induced necroptosis was independent of IDO activity.

Although necroptosis was initially defined as the type of cell death mediated by RIPK1, RIPK3 and MLKL, a number of recent articles have shown major role of RIPK3 in launching necroptosis in the absence of RIPK1 (Vanlangenakker *et al.*, 2011; Moujalled *et al.*, 2013; Orozco *et al.*, 2014), and even in this latter work it was found that in contrast to RIPK3, knockdown of RIPK1 did not block TNF cytotoxicity (Vanlangenakker *et al.*, 2011). In this regard, it is also worthwhile to quote some sentences of the work by Cho *et al.* (2011): "(…) siRNA-mediated silencing of RIPK1 had no effects on TNF-induced necrosis in L929 cells. Western blot analysis shows that the lack of protection against TNF-induced necrosis in L929 cells was not due to inefficient silencing of RIP1 expression (…) Furthermore, siRNA-mediated silencing of another essential programmed necrosis mediator, RIPK3, effectively inhibited zVAD-fmk and TNF-induced necrosis in L929 cells, and TNF-induced necrosis in NIH 3T3 cells. Our results are consistent with those of Hitomi (Hitomi *et al.*, 2008), which show that siRNA knock-down of RIPK1 in L929 cells exhibited disparate effects on necrosis induced by zVAD-fmk or TNF (…) Nec-1 effectively inhibited TNF-induced necrosis in RIP1 siRNA and control siRNA transfected cells. Nec-1 also inhibited cell death induced by TNF and zVAD-fmk in RIP1 siRNA transfected cells." Interestingly, we found that silencing RIPK3, but not RIPK1, inhibited necrotic cell death and increased apoptosis in edelfosine-treated U118 cells, which was blocked by caspase inhibition. However, Nec-1 prevented necrosis in RIPK1-silenced cells following edelfosine treatment. Silencing of RIPK1 largely decreased its protein expression, but we cannot rule out that the remaining levels of RIPK1 can still mediate necroptosis, or that Nec-1 may affect other proteins besides RIPK1. In this context, RIPK1-dependent and independent actions of Nec-1 in necrosis induction have been reported (Holler *et al.*, 2000). Furthermore, inhibition of the RIPK3 substrate MLKL with necrosulfonamide also increased apoptosis in edelfosine-treated cells. The data reported here highlight a major role for RIPK3 in the induction of necroptosis as well as in the switch from necrosis to apoptosis when RIPK3 is knockdown in edelfosine-treated U118 cells. Preliminary data suggest that Nec-1 inhibits the apoptotic response (~43%) induced by edelfosine in U118 after silencing RIPK3. Taken together, these data suggest a major role of RIPK1/RIPK3

complexes in the cell death response induced by edelfosine in glioblastoma U118 cells, either necrotic or apoptotic, and they might also suggest that RIPK1 function in cell death could be modulated by RIPK3, thus involving RIPK1 in apoptosis when RIPK3 is absent. In line with these findings, Remijsen *et al* (Remijsen *et al.*, 2014) showed in a recent paper that knockdown of RIPK3 or MLKL blocks TNF-induced necroptosis in L929 fibrosarcoma cells but that the repression of either of these proteins did not protect the cells from death, but instead induced a switch from TNF-induced necroptosis to RIPK1 kinase-dependent apoptosis. Because, unlike Nec-1, Nec-1s or RIPK3 silencing, neither pan-caspase nor autophagy inhibitors were able to rescue U118 cells from the cell death induced by edelfosine, these data suggest that this glioma cell line might be a useful model to study molecular signalling transducers involved in necroptosis.

Our results also show that necroptosis inhibition by RIPK1 inhibition and RIPK3 silencing causes U118 cells to undergo caspase-dependent apoptosis upon edelfosine treatment, thus turning the cell death response to caspase-dependent apoptosis when necroptosis is blocked. Edelfosine has been previously reported to promote caspase-independent cell death in LN18 malignant glioma cell line (Naumann *et al.*, 2004). Another APL, perifosine, has been reported to induce caspase-independent cell death in human prostate cancer PC-3 cells (Floryk & Thompson, 2008). The APL miltefosine promotes cell-type-dependent apoptotic and non-apoptotic cell death processes in several human breast cancer cell lines (Chakrabandhu *et al.*, 2008). However, necroptosis was not examined in the above studies. The alkylating agent temozolomide, which penetrates the blood-brain barrier and is the new gold standard for brain tumor therapy, has been reported to induce autophagy in malignant glioma cells (Carmo *et al.*, 2011). Proautophagic drugs are being considered as a putative novel means in the treatment of devastating cancers, such as glioblastoma, that show resistance to radiotherapy and pro-apoptotic-related chemotherapy (Vanlangenakker *et al.*, 2012). Our data indicate that the triggering of autophagy by edelfosine, which correlated in time with the induction of necrotic cell death, was not relevant for the induction of the major necroptotic cell death response, and in this regard the mechanism of action of edelfosine shows clear-cut differences from that of temozolomide. Suppression of autophagy promoted a rather slight increase of apoptosis, thus suggesting autophagy could work as a poor protective scenario for apoptosis in this cell line following edelfosine treatment. The potent necroptotic activity of edelfosine was exerted when this ether lipid was used at 10 μM, a concentration that fits well with the drug plasma levels (10-20 μM) found in pharmacokinetic and in vivo studies (De Mendoza *et al.*, 2009; Mollinedo *et al.*, 2010, 2010). Temozolomide at the rather high concentration, but clinically achievable, of 100 μM and after 72 h incubation induces autophagy, but not apoptosis in several malignant glioma cell lines (Kanzawa *et al.*, 2004). Temozolomide inhibited cell proliferation of U118 glioma cells at concentrations of >100 μM and induced ~15% apoptosis at 250 μM after 48-h incubation (Carmo *et al.*, 2011). On these grounds, the results reported here suggest that certain features of U118 glioma cells make them particularly sensitive to edelfosine and turn the usual pro-apoptotic action of the ether phospholipid into necroptotic activity. The identification of these features could be of interest

in the advent of new chemotherapy approaches for glioma treatment.

We also found that edelfosine prompted an increase in free intracellular Ca^{2+} concentration in U118 cells that was mainly due to the entry of extracellular calcium. This increase in intracellular Ca^{2+} was not relevant to the induction of the necroptotic response, but seemed to play a major role in the triggering of autophagy. In this regard, an increase in cytosolic Ca^{2+} concentration has been reported to induce autophagy (Høyer-Hansen *et al.*, 2007). Our data suggest that most of the increase in intracellular Ca^{2+} detected in U118 cells treated with edelfosine comes from extracellular calcium and promotes autophagy, whereas a minor release of intracellular calcium from internal stores seems to promote apoptosis. Inhibition of necroptosis by Nec-1 reduced autophagy, suggesting that autophagy is a side effect of the stress imposed to the cells undergoing necrosis. Because edelfosine promotes rapidly the loss of membrane integrity in U118 cells, it might be envisaged that the increase in cytosolic Ca^{2+} concentration could be due, at least in part, to damage at the plasma membrane. In fact, U118 cells pretreated with Nec-1, prior to edelfosine administration, showed a lower increase, even though not statistically significant, in the intracellular free calcium level. This might be due to the better preservation of plasma membrane integrity following Nec-1 treatment. The effect of Nec-1 in reducing autophagy might be also due to the lower levels of intracellular calcium.

Figure 7.1 (from Melo-Lima *et al.*, 2014) depicts a scheme for the involvement and relative participation of the three major types of cell death in the demise of U118 cells upon edelfosine treatment. As stated above, we have found that U118 cells treated with the ether phospholipid edelfosine primarily undergo necroptosis (Figure 7.1, upper), and inhibition of this necrotic response results in an increase in apoptosis (Figure 7.1, lower), thus highlighting the potent pro-cell death signalling triggered by edelfosine in this glioma cell line. This warrants further studies on the putative effects of this ether lipid in glioblastoma and the underlying mechanisms. Although Nec-1 conferred protection to U118 cells for some time, it did not completely abolish cell death at protracted incubation times with edelfosine. Interestingly, after 9-24 h incubation of U118 cells with 10 μM edelfosine, we found that a combination of Nec-1, EGTA and z-VAD-fmk, thus blocking necroptosis, extracellular calcium entry and caspase-mediated apoptosis, inhibited cell death about 1.3 times more efficiently than Nec-1 alone, as assessed by SSC/FSC flow cytometry analysis. These results suggest that there are different processes contributing to the overall cell death process in U118 cells after edelfosine treatment, namely a major activation of necroptosis, mainly mediated by RIPK3, a minor caspase-dependent apoptosis, and an increase in intracellular calcium level (Figure 7.1). The existence of several distinct pathways that exert cell death would imply that they all need to be interrupted simultaneously for cytoprotection. The fact that blockade of necroptosis led to increased apoptosis shows that edelfosine can activate both cell death pathways in U118 cells, and therefore it can be an effective drug for the demise of glioblastoma cells. The data reported here also suggest that U118 cells can constitute a good tool to further analyze the mechanisms that dictate the cellular decision to undergo alternative cell death pathways, such as apoptosis or necroptosis, as well as the processes mediating the execution of necroptosis

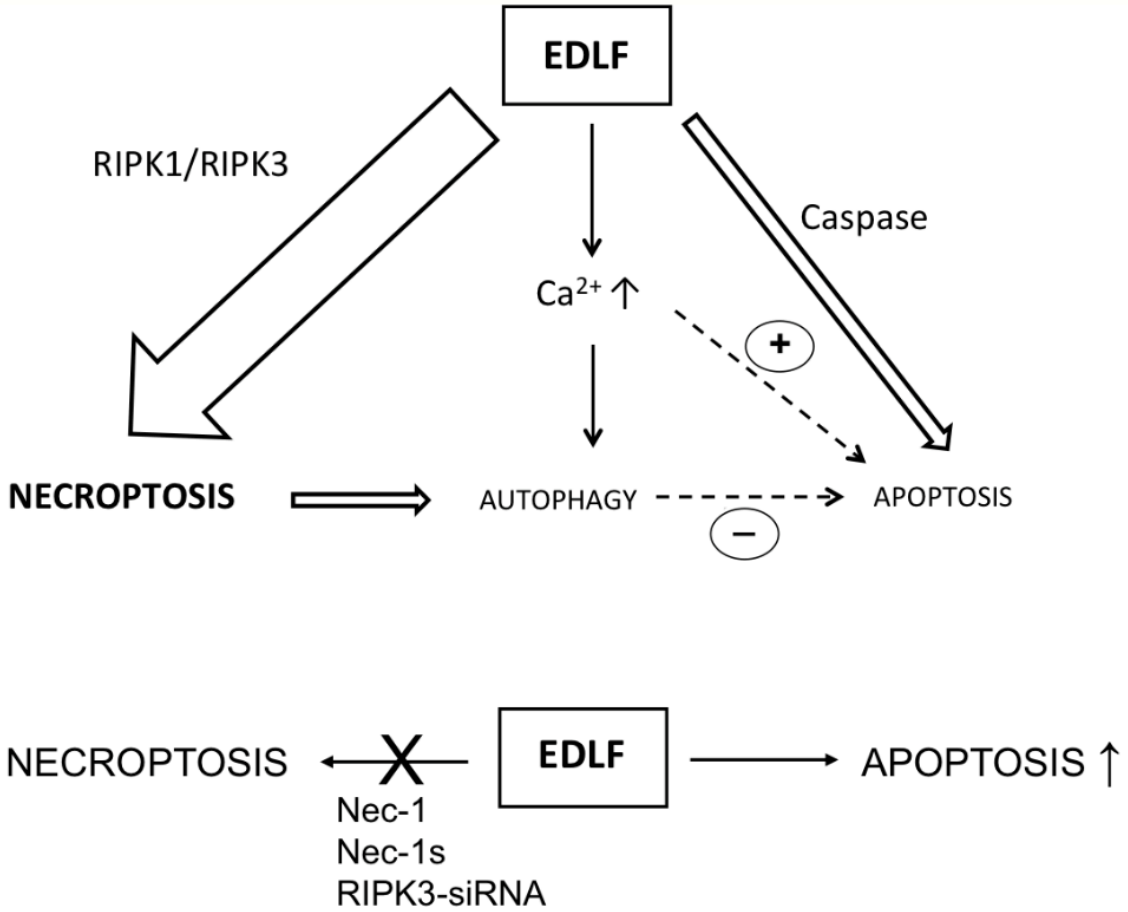

Figure 7.1: Schematic model for edelfosine-induced cell death in U118 cells. (*upper*) This is a schematic diagram that depicts the cell death mechanisms triggered during the edelfosine killing action in U118 glioblastoma cells, and highlights the involvement of RIPK1/RIPK3-mediated necroptotosis in the process. (*lower*) When necroptosis is inhibited, the caspase-dependent apoptotic response is potentiated following edelfosine treatment. *(Melo-Lima et al., 2014).*

and its relevance in the search for new therapeutic approaches to treat glioblastoma.

Results II

The data reported in chapter 4, *Inhibition of ERK1/2 phosphorylation by MEK1/2 inhibitor U0126 shifts the predominantly necrotic response induced by edelfosine to an apoptotic type of cell death in U118 cells*, suggest that ERK1/2 phosphorylation acts as a major regulator of apoptotic cell death, triggering signals that lead to apoptosis inhibition in U118 cells following edelfosine treatment. Taken together, our results indicate that the MEK1/2 inhibitor U0126, leading to ERK1/2 inhibition, dramatically shifts the response of U118 glioblastoma cell line to edelfosine from necrosis/necroptosis to apoptosis. U0126 alone reduced ERK1/2 phosphorylation, but its effect was further potentiated when used in combination with edelfosine,

leading to manifold actions, namely: (a) RIPK1 degradation, likely underlying inhibition of necroptosis; (b) RelA/NF-κB p65 degradation, thus inhibiting survival signalling; (c) caspase activation, leading to caspase-dependent apoptosis. The dramatic increase in apoptosis after U0126 plus edelfosine treatment was assessed by an increase in the rate of cells displaying apoptotic morphology and DNA degradation (Sub-G_1 cell population), as well as by caspase activation and prevention of cell death through caspase inhibition.

Figure 7.2 (from Melo-Lima *et al.*, 2015) depicts a putative model of how ERK1/2 may regulate the final outcome in U118 cells upon edelfosine treatment. Interestingly, our data suggest that three major cellular responses (survival, apoptosis, necrosis/necroptosis) can be generated following edelfosine treatment of U118 cells. RIPK1-containing complexes could lead to the triggering of distinct cellular outcomes depending on the RIPK1 partner (Christofferson & Yuan, 2010), namely (Figure 7.2) : (a) cell survival, through its interaction with NF-κB essential modulator (NEMO), leading to the activation of the NF-κB pathway; (b) apoptosis, through its interaction with caspase-8 and FADD, thus activating a caspase cascade and leading to apoptosis and RIPK1 degradation; (c) necrosis/necroptosis, through its interaction with RIPK3 forming the so-called necrosome complex, leading to necrosis/necroptosis. The formation and setting in motion of each of the above different triggers would depend on the inherent characteristics of each cell type regarding gene expression and on the distinct stimuli. Based on the results reported here, edelfosine seems to be able to induce the above three major cellular responses in U118 cells, namely survival, apoptosis and necrosis/necroptosis, and two major factors regulating the eventual cellular outcome include drug concentration and ERK1/2 phosphorylation (Figure 7.2).

At low edelfosine concentrations (1 μM), the triggering of cell death-promoting processes is suggested not to be potent enough to outweigh the anti-apoptotic signals delivered by ERK1/2 phosphorylation, and therefore apoptosis is not taking place, but instead survival signals, likely involving ERK1/2 and NF-κB, are delivered (Figure 7.2). At higher drug concentration (10 μM), edelfosine treatment generates cell death-promoting signals in U118 cells that overcome survival signalling, leading to necrotic cell death, provided apoptosis is suppressed by ERK1/2 phosphorylation (Figure 7.2). Thus, necrosis/necroptosis would act as a backup mechanism of cell death when apoptosis is blocked in edelfosine-treated U118 cells. However, ERK1/2 inhibition leads to permissive conditions for apoptosis in edelfosine-treated U118 cells, diminishing the threshold for edelfosine-induced apoptosis and highly potentiating cell demise. Interestingly, caspase-8 activation was only detectable following ERK1/2 dephosphorylation, suggesting a role for ERK1/2 phosphorylation in blocking the apoptotic pathway at the level of caspase-8 activation in edelfosine-treated U118 cells. The fact that ERK1/2 inhibition dramatically potentiates edelfosine-induced apoptosis in U118 cells, and turns either the survival or necrotic responses into potent apoptosis, suggests that edelfosine is a potent inducer of apoptotic signalling, but this apoptotic response is highly modulated by ERK1/2 phosphorylation. Caspase-8 activation engages downstream caspases, thus leading to RIPK1 degradation and inhibition of the necrosis and survival triggers (Figure 7.2), as RIPK1 is involved in both survival and necrotic signalling (Christofferson & Yuan, 2010).

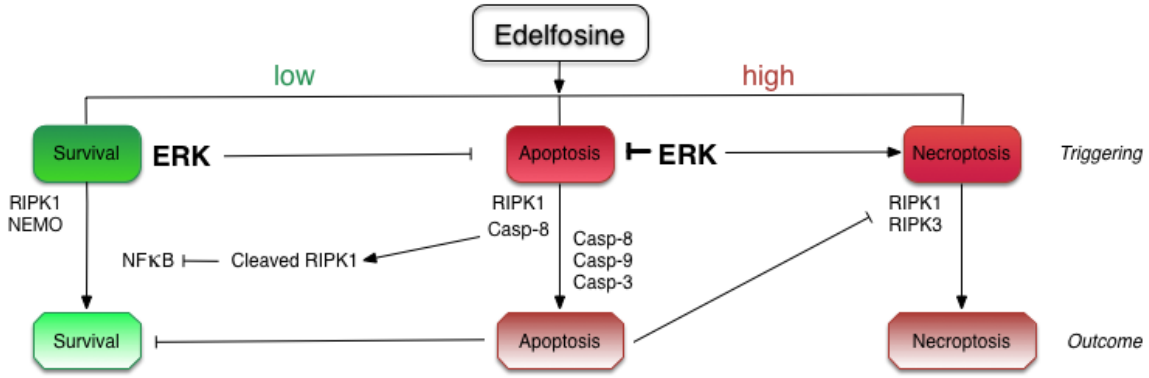

Figure 7.2: Schematic model of ERK1/2 involvement in a regulatory cell death switch for apoptosis induction in edelfosine-treated U118 glioblastoma cells. This scheme portrays a putative mechanism by which ERK1/2 activation modulates the distinct responses (survival signalling, green; cell death signalling, red) induced by edelfosine in U118 cells, with a major role in apoptosis regulation. Edelfosine is able to induce three different responses in U118 cells depending on drug concentration and the state of ERK1/2 phosphorylation, namely: survival (low drug concentration; ERK activation); necrosis (high drug concentration; ERK1/2 activation); and apoptosis (high drug concentration; ERK1/2 inhibition). RIPK1 forms complexes with distinct proteins, being involved in the triggering of the above mentioned cellular processes and leading to various cellular outcomes. When RIPK1 is degraded by caspase-8, both RIPK1-dependent survival and necrotic responses are inhibited, thus potentiating caspase-dependent apoptosis as the major cellular response. *From Melo-Lima et al. (2015).*

Regarding NF-κB-mediated survival signalling, cleaved RIPK1 has been shown to inhibit NF-κB activation (Rébé *et al.*, 2007), and RIPK1 cleavage by caspase-8 results in blockage of the TNF-induced NF-κB activation and prompts tumor necrosis factor (TNF)-induced apoptosis (Lin *et al.*, 1999a). Taken together, our data suggest that ERK1/2 activation blocks caspase-8 activity through not yet known mechanisms, thus limiting the initiation and amplification of both extrinsic and intrinsic apoptotic pathways, and thereby favoring survival at low concentrations of edelfosine or the necrotic pathway when edelfosine concentration reaches 10 μM. Our data suggest that ERK1/2 acts as a major regulator or a gatekeeper for apoptosis in edelfosine-treated cells. The drastic change from necrosis to apoptosis in edelfosine-treated U118 cells following ERK1/2 inhibition suggests that ERK1/2 phosphorylation regulates a switch determining the cell death type response in edelfosine-treated U118 glioblastoma cells. This switch, between apoptosis (ERK1/2 inactivation) and necroptosis (ERK1/2 activation), could be of importance in order to modulate the cell death response induced in specific cancer cells, which could be of special importance in the treatment of glioblastoma, a necrosis-prone neoplasm, where necrosis raises some concerns about undesirable side effects.

Furthermore, we also found that treatment with edelfosine alone induced a potent necrotic response accompanied by rapid $\Delta\Psi_m$ dissipation and high increase in ROS generation, but a small percentage of cells still remained viable. However, following U0126 preincubation, U118 cells became extremely sensitive to edelfosine, and practically all the cells underwent $\Delta\Psi_m$ loss and apoptosis while showing much lower levels of ROS. The

mitochondrion is a significant source of ROS that are associated with the pathogenesis of many diseases. The oxygen species that are typically linked to oxidative stress include superoxide anion, hydroxyl radical (OH), hydrogen peroxide (H_2O_2), nitric oxide (NO) and peroxynitrite ($ONOO^-$) (Hong *et al.*, 2006). Although generation of these species from molecular oxygen is a normal feature of mammalian respiration, ROS can cause severe damage to cellular proteins, lipids and DNA when produced at high levels and may lead to necrosis. Some studies also linked ERK phosphorylation with increased ROS production (Cagnol & Chambard, 2010). Another executional step of necrosis may be refrained in U0126 pre-treated cells by lowering ROS levels, favoring apoptotic execution and overall cellular demise.

Hsp90 inhibition has been reported to inhibit ERK1/2 signalling (Zhang & Burrows, 2004; Georgakis *et al.*, 2006), as well as to promote proteasomal degradation of RIPK1 (Fearns *et al.*, 2006). We have also found that the combined treatment of the Hsp90 inhibitor geldanamycin and edelfosine downregulated ERK1/2 and RIPK1, leading to a dramatic activation of caspases 3, 8 and 9, and a potent apoptotic response in U118 cells. These data are in agreement with the results described here and further support that ERK1/2 inhibition potentiates edelfosine-induced apoptosis in glioblastoma U118 cells. Hsp90 inhibition has been reported to induce tumor regression in glioblastoma (Zhu *et al.*, 2010), and thereby the combined use of Hsp90 inhibitors and edelfosine could be an interesting approach in the induction of apoptotic cell death in glioblastoma. Geldanamycin favored a fast cell death, mainly, but not totally, apoptotic as observed by morphological changes, increase in Sub-G_1 population by cell cycle analysis, and caspases activation. We could also detect caspase-8 activation after a short period of incubation. Again, ERK phosphorylation decrease might favor the activation of the apoptotic machinery instead of the necroptotic one, while RIPK1 degradation/cleavage may block the necroptotic pathway. The complete change from a necroptotic type of cell death to an apoptotic one is not as sharp as in the case of U0126 combination with edelfosine; this could be due to a smaller decrease in ERK phosphorylation with the use of geldanamycin, and because Hsp90 function could interfere with many other client proteins and signalling pathways regulating cell death/survival might be affected, influencing cellular fate outcome.

On the other hand, different studies have shown that in necrotic cell death, RIPK1 leads to anti-apoptotic signals by the activation of NF-κB and the MAPKs. Could also the cleaved RIPK1 or the fact that there is less intact RIPK1, limit the extent of ERK phosphorylation? Zheng-gang Liu *et al* reported that the kinase activity of RIPK1 is required for ERK activation (Zheng *et al.*, 2003). This could help to explain why ERK phosphorylation keeps diminishing over time with edelfosine treatment combined with U0126 and virtually disappears when there is no RIPK1 (78kDa band). One of the essential functions of RIPK1 is to mediate TNF-induced NF-κB activation, and overexpression of RIPK1 activates NF-κB (Hsu *et al.*, 1996). Here, we found an important downregulation of total protein NF-κB, that coincide with RIPK1 cleavage and increased apoptosis levels.

We also found that U0126 caused an important reduction in the autophagic marker

LC3B-II, and also in LC3B-I. Autophagy has been described as a side effect of the stress imposed to cells undergoing necrosis, and many studies associated ERK activity with autophagy in different models, in response to different stresses (Cagnol & Chambard, 2010). Moreover, direct ERK activation by overexpression of constitutively active MEK can promote autophagy without any other stimulus (Corcelle *et al.*, 2006). Also, some recent studies suggest a correlation between caspase-8 inhibition and excessive autophagy. Taken together, the data reported here suggest that ERK1/2 inhibition leads to permissive conditions that facilitate apoptosis upon addition of certain cell death-promoting stimuli such as edelfosine, and that the phosphorylation state of ERK1/2 behaves as a switch in the onset of either apoptosis or necrosis in glioblastoma U118 cells to execute the internal cell death program, deciding the prevalence of either apoptosis or necrosis, which could be of major importance in the treatment of necrosis-prone tumors, such as glioblastoma. Thus, our data suggest that MEK1/2-ERK1/2 signalling acts as a master on/off switch in controlling apoptosis of U118 glioblastoma cells following edelfosine treatment.

Results III

In chapter 5, *Identification of a subpopulation of edelfosine-resistant U118 cells*, we describe that with edelfosine treatment, although the majority of the cells died through a necrotic process in a short period of time, a small proportion of the cells was resistant to the drug: this population did not lose mitochondrial membrane potential, and expressed high levels of the anti-apoptotic protein Bcl-x_L. We also observed that after removing edelfosine, the resistant cells that survived could proliferate again after a few days, and generated multinucleated cells; these cells were efficiently killed with a mixture of necrosis and apoptosis by the BH3-mimetic inhibitor ABT-737. Pre-incubating the cells with U0126, besides increasing apoptotic execution, led to a much lower number of resistant, edelfosine surviving cells. Bcl-x_L was downregulated by pretreatment with U0126 and in that case practically all the cells underwent a total $\Delta\Psi_m$ loss (~95%). Bcl-x_L appears to play a prominent role in the regulation of multiple distinct types of cell death, including apoptosis and regulated necrosis (Michels *et al.*, 2013). Bcl-2 and Bcl-x_L, which reside at the outer layer of the mitochondrial membrane, act to negatively regulate the intrinsic apoptosis pathway, preventing mitochondrial permeabilization and the release of cytochrome c, formation of the apoptosome and the activation of caspase-9 (Johnson, 2013). However, Bcl-2 and Bcl-x_L appear to control cell survival beyond the APAF1-caspase-9 axis. If caspase activation is inhibited by loss of APAF1 or caspase-9, or even by the combined loss of caspase-9 and caspase-2, the rate of acquisition of apoptotic morphology after stress-induced apoptosis was seen to be significantly delayed in myeloid progenitors and mast cells, but these cells still lose clonogenic potential and die, unlike cells that overexpress Bcl-2 or Bcl-x_L (Youle & Strasser, 2008). The step of apoptosis regulation that is controlled by the Bcl-2 family thus appears to be the most general final commitment for the decision between cell life and death.

Our results suggest that although the necroptotic pathway is a very fast and highly effi-

cient form of cellular demise after edelfosine treatment in the U118 cell line, the activation of this program instead of the apoptotic one is also allowing the survival of some cells that seem not to be resistant to the apoptotic cell death program, but that are allowed to survive when apoptosis is blocked (these cells are not resistant to apoptosis but are resistant to necroptosis). This raises different questions: is the necroptotic pathway acting as a backup mechanism since apotosis is blocked through p-ERK activation, or is it being enhanced by the factors blocking apoptotic signalling? p-ERK activation blocks apoptosis but allows necroptotic pathway to proceed; is Bcl-x_L protecting from cell death, both apoptotic and necroptotic? How could we balance between these cell death pathways, and favor the maximum cellular demise?

U118 surviving cells expressed high levels of Bcl-x_L, and although ERK expression was downregulated, levels of p-ERK remained high, pointing out that the majority, if not all, the remaining protein was in its activated state. As mentioned by Flusberb and Sorger (Flusberg & Sorger, 2015), it is technically challenging to observe both the initial state of a cell and its ultimate fate, and to know whether markers that characterize survivors pre-date drug treatment or arise in response to it. So, we cannot say if the surviving cells always displayed autophagy or expressed high levels of Bcl-x_L or p-ERK, but the fact that the surviving cells at 24 h treatments present these characteristics, while almost 80% of the cells were already dead, make it reasonable to think that the activated pathways and proteins with increased expression are allowing cell survival. Furthermore, the fact that autophagy is mantained during the recovery phase after drug removal, for few days, might suggest that this mechanism favors cell survival. However, most of the cells dying within the 24 hours treatment displayed signs of autophagy and still died through necroptosis; in fact, as mentioned above, autophagy seems to be a parallel phenomenon to the necroptotic process, since autophagy was importantly diminished when necroptosis was inhibited by either Necrostatin-1 or the use of MEK1/2 inhibitor. Also, autophagy does not seem to be of great importance to cellular outcome, since its inhibition alone did not produce a significant change in cell survival or type of induced cell death. In the case of the surviving cells, we did not find a significant change in the apoptotic or total rate of cell death after treatment with autophagy inhibitors bafilomycin or wortmannin following edelfosine wash-off (preliminary results). Again, autophagy may be a parallel mechanism that is activated due to the induced stress, but in this case it does not seem to be determinant to cell death in the continuous presence of the drug, or to cell survival after drug withdrawal. It might be suggested, however, that surviving cells are cells that activate autophagy and are somehow resistant to necrotic execution of cell death.

By selecting these surviving cells, gradually increasing the time of exposure to edelfosine and the drug concentration, we could generate super-resistant cells, which were able to tolerate ~10 times higher doses of edelfosine than the original U118 cell line. Different studies suggest that cell-to-cell variability that can result from differences in genetic, epigenetic, phenotypic, stochastic flutuations, cell cycle differences, etc, plays an important role in cell fate decisions, and may explain variations in the timing of cell death as well as the fate of individual cells (Raj & Oudenaarden, 2008; Brock *et al.*, 2009). Cell variability may affect both the extent of death activation and the magnitude of survival pathway induction, con-

tributing to fractional killing within a cell population. At each increasing concentration step, a part of the population died but another one survived, and the proportion of surviving cells increased at each additional step, supporting the notion that a "memory" of the first stress, activated in U118 cells that responded with the induction of stress rather than death, leads to preferential protection of these cells over others when a future exposure arises. Accumulating observations suggest that non-killed, residual tumor cells actively acquire a new phenotype simply by exploiting their developmental potential. These surviving cells are stressed by the cytotoxic treatment, and owing to phenotype plasticity, exhibit a variety of responses (Pisco & Huang, 2015). These cells that survive may activate not only counter-balancing adaptive pathways that protect themselves against death in a future insult, but also inflammation and differentiation programs that promote repair of damage and clearance of apoptotic cells caused by death of neighboring cells (Flusberg & Sorger, 2015). The clearance of apoptotic cells was also strongly suggested in U118 surviving cells following edelfosine withdrawal and could possibly favor the formation of multinucleated cells.

The phenomenon of multinucleation and formation of multinucleated cells could be due to at least three mechanisms: endomitosis, cell engulfment and/or cell fusion. Our results do not clearly define which of these mechanisms are implicated in this case, but we found that Bcl-x_L is important for both the survival and the multinucleation process at that stage, suggesting that these two processes may be connected and interdependent. Also, blocked cytokinesis and probably cell fusion seem to be involved, from the data herein reported. Cell fusion may occur more often or more easily when cancer cells are in a more stressful situation, such as during therapies. In fact, resistance to chemotherapy has been interpreted more in terms of gross changes in chromosome number (aneuploidy) or chromosome aberrations (instability) rather than of point mutations, and a role for Bcl-x_L in this process has already been described (Nuydens *et al.*, 2000). Minn *et al* (Minn *et al.*, 1995) also found that Bcl-x_L expressing cells treated with chemotherapeutic drugs retained their proliferative ability after the drugs were removed, and that vincristine-treated cells expressing Bcl-x_L become polyploid after drug removal. The ability of Bcl-x_L to prevent apoptotic cell death in response to chemotherapy may contribute to accumulation of chromosomal aberrations within tumors, favoring even more the development of drug resistance. Furthermore, Bcl-2-like proteins have recently been shown to modulate multiple processes not directly connected to the execution of cell death, including - among others- bioenergetic metabolism, mitochondrial functions, mitosis, and autophagy (Michels *et al.*, 2013).

In the review "Surviving apoptosis: life-death signaling in single cells", the authors question if acquired resistance to any death-inducing stimulus is a manifestation of trasiently induced resistance that is reversible following drug removal or if it results from stable genetic mutations or from a more slowly reversible epigenetic adaptation (Flusberg & Sorger, 2015). It seems reasonable that some changes after one insult or persistance of that insult favoring cell survival would be mantained in the presence of the stimulus, and then return to "normal state" following drug withdrawal. However, it is known that cells faced with a sublethal stress may induce protective mechanisms against a future exposure to that stress, a concept

known as preconditioning, acquiring a "memory" of their resistant state. This "memory" would depend on the lenght of exposure and subsequent exposures; the survival and/or adaptive state can either be sustained by continued treatment during this resistance stage or lost when treatment is removed and this may occur at different timescales. In fact, what we could observe in the U118 cell line when generating the U118-R edelfosine-resistant cell line, was most probably an increased preconditioning as we further increased the concentration and the time of exposure to edelfosine. Possibly, after a certain threshold, the cells are mantained in their "resistant state" and challenging them with the same stimulus no longer induces cell death. In addition, from the stress pressure imposed to the cells, an increased heterogenity and adaptability are progressively selected.

In this chapter, we described that U118-R cells present higher levels of basal ERK1/2 phosphorylation. In U118 cells, ERK1/2 and JNK1/2 followed similar patterns of activation after edelfosine treatment, but in U118-R untreated cells ERK is strongly phosphorylated whereas JNK1/2 is not phosphorylated. In this way, it seems reasonable to think that cells that survived and led to the generation of the U118-R cell line had higher levels of ERK activation and lower levels of p-JNK. Possibly, p-ERK and p-JNK contributed to cell survival and to cell death respectively, in the U118 cell line. However, the role of JNK in cell death is controversial, since both pro-apoptotic and pro-survival roles have been attributed to JNK, and the underlying mechanisms mediating both functions remain unclear. Interestingly, the resistant cell line did not activate ERK1/2 or JNK1/2 when treated with edelfosine, at least until up to a 50 μM concentration. However, even though ERK is not further phosphorylated following edelfosine treatment in U118-R cells, p-ERK acts as a protector from apoptosis execution, since incubation with U0126 prior to edelfosine treatment also led to an increase in apoptotic cell death in U118-R cells, showing again the importance of p-ERK in mediating cell death and blocking apoptosis; this effect was maintained through the process of generating the resistant cell line.

U118-R cells showed different levels of expression and activation status in many distinct proteins when compared with the original cell line, and some of these correlated with changes observed in the microarrays analysis performed. Figure 7.3 graphically represents the results for singular enrichment analysis on molecular functions and related *PANTHER* and *KEGG* pathways for differentially expressed genes in U118-R cells. In Table 7.1, differentially expressed genes corresponding to each group of potentially affected signalling *KEGG* pathways are indicated. The GeneCodis (Gene Annotation Co-occurrence Discovery) was used to perform these analyses (Carmona-Saez *et al.*, 2007; Nogales-Cadenas *et al.*, 2009; Tabas-Madrid *et al.*, 2012). Although these results need validation by qPCR, they constitute a preliminary evaluation of the changes undergone by cells that are continuously exposed to edelfosine.

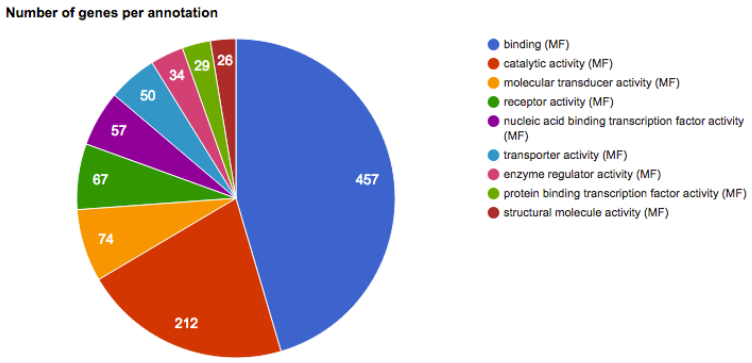

(a) GO Molecular Function

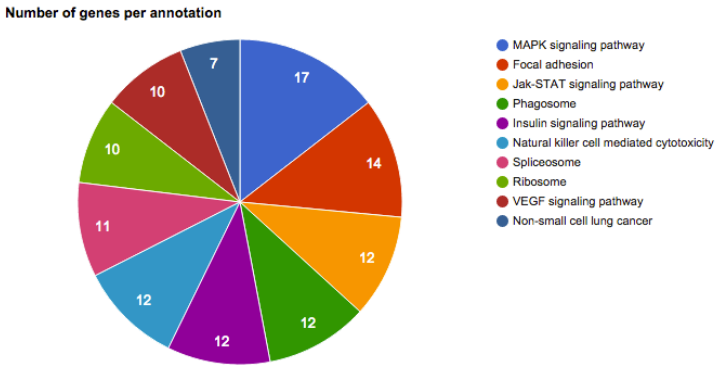

(b) KEGG Pathways

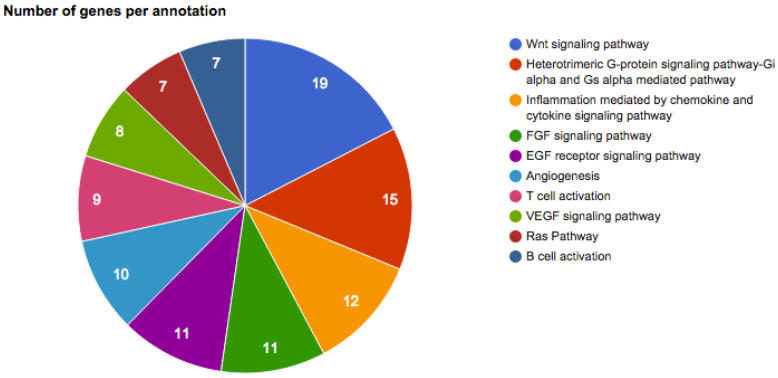

(c) Pantherpathways

Figure 7.3: The GeneCodis (Gene Annotation Co-occurrence Discovery) was used to identify statistically significant functional associations linking particular gene subsets contained within the list of differentially expressed genes in U118-R cells (FDR=0.1) to specific cellular functionalities, including particular Molecular Functions (a) and signalling pathways - KEGG (b) and PANTHER (c) Pathways.

Annotations	KEGG Pathway	Hyp	Hyp c	Genes
Kegg:04722	Neurotrophin signaling pathway	0.001983	0.017038	HRAS, SHC3, MAPKAPK2, BRAF, AKT1, PIK3CD, MAPK14, PIK3CG, IRS2
Kegg:04910	**Insulin signaling pathway**	4.85E-05	0.002292	**CBLC, HRAS, SHC3, SLC2A4, PRKACA, BRAF, AKT1, PIK3CD, PIK3CG, PCK2, IRS2, PRKAG2**
Kegg:04920	Adipocytokine signaling pathway	0.000756	0.00841	SLC2A4, AKT1, ACSL4, RXRA, PCK2, IRS2, PRKAG2
Kegg:04630	**Jak-STAT signaling pathway**	0.000186	0.002704	**CBLC, GH1, CCND2, OSM, AKT1, PIK3CD, CCND3, CTF1, PIK3CG, IL2RB, SPRY4, IFNA10**
Kegg:00190	Oxidative phosphorylation	0.002735	0.022476	COX11, ATP5J, ATP5D, ATP6V1A, COX6A1, NDUFA7, NDUFA13, ATP6V1B2, NDUFS6
Kegg:04810	Regulation of actin cytoskeleton	0.000953	0.010007	HRAS, SSH3, ACTG1, FGFR3, FGF17, FGF19, BRAF, ACTB, TMSB4X, PIK3CD, ARHGEF4, PIK3CG, ACTN4
Kegg:04010	**MAPK signaling pathway**	0.000102	0.002754	**MEF2C, HRAS, FGFR3, MAPKAPK2, FLNA, FGF17, FGF19, PRKACA, ARRB2, BRAF, PLA2G2E, AKT1, MAPK14, PPP3CA, PLA2G12B, ARRB1, GADD45B**
Kegg:04370	**VEGF signaling pathway**	6.83E-06	0.00129	**HRAS, MAPKAPK2, PLA2G2E, SPHK1, AKT1, PIK3CD, MAPK14, PPP3CA, PLA2G12B, PIK3CG**
Kegg:05200	**Pathways in cancer**	0.000155	0.002929	**VEGFB, RARB, CBLC, HRAS, WNT9B, WNT7A, FZD7, NKX3-1, FGFR3, FGF17, FGF19, BRAF, FZD1, FZD9, AKT1, PIK3CD, SMAD4, PIK3CG, RXRA**
Kegg:05223	Non-small cell lung cancer	0.000176	0.002768	RARB, HRAS, BRAF, AKT1, PIK3CD, PIK3CG, RXRA
Kegg:03040	Spliceosome	7.38E-05	0.002325	TCERG1, HNRNPA1, PPIE, U2AF1, MAGOHB, ZMAT2, SNRPG, TRA2A, SNRPE, LSM3, DHX8
Kegg:04062	Chemokine signaling pathway	0.000318	0.004008	HRAS, SHC3, GRK6, ELMO1, PRKACA, ARRB2, BRAF, GNG5, AKT1, CCR10, PIK3CD, ARRB1, PIK3CG
Kegg:04145	Phagosome	6.48E-05	0.00245	HLA-A, TUBB2B, ACTG1, ATP6V1A, FCAR, LAMP1, HLA-C, ACTB, FCGR3A, TUBB6, CORO1A, ATP6V1B2
Kegg:03010	Ribosome	2.34E-05	0.002208	RPS9, RPL36, RPL13A, RPL10, RPL22, RPL18A, RPL34, RPS2, RPL28, RPL3
Kegg:04080	Neuroactive ligand-receptor interaction	0.00801	0.042052	UTS2R, HRH4, ADRA2B, GH1, DRD5, CHRNB4, ADRA2A, CHRNA7, GALR3, MTNR1A, ADRA2C, SSTR2, PTGDR
Kegg:04650	Natural killer cell mediated cytotoxicity	2.62E-05	0.001651	HRAS, SHC3, HLA-A, RAET1L, HLA-C, BRAF, HCST, PIK3CD, PPP3CA, FCGR3A, PIK3CG, IFNA10
Kegg:03015	mRNA surveillance pathway	0.008731	0.0446	GSPT1, SMG1, PABPC3, MAGOHB, PPP2R3B, PPP2R5D
Kegg:04510	Focal adhesion	0.00016	0.002743	VEGFB, HRAS, SHC3, ACTG1, CCND2, FLNA, TLN1, BRAF, ACTB, AKT1, PIK3CD, CCND3, PIK3CG, ACTN4
Kegg:04144	**Endocytosis**	0.000129	0.003041	**CBLC, HRAS, HLA-A, GRK6, FGFR3, ARRB2, HLA-C, PARD6B, IQSEC3, SMAP2, VPS37D, ARRB1, IL2RB, PARD6G**
Kegg:05110	Vibrio cholerae infection	0.006643	0.039237	ACTG1, ATP6V1A, PRKACA, ACTB, ATP6V1B2
Kegg:04660	T cell receptor signaling pathway	0.010553	0.049864	CBLC, HRAS, AKT1, PIK3CD, MAPK14, PPP3CA, PIK3CG
Kegg:04310	Wnt signaling pathway	0.000145	0.003045	WNT9B, WNT7A, FZD7, CCND2, PRKACA, FZD1, FZD9, PPP3CA, TBL1XR1, SMAD4, PPP2R5D, CCND3
Kegg:05218	Melanoma	0.000984	0.0093	HRAS, FGF17, FGF19, BRAF, AKT1, PIK3CD, PIK3CG
Kegg:04916	Melanogenesis	0.006643	0.038049	HRAS, WNT9B, WNT7A, FZD7, PRKACA, FZD1, FZD9
Kegg:04530	Tight junction	0.000729	0.00861	HRAS, ACTG1, CSDA, EPB41L1, ACTB, AKT1, PARD6B, EPB41, ACTN4, PARD6G
Kegg:05211	Renal cell carcinoma	0.004874	0.031763	VEGFB, HRAS, BRAF, AKT1, PIK3CD, PIK3CG
Kegg:04150	**mTOR signaling pathway**	0.006127	0.037358	**VEGFB, BRAF, AKT1, PIK3CD, PIK3CG**
Kegg:05212	Pancreatic cancer	0.004874	0.031763	VEGFB, BRAF, AKT1, PIK3CD, SMAD4, PIK3CG
Kegg:04380	Osteoclast differentiation	0.007704	0.042823	TNFRSF11A, SIRPG, AKT1, PIK3CD, MAPK14, PPP3CA, FCGR3A, PIK3CG
Kegg:04012	ErbB signaling pathway	0.003462	0.024231	CBLC, HRAS, SHC3, BRAF, AKT1, PIK3CD, PIK3CG
Kegg:05220	Chronic myeloid leukemia	0.000231	0.003122	CBLC, HRAS, SHC3, BRAF, AKT1, PIK3CD, SMAD4, PIK3CG
Kegg:05213	Endometrial cancer	0.006127	0.037358	HRAS, BRAF, AKT1, PIK3CD, PIK3CG
Kegg:05217	Basal cell carcinoma	0.007765	0.04193	WNT9B, WNT7A, FZD7, FZD1, FZD9
Kegg:05221	Acute myeloid leukemia	0.009011	0.04482	HRAS, BRAF, AKT1, PIK3CD, PIK3CG
Kegg:05214	Glioma	0.00288	0.022684	HRAS, SHC3, BRAF, AKT1, PIK3CD, PIK3CG

Table 7.1: The GeneCodis (Gene Annotation Co-occurrence Discovery) was used to identify statistically significant functional associations linking particular gene subsets contained within the list of differentially expressed genes in U118-R cells (FDR=0.1) to specific signalling pathways. The column "Annotations" identifies KEGG number, "KEGG Pathways" the denomination of signalling pathways potentially affected by the corresponding group of differentially expressed genes listed in each case under the "Genes" column. The column labeled "Hyp" refers to the statistical significance of the functional associations identified, and contains p-values calculated using the Hypergeometric Distribution and subsequently corrected by implementing the False Discovery Rate method ("Hyp c"). Total number of genes in the input list, 768.

Further analysis, however, must be carefully performed, in order to distinguish the changes that represent a consequence of that exposure and do not have a direct impact on cell survival from others that may in fact constitute alterations that favor/allow cell survival. Still remains the question if these factors were already there and were selected through selection of the surviving cells, or if they were induced by edelfosine exposure and continuous adaptation of the cells, that due to different characteristics were already able to tolerate the drug for more time or at a higher concentration, as previously discussed. Likely, these changes result from a combination of both. The high number of genes and pathways implicated and identified in the preliminary analysis of the microarray data, point out to already described effects on lipid metabolism, EGF receptor and PDGF signalling pathways and insulin/IGF pathway-PKB signalling cascades. These findings also contribute to the notion that edelfosine affects many different cellular processes and exerts changes in lipid metabolism and lipid-dependent signal transduction pathways.

The results presented in this thesis were focused on the cascades of protein kinases and their cytoplasmic substrates that become activated in response to edelfosine. However, lipids, lipid kinases, and lipid phosphatases serve a variety of roles in signal transduction. Lipids act as ligands that activate signal transduction pathways as well as mediators of signalling pathways, and are the substrates of lipid kinases and lipid phosphatases (Eyster, 2007). In order to gain insight into edelfosine-induced changes in the content of different lipid molecular species, lipidomic studies were performed in U118 and U118-R untreated and treated cells and important changes were found between the two groups. Importantly, we found ceramides were increased in U118-R cells (preliminary lipidomics analyses). In this context, miltefosine has been shown to inhibit sphingomyelin synthesis leading to elevated levels of ceramide (Wieder *et al.*, 1998).

Generation of ceramide, a sphingolipid bioactive molecule that induces apoptosis and other forms of cell death, and triggers autophagy (Pattingre *et al.*, 2009) may constitute an important signalling event activated by cellular stresses, including activation of tumor necrosis factor receptor, ultraviolet radiation, chemotherapeutic drugs, and hyperosmolarity (Schubert *et al.*, 2000). Ceramides increase can lead to cell death by apoptosis, but U118 cells are resistant to apoptotic execution, and it is thus possible that ceramide's increased content in the resistant cells is a consequence of exposure to edelfosine; those cells however, even in the presence of high levels of ceramides were able to survive, probably having acquired ways to cope with that increase.

Autophagy was also proven to be activated during ceramide increase as a way do deal with the imposed stress (Lavieu *et al.*, 2007). The sphingolipid rheostat, ceramide/sphingosine-1-phosphate (S1P), has been proposed to orchestrate the balance between cell survival and cell death where sphingosine-1-phosphate is an anti-apoptotic molecule that increases cell survival and ceramide is a pro-apoptotic mediator (Lavieu *et al.*, 2007). Sphingosine kinase (SphK), the enzyme that synthesizes S1P, is a crucial enzyme in the regulation of the balance of these sphingolipids and has been shown to play dynamic roles in the responses of cells to stress, leading to modulation of cell fate through a variety of signalling pathways impinging

on the processes of cell proliferation, apoptosis, autophagy and senescence (Van Brocklyn & Williams, 2012). We found that ceramides were increased and that sphingosine kinase was upregulated in U118-R cells (~1,44 x , p value= 0.0024, microarrays data). Both ceramide and S1P have been shown to stimulate autophagy, however, ceramide induces autophagy via upregulation of Beclin-1 and BNIP-3 usually resulting in autophagic cell death, whereas SphK/S1P-induced autophagy appears to be mediated by different pathways and is generally a survival response (Van Brocklyn & Williams, 2012). The balance of Beclin-1 and Bcl-2 may be important in determining cellular outcome, as Bcl-2 has been shown to interact with Beclin-1 to inhibit autophagy, and the Beclin-1/Bcl-2 balance has been suggested to maintain moderate levels of autophagy compatible with cell survival (Van Brocklyn & Williams, 2012). SphK can upregulate Bcl-2 and Bcl-2 overexpression can also induce increased SphK expression, thus, by causing only a modest increase in Beclin-1 and an increase in Bcl-2, SphK favors the survival side of autophagy (Van Brocklyn & Williams, 2012). Based on the interplay of SphK-regulated autophagic and apoptotic pathways it has been suggested that autophagy may be the key mechanism by which the sphingolipid rheostat controls cell survival (Lavieu *et al.*, 2007).

Following activation, SphK can translocate to the plasma membrane, where it phosporylates sphingosine to S1P. S1P is a bioactive lipid molecule, which can function as an intracellular messenger or is secreted out of the cell and coupled to its G-protein-coupled receptors (S1PRs) in an autocrine and/or paracrine manner to mediate prosurvival, cell proliferation, tumor growth and/or metastasis (Ponnusamy *et al.*, 2010). S1P signalling through S1P receptors can activate anti-apoptotic pathways, such as PI3 kinase/Akt and ERK MAP kinases (Young & Van Brocklyn, 2006). Furthermore, transporters of the ATP-binding cassette (ABC) family, which are known to export S1P extracellularly, have in some cases been shown be necessary for S1P-mediated survival responses (Ponnusamy *et al.*, 2010). In addition, ceramide metabolism to generate S1P by sphingosine kinase-1 (upregulated in U118-R cells) and -2 mediates, with or without the involvement of G-protein-coupled S1P receptor signalling, prosurvival, angiogenesis, metastasis and/or resistance to drug-induced apoptosis (Ponnusamy *et al.*, 2010).

The opposite cell survival/death signalling and the important changes observed in U118 *versus* U118-R cells related to lipid mediators and affected pathways warrants further investigation possibly through analysis of lipidomic studies and testing which related lipid kinases and phosphatases actually interfere with resistance to edelfosine. Analysis of these results may also shed light into possible changes occurring in membrane lipid composition that could have an impact in drug incorporation. In this chapter we described that resistant cells incorporated significantly much less edelfosine than U118 cells, and reduced incorporation of the drug could be an explanation, at least in part, for the fact that the dose that used to kill the normal cell line (10 μM) was insufficient to cause cell death in the resistant cell line.

Although changes in the fluidity/composition of the cell membrane may account for reduced edelfosine incorporation, other reasons for decreased incorporation could be decreased expression of proteins involved in edelfosine uptake and increase in expression and/or activ-

ity of edelfosine extrusion pumps. In this regard, microarrays data indicate that ABCC3, a member of the ATP-binding cassette transporters family which is involved in multidrug resistance (Zelcer *et al.*, 2001), is upregulated ~1.2 x in the U118-R cell line (p value=0.007). ABCC3 has been shown to confer resistance to the anticancer drugs methotrexate, etoposide, and teniposide (Uchiumi *et al.*, 1998; Kool *et al.*, 1999).

Results IV

In chapter 6, *Types of cell death induced by edelfosine in other glioblastoma cell lines and possible ways to increase cell death - where to interfere in order to maximize cell death and avoid drug resistance*, we analyzed the effects of edelfosine on the induction of cell death in the SF268, T98G, GOS-3 and A172 cell lines. In the next sections a short discussion of the main findings for each cell line will be made, and then a general comment for all the evaluated cell lines.

SF268 cell line

We found that edelfosine did not induce significant cell death in the SF268 cell line and that Bcl-x_L expression increased with the treatment. Similar to Bcl-2, Bcl-x_L binds to its multidomain pro-apoptotic counterparts Bax and Bak, preventing the formation of lethal pores in the mitochondrial outer membrane, as well as to multiple BH3-only proteins, interrupting apical pro-apoptotic signals (Michels *et al.*, 2013). Bcl-x_L has also been suggested to exert cytoprotective functions by binding to the voltage-dependent anion channel 1 (VDAC1), thereby inhibiting the so-called mitochondrial permeability transition (MPT), by preventing the generation of pro-apoptotic cytosolic Ca^{2+} waves by reducing capacity of ER Ca^{2+} stores and also by sequestering a cytosolic pool of the pro-apoptotic transcription factor p53, (Michels *et al.*, 2013). Bcl-x_L thus exerts cytoprotective effects not only as it antagonizes its pro-apoptotic counterparts but also as it counteracts the activity of p53. In addition, Bcl-x_L has recently been reported to interact with the mitochondrial phosphatase phosphoglycerate mutase family member 5 (PGAM5), a central effector of regulated necrosis (Sun *et al.*, 2012).

The BH3-mimetic inhibitor ABT-737 was able to increase cell death in SF268 cells by potentiating the execution of the intrinsic apoptotic pathway after edelfosine treatment. As found for the U118 cell line, possibly Bcl-x_L plays an important role mediating resistance to apoptosis induced by edelfosine in SF268 cells, in which limitation of the intrinsic apoptotic pathway has an important impact on cell death execution. Although a decrease in caspase-8 proform was observed at 8 h treatment with edelfosine, only a residual signal could be detected in the molecular weight corresponding to the active fragments. Caspase-8 may suffer modifications that alter its molecular weight or its expression may be decreased, but the active fragments are not present, thus limiting execution of cell death through the intrinsic

apoptotic pathway. ABT-737 potentiates apoptotic cell death through activation of the instrinsic pathway, as demonstrated by $\Delta\Psi_m$ loss, increased release of citochrome c into the cytosol and increased activation of caspases -9 and -3. Caspase-8 active 43 kDa fragment could be detected when the BH3-mimetic inhibitor was used, but its slight activation occurred approximately at the same time, or later, than activation of the other caspases, suggesting that its activation may be secondary to caspase-9 activation and that the intrinsic apoptotic pathway is preferently executed in SF268 cells.

ABT-737 is a small molecule that targets anti-apoptotic Bcl-2 family proteins (Bcl-2, Bcl-x_L, and Bcl-w), sequestering pro-apoptotic BH3 domain proteins, promoting Bax and Bak oligomerization and ultimately programmed cell death. ABT-737 markedly increased the response to radiation as well as multiple chemotherapy agents *in vitro*, showed good activity as a single agent in two small cell lung cancer xenograft models and preclinical activity as a single agent or in combination with various cytotoxic agents against AML, multiple myeloma, lymphoma, CLL, acute lymphoblastic leukemia, and small cell lung cancer (Kang & Reynolds, 2009).

PARP and AIF expression were affected by edelfosine treatment and also by pre-incubation with ABT-737; these proteins could be involved in alternative mechanisms of cell death execution or in resistance to cell death. PARP and AIF expression were importantly upregulated by edelfosine treatment. The consequences of this upregulation were not fully explored in this work; however, the fact that SF268 cells were resistant to cell death execution and that ABT-737 increased cell death but refrained the increase in both proteins, raises the possibility that PARP and AIF may have a protective effect on SF268 edelfosine-treated cells. However, it is also possible that the upregulation of these proteins may be due to, or lead to, the activation of another pathway of cell death execution that is limited for some reason, since both PARP and AIF may play dual roles, favoring cell death or cell survival. AIF is a mitochondrial flavoprotein, which normally resides in the inner mitochondrial membrane and possesses an NADH oxidase activity (Stambolsky *et al.*, 2006). It can exert a cytoprotective role in the mitochondria, enabling cells to cope more effectively with oxidative stress, but contrasting to its cytoprotective role in the mitochondria, translocation of AIF to the nucleus exerts an opposite effect on cell survival, and serves as a potent pro-apoptotic trigger (Stambolsky *et al.*, 2006). The DNA-repair and protein-modifying enzyme PARP, which is also called poly(ADP-ribose) synthetase and poly(ADP-ribose) transferase, is an abundant nuclear protein that is involved in the DNA-base-excision-repair system (Hong *et al.*, 2004). Many of the proteins involved in DNA repair systems can also be recruited to contribute to cell death, including p53, PARPs, BRCA1, ATM, etc. (Hong *et al.*, 2006). PARP has been implicated in caspase-independent cell death: its activation has been related to the translocation of a 57-kDa form of AIF into the cell nucleus, where it promotes chromatin condensation, DNA fragmentation and nuclear shrinkage (Martín-Oliva *et al.*, 2011). The broad-spectrum cytoprotective molecules Bcl-2 can delay or prevent AIF mediated toxicity, but their mechanism of action is unknown (Hong *et al.*, 2004). In the SF268 cell line, we found that pre-incubation with the BH3-mimetic inhibitor ABT-737

prevented the increase in both PARP and AIF expression observed with edelfosine treatment, and resulted in increased cell death through activation of the intrinsic apoptotic pathway. PARP functions at the center of cellular stress responses, where it processes diverse signals and, in response, directs cells to specific fates (e.g., DNA repair vs. cell death) based on the type and strength of the stress stimulus (Luo & Kraus, 2012). PARP may also suffer postranslational modifications that include ADP-ribosylation, phosphorylation, acetylation, ubiquitylation or SUMOylation. Postranslational modifications of PARP could occur in this cell line since we immunodetected bands of different molecular weights in edelfosine treated SF268 cells. Further investigation would be needed in order to evaluate these modifications and also the location and role of PARP and AIF in cell death/cell survival in edelfosine and ABT-737+edelfosine-treated cells. The correlation in the upregulation of both proteins and its inhibition through ABT-737 makes them an interesting subject for further studies.

T98G cell line

In the T98G cell line, edelfosine induced an apoptotic response, mediated through the extrinsic pathway. T98G was the only tested cell line in which activation of caspase-8 could be clearly seen after edelfosine treatment, followed by a progressive increase in caspase-3 activation, PARP cleavage and DNA degradation reflected an increase in the Sub-G_1 population. Contrary to the other cell lines, where the scarce apoptosis appeared to be due to the activation of the intrinsic apoptotic pathway, in T98G cells caspase-9 activation was not marked and loss of $\Delta\Psi_m$ was not generally observed as in other cell lines. In order to evaluate if the execution of the apoptotic response could be potentiated, we tested whether interferon-γ preincubation would affect apoptosis induction in the T98G cell line. Others have shown that IFN-γ sensitizes KB cells for apoptosis induction by facilitating death-inducing signalling complex (DISC)-mediated caspase 8 processing (Siegmund *et al.*, 2005). IFN-γ was also previously shown to upregulate many apoptosis-related molecules, including Fas, caspase-3, caspase-4, caspase-7, caspase-8 and Bak (Ahn *et al.*, 2002). While IFN-α and IFN-β are produced by most cells in response to virus infections and double-stranded RNA (dsRNA), IFN-γ is secreted from activated Th1 T cells and natural killer cells (Chawla-Sarkar *et al.*, 2003). Interferons are able to block viral replication and additionally induce a variety of other effects, including immune modulation, differentiation, apoptosis, and inhibition of proliferation and angiogenesis, thus IFNs may mediate anti-tumor effects either indirectly by modulating immunomodulatory and anti-angiogenic responses or by directly affecting proliferation or cellular differentiation of tumor cells (Chawla-Sarkar *et al.*, 2003). We found that IFN-γ upregulated Fas death receptor expression and caspase-8 in the T98G cell line, and that coadministration of interferon-γ with edelfosine resulted in increased caspase -8 and -3 activation and DNA degradation.

IFN-γ-mediated sensitization required pre-treatment for 1 to 2 days, suggesting the involvement of IFN-γ-induced genes (Chawla-Sarkar *et al.*, 2003). Here we found that Fas ex-

pression increased progressively with incubation time, and thus we selected a 48 hours period of incubation for further testing the effects of IFN on the T98G cell line. IFN-stimulated genes (ISGs) comprise several pro-apoptotic genes, including those encoding caspase 8, TRAIL, and FasL (Apelbaum *et al.*, 2013). Treating IFN-γ-preincubated cells with edelfosine resulted in an earlier and potentiated apoptotic response and increased initiator caspase-8 activation as well as of effector caspases -3 and -9, probably this later due to stronger caspase-8 mediated cleavage of Bid.

GOS-3 cell line

GOS-3 cells were quite resistant to edelfosine induced cell death; a relatively high concentration of 30 μM was needed in order to achieve measurable apoptosis activation in this cell line. Although apoptosis induction was less than 30% at 72 hours, execution of other cell death modalities may occur in GOS-3 edelfosine-treated cells as necrotic morphology and also extensive vacuolization could be observed following the treatment. Progressive increase in the Sub-G_1 population was seen from 24 h to 72 hours, but apoptotic markers such as caspases activation and the PARP fragment of 85 kDa were more strongly detected at 24 hours and decreased after that period of time. Time-lapse showed a relatively early activation of apoptosis in many cells, but then they remained attached and did not form the typical apoptotic blebbing. Since GOS-3 cells expressed Bcl-x_L and its levels did not change with edelfosine treatment, and we have seen that Bcl-x_L had an impact in refraining apoptosis execution in other cell lines, we decided to evaluate if ABT-737 inhibitor could also increase cell death in GOS-3 cells. ABT-737 increased DNA degradation and the number of dying cells. Although we did not further study the effects of ABT-737 in the execution of other cell death modalities, it is possible that ABT-737 could also have an impact in autophagy given the increase in the number of vacuolized cells and the known effects that the Bcl-x_L inhibitor can exert on this route.

A172 cell line

Edelfosine induced apoptosis in the A172 cell line: we found that p-ERK and Bcl-x_L levels were reduced at 72 h, possibly favoring apoptotic execution, further supporting the notion that ERK phosphorylation status and Bcl-x_L are key players in edelfosine-induced cell death. In the A172 cell line, autophagy was activated and autophagy inibitors bafilomycin and chloroquine increased apoptotic execution, pointing out that autophagy acts as a protective mechanism, so autophagy may delay the onset of apoptosis and limit the extent of its execution in this cell line.

PI3K/AKT/ERK signalling in the evaluated cell lines

The phosphoinositide 3-kinase (PI3K)/Akt and RAF/MEK/ERK signalling pathways are activated in a wide range of human cancers and in many cases, concomitant inhibition of both pathways is necessary to block proliferation and induce cell death and tumor shrinkage (Turke *et al.*, 2012). Several feedback systems have been described in which inhibition of one intracellular pathway leads to activation of a parallel signalling pathway, thereby decreasing the effectiveness of single-agent targeted therapies (Turke *et al.*, 2012).

Data from Will *et al* (Will *et al.*, 2014) strongly suggest that PI3K inhibitors induce a greater degree of cell death than Akt inhibitors because they inhibit ERK signalling. Will *et al* (Will *et al.*, 2014) found that whereas Akt inhibitors inhibit Akt/mTOR and activate ERK signalling due to relieve feedback inhibition of receptor signalling, PI3K inhibitors inhibit both. They cause durable inhibition of Ras activation and ERK signalling, both of which are required for induction of apoptosis. Moreover, induction of apoptosis by an Akt inhibitor is significantly enhanced when combined with a MEK inhibitor. ERK and PI3K pathways converge on key targets that regulate cell survival and proliferation, including the BH3 domain protein Bad, the regulator of cap-dependent-translation 4E-BP1, and Bcl-2 (Will *et al.*, 2014).

Edelfosine and other ATLs, perifosine in particular, have been reported to inhibit the PI3K-Akt survival pathway (Ruiter *et al.*, 2003; Li *et al.*, 2010; Dineva *et al.*, 2012). In the U118 cell line, Akt activation and even total levels of Akt were downregulated few hours after edelfosine treatment, and its levels were recovered following edelfosine withdrawal, pointing out again for edelfosine acting as an Akt inhibitor. Others have shown that Akt or mTOR inhibition causes activation of ERK signalling. We found that edelfosine downregulated Akt and mTOR in U118 cells, while it activated ERK. Adding the MEK1/2 inhibitor U0126 not only changed the type of executed cell death from necroptosis to apoptosis but also diminished the number of surviving cells, supporting Will's notion that ERK inhibition synergizes with PI3K-Akt inhibition to cause cell death. Moreover, in the other evaluated glioblastoma cell lines, we found apoptosis and other uncharacterized cell death modalities to be induced when both p-ERK and p-Akt were downregulated, and if both protein levels were raised again, that matched with a stronger resistance to cell death execution, as is the case for SF268 cells at 72 h and for GOS-3 at 48 h treatments. Interestingly, although Bcl-x_L increased temporarily at 48 h in the T98G cell line, both p-ERK levels and p-Akt levels were downregulated, possibly favoring the higher apoptosis and cell death execution observed in this cell line.

General discussion, future perspectives and concluding remarks

In conclusion, from the exposed results, we found that ERK phosphorylation specifically blocked apoptotic execution in the evaluated cell lines, and that Bcl-x_L prevented apoptosis and cell death execution in general. These two conditions (ERK activation and Bcl-x_L over-expression) favored cell survival, and opposed to a strong activation of an apoptotic response. In the U118 cell line, specifically, we studied the ability of edelfosine to induce different cell death modalities and identified some of the "switches" or main regulators in the decision to execute cell death. However, in order to better understand the regulation of these complex processes, further investigation of different aspects would be needed, namely the role of RIPK1, RIPK3 and other components of the necrosome and ripoptosome in the execution of cell death in the U118 cell line (see schematic model, Figure 7.4).

Comments on RIPK1 and RIPK3 involvement in cell death execution

Recent studies indicate that ubiquitination of RIPK1 functions as a major cytoprotective event and that disruption of RIPK1 ubiquitination converts RIPK1 into a death-inducing molecule (O'Donnell & Ting, 2011). In U118 cells we found that RIPK1 plays a role in the decision between cell death execution/cell survival and in the type of executed cell death following edelfosine treatment. The use of the RIPK1 inhibitors Nec-1 and Nec-1s delayed cell death execution and limited necroptosis while potentiated apoptosis following edelfosine treatment, however RIPK1-silenced cells still died with necrotic morphology; in U0126 and geldanamycin pre-treated cells we found RIPK1 degradation and strong activation of apoptosis. Ubiquitination studies, as well as co-immunoprecipitation of RIPK1 and identification of its partners for these different treatments should shed light into the processes occurring and on the outcomes produced. Also, if distinct domains of RIPK1 could play a role on different processes or steps of cell death regulation/execution, that might explain how treatments that produce catalytically inactive RIPK1, RIPK1 silencing or the cleavage of RIPK1 into different fragments, can result in different cellular outcomes.

In the minireview "RIP1 comes back to life as a cell death regulator in TNFR1 signaling", O'Donnell and Ting (O'Donnell & Ting, 2011) explain that there are two cell-death checkpoints in the TNFR1 pathway controlled by RIPK1 (Figure 7.5). In the first checkpoint, ubiquitination of RIPK1 by the E3 ligases TRAF2, cIAP1 and cIAP2 hinders RIPK1 from binding cell-death molecules early after TNF stimulation. When RIPK1 is ubiquitinated it does not associate with caspase-8, whereas when it is not ubiquitinated, it rapidly associates with caspase-8 to trigger apoptosis (O'Donnell *et al.*, 2007). This checkpoint does not require new protein synthesis but it can be rapidly altered by ligation of other TNFR family members that trigger degradation of E3 ligases. The ubiquitination of RIPK1 and recruitment of NEMO function as the first pro-survival checkpoint at early time-points after TNFR1 ligation, since it restrains the apoptosis-inducing property of RIPK1 by sequestering it from caspase-8

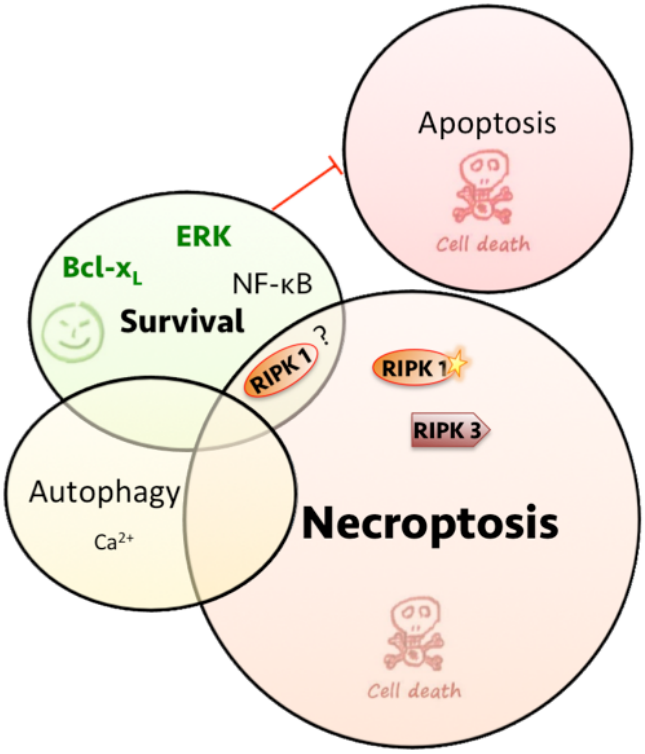

Figure 7.4: ERK activation and Bcl-x_L overexpression favored cell survival in the U118 cell line, blocking apoptosis execution. The adaptor function of RIPK1 may be important for activation of MAPK and NF-κB resulting in cell death inhibition but RIPK1 kinase activity can be involved in cell death: further studies will be needed to clarify the role of RIPK1 and RIPK3 in the execution of cell death in the U118 cell line.

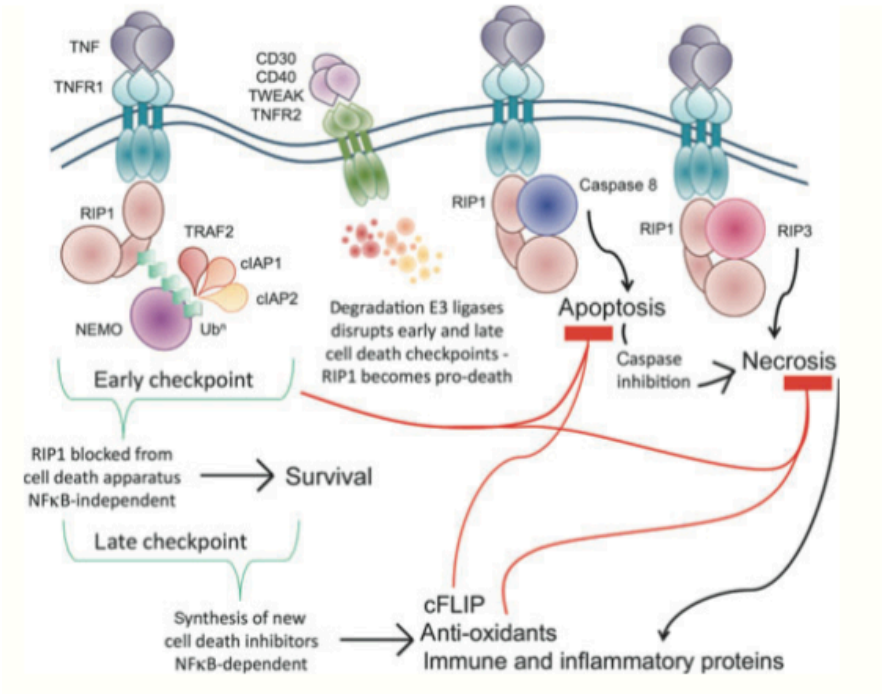

Figure 7.5: There are two cell-death checkpoints well described in the TNFR1 pathway. In the first checkpoint, ubiquitination of RIPK1 by the E3 ligases TRAF2, cIAP1 and cIAP2 hinders RIPK1 from binding cell-death molecules early after TNF stimulation. This checkpoint does not require new protein synthesis. In the second checkpoint, NF-κB activation by ubiquitinated RIPK1 leads to the production of new proteins that can block cell death, keeping cells alive in the long-term. However, the early checkpoint can be rapidly altered by ligation of the other TNFR family members, which trigger degradation of the E3 ligases. Nonubiquitinated RIPK1 becomes a pro-death signaling molecule and quickly binds caspase 8 to initiate apoptosis. If caspase activity is blocked, RIPK1 binds RIPK3 and triggers the back-up cell death pathway by programmed necrosis. *From O'Donnell & Ting (2011).*

(O'Donnell *et al.*, 2007). The interaction between NEMO and ubiquitinated RIPK1 subsequently leads to the activation of NF-κB, and NF-κB-dependent gene transcription acts as the second cell-death checkpoint to inhibit apoptosis at later time-points; this delayed protection from apoptosis does depend on the synthesis of new proteins such as c-FLIP (O'Donnell & Ting, 2011).

Binding of FasL to Fas, or of TRAIL to TRAILR1 or TRAILR2 induces the assembly of the membrane-associated death-inducing signalling complex (DISC) through the adaptor protein FADD, leading to recruitment and activation of caspase-8 and subsequent apoptosis (Pasparakis & Vandenabeele, 2015). Under particular conditions such as the absence of IAPs, which favours the recruitment of RIPK1 to Fas and the formation of a cytosolic ripoptosome complex IIb (made up of RIPK1, RIPK3, FADD and caspase-8), these ligands also mediate necroptosis when caspase-8 is blocked (Pasparakis & Vandenabeele, 2015).

Pre-treating U118 cells with U0126, resulted in strong activation of caspase-8 and cleavage of RIPK1 leading to its depletion and to the induction of apoptosis following edelfosine

treatment. The new RIPK1 fragment of 45 kDa was not produced when U0126+edelfosine-treated cells were pre-incubated with z-VAD-fmk, suggesting that this RIPK1 cleavage was caspase mediated. Inhibition of ERK1/2 phosphorylation by U0126 completely shifted the necrotic response to an apoptotic type of cell death. Caspase-8 activity was shown to be essential for controlling RIPK1/RIPK3-dependent necroptosis in activated T cells and further studies revealed that caspase-8 possibly protects from necroptosis by cleaving RIPK1 and/or RIPK3 (Ch'en *et al.*, 2011; Lu *et al.*, 2011). It was also shown that caspase-8 is the most crucial factor for preventing necroptosis and in most *in vivo* experimental systems; sensitization to necroptosis was achieved by a genetic defect compromising FADD-caspase-8 signalling, and thus inhibiting apoptosis (Pasparakis & Vandenabeele, 2015). Accordingly, we were only able to detect caspase-8 activity in U0126 pre-treated cells, and its activation led to apoptotic execution and to the suppression of necroptotic signalling (see schematic model, Figure 7.6).

With the available data, we may construct the following hypothesis: in the U0126 pre-treated cells, RIPK1 is unubiquitinated and can thus associate with caspase-8, leading to apoptosis activation. The second cell-death checkpoint leading to NF-κB activation would also be suppressed if RIPK1 is not ubiquitinated since there is no interaction between NEMO and RIPK1. NF-κB activation by ubiquitinated RIPK1 leads to the production of new proteins that can block cell death, keeping cells alive in the long-term: translocation of NF-κB transcription factors to the nucleus drive expression of antiapoptotic proteins such as c-FLIP, Bcl-2 family members, TRAFs and IAPs (O'Donnell & Ting, 2011). Overexpression of NF-κB promotes cell survival by suppressing induction of apoptosis in various cell types. We suggest that in edelfosine-treated cells this survival checkpoint is "ON", which could explain why some cells survive long periods of incubation with the drug while showing an increase in some antiapoptotic proteins such as Bcl-x_L and resistance to both apoptotic and necrotic execution, whereas in U0126 pre-treated cells the survival checkpoint is "OFF". In this regard, a few studies have pointed to a protective gene expression program mediated by NF-κB and other transcription factors that can reduce cell death by necrosis (O'Donnell & Ting, 2011).

We observed an increase in NF-κB expression in edelfosine treated cells, while in U0126 pre-treated cells its expression was importantly reduced. U0126 treatment could cause loss/affect E3 ligases, leaving RIPK1 unubiquitinated and thus allowing RIPK1 to function as a pro-apoptotic molecule. The consequent suppression of the second checkpoint would also favor cell death and limit resistance to apoptotic execution. IAPs, e.g., readily ubiquitinate RIPK1 during *in vitro* reactions and the loss of IAP1 and IAP2 abrogates ubiquitination of RIPK1 in response to TNF (Varfolomeev *et al.*, 2008). In U118 cells we found loss of IAP1 increasing with drug concentration used and no loss in U118-R cells (preliminary results). RIPK1 deficiency also sensitizes cells to both apoptosis and necroptosis, and we found resistant cells to have increased expression of RIPK1 and RIPK3.

However, the factors determining whether a cell that lacks RIPK1 will die by apoptosis or necroptosis remain elusive. Blockade of the E3 ligase activity of TRAF2 in NF-κB-deficient T

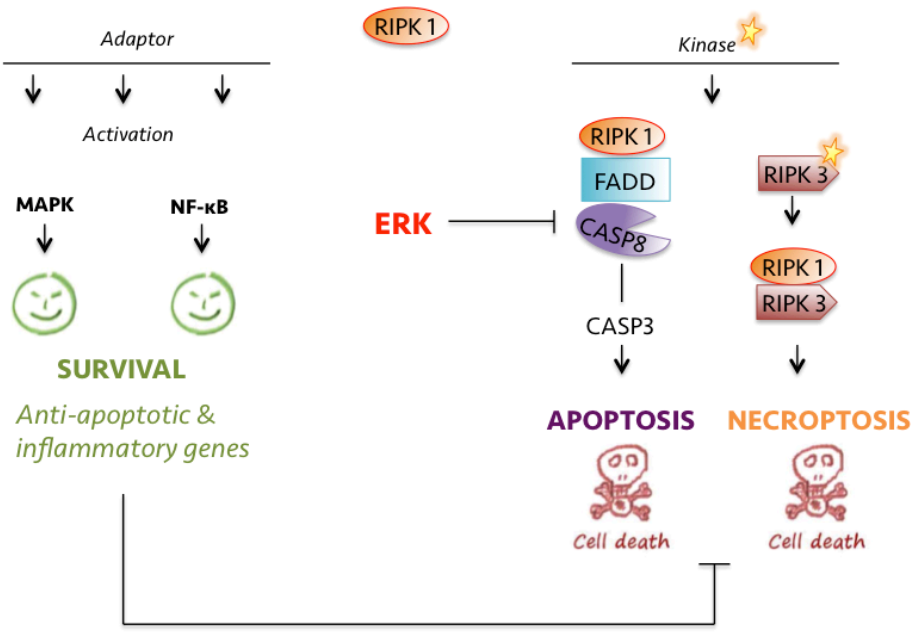

(a)

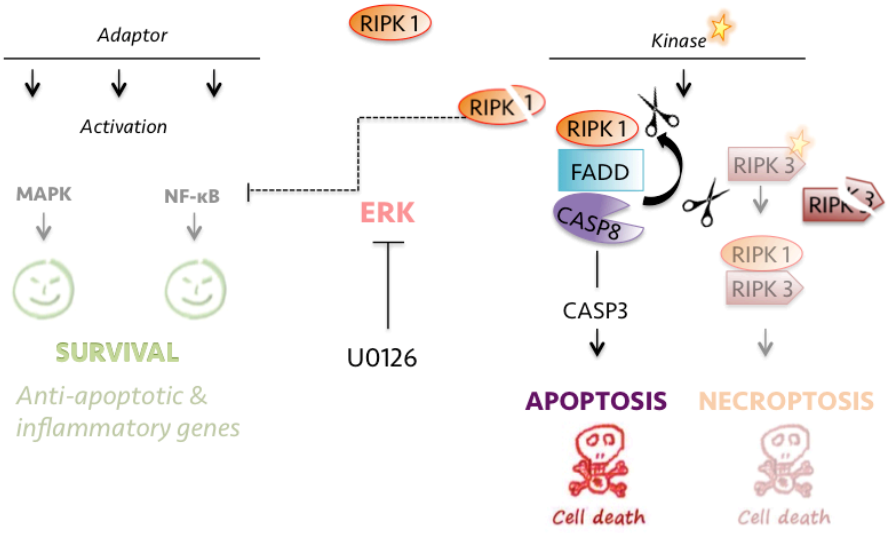

(b)

Figure 7.6: (a) ERK seems to play a major role in regulating cell death processes in the U118 cell line, mainly blocking apoptosis execution following edelfosine treatment. (b) When ERK activation is inhibited by the use of MEK1/2 inhibitor U0126, an apoptotic response is promoted, with strong caspase-8 activation. Caspase-8 activation may lead to RIP kinases cleavage, thus blocking necroptotic execution and further favoring apoptosis execution through simultaneous inhibition of survival signalling.

cells, resulted in apoptosis that is dependent on RIPK1 (O'Donnell *et al.*, 2007). Interestingly, we found that *in U0126 pre-treated cells, adding Nec-1 reduced the apoptosis induced by edelfosine*. If Nec-1 only affects RIPK1, then RIPK1, or the fragment produced by caspase-8-dependent cleavage, might be involved in apoptosis execution, at least in the presence of U0126, and Nec-1 affects that RIPK1 function. In this regard, it has been shown that the c-terminal fragment of RIPK1 produced by caspase-8 activates the DISC, attenuates NF-κB signalling and amplifies the activation of caspase-8 which initiates the downstream apoptotic events (Kim *et al.*, 2000). From the previous assumptions, RIPK1 would be ubiquitinated when cells are treated with edelfosine and thus can not interact with caspase-8. When RIPK1 is ubiquitinated, it generates survival signals; the survival signal generated by ubiquitinated RIPK1 is NF-κB-independent at early time points but shifts to a NF-κB- dependent manner at later time points.

Why there is no necroptosis when Nec-1 is used? Impaired kinase function of RIPK1 limits RIPK3 activation or progression of necroptosis dependent on RIPK1 itself? Nec-1 should affect RIPK1's abillity to cause necroptosis and cell death, and also its ability to limit apoptosis execution, since pre-incubation with Nec-1 diminished necroptosis and increased apoptosis following edelfosine treatment. In the absence of RIPK1, however, obtained by siRNA-RIPK1, we do not observe any protection from necroptosis, instead cell death seems to occur with necrotic morphology even at a more accelerated pace. Because necrostatin is a RIPK1 inhibitor, it is widely believed that RIPK1 kinase activity is required to promote RIPK3 activation and necroptosis, however, an alternative interpretation of the effects of necrostatin is that *the kinase-inhibited form of RIPK1 could act as a dominant-negative inhibitor of necroptosis* (Kearney *et al.*, 2014). In this latter scenario, the absence of RIPK1 would not allow for the inhibition of necroptosis elicited by Nec-1, possibly explaining why RIPK1-silenced cells are not protected from necroptosis. In this regard, it was shown that cells lacking RIPK1 undergo increased spontaneous RIPK3-dependent death on accumulation of the RIPK3 protein, while cells containing a chemically inhibited or catalytically inactive form of RIPK1 were protected from this form of cell death (Orozco *et al.*, 2014). Data presented by Orozco *et al* (Orozco *et al.*, 2014) indicate that RIPK1 can activate RIPK3 in response to receptor signalling, but also acts as a negative regulator of spontaneous RIPK3 activation in the cytosol. Thus, inhibiting RIPK1 with necrostatin-1 or silencing the protein could have different effects.

A major difference between inhibition of RIPK1 kinase activity by necrostatin and RIPK1 knockdown is that while RIPK1 knockdown eliminates both its scaffold function in NF-κB activation and its kinase activity, necrostatin does not impede RIPK1-dependent NF-κB activation, as the kinase activity of RIPK1 is not required for its role as a scaffold for NEMO recruitment (Kearney *et al.*, 2014). This raises the possibility that RIPK1-dependent gene expression events could, at least in principle, contribute to its ability to suppress necroptosis in the presence of necrostatin (Kearney *et al.*, 2014). Another possiblity is that necrostatin may promote a conformational change in RIPK1 that permits the necrostatin-inhibited form of RIPK1 to act in a dominant-negative fashion, perhaps through binding and inhibiting

RIPK3 or MLKL (Kearney *et al.*, 2014).

Kearney *et al* have shown that RIPK1 can function as an inhibitor rather than an initiator of RIPK3-dependent necroptosis: necrostatin potently inhibited TNF-induced necroptosis but RIPK1 knockdown unexpectedly potentiated this process, while RIPK3 knockdown potently suppressed necroptosis, leading the authors to suggest that necrostatin enhances the inhibitory effects of RIPK1 on necroptosis, as opposed to blocking its participation in the process (Kearney *et al.*, 2014). To resolve whether necrostatin had an off-target effect on necroptosis, Kearney *et al* investigated whether the inhibitor still protected cells from necroptosis upon RIPK1 knockdown, and found that whereas necrostatin efficiently blocked TNF/zVAD-induced necroptosis in L929 cells in the presence of RIPK1, it failed to do so upon RIPK1 knockdown (Kearney *et al.*, 2014). This was not the case in U118 cells, where necrostatin-1 was also able to protect RIPK1-silenced cells from necroptosis, suggesting either that necrostatin is operating in an off-target manner, or that the role of RIPK1 is even more complex than currently understood. To exclude the possibility that RIPK1 knockdown enhanced edelfosine-induced cell death in a manner unrelated to the necroptotic pathway, we also investigated whether the necroptosis seen upon RIPK1 knockdown was RIPK3-dependent. Edelfosine-induced necrosis after RIPK1 knockdown was abolished by simultaneous RIPK3 knockdown, but in turn we observed an increase in apoptotic cell death. Interestingly, we found that Nec-1 also reduced apoptosis in this setting, although the cells were RIPK1-silenced cells. The data point to an off-target effect of necrostatin-1, but this effect seems to interfere with important regulatory mechanisms of the same pathway. Contrary to Kearney *et al*, but in line with our findings, Cho *et al* (Cho *et al.*, 2011) first reported that TNF-induced necroptotic cell death in RIPK1 knocked down L929 cells could be inhibited by Nec-1.

Kaiser *et al* (Kaiser *et al.*, 2014) described how in the face of complete RIPK1 deficiency, cells developed sensitivity to RIPK3-mixed lineage kinase domain-like-mediated apoptosis as well as to caspase-8 mediated apoptosis. Although cells died with necrotic morphology, we found that z-VAD-fmk partially protected the RIPK1-silenced U118 cells treated with edelfosine from cell death (preliminary results).

In the absence of RIPK1, it remains unclear whether RIPK3 undergoes autoactivation under necroptotic conditions or whether an upstream kinase is involved. The presence of a RHIM domain-containing adaptor may be essential to facilitate recruitment of RIPK3 to the stimulated receptor (Kearney *et al.*, 2014). In the absence of RIPK1, it is possible that an as yet unidentified RHIM adaptor facilitates RIPK3 recruitment; alternatively, deregulated activation of an as yet unidentified kinase may activate RIPK3 in the absence of RIPK1 (Kearney *et al.*, 2014). We speculate that Nec-1 can exert an effect in this process, given the above-mentioned effects of necrostatin on RIPK1-silenced cells.

In RIPK3-silenced cells, cell death was also quickly induced following edelfosine treatment, but the majority of the cells died with apoptotic morphology instead of necrotic. Possibly RIPK3 absence limited necroptotic execution, and it is conceivable that RIPK1 was involved in the apoptotic execution under these circumstances, since Nec-1 was able to re-

duce apoptosis (by ~43%) in this case. When simultaneously silencing RIPK3 and RIPK1, cells did not die through necrosis but mainly by an apoptotic type of cell death, pointing again for RIPK3 as the essential player for necroptotic induction and RIPK1 as a possible but not necessary intervenient in apoptosis execution following RIPK3 absence.

From the above, it is conceivable that edelfosine treatment could lead to the activation of NF-κB and also to the activation of necroptosis that is independent from RIPK1, through RIPK3-RIPK3 interaction. If RIPK1 is needed for NF-κB activation but not for the RIPK3-RIPK3 interaction and induction of necroptosis, that could explain why silencing RIPK1 would not protect from cell death but rather potentiate it, through inibition of NF-κB-dependent gene expression. However, if RIPK1 is not needed for necroptosis, Nec-1 would have to affect other targets or induce changes in RIPK1 that would interfere/limit RIPK3 activation and suppress necroptotic or apoptotic signalling mediated by RIPK1, and allow for NF-κB activation, for necrosis to be prevented and cell death delayed in Nec-1 treated cells. But how is Nec-1 still able to protect from necroptosis in RIPK1-silenced cells? Does Nec-1 have an effect on RIPK3? Or possibly RIPK1 silencing was incomplete and Nec-1 affected the remaining RIPK1 in a way that limited RIPK3 activation? If the kinase-inhibited form of RIPK1 acts as a dominant-negative inhibitor of necroptosis, in RIPK1-silenced cells the few amount of RIPK1 that remains (since 100% silencing was not achieved) is not kinase inhibited, and would not be able to limit necroptosis, hence the cell death execution would proceed through necroptosis via RIPK3; however, we speculate that inhibition of the kinase activity of the remaining RIPK1 would be sufficient to prevent again necroptosis when necrostatin-1 is added.

In order to answer these questions, changes in RIPK1 protein, such as its ubiquitination and phosphorylation status and also the expression of IAPs and c-FLIP should be evaluated. Co-immunoprecipitation of caspase-8 would be useful to evaluate the complexes in which caspase-8 participates and its undergoing modifications. We found important changes in the immunodetected bands for caspase-8, particularly the appearence of a very strong band at a very high molecular weight (> 200 kDa) that was only detectable in the case of pre-incubation with U0126, and hypothesize that it may represent the formation of a complex that allows apoptotic execution or/and blocks necroptosis. Comparison between the different treatments, EDLF, Nec-1+EDLF, siRNA-RIPK1+EDLF, U0126+EDLF, and also between the resistant cell line and the U118 normal cell line treated at different drug concentrations should shed light into the complexes formed and give further understanding of how necroptosis and apoptosis are controlled in this particular cell line.

Comments on the role of p-ERK in refraining apoptosis and potentiating cell survival

For the evaluated cell lines, we found that ERK activation played an important role in regulating cell death, and particularly in refraining apoptotic cell death. In U118 cells, apoptosis was only induced following ERK inhibition through the use of MEK1/2 inhibitor

U0126; in the T98G cell line, stronger activation of caspases -8 and -3 could be seen following reduction of ERK phosphorylation at 48 h, and in the GOS-3 cell line apoptotic markers could only be detected at 24 h, after that period of time ERK phosphoylation increased again and cells no longer activated apoptosis. In this regard, it was shown that transient or prolonged activation of ERK1/2 in response to a wide range of stimuli including tumor necrosis factor (TNF), Fas ligand, TNF-related apoptosis-inducing ligand (TRAIL), radiation, osmotic stress, hypoxia, growth factor withdrawal, nitric oxide, hydrogen peroxide, matrix detachment, and chemotherapeutic agents results in an antiapoptotic effect and that its inhibition promotes apoptosis (Lu & Xu, 2006). The mechanism of this antiapoptotic effect is complex and varies among cell types, most likely due to differences in many other regulators of this activity.

The antiapoptotic effect of ERK1/2 activation may be diminished after prolonged stimulation, because ERK1/2 activity can be downregulated by dephosphorylation or degradation of ERK1/2 (Lu & Xu, 2006); the latter appears to be the case in the U118 cell line, where we found that ERK1/2 was activated but the total protein levels after 24 hours of incubation with edelfosine were much lower than in untreated control levels.

ERK1/2 anti-apoptotic effects can be achieved by downregulating pro-apoptotic molecules via a decrease in their activity or a reduction of their protein expression, such as inactivation of Bad through phosphorylation at Ser112 by ERK-activated p90 ribosomal S6 kinase (RSK), MEK/ERK1/2-dependent phosphorylation of Bim or downregulation of Bim protein expression, or caspase-9 inhibition by phosphorylation at Thr125, resulting in inhibition of caspase-9 processing and subsequent caspase-3 activation (Lu & Xu, 2006).

Besides inhibiting pro-apoptotic proteins, ERK1/2 can also promote cell survival by enhancing the activity of anti-apoptotic molecules. IEX-1, an early response and nuclear factor kappa B (NF-κB) target gene, interacts with phosphorylated ERK1/2 and is phosphorylated by ERK1/2 primarily at Thr18 (Garcia *et al.*, 2002). Upon phosphorylation by ERK1/2, IEX-1 acquires the ability to prevent the release of cytochrome c from mitochondria and to inhibit cell death induced by cytokine deprivation and stimulation with staurosporine, TNF, or etoposide. In addition to acting as an ERK1/2 downstream effector mediating survival, IEX-1 functions as a regulator of ERK1/2 by enhancing ERK1/2 activation in response to various growth factors (Garcia *et al.*, 2002).

In the U118 cell line, we found that limiting ERK activation by inhibiting MEK1/2, resulted in increased loss of $\Delta\Psi_m$ and caspase-9 activation, possibly due to the mentioned effects of activated ERK. Moreover, different studies point to the fact that ERK1/2 signalling can block apoptosis at levels upstream, downstream, or unrelated to change of mitochondrial transmembrane potential and cytochrome c release (Lu & Xu, 2006). Inhibition of ERK1/2 activity causes arrest at the G_1 phase of the cell cycle and downregulation of the expression levels of Mcl-1 and Bcl-x_L (Boucher *et al.*, 2000).

Boucher *et al* (Boucher *et al.*, 2000) described that MIA PaCa-2 cells express the anti-apoptotic members Bcl-2, Mcl-1 and Bcl-x_L along with the pro-apoptotic members Bak, Bad and Bax, and interestingly, inhibition of ERK1/2 activities by PD98059 resulted in significant reductions in the expression of all the anti-apoptotic molecules studied. In U0126-pretreated

U118 cells, Bcl-x_L was importantly downregulated, which we related to an increased activation of the intrinsic apoptotic pathway. However, p-ERK inhibition also led to an increase in caspase-8 activation. Others reported that activation of ERK1/2 by constitutive expression of MEK1 inhibits caspase 8 activation/Bid cleavage induced by ionizing radiation or activation of Fas/CD95, TNF, and TRAIL receptors, suppressing activation of the caspase effector machinery (Holmström *et al.*, 2000; Tran *et al.*, 2001). Tran *et al* (Tran *et al.*, 2001) observed that a number of FasR-insensitive cell lines could redirect the pro-apoptotic signal to an anti-apoptotic ERK1/2 signal resulting in inhibition of caspase activation. Activation of the FasR, TNF-R1 and TRAIL-R, rapidly induced subsequent ERK1/2 activation, an event independent from caspase activity, whereas inhibition of the death receptor-mediated ERK1/2 activation was sufficient to sensitize the cells to apoptotic signalling from FasR and TRAIL-R (Tran *et al.*, 2001).

Caspase-8 is now appreciated to govern both apoptosis following death receptor ligation, and cell survival and growth via inhibition of the ripoptosome, a 2 MDa complex containing RIPK1, FADD, caspase-8 and c-FLIP (Koenig *et al.*, 2014). Cellular FLICE-like inhibitory protein (c-FLIP) has been identified as a protease-dead, procaspase-8-like regulator of death ligand-induced apoptosis, based on observations that c-FLIP impedes TNF-α, Fas-L, and TNF-related apoptosis-inducing ligand (TRAIL)-induced apoptosis by binding to FADD and/or caspase-8 or -10 in a ligand-dependent fashion, which in turn prevents death-inducing signalling complex (DISC) formation and subsequent activation of the caspase cascade (Safa *et al.*, 2008).

Besides regulation of death ligand-induced apoptosis, recent studies revealed additional roles for c-FLIP in cell death/survival. Tsuchiya *et al* (Tsuchiya *et al.*, 2015) reported that c-FLIP controls the classical death receptor-mediated extrinsic apoptosis pathway, regulates the formation of the death receptor-independent apoptotic platform named the ripoptosome and is also involved in necroptosis. c-FLIP plays a critical role as a switch to determine the destiny of cells among survival, apoptosis, and necroptosis (Tsuchiya *et al.*, 2015). Full lenght c-FLIPL can heterodimerize with caspase-8 independent of death receptor ligation and activate caspase-8 via an activation loop in the C terminus of c-FLIPL, which triggers cleavage of c-FLIPL at Asp-376 by caspase-8 to produce p43FLIP (Koenig *et al.*, 2014). p43FLIP associates with Raf1, TRAF2, and RIPK1, which augments ERK and NF-κB activation, IL-2 production, and T cell proliferation (Koenig *et al.*, 2014).

Kataoka *et al* (Kataoka *et al.*, 2000) had previously described that Fas-recruited c-FLIP interacts with TNF-receptor associated factors 1 and 2, as well as with the kinases RIP and Raf-1, resulting in the activation of the NF-κB and ERK signalling pathways and postulate that c-FLIP is not simply an inhibitor of death-receptor-induced apoptosis, but that it also mediates the activation of NF-κB and ERK by virtue of its capacity to recruit adaptor proteins involved in these signalling pathways. In the U118 cells, ERK inhibition led to the switch from necroptosis to apoptosis enabling caspase-8 activation, and we speculate that c-FLIP could be a determinant factor in these processes. Recent studies showed that RIPK1 activates MAPKs such as p38 MAPK, JNK and ERK during apoptosis after TNF-α

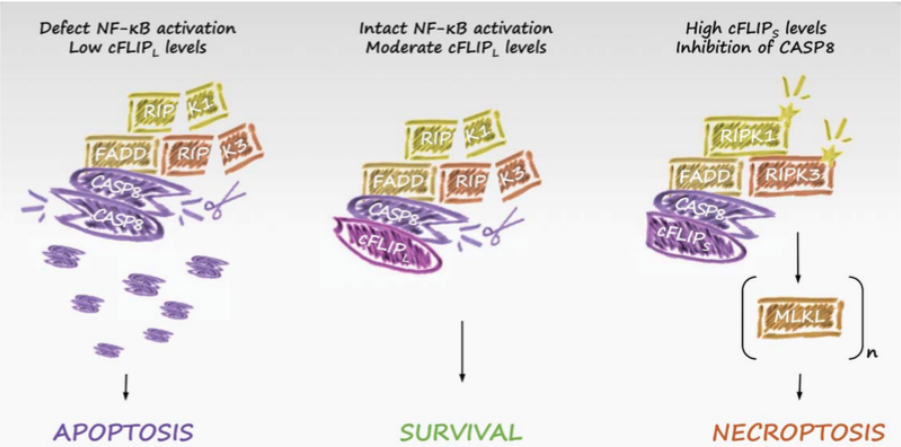

Figure 7.7: The role of FLIP in TNFR1-induced complex II activity is depicted. TNFR1 stimulation typically induces NF-κB-mediated survival signalling, for example through up-regulation of FLIPL (central panel). Caspase-8/FLIPL heterodimers allow local caspase-8 activity within complex II, resulting in cleavage of RIPK1 and RIPK3. As a result, apoptosis and necroptosis are inhibited. However, when FLIPL levels are low (for example due to defective NF-κB activation) active caspase-8 homodimers form, are released from complex II, and induce apoptosis (left panel). In conditions where FLIPs levels are upregulated, caspase-8/FLIPs heterodimers inhibit local caspase-8 activity, allowing RIPK1/3-mediated necroptosis (right panel). *From Vandenabelee et al (2015).*

treatment (Festjens *et al.*, 2007; Alvarez *et al.*, 2010). However, the activation of MAPKs and its role in necroptosis are unknown.

Aoudjit and Vuori (Aoudjit & Vuori, 2001) reported that inhibition of the ERK pathway in adherent HUVECs downregulates c-FLIP expression. It is thus conceivable that ERK1/2 inhibition could downregulate c-FLIP, favoring apoptosis instead of necroptosis. Interestingly, Zheng *et al* reported that the MEK1/2 inhibitor U0126 modulated the levels of several intracellular proteins including Bcl-2, Mcl-1 and c-FLIP (Zheng *et al.*, 2003). In the model proposed by Schilling *et al* (Schilling *et al.*, 2014), procaspase-8 incorporated in the ripoptosome is activated and fully processed through homodimerization, cleaves and inactivates RIPK1 and leads to ripoptosome disassembly. As a consequence, only caspase-8-mediated apoptosis is executed. When c-FLIPL is incorporated in the ripoptosome, it activates procaspase-8 through heterodimerization. However, cFLIPL-activated procaspase-8 is able to cleave limited substrates and inactivate RIPK1, but becomes inactive again after ripoptosome disassembly (Schilling *et al.*, 2014). As a consequence, c-FLIPL blocks apoptosis and maintains cell survival. In contrast, cFLIPS promotes ripoptosome assembly but cannot activate procaspase-8 to inactivate RIPK1 and under these conditions, cells undergo necroptosis. The role of FLIP in TNFR1-induced complex II activity, determining the destiny of cells among survival, apoptosis and necroptosis is depicted in Figure 7.7 (Vanden Berghe *et al.*, 2015).

Feoktistova *et al* reported that necroptosis promoted by the elimination of IAPs was dependent on the kinase activity of RIPK3. Inhibition of RIPK3 kinase activity by either chemical compounds or active site D161N mutation (but not other inactive mutants) blocked necroptosis, but unexpectedly induced apoptosis via the formation of ripoptosome-like platform (Feoktistova *et al.*, 2012). Therefore, there is a close interplay between two cell death pathways, one leading to caspase-8-dependent apoptosis, and one leading to RIPK3-dependent necrosis. The functional RIPK1-RIPK3-MLKL axis and the balance of c-FLIP isoforms are both critical determinants of cell fate switching among survival, apoptosis, and necroptosis (Tsuchiya *et al.*, 2015). Therefore, we would proceed the investigation on this subject by performing studies on RIPK1 phosphorylation/ubiquitination, caspase-8, c-FLIP and other downstream signalling components of death receptors multicomplexes and NF-κB signalling complexes, such as E3 ligases, IAP-1, and IAP-2, deubiquitinases, CYLD, A20, and HOIL-1/HOIP/Sharpin (LUBAC) as very important cell death decision checkpoints to apoptosis and necroptosis. Co-immunoprecipitation and quantitative mass spectrometric analysis of the complexes formed following edelfosine treatment in U118 cells or RIPK1-silenced and RIPK3-silenced cells, and also changes induced by pre-incubation with necrostatin, U0126 and geldanamycin could elucidate which specific complexes are formed under specific circunstances and how they influence cell death execution/cell survival.

Comments on the role of Bcl-x_L

Regarding Bcl-x_L, its expression was reduced following ERK1/2 inhibition and this protein may also play important roles protecting from cell death execution and allowing cell survival. Many studies analyzed Bcl-x_L implications for cell survival and resistance to chemotherapy. Importantly, antiapoptotic multidomain members of the Bcl-2 protein family, including Bcl-2 itself, Bcl-x_L, and Mcl-1, not only counteract the pore-forming activity of Bax and Bak by engaging in direct inhibitory interactions, but also intercept upstream pro-apoptotic signals such as those mediated by BH3 only proteins like Bad, Bid, Bim, and PUMA (p53-upregulated modulator of apoptosis); bind to and regulate several components of the PTPC, including VDAC1 and ANT, and prevent the generation of pro-apoptotic cytosolic Ca^{2+} waves, either by interacting with inositol 1,4,5- trisphosphate (IP3)-gated Ca^{2+} channels on the endoplasmic reticulum or by limiting the capacity of ER Ca^{2+} stores (Michels *et al.*, 2013).

It has also been shown that Bcl-x_L is capable of inhibiting DISC formation and Bid processing or activation (Wang *et al.*, 2004). In addition, although the caspase inhibitor z-VAD-fmk could not block the alkylphosphocholine (APC)-induced formation of large vacuoles and typical features of apoptosis in human glioma cell lines, Bcl-x_L blocked caspase activation and also cell death (Naumann *et al.*, 2004). Naumann *et al* reported that Bcl-x_L inhibited both the apoptotic and necrotic cell death pathways activated by APC, possibly by preventing the breakdown of the mitochondrial membrane potential (Naumann *et al.*, 2004). Thus, there

was a close correlation between the loss of $\Delta\Psi_m$ and ensuing cell death, and their modulation occurred in parallel.

Bcl-x_L played a crucial role in detaining the loss of $\Delta\Psi_m$ in U118 and SF268 cell lines, thereby limiting apoptotic execution after edelfosine treatment. Moreover, because the overexpression of Bcl-x_L inhibits the loss of $\Delta\Psi_m$ and the production of ROS as well as mitochondrial membrane permeabilization, Bcl-x_L can largely affect the inhibition of apoptotic and nonapoptotic cell death pathways: e.g. Bcl-x_L effectively inhibits nonapopotic cell death pathways such as necrosis and autophagy in TRAIL-induced cell death (Kim, 2005). In U118 cells, inhibition of ERK1/2 activity led to downregulation of Bcl-x_L and increased cell death; surviving U118 cells overexpressing Bcl-x_L were efficiently killed by the BH3-mimetic inhibitor ABT-737, so Bcl-x_L plays a role in protecting U118 cells from both apoptosis and necroptosis following edelfosine treatment.

Back to "a matter of life and death", concluding remarks

From all the points explored in this thesis, it becomes clear that the same stimulus can lead to different outcomes depending on an array of circumstances. Particularly, the fact that edelfosine may stimulate survival signalling at the same time that it induces cell death claims for deeper undertanding of the regulation of these intricate signals in order to effectively induce cell death in the context of cancer therapy and prevent development of resistance.

Interestingly, it has been known for a long time that cell death receptors can transduce both survival and death signals. "Conditions that promote cell proliferation necessarily engage the cell death process" (Green & Evan, 2002), and it is reasonable to ask if conditions that promote cell death would also engage the opposite process of cell survival and proliferation. In the review "Surviving apoptosis: life-death signaling in single cells" (Flusberg & Sorger, 2015), the authors point out that the extrinsic apoptotic cell death pathway plays a multifaceted role in the immune system and, therefore, it is not surprising that death receptors can induce both apoptosis and cell survival, processes that are equally important in the regulation of inflammation and immunity. They also advance with possible evolutionary explanations: for cell death to have evolved, proteins necessary for initiating death must originally have had non-apoptotic roles, making cells dependent on them for survival; hence the close relation between death and survival mechanisms. Or, death and survival pathways may be coupled such that a chronic pro-death signal is inhibited until a survival signal is turned off (Flusberg & Sorger, 2015). But this systems must have evolved in such a complex way, that it is now the level of multiple proteins in these pathways, and how they interact among them, that determine cellular fate in response to a death signal. Supporting this notion, receptor-mediated apoptosis can be regulated and fine-tuned at many levels, including interaction among receptors, receptor post-translational modifications and localization to different membrane compartments determine the strength of pro-apoptotic signalling, for example by preventing the formation of higher-order receptor aggregates. DISC, where c-FLIP

can exert its antiapoptotic activity, is also subject of regulation, and downstream of that, anti- or pro-apoptotic proteins such as IAPs and others that regulate mitochondrial outer membrane permeabilization are also determinant for cellular fate (Flusberg & Sorger, 2015). Furthermore, many proteins exhibit both pro-apoptotic and anti-apoptotic activities, adding complexity to the understanding of the exact roles of each player at a given time.

Analyzing edelfosine effects in the U118 cell line, we found that a minority of the cells activated apoptosis in response to 10 μM edelfosine, but the majority of the cells died through a necroptotic process. This process was dependent on RIPK1 and RIPK3, and both proteins played an important role determining cell fate, although further studies are needed in order to better understand their interplay on necroptosis/apoptosis and cell survival.

Another important regulator of cell death execution in the U118 cells is ERK, as inhibition of its phosphorylation led to a change in the executed cell death modality and also to a change in the number of resistant cells surviving the treatment. Possibly, edelfosine treatment leading to necroptotic cell death could also activate survival signalling in U118 cells, but the change to an apoptotic type of cell death execution, obtained by p-ERK inhibition, abolished those signals. Caspase-8 activation engaged downstream caspases, thus leading to RIPK1 degradation and inhibition of the necrosis and survival triggers.

Interestingly, we found that treating U118 cells with low concentrations of edelfosine (between 0.1 μM and 1 μM) increased cell proliferation, proving that edelfosine is indeed able to stimulate survival/proliferation pathways in these cells. Edelfosine induced a rapid and transient activation of ERK phosphorylation and the duration of that activation was dependent on drug concentration; the higher the concentration, the more prolonged was ERK activation. Edelfosine was able to promote cell proliferation or necrotic cell death in U118 cells depending on the drug concentration used, but the apoptotic response remained largely blocked. Whether or not cell death occurred, edelfosine appears to be an inducer of cell proliferation. In the presence of survival factors, U118 cells survive and accumulate; in other cases, edelfosine may provide both cell death signals and survival signals, albeit through different effector pathways.

The functional role of Fas/CD95 signalling in edelfosine-induced apoptosis has been demonstrated in different studies in our laboratory (Gajate & Mollinedo, 2001, 2007; Gajate *et al.*, 2004). A few reports demonstrated that CD95 is not only a potent apoptosis inducer, but is also capable of activating multiple survival pathways (Lavrik *et al.*, 2007). Namely, in tumor cells resistant to CD95-induced apoptosis the triggering of CD95 was reported to result in activation of survival pathways involving NF-κB, ERK1/2, p38, JNK and Akt.

Lavrik *et al* (Lavrik *et al.*, 2007) developed a mathematical model to gain insight into CD95-induced apoptosis and the decision-making steps of CD95 signalling. They arrived to the conclusion that the initial concentration of CD95L and the concentration of the inhibitor c-FLIP at the DISC were the most important factors contributing to the cellular decisions for CD95-induced life and death. At threshold stimulation of CD95, c-FLIP was upregulated at the DISC due to the highest affinity of c-FLIP to the DISC compared with other DED proteins,

leading to the inhibition of caspase-8 activation and further downstream apoptotic events. Lavrik *et al* also observed from their experimental data that triggering of CD95 with low amounts of a CD95 stimulus did not result in apoptosis but in MAP kinase activation (Lavrik *et al.*, 2007). Similar to our findings for U118 cells stimulated with edelfosine, they observed that reducing concentrations of anti-CD95 antibodies down to the threshold level did not result in blockage of MAP kinase activation, but to different kinetics in ERK phosphorylation upon stimulation with different concentrations.

That apoptosis is triggered when some buffered threshold is exceeded is suggested by the binary nature of the life-death decision (Green & Evan, 2002). It is also indicated by observations that cells can be subjected to a variety of independently subcritical apoptotic insults that when administered together trigger dramatic apoptosis. In U118 cells, edelfosine is able to induce both survival and death signals, and surviving signals are efficiently transduced in the presence of ERK phosphorylation. ERK phosphorylation may also be the responsible for increased cell proliferation below the 5 μM threshold. The question is whether it is this same signal that triggers necroptotic execution or is this upstream blockade in conjugation with other events that leads to cell death, executed in an alternative way to apoptosis. The referred cell-to-cell variablilty could allow some cells with lower death pathways activation and higher survival pathways induction to resist to edelfosine treatment. These cells could then activate adaptive pathways that allow them to survive to further exposure to edelfosine.

If activation of apoptosis can lead to blockage of necroptosis, could also necroptosis inhibit apoptosis execution? Or is each type of cell death induced by a different effector mechanism? Importantly, apoptosis signalling opposes the stabilization of necrosomes following death receptor ligation and both RIPK1 and RIPK3 are known targets of caspase-8 mediated cleavage (Lin *et al.*, 1999b). Co-evolution of necroptosis with caspase-dependent apoptosis is suggested by the aforementioned cross-inhibition (Walsh, 2014). Several viral encoded genes are produced to prevent apoptosis, and thus it is clear that inhibition of apoptosis is an important means viruses have exploited to avoid immune clearance. Interestingly, cytomegalovirus induces RIPK3-mediated necroptosis via the interferon regulatory factor DAI but the virus also produces a protein that disrupts assembly of RIPK1/RIPK3 necrosomes and consequent necroptosis (Walsh, 2014). While the physiological function of necroptosis remains to be fully elucidated, Walsh point out that it is clear that this cellular process has been around for a long time during evolution (Walsh, 2014).

If necroptosis constitutes a backup mechanism for cell death execution, could it be activated due to parallel received signals for proliferation when those signals can no longer be sustained? Is it the proliferation signal the same that limits apoptotic execution? And was necroptosis activated due to proliferation induction or by an independent mechanism? Does necroptosis execution blocks apoptosis, like apoptosis seems to limit necroptosis progression? Many questions remain to be answered with respect to the interplay between apoptosis and necroptosis, but the U118 cell line and edelfosine treatment appear to be a good model for further evaluation of these questions.

At low drug concentrations (0.1- 5 μM) there was transduction of proliferation signals

and no necroptotic induction. Although apoptosis was extremely low, we did detect caspase-3 activation following downregulation of ERK survival signalling at this low concentration; the removal of the stimulus that induced proliferation was able to induce death in some cells. We also found that ERK inhibition through the use of the MEK inhibitor U0126 led to apoptotic cell death at concentrations that would increase proliferation in case ERK1/2 was phosphorylated. Blocking ERK phosphorylation at 10 μM diminished not only necroptotic execution but also the number of surviving cells, pointing to a connection between execution of necroptosis and survival, as opposed to apoptotic induction. Inhibition of ERK activation decreased tolerance to edelfosine in both U118 and U118-R cells, pointing out again to ERK as a very important anti-apoptotic player. Interestingly, we found that challenging U118-R cells with edelfosine no longer increased ERK activation, but pre-incubation with U0126 would still lead to an increase in apoptotic execution, suggesting that ERK's role as a suppressor of apoptosis is mantained during the selective pressure imposed by edelfosine.

It would be interesting to study the different signalling complexes mediating cell death, namely by performing co-imunoprecipitation of CD95, caspase-8 or RIPK1; and compare which complexes are formed at low edelfosine concentration, when survival signal prevails, at higher dosis (10 μM) when necroptosis prevails and at 10 μM, but pre-treating the cells with U0126 in order to evaluate which changes account for the executed cell death modality.

Could edelfosine-induced ERK activation in U118 cells be related to the ability of edelfosine to induce necroptosis? If conditions that promote cell proliferation necessarily engage the cell death process, possibly ERK activation together with other factors and the inhibition of apoptosis, could lead to activation of necroptosis. Because when ERK activation is limited apoptosis increases and necroptosis is not activated, p-ERK could work as survival factor and at the same time allow for necroptosis execution under a set of determined conditions. If we remove the survival factor however, apoptosis would be restored. Cells might become "addicted" to survival signalling and perhaps the execution of cell death will only take place if those signals are shuted off. One idea, arising from this conception, is that the triggering of proliferation/survival signals followed by removal of the trigger/survival stimulus in cells with unblocked apoptotic machinery should cause cell death.

This has been proved to be true with the death receptor CD95. In their review "The role of CD95 and CD95 ligand in cancer", ME Peter *et al* (Peter *et al.*, 2015) expose the findings that led to the recognition of CD95 as an inducer of proliferation in various cell types and that stimulation of Fas/CD95 on 22 apoptosis-resistant cancer cell lines increased their motility and invasiveness *in vitro*. Nonapoptotic signalling through CD95 involved activation of NF-κB and the three MAP kinases, ERK1/2, JNK1/2, and p38.

Interestingly, Peter *et al* (Peter *et al.*, 2015) found that elimination of either CD95 or CD95L killed cancer cells *in vitro* and *in vivo*, pointing the activity of CD95 as a survival factor most relevant for cancer cells that died under a necrotic form of mitotic catastrophe with signs of apoptosis, autophagy and senescence. Importantly, the authors mention that this form of cell death, induced in cancer cells following CD95 or CD95L elimination could not be inhibited by any of 1200 tested drugs or by any single gene in a genome wide sh-RNA screen (Peter *et*

al., 2015). This brings us to the previoulsy discussed theory that cancer cells would be more sensitive to restoration of the killing pathways that they suppressed and possibly even more sensitive to the shutdown of survival pathways to which they became dependent on. If the suppressed killing pathways became responsible for cell survival somehow, their elimination in a stress-adapted cell, in which the pathway now only promotes cell survival, would be deleterious to the cell. It seems plausible that if cells became addicted to a ligand that activates pathways implicated in survival, when cells fail to receive that signal, the activation of death would be elicited. This seems to be the case in cancer cells in which elimination of the CD95 receptor or of the ligand induces cell death, and in these cells CD95 could be working as a "dependence receptor". "Dependence receptors" have the ability to trigger two opposite signalling pathways: in the presence of the ligand they activate pathways implicated in cell survival, migration and differentiation, while in the absence of the signal they do not stay inactive but rather elicit an apoptotic signal (Goldschneider & Mehlen, 2010). If cancer cells were selected because they activated survival pathways and proliferated in response to CD95L, and that signal also blocked cell death, then when they adapted in a certain way, "forgetting" the inactivation of the death signal due to stronger induction of proliferation pathways, if the stimulus is removed, death activation would be elicited again. By definition, the cell death induced by elimination of CD95 or CD95L has never been triggered in any cancer cell found in a cancer patient, the implication being that cancer cells do not become resistant to this cell death, but they become resistant to apoptosis and may evade cell death by retaining expression of CD95 and CD95L (Goldschneider & Mehlen, 2010).

The idea of making cells addicted to a certain stimulus that will induce cell survival while blocking cell death, if death machinery remains intact, brings a potential weakness to explore later: removal of the signal that allowed these cells to live would leave the death signal unchecked. This could happen in cancer cells that became resistant but also dependent on chemotherapeutic drugs. However, if this same process naturally occurred in cancer cells, that learned how to avoid death, if they co-evolved in such a way that the system developed for survival also blocks death pathways originally transduced by it, finding out which these systems are and how to block them, would possibly be a way to induce cellular demise with little or no resistance emerging.

However, the fact that other types of cell death besides apoptosis may be activated by chemotherapeutic drugs should be better explored, as it is important to understand the molecular and regulatory features of the early/primary cell death triggers and initiators, as well as of the switches leading to the different types of cell death, in order to efficiently manipulate cell death execution. Apoptosis and necrosis can occur simultaneously in tissues or cell cultures exposed to the same stimulus and, often, the intensity of the same initial insult decides the prevalence of either apoptosis or necrosis (Nicotera *et al.*, 1999). The execution of the death programme seems to involve a relatively limited number of pathways, but the interconnections between these seem to be extremely complex and are far from being completely understood.

In conclusion, for the evaluated glioblastoma cell lines, our results point out to the fact

that blockage of apoptosis is the main responsible for the lack of response to edelfosine, that in turn it is limited mainly by p-ERK activation and Bcl-x_L expression, and that the activation and execution of other mechanisms of cell death, like necroptosis, are also limited by Bcl-x_L expression. These mechanisms should be further explored in order to take advantage of alternative cell death pathways to overcome natural resistance to apoptosis commonly observed in cancer cells, but caution is needed to understand other possible mechanisms of resistance, possibly shared between apoptosis and necroptosis.

New insights on the identification of the repertoire of anti-apoptotic mechanisms in cancer and on how survival signalling and cell death blockage contribute to tumor progression, deregulated cell proliferation and drug resistance, are key to better understand cell death and cancer itself. Elucidation of the cell survival and death signalling mechanisms and their interrelationships in cancer will provide us with important knowledge to therapeutically explore its weaknesses.

8

Materials and methods

Reagents

Edelfosine was obtained from R. Berchtold (Biochemisches Labor, Bern, Switzerland). A stock solution was prepared at 2 mM in culture medium containing 10% (v/v) fetal bovine serum (FBS) by heating at 50ºC for 45 min, as previously described (Mollinedo *et al.*, 1997).Perifosine and erucylphosphocholine were from Zentaris (Frankfurt, Germany), miltefosine was from Calbiochem (Billerica, MA, USA), erufosine and oleylphosphocholine were obtained from Lars H. Lindner (University Hospital, Ludwig Maximilians University, Munich, Germany). Versene, FBS, L-glutamine, penicillin, and streptomycin were from Gibco, Life Technologies Corporation (Carlsbad, CA). Necrostatin-1 was from Sigma (St. Louis, MO), necrosulfonamide and Nec-1s were from Calbiochem (Billerica, Massachusetts). U0126 was also from Calbiochem and 10 mM stock solutions were prepared in DMSO, in order to use the solvent at 0.1% final concentration that did not affect any of the parameters analyzed in this study. ABT-737 was from Santa Cruz Biotechnology Inc. (Santa Cruz, CA), Geldanamycin was from InvivoGen (San Diego, CA), z-VAD-fmk was from Alexis Biochemicals-Enzo Life Sciences.

Et-BDP-ET (1-*O*-(11′-(6″-ethyl-1″,3″,5″,7″-tetramethyl-4″,4″-difluoro-4″-bora-3a″,4a″-diaza-*s*-indacen-2″-yl)undecyl)-2-*O*-metil-*rac*-glycero-3-phosphocholine was synthesized by Francisco Amat-Guerri and A. Ulises Acuña (CSIC, Madrid), who kindly provided the fluorescent analogue. It was stored frozen in 1-10 mM stock solutions in DMSO protected from the light and used at a 10 μM final concentration.

LysoTracker Green DND-26, MitoTracker Red CMXRos Molecular Probes, as well as Alexa Fluor 594 phalloidin, were from Thermo Fisher Scientific Inc.

All other chemicals and reagents were from Sigma (St. Louis, MO) unless otherwise indicated.

Cell culture

The human U118 (U-118 MG), GOS-3, SF268 and A172 cell lines derived from malignant gliomas, and HeLa, derived from a cervical cancer, were grown at 37°C in Dulbecco's modified Eagle's medium (DMEM) (Gibco, Life Technologies Corporation) supplemented with 10% heat-inactivated FBS, 2 mM L-glutamine, 100 U/ml penicillin, 100 μg/ml streptomycin in a humidified atmosphere containing 5% CO_2. The human acute T-cell leukemia Jurkat cell line, Ewing's sarcoma CADO-ES1 and T98G cell lines were grown in RPMI-1640 (Gibco), supplemented with 10% heat-inactivated FBS, 2 mM L-glutamine and antibiotics as above.

Cell proliferation and viability assays

MTT assay

Cell proliferation and viability was assessed by the MTT (3-(4,5-dimethylthiazol-2-yl)-2,5-diphenyltetrazolium bromide) assay, which is based on the conversion of this tetrazolium salt to a colored product, formazan, by metabolically active cells. 200 μl of MTT solution (5 mg/ml in PBS) were added to each well (containing the cells in 2 ml medium) of the 6-well plate 30 min before the end of incubation. Medium was centrifuged to pellet the cells that detached from the plates during drug treatment, and supernatant was discarded. The precipitated formazan was dissolved using acidic isopropanol (0.1 N HCl in isopropanol). Absorbance was measured using a spectrophotometric microplate reader with reference filter at 630 nm and reading filter at 570 nm. Each determination was performed in triplicate.

Trypan blue

Cell viability was also evaluated by using Trypan Blue dye reagent. Non-viable cells stained blue, while viable cells excluded Trypan Blue and showed normal refringent cytoplasm. Samples were counted under a light microscope, and the percentage of non-viable cells was determined.

LDH

Cytotoxicity was also analyzed by lactate dehydrogenase (LDH) assay by using the Cytotoxicity Detection Kit (LDH) (Roche, Basel, Switzerland), according to the manufacturer's instructions. LDH is a stable cytoplasmic enzyme that is rapidly released into the cell culture supernatant upon damage of the plasma membrane. Background control values from untreated cells were subtracted from all readings, and the maximum releasable LDH activity in the cells was obtained by adding 2% Triton X-100 to the culture medium, which corresponded to 100% cell lysis or 100% non-viable cells. Absorbance was read in a spectrophotometric microplate reader at 450 nm. Values were normalized as percentages to untreated cells and shown as % viability relative to untreated cells.

Flow cytometry

Measurement of apoptosis by flow cytometry

Following drug treatment, both cells in suspension and adherent cells, which were detached with Versene, were collected and brought together, centrifuged at 1200 rpm for 5 min, and fixed overnight in 70% ethanol at 4ºC. Cells were washed three times with PBS, incubated for 1 h with 100 μgml RNase A and 20 μg/ml propidium iodide (PI) at room temperature and then analyzed with a Becton Dickinson (San Jose, CA, USA) FACSCalibur flow cytometer. Quantitation of apoptotic cells was calculated as the percentage of cells in the Sub-G_1 region (hypodiploidy) following cell-cycle analysis as previously described (Gajate *et al.*, 2000).

PI exclusion assay

This assay was used to evaluate the integrity of the plasma membrane. Attached and detached cells from each experimental point were collected, brought together, centrifuged and washed once with PBS. Cells were then resuspended in PBS containing 10 μg/ml PI. After incubation in the dark for 15 min at room temperature, cells were analyzed by flow cytometry at 590 nm. The proportion of cells with increased permeability to PI (PI^+ cells) was calculated as the percentage of cells with increased red fluorescence (strong shift in FL-2 values, *log* scale) with respect to the basal red fluorescence observed in untreated control cells using FCS Express 4 Plus software.

Annexin V/PI assay

For the quantification of apoptotic cells, phosphatidylserine exposure was monitored. Control and treated cells were collected, washed with PBS, and incubated in 100 μl annexin V binding buffer 1x (BD Pharmingen, San Jose, CA) with 5 μl of annexin V-FITC (BD Pharmingen) and 10 μg/ml PI for 15 min at room temperature. Then, 400 μl of annexin V binding buffer 1x were added and samples were analyzed by flow cytometry with simultaneous monitoring of green fluorescence (530 nm, 30 nm band-pass filter) for annexin V-FITC (FL-1) and red fluorescence (long-pass emission filter that transmits light >650 nm) for PI (FL-3).

Lysosomal membrane permeabilization

LysoTracker probe is a fluorescent acidotropic probe for labeling and tracing acidic organelles in live cells. Cells were incubated with 100 ng of LysoTracker (Molecular Probes)/ml for 30 min at 37ºC. Cells were then detached, washed, pelleted and resuspended in 1 ml of PBS for measurement of mean fluorescence by flow cytometry.

Cytofluorimetric analysis of mitochondrial transmembrane potential ($\Delta\Psi_m$) and generation of reactive oxygen species (ROS)

To evaluate $\Delta\Psi_m$ and the generation of ROS, cells were incubated in PBS with 20 nM 3,3 - dihexyloxacarbocyanine iodide ($DiOC_6(3)$; green fluorescence; Molecular Probes, Leiden, The Netherlands) and 2 μM dihydroethidine (DHE; red fluorescence after oxidation; Sigma) for 15 min at 37ºC, followed by analysis on a Becton Dickinson (San Jose, CA, USA) fluorescence-activated cell sorting FACSCalibur flow cytometer as previously described (Gajate *et al.*, 2000).

Cell surface death receptor expression

To analyze Fas/CD95 by flow cytometry assays, cells (2.5 x 10^5) were incubated with anti-human Fas SM1/1 IgG_{2a} mAb (Bender MedSystems) in PBS (1:150 dilution) for 1h at 4ºC, washed with cold PBS, and incubated for 1 h at 4ºC with FITC-conjugated goat anti-mouse immunoglobulin (Dakopatts, Glostrup, Denmark). After washing, cells were fixed with 1.5% (w/v) formaldehyde, and subjected to immunofluorescence flow cytometry in a FACSCan cytofluorometer (MFI values). Percentage of death receptor positive cells were estimated using P3X63 myeloma supernatant as a negative control, provided by F. Sanchez-Madrid (Hospital La Princesa, Madrid, Spain).

Analysis of DNA fragmentation in agarose gels

To assess apoptosis, we isolated fragmented DNA as previously described (Mollinedo *et al.*, 1997). In brief, at the indicated times, 4 x 10^6 cells were pelleted at 1200 rpm for 8 min. Supernatants were discarded and pellets were washed with PBS. Cells were then resuspended in hypotonic detergent buffer (10 mM Tris/HCl, pH 7.5-8.0, 1 mM EDTA, 0.2% Triton X-100) and incubated for 30 min at 4ºC. Cells were centrifuged at 1200 rpm for 20 min and the pellet was discarded. 75 μg/ml RNase A was added to the supernatant and incubated at 37ºC for 1 h. After adding 200 μg/ml proteinase K and 0.5% SDS, samples were incubated for another hour at 37ºC. Extraction of the aqueous phase with phenol/Tris/HCl, pH 7.5 was performed twice, and followed by a third extraction with phenol/chloroform/isoamilic alcohol. 300 mM NaCl was added and then DNA was precipitated with absolute ethanol (at -20ºC, overnight). After centrifugation and washing with ethanol, samples were dried with speed-vacuum and resuspended in TE buffer (10 mM Tris/HCl, pH 8.0.1 mM EDTA). 25 μl of each sample were loaded on a 1% agarose gel (containing 0.5 μg/ml ethidium bromide) and the typical DNA ladder was visualized with an UV transillumination system.

Supravital cell staining with acridine orange - autophagy studies

Cells were incubated with 1 μg/ml acridine orange (Molecular Probes, Leiden, The Netherlands) for 15 min at 37ºC, and then analyzed under a Nikon Eclipse Ti-S fluorescence microscope using an excitation filter of 550 nm (540-560 nm) and a long pass >610 nm emission/ barrier filter. Photographs were acquired with ProgRes Capture Pro 2.6. For flow cytometry studies, following incubation with acridine orange cells were detached, washed, pelleted and resuspended in PBS; fluorescence was read in chanels FL-1 and FL-3 with a Becton Dickinson (San Jose, CA, USA) FACSCalibur flow cytometer.

Monodansylcadaverine staining

Monodansylcadaverine (MDC) is a fluorescent compound that is incorporated into multilamellar bodies by both an ion trapping mechanism and the interaction with membrane lipids, used as a probe for detection of autophagic vacuoles in cultured cells. Following the appropriate treatment, U118 cells were incubated with MDC at a final concentration of 0.05 mM for 15 min at 37ºC and observed under a fluorescence microscope with a UV filter; photographs were acquired using ProgRes Capture Pro 2.6.

Measurement of intracellular calcium

After treatment, cells were incubated with 2 μM Fluo-4 AM dye (Molecular Probes) for 30 min at 37ºC, and then examined under an inverted fluorescence microscope or collected and analyzed by flow cytometry.

SYTOX-Green Stain

Apoptosis was also measured by observing morphological changes in the nuclear chromatin of cells detected by staining with 100 nM SYTOX-Green Nucleic Acid Stain (Invitrogen, Eugene, OR) for 15 min at 37ºC, followed by examination on a Nikon Eclipse Ti-S inverted fluorescence microscope (Tokyo, Japan). Photographs were acquired with ProgRes Capture Pro 2.6.

siRNA transfection

ON-TARGETplus SMART pools for human RIPK1 (cat. # L-004445-00) and RIPK3 (cat. # L-003534-00) siRNAs, which included a mixture of four specific siRNAs provided as a single reagent, as well as a non-targeting pool siRNA (cat. # D-001810-10-05) were purchased from Thermo Scientific (Pittsburgh, PA). U118 cells at a density of 8×10^4 cells per well in 6-well plates were transfected with 200 nM RIPK1-siRNA and 100 nM RIPK3-siRNA

using siPORT NeoFX transfection agent (Life Technologies) according to the manufacturer's instructions. Protein knockdown was assessed between two and five days after transfection, and best knockdown rates were obtained following 5 days after transfection and used in the experiments shown in this work. Efficiency of RIPK1 and RIPK3 knockdown was quantified with ImageJ software after Western blotting and using β-actin as protein control.

Western blot analysis

Cells (4-5 x 10^6) were detached using Versene, washed twice with PBS, and lysed with 60 μl of lysis buffer containing HEPES (pH 7.7), 0.3 M NaCl, 1.5 mM $MgCl_2$, 0.2 mM EDTA, 0.1% Triton X-100, 20 mM β-glycerophosphate, 0.1 mM sodium orthovanadate, supplemented with protease inhibitors (1 mM phenylmethylsulfonyl fluoride, 20 μg/ml aprotinin and 20 μg/ml leupeptin). Thirty to fifty micrograms of protein extract was subjected to SDS-polyacrylamide gels, transferred to Immobilon-P PVDF membranes (Merck Millipore, Darmstadt, Germany), blocked with 5% (w/v) defatted milk powder in TBST (50 mM Tris-HCl, pH 8.0, 150 mM NaCl, 0.1% Tween 20) for 1 h at room temperature, and incubated for 1 h at room temperature, or overnight at 4 °C, with the specific antibodies indicated in Table 8.1.

Secondary antibodies were anti-mouse or anti-rabbit immunoglobulins conjugated to horseradish peroxidase (GE Healthcare, Princeton, NJ) or from Santa Cruz Biotechnology Inc. as indicated in the Table 8.1. Signals were detected using an ECL (enhanced chemiluminescence) kit (GE Healthcare).

Table 8.1: List of the antibodies used in Western blotting (WB), confocal microscopy immunofluorescence (IF) and flow cytometry (FC) studies. The origin of the antibody, the molecular weight of the immunodetected bands, the company in which the antibody was produced, and the dilutions used are indicated. The phosphorylated residues recognized by the phospho-specific antibodies are indicated between parentheses.

Antibody	**Origin**	**Molecular weight (kDa)**	**Company**	**Dilution**	**Technique**
Cleaved caspase-3 (Asp 175)	Rabbit mAb	19, 17	Cell Signaling	1:1000	WB
PARP	Mouse mAb	116, 85	BD Biosciences	1:1000	WB
β-actin	Mouse mAb	42	Sigma	1:5000	WB
LC3B-I/LC3B-II	Rabbit pAB	16, 14	Cell Signaling	1:1000, 1:200	WB, IF
RIPK1	Rabbit mAB	79	Cell Signaling	1:1000	WB
RIPK1	Rabbit pAB	79, 45	Cell Signaling	1:1000	WB
Fas/CD95	Rabbit pAB	48	Santa Cruz Biotechnology	1:500	WB
Fas SM1/1 IgG_{2a}	Mouse mAb	48	Bender MedSystems	1:150	FC
FADD	Mouse mAb	24	BD Transduction Laboratories	1:1000	WB
RIPK3	Rabbit mAB	62	Cell Signaling	1:1000	WB
Caspase-8 (1C12)	Mouse mAb	57, p43/41, p18	Cell Signaling	1:1000	WB
Phosphorylated p44/42 MAPK (ERK1/2)	Mouse mAb	44, 42	Santa Cruz Biotechnology	1:1000	WB
ERK 2 (D-2): sc-1647	Mouse mAb	42	Santa Cruz Biotechnology	1:1000	WB
p44/42 MAPK (ERK1/2)	Rabbit mAb	44, 42	Cell Signaling	1:1000	WB
Phospho-p44/42 MAPK (ERK1/2) (Thr202/Tyr204)	Rabbit mAb	44.42	Cell Signaling	1:1000	WB
NF-κB	Rabbit mAb	65	Cell Signaling	1:1000	WB
Cytochrome c	Mouse	15	BD Pharmingen	1:1000	WB
Bcl-x_L	Rabbit	30	Cell Signaling	1:1000	WB
Caspase-9 (proforma and cleaved active fragments)	Mouse mAb	47, p37, p35	Cell Signaling	1:1000	WB
Cleaved caspase-9 (Asp 153)	Rabbit pAb	38	Calbiochem	1:1000	WB
Akt 1/2/3 (H-136)	Rabbit pAb	60	Santa Cruz Biotechnology	1:1000	WB
Akt (Akt 1/2/3)	Rabbit	60	Cell Signaling	1:1000	WB
Phospho-Akt (Ser473)	Rabbit pAb	60	Cell Signaling	1:1000	WB
Cyclin D1 (H-295):sc-753	Rabbit pAb	36	Santa Cruz Biotechnology	1:1000	WB
c-Myc (N-262): sc-764	Rabbit pAb	57-65	Santa Cruz Biotechnology	1:1000	WB
Phospho-SAPK/JNK (Thr183/Tyr185) (G9)	Rabbit mAb	46, 54	Cell Signaling	1:1000	WB
JNK1	Mouse mAb	46	Santa Cruz Biotechnology	1:1000	WB
AIF	Rabbit pAb	57, 67	Cell Signaling	1:1000	WB
Phospho-GSK-3α/β (Ser21/9) (37F11)	Rabbit mAb	51, 46	Cell Signaling	1:1000	WB
GSK-3α/β	Rabbit pAb	51, 46	Cell Signaling	1:1000	WB
Bid	Goat pAb	23	Santa Cruz Biotechnology	1:500	WB
Bad	Mouse mAb	23	BD Transduction Laboratories	1:1000	WB
Phospho-Bad (Ser136)	Rabbit pAb	23	Cell Signaling	1:1000	WB
Anti-Mouse IgG-HRP: sc-358914	Rabbit	-	Santa Cruz Biotechnology	1:2000	WB
Anti-Rabbit IgG-HRP: sc-2317	Donkey	-	Santa Cruz Biotechnology	1:2000	WB
Anti-Goat IgG-HRP: sc-2768	Rabbit	-	Santa Cruz Biotechnology	1:2000	WB
α-tubulin	Mouse mAb	-	Cabiochem	1:250	IF
Cy3-conjugated AffiniPure Goat anti-rabbit/mouse IgG	Goat	-	Jackson ImmunoResearch	1:150	IF
FITC- conjugated anti-Ki-67	Mouse mAb	-	BD Pharmingen	1:500	IF
FITC-conjugated goat anti-mouse Immunoglobulin	Goat	-	Dakopatts	1:100	FC

Separation of mitochondrial and cytosolic extracts

In order to analyze by Western blot the release of cytochrome c and AIF to the cytosol, separation of mitochondrial and cytosolic extracts was performed as described previously (Piqué *et al.*, 2000). Briefly, cells were harvested by centrifugation, washed once in cold PBS and gently lysed for 30 s by passing through a 26-gauge needle in a lysis buffer containing 250 mM sucrose, 1 mM EDTA, 0.05% digitonin, 25 mM Tris (pH 6.8), 1 mM DTT, 20 μg/ml aprotinin, 20 μg/ml leupeptin and 1 mM PMSF. Lysates were then centrifuged at 13000 rpm at 4ºC for 3 min to obtain the supernatants, that correspond to the *cytosolic fraction* (cytosolic extracts free of mitochondria) and the pellets, corresponding to the nuclear and mitochondrial fractions. Supernatants (40 μg protein) were then analyzed by Western-blot using specific antibodies against cytochrome c and AIF (Table 8.1).

Time-lapse videomicroscopy

Cells were recorded by time-lapse microscopy using a Nikon Eclipse TE2000-E microscope that was enclosed in a Plexiglass box where cells were maintained under a humidified air of 5% CO_2 at 37ºC using OKO-Lab technology. MetaMorph software was used for image acquisition and processing. Frames were taken every 10 min for 9 h for the U118 cell line. SF268 video was recorded for 68 h and frames were taken every 10 min; A172 video for 72 hours with frames taken every 10 min; GOS-3 cells were recorded for 48 h and frames were taken every 5 min. The elapsed time is shown in the inferior right corner for each video.

Files recorded in CD as Supplementary_Videos: U118.AVI; SF268.AVI; A172.AVI; GOS3.AVI

Confocal microscopy

1×10^6 cells were seeded on 6-well plates, each well containing a sterile glass coverslip coated with poly-L-lysine. Untreated and edelfosine-treated cells were fixed in formaldehyde (4% in PBS) for 20 min at room temperature. After fixation, cells were permeabilized in cold PBS containing 0.1% Triton X-100 for 1 min and rinsed thoroughly with PBS. Staining was performed incubating the coverslip with specific antibodies anti-LC3B, anti-α-tubulin or FITC-conjugated anti-Ki-67 for 1-h at room temperature followed by 1-h at room temperature with CY3-conjugated anti-rabbit or anti-mouse immunoglobulin (Ig) antibody (diluted 1:150 in PBS; Jackson ImmunoResearch, West Grove, PA) for LC3B and α-tubulin respectively, and DAPI staining (0.5 μg/ml; 5 min). Each incubation was followed by 2 washes in PBS. Stained coverslips were then mounted on slides using the antifading reagent SlowFade Gold (Invitrogen, Eugene, OR) to preserve fluorescence signal intensity. Samples were analyzed by microscopy using a confocal Leica SP5 microscope and LAS AF software.

Drug subcellular localization

The subcellular localization of edelfosine in U118 cells was examined with the edelfosine fluorescent analog Et-BDP-ET, a kind gift from F. Amat-Guerri and A. U. Acuña (Consejo Superior de Investigaciones Científicas, Madrid, Spain). Cells seeded in sterile coverslips coated with poly-L-lysine and mantained in DMEM as referred in *cell culture*, were incubated with the fluorescent analog for 45 min at 37ºC, and then with 100 nM MitoTracker Red for 15 min. Cells were then washed with PBS, stained with DAPI (0.5 μg/ml; 5 min) and coverslips were mounted on slides using SlowFade Gold to preserve fluorescence signal intensity. Samples were analyzed by microscopy using a confocal Leica SP5 microscope and LAS AF software.

IFN-γ treatment

To examine the effect of IFN-γ incubation on protein expression, 4-5 x 10^6 cells were treated with 50 ng/ml IFN-γ (Upstate Biotechnology, Lake Placid, NY, USA) in RPMI-1640/10% FBS complete culture medium for 24 or 48 h, and Fas/CD95 and caspase-8 expression were analyzed by western blot (see western blot section).

To analyze the effect of IFN-γ on caspase-8 and caspase-3 activation and Bid cleavage, cells were pre-treated with 50 ng/ml IFN-γ for 48 h in RPMI-1640/10% FBS complete culture medium, before incubation with edelfosine. Then, fifty micrograms of protein extract were subjected to Western blot analysis. For cell cycle analysis, T98G cells (4 x 10^5) were treated with 50 ng/ml IFN-γ plus 10 μM edelfosine for 24, 48 and 72 h and the percentage of cells in the Sub-G_1 and G_2 phases of the cell cycle were measured by flow cytometry.

Statistical analysis

Results are expressed as means ± SD of the number of experiments indicated. Comparisons between two experimental groups were determined using Student's t-test with P-value <0.05 indicating statistical significance.

References

Adamson, C., Kanu, O.O., Mehta, A.I., Di, C., Lin, N., Mattox, A.K., & Bigner, D.D. (2009) Glioblastoma multiforme: a review of where we have been and where we are going. *Expert opinion on investigational drugs*, **18**, 1061–1083.

Ahn, E.-Y., Pan, G., Vickers, S.M., & McDonald, J.M. (2002) IFN-gammaupregulates apoptosis-related molecules and enhances Fas-mediated apoptosis in human cholangiocarcinoma. *International journal of cancer. Journal international du cancer*, **100**, 445–451.

Alvarez, S.E., Harikumar, K.B., Hait, N.C., Allegood, J., Strub, G.M., Kim, E.Y., Maceyka, M., Jiang, H., Luo, C., Kordula, T., Milstien, S., & Spiegel, S. (2010) Sphingosine-1-phosphate is a missing cofactor for the E3 ubiquitin ligase TRAF2. *Nature*, **465**, 1084–1088.

Andreesen, R., Modolell, M., & Munder, P.G. (1979) Selective sensitivity of chronic myelogenous leukemia cell populations to alkyl-lysophospholipids. *Blood*, **54**, 519–523.

Andreesen, R., Modolell, M., Weltzien, H.U., Eibl, H., Common, H.H., Löhr, G.W., & Munder, P.G. (1978) Selective destruction of human leukemic cells by alkyl-lysophospholipids. *Cancer Research*, **38**, 3894–3899.

Anton, K., Baehring, J.M., & Mayer, T. (2012) Glioblastoma Multiforme: Overview of Current Treatment and Future Perspectives. *Hematology/Oncology Clinics of North America*, **26**, 825–853.

Antonios, D. (2011) *Imaging of Brain Tumors with Histological Correlations*. Springer Berlin Heidelberg, Berlin, Heidelberg.

Antunes, F., Cadenas, E., & Brunk, U.T. (2001) Apoptosis induced by exposure to a low steady-state concentration of H2O2 is a consequence of lysosomal rupture. *The Biochemical journal*, **356**, 549–555.

Aoudjit, F. & Vuori, K. (2001) Matrix attachment regulates Fas-induced apoptosis in endothelial cells: a role for c-flip and implications for anoikis. *The Journal of cell biology*, **152**, 633–643.

Apelbaum, A., Yarden, G., Warszawski, S., Harari, D., & Schreiber, G. (2013) Type I Interferons Induce Apoptosis by Balancing cFLIP and Caspase-8 Independent of Death Ligands. *Molecular and Cellular Biology*, **33**, 800–814.

Attard, G.S., Templer, R.H., Smith, W.S., Hunt, a N., & Jackowski, S. (2000) Modulation of CTP:phosphocholine cytidylyltransferase by membrane curvature elastic stress. *Proceedings of the National Academy of Sciences of the United States of America*, **97**, 9032–9036.

Ausili, A., Torrecillas, A., Aranda, F.J., Mollinedo, F., Gajate, C., Corbalán-García, S., Godos, A. de, & Gómez-Fernández, J.C. (2008) Edelfosine is incorporated into rafts and alters their organization. *The journal of physical chemistry. B*, **112**, 11643–11654.

Baburina, I. & Jackowski, S. (1998) Apoptosis triggered by 1-O-octadecyl-2-O-methyl-rac-glycero-3-phosphocholine is prevented by increased expression of CTP:phosphocholine cytidylyltransferase. *The Journal of biological chemistry*, **273**, 2169–2173.

Bala, A.D. & Bhattacharjee, A. (2011) Treatment of Glioblastoma Multiforme. *Journal of Pharmaceutical and Biomedical Sciences*, **12**, 1–7.

Barker, F.G., Chang, S.M., Huhn, S.L., Davis, R.L., Gutin, P.H., McDermott, M.W., Wilson, C.B., & Prados, M.D. (1997) Age and the risk of anaplasia in magnetic resonance - Nonenhancing supratentorial cerebral tumors. *Cancer*, **80**, 936–941.

Berghe, T.V., Kaiser, W.J., Bertrand, M.J.M., & Vandenabeele, P. (2015) Molecular crosstalk between apoptosis, necroptosis and survival signaling. *Molecular & Cellular Oncology*, 00–00.

Berghe, T.V., Linkermann, A., Jouan-Lanhouet, S., Walczak, H., & Vandenabeele, P. (2014) Regulated necrosis: the expanding network of non-apoptotic cell death pathways. *Nature Reviews Molecular Cell Biology*, **15**, 135–147.

Bénéteau, M., Pizon, M., Chaigne-Delalande, B., Daburon, S., Moreau, P., De Giorgi, F., Ichas, F., Rebillard, A., Dimanche-Boitrel, M.-T., Taupin, J.-L., Moreau, J.-F., & Legembre, P. (2008) Localization of Fas/CD95 into the lipid rafts on down-modulation of the phosphatidylinositol 3-kinase signaling pathway. *Molecular cancer research : MCR*, **6**, 604–613.

Blanc, J.L., Wager, M., Guilhot, J., Kusy, S., Bataille, B., Chantereau, T., Lapierre, F., Larsen, C.J., & Karayan-Tapon, L. (2004) Correlation of clinical features and methylation status of MGMT gene promoter in glioblastomas. *Journal of Neuro-Oncology*, **68**, 275–283.

Blink, E.J. (2004) Basic mri : Physics For anyone who does not have a degree in physics 0–75.

Blitterswijk, W.J. van & Verheij, M. (2008) Anticancer alkylphospholipids: mechanisms of

action, cellular sensitivity and resistance, and clinical prospects. *Current pharmaceutical design*, **14**, 2061–2074.

Blitterswijk, W.J. van, Luit, A.H. van der, Veldman, R.J., Verheij, M., & Borst, J. (2003) Ceramide: second messenger or modulator of membrane structure and dynamics? *The Biochemical journal*, **369**, 199–211.

Bonilla, X., Dakir, E.-H., Mollinedo, F., & Gajate, C. (2015) Endoplasmic reticulum targeting in Ewing's sarcoma by the alkylphospholipid analog edelfosine. *Oncotarget*, **6**, 14596–14613.

Bononi, A., Agnoletto, C., De Marchi, E., Marchi, S., Patergnani, S., Bonora, M., Giorgi, C., Missiroli, S., Poletti, F., Rimessi, A., & Pinton, P. (2011) Protein kinases and phosphatases in the control of cell fate. *Enzyme research*, **2011**, 329098.

Boucher, M.J., Morisset, J., Vachon, P.H., Reed, J.C., Lainé, J., & Rivard, N. (2000) MEK/ERK signaling pathway regulates the expression of Bcl-2, Bcl-X(L), and Mcl-1 and promotes survival of human pancreatic cancer cells. *Journal of cellular biochemistry*, **79**, 355–369.

Boya, P. & Kroemer, G. (2008) Lysosomal membrane permeabilization in cell death. *Oncogene*, **27**, 6434–6451.

Brady, C. a & Attardi, L.D. (2010) P53 At a Glance. *Journal of cell science*, **123**, 2527–2532.

Brat, D.J. (2012) Glioblastoma: biology, genetics, and behavior. *American Society of Clinical Oncology educational book / ASCO. American Society of Clinical Oncology. Meeting*, 102–107.

Bravo, R., Parra, V., Gatica, D., Rodriguez, A.E., Torrealba, N., Paredes, F., Wang, Z.V., Zorzano, A., Hill, J. a, Jaimovich, E., Quest, A.F.G., & Lavandero, S. (2013) Endoplasmic Reticulum and the Unfolded Protein Response. Dynamics and Metabolic Integration. *International Review of Cell and Molecular Biology*, **301**, 215–290.

Brock, A., Chang, H., & Huang, S. (2009) Non-genetic heterogeneity–a mutation-independent driving force for the somatic evolution of tumours. *Nature reviews. Genetics*, **10**, 336–342.

Bulik, M., Jancalek, R., Vanicek, J., Skoch, A., & Mechl, M. (2013) Potential of MR spectroscopy for assessment of glioma grading. *Clinical Neurology and Neurosurgery*, **115**, 146–153.

Busto, J.V., Del Canto-Jañez, E., Goñi, F.M., Mollinedo, F., & Alonso, A. (2008) Combination of the anti-tumour cell ether lipid edelfosine with sterols abolishes haemolytic side effects of the drug. *Journal of chemical biology*, **1**, 89–94.

Busto, J.V., Sot, J., Goñi, F.M., Mollinedo, F., & Alonso, A. (2007) Surface-active properties of the antitumour ether lipid 1-O-octadecyl-2-O-methyl-rac-glycero-3-phosphocholine

(edelfosine). *Biochimica et Biophysica Acta - Biomembranes*, **1768**, 1855–1860.

Butowski, N.A., Sneed, P.K., & Chang, S.M. (2006) Diagnosis and treatment of recurrent high-grade astrocytoma. *Journal of Clinical Oncology*, **24**, 1273–1280.

Cagnol, S. & Chambard, J.C. (2010) ERK and cell death: Mechanisms of ERK-induced cell death - Apoptosis, autophagy and senescence. *FEBS Journal*, **277**, 2–21.

Cai, Z., Jitkaew, S., Zhao, J., Chiang, H.-C., Choksi, S., Liu, J., Ward, Y., Wu, L.-G., & Liu, Z.-G. (2013) Plasma membrane translocation of trimerized MLKL protein is required for TNF-induced necroptosis. *Nature cell biology*, **15**, 1–13.

Cairns, R.a. & Mak, T.W. (2013) Oncogenic isocitrate dehydrogenase mutations: Mechanisms, models, and clinical opportunities. *Cancer Discovery*, **3**, 730–741.

Carmo, A., Balça-Silva, J., Matias, D., & Lopes, M.C. (2013) PKC signaling in glioblastoma. *Cancer Biology and Therapy*, **14**, 287–294.

Carmo, A., Carvalheiro, H., Crespo, I., Nunes, I., & Lopes, M.C. (2011) Effect of temozolomide on the U-118 glioma cell line. *Oncology Letters*, **2**, 1165–1170.

Carmona-Saez, P., Chagoyen, M., Tirado, F., Carazo, J.M., & Pascual-Montano, A. (2007) GENECODIS: a web-based tool for finding significant concurrent annotations in gene lists. *Genome biology*, **8**, R3.

Castellano, E. & Downward, J. (2011) RAS Interaction with PI3K: More Than Just Another Effector Pathway. *Genes & cancer*, **2**, 261–274.

Chakrabandhu, K., Huault, S., & Hueber, A.O. (2008) Distinctive molecular signaling in triple-negative breast cancer cell death triggered by hexadecylphosphocholine (miltefosine). *FEBS Letters*, **582**, 4176–4184.

Chan, F.K.M., Shisler, J., Bixby, J.G., Felices, M., Zheng, L., Appel, M., Orenstein, J., Moss, B., & Lenardo, M.J. (2003) A Role for Tumor Necrosis Factor Receptor-2 and Receptor-interacting Protein in Programmed Necrosis and Antiviral Responses. *Journal of Biological Chemistry*, **278**, 51613–51621.

Chautan, M., Chazal, G., Cecconi, F., Gruss, P., & Golstein, P. (1999) Interdigital cell death can occur through a necrotic and caspase-independent pathway. *Current Biology*, **9**, 967–970.

Chawla-Sarkar, M., Lindner, D.J., Liu, Y.-F., Williams, B.R., Sen, G.C., Silverman, R.H., & Borden, E.C. (2003) Apoptosis and interferons: role of interferon-stimulated genes as mediators of apoptosis. *Apoptosis : an international journal on programmed cell death*, **8**, 237–249.

Chen, R., Brady, E., & McIntyre, T.M. (2011) Human TMEM30a promotes uptake of anti-

tumor and bioactive choline phospholipids into mammalian cells. *Journal of immunology (Baltimore, Md. : 1950)*, **186**, 3215–3225.

Chen, W.W., Yu, H., Fan, H.B., Zhang, C.C., Zhang, M., Zhang, C., Cheng, Y., Kong, J., Liu, C.F., Geng, D., & Xu, X. (2012) RIP1 mediates the protection of geldanamycin on neuronal injury induced by oxygen-glucose deprivation combined with zVAD in primary cortical neurons. *Journal of Neurochemistry*, **120**, 70–77.

Cho, Y., McQuade, T., Zhang, H., Zhang, J., & Chan, F.K.M. (2011) RIP1-dependent and independent effects of necrostatin-1 in necrosis and T cell activation. *PLoS ONE*, **6**.

Christofferson, D.E. & Yuan, J. (2010) Necroptosis as an alternative form of programmed cell death. *Current Opinion in Cell Biology*, **22**, 263–268.

Ch'en, I.L., Tsau, J.S., Molkentin, J.D., Komatsu, M., & Hedrick, S.M. (2011) Mechanisms of necroptosis in T cells. *The Journal of experimental medicine*, **208**, 633–641.

Cohen, M.H., Shen, Y.L., Keegan, P., & Pazdur, R. (2009) FDA drug approval summary: bevacizumab (Avastin) as treatment of recurrent glioblastoma multiforme. *The oncologist*, **14**, 1131–1138.

Corcelle, E., Nebout, M., Bekri, S., Gauthier, N., Hofman, P., Poujeol, P., Fénichel, P., & Mograbi, B. (2006) Disruption of autophagy at the maturation step by the carcinogen lindane is associated with the sustained mitogen-activated protein kinase/extracellular signal-regulated kinase activity. *Cancer Research*, **66**, 6861–6870.

Cui, H., Kong, Y., & Zhang, H. (2012) Oxidative Stress, Mitochondrial Dysfunction, and Aging. *Journal of Signal Transduction*, **2012**, 1–13.

Danker, K., Reutter, W., & Semini, G. (2010) Glycosidated phospholipids: uncoupling of signalling pathways at the plasma membrane. *British journal of pharmacology*, **160**, 36–47.

Daumas-Duport, C., Scheithauer, B., O'Fallon, J., & Kelly, P. (1988) Grading of astrocytomas. A simple and reproducible method. *Cancer*, **62**, 2152–2165.

Davis, R.J. (2000) Signal transduction by the JNK group of MAP kinases. *Cell*, **103**, 239–252.

De Mendoza, a.E.H., Campanero, M.a., De La Iglesia-Vicente, J., Gajate, C., Mollinedo, F., & Blanco-Prieto, M.J. (2009) Antitumor alkyl ether lipid edelfosine: Tissue distribution and pharmacokinetic behavior in healthy and tumor-bearing immunosuppressed mice. *Clinical Cancer Research*, **15**, 858–864.

Degterev, a, Maki, J.L., & Yuan, J. (2013) Activity and specificity of necrostatin-1, small-molecule inhibitor of RIP1 kinase. *Cell death and differentiation*, **20**, 366.

Degterev, A., Hitomi, J., Germscheid, M., Ch'en, I.L., Korkina, O., Teng, X., Abbott, D., Cuny, G.D., Yuan, C., Wagner, G., Hedrick, S.M., Gerber, S.A., Lugovskoy, A., & Yuan, J. (2008) Identification of RIP1 kinase as a specific cellular target of necrostatins. *Nature chemical biology*, **4**, 313–321.

Degterev, A., Huang, Z., Boyce, M., Li, Y., Jagtap, P., Mizushima, N., Cuny, G.D., Mitchison, T.J., Moskowitz, M.A., & Yuan, J. (2005) Chemical inhibitor of nonapoptotic cell death with therapeutic potential for ischemic brain injury. *Nature chemical biology*, **1**, 112–119.

Delorme, S. & Weber, M.-A. (2006) Applications of MRS in the evaluation of focal malignant brain lesions. *Cancer Imaging*, **6**, 95–99.

Dineva, I.K., Zaharieva, M.M., Konstantinov, S.M., Eibl, H., & Berger, M.R. (2012) Erufosine suppresses breast cancer in vitro and in vivo for its activity on PI3K, c-Raf and Akt proteins. *Journal of cancer research and clinical oncology*, **138**, 1909–1917.

Dumontet, C., Thomas, L., Bérard, F., Gimonet, J.F., & Coiffier, B. (2006) A phase II trial of miltefosine in patients with cutaneous T-cell lymphoma. *Bulletin du cancer*, **93**.

Duque-Parra, J.E. (2005) Note on the origin and history of the term "apoptosis". *Anatomical record. Part B, New anatomist*, **283**, 2–4.

Eisele, G. & Weller, M. (2013) Targeting apoptosis pathways in glioblastoma. *Cancer Letters*, **332**, 335–345.

Eisenberg, T., Knauer, H., Schauer, A., Büttner, S., Ruckenstuhl, C., Carmona-Gutierrez, D., Ring, J., Schroeder, S., Magnes, C., Antonacci, L., Fussi, H., Deszcz, L., Hartl, R., Schraml, E., Criollo, A., Megalou, E., Weiskopf, D., Laun, P., Heeren, G., Breitenbach, M., Grubeck-Loebenstein, B., Herker, E., Fahrenkrog, B., Fröhlich, K.-U., Sinner, F., Tavernarakis, N., Minois, N., Kroemer, G., & Madeo, F. (2009) Induction of autophagy by spermidine promotes longevity. *Nature cell biology*, **11**, 1305–1314.

England, B., Huang, T., & Karsy, M. (2013) Current understanding of the role and targeting of tumor suppressor p53 in glioblastoma multiforme. *Tumor Biology*, **34**, 2063–2074.

Eramo, A., Pallini, R., Lotti, F., Sette, G., Patti, M., Bartucci, M., Ricci-Vitiani, L., Signore, M., Stassi, G., Larocca, L.M., Crinò, L., Peschle, C., & De Maria, R. (2005) Inhibition of DNA methylation sensitizes glioblastoma for tumor necrosis factor-related apoptosis-inducing ligand-mediated destruction. *Cancer Research*, **65**, 11469–11477.

Estella-Hermoso De Mendoza, A., Préat, V., Mollinedo, F., & Blanco-Prieto, M.J. (2011) In vitro and in vivo efficacy of edelfosine-loaded lipid nanoparticles against glioma. *Journal of Controlled Release*, **156**, 421–426.

Evan, G. & Littlewood, T. (1998) A matter of life and cell death. *Science (New York, N.Y.)*, **281**, 1317–1322.

Evans, C. (2011) TCGA Scientists Discover Four Distinct Subtypes of Glioblastoma Distinguished by Gene Expression Patters and Clinical Characteristics.

Eyster, K.M. (2007) The membrane and lipids as integral participants in signal transduction: lipid signal transduction for the non-lipid biochemist. *AJP: Advances in Physiology Education*, **31**, 5–16.

Faivre, S., Kroemer, G., & Raymond, E. (2006) Current development of mTOR inhibitors as anticancer agents. *Nature reviews. Drug discovery*, **5**, 671–688.

Fearns, C., Pan, Q., Mathison, J.C., & Chuang, T.H. (2006) Triad3A regulates ubiquitination and proteasomal degradation of RIP1 following disruption of Hsp90 binding. *Journal of Biological Chemistry*, **281**, 34592–34600.

Feoktistova, M., Geserick, P., Panayotova-Dimitrova, D., & Leverkus, M. (2012) Pick your poison: the Ripoptosome, a cell death platform regulating apoptosis and necroptosis. *Cell cycle (Georgetown, Tex.)*, **11**, 460–467.

Festjens, N., Vanden Berghe, T., & Vandenabeele, P. (2006) Necrosis, a well-orchestrated form of cell demise: Signalling cascades, important mediators and concomitant immune response.

Festjens, N., Vanden Berghe, T., Cornelis, S., & Vandenabeele, P. (2007) RIP1, a kinase on the crossroads of a cell's decision to live or die. *Cell death and differentiation*, **14**, 400–410.

Fine, H.A., Dear, K.B., Loeffler, J.S., Black, P.M., & Canellos, G.P. (1993) Meta-analysis of radiation therapy with and without adjuvant chemotherapy for malignant gliomas in adults. *Cancer*, **71**, 2585–2597.

Floryk, D. & Thompson, T.C. (2008) Perifosine induces differentiation and cell death in prostate cancer cells. *Cancer Letters*, **266**, 216–226.

Flusberg, D.A. & Sorger, P.K. (2015) Surviving apoptosis: life-death signaling in single cells. *Trends in cell biology*, **25**, 446–458.

Friedman, H., Kerby, T., & Calvert, H. (2000) Temozolomide and treatment of malignant glioma **6**, 2585–2597.

Fujisawa, H., Reis, R.M., Nakamura, M., Colella, S., Yonekawa, Y., Kleihues, P., & Ohgaki, H. (2000) Loss of heterozygosity on chromosome 10 is more extensive in primary (de novo) than in secondary glioblastomas. *Laboratory investigation; a journal of technical methods and pathology*, **80**, 65–72.

Fulda, S. (2014) Targeting Inhibitor of Apoptosis Proteins for Cancer Therapy: A Double-Edge Sword? *Journal of Clinical Oncology*, **32**, 11–12.

Fults, D. & Pedone, C. (1993) Deletion mapping of the long arm of chromosome 10 in glioblas-

toma multiforme. *Genes, chromosomes & cancer*, **7**, 173–177.

Furnari, F.B., Fenton, T., Bachoo, R.M., Mukasa, A., Stommel, J.M., Stegh, A., Hahn, W.C., Ligon, K.L., Louis, D.N., Brennan, C., Chin, L., DePinho, R.a., & Cavenee, W.K. (2007) Malignant astrocytic glioma: Genetics, biology, and paths to treatment. *Genes and Development*, **21**, 2683–2710.

Gaillard, F. (2015) Radiopaedia.org Glioblastoma.

Gajate, C. & Mollinedo, F. (2001) The antitumor ether lipid ET-18-OCH3 induces apoptosis through translocation and capping of Fas/CD95 into membrane rafts in human leukemic cells. *Blood*, **98**, 3860–3863.

Gajate, C. & Mollinedo, F. (2002) Biological activities, mechanisms of action and biomedical prospect of the antitumor ether phospholipid ET-18-OCH(3) (edelfosine), a proapoptotic agent in tumor cells. *Current drug metabolism*, **3**, 491–525.

Gajate, C. & Mollinedo, F. (2007) Edelfosine and perifosine induce selective apoptosis in multiple myeloma by recruitment of death receptors and downstream signaling molecules into lipid rafts. *Blood*, **109**, 711–719.

Gajate, C. & Mollinedo, F. (2011) Lipid Rafts and Fas/CD95 Signaling in Cancer Chemotherapy. *Recent patents on anti-cancer drug discovery*, **6**, 274–283.

Gajate, C. & Mollinedo, F. (2014) Lipid Rafts, Endoplasmic Reticulum and Mitochondria in the Antitumor Action of the Alkylphospholipid Analog Edelfosine. *Anti-Cancer Agents in Medicinal Chemistry*, **14**, 509–527.

Gajate, C. & Mollinedo, F. (2015) Lipid rafts and raft-mediated supramolecular entities in the regulation of CD95 death receptor apoptotic signaling. *Apoptosis : an international journal on programmed cell death*, **20**, 584–606.

Gajate, C., Del Canto-Jañez, E., Acuña, a U., Amat-Guerri, F., Geijo, E., Santos-Beneit, A.M., Veldman, R.J., & Mollinedo, F. (2004) Intracellular triggering of Fas aggregation and recruitment of apoptotic molecules into Fas-enriched rafts in selective tumor cell apoptosis. *The Journal of experimental medicine*, **200**, 353–365.

Gajate, C., Gonzalez-Camacho, F., & Mollinedo, F. (2009) Involvement of raft aggregates enriched in Fas/CD95 death-inducing signaling complex in the antileukemic action of edelfosine in Jurkat cells. *PloS one*, **4**, e5044.

Gajate, C., Matos-da-Silva, M., Dakir, E.L.-H., Fonteriz, R.I., Alvarez, J., & Mollinedo, F. (2012) Antitumor alkyl-lysophospholipid analog edelfosine induces apoptosis in pancreatic cancer by targeting endoplasmic reticulum. *Oncogene*, **31**, 2627–2639.

Gajate, C., Santos-Beneit, A., Modolell, M., & Mollinedo, F. (1998) Involvement of c-Jun NH2-terminal kinase activation and c-Jun in the induction of apoptosis by the ether phos-

pholipid 1-O-octadecyl-2-O-methyl-rac-glycero-3-phosphocholine. *Molecular pharmacology*, **53**, 602–612.

Gajate, C., Santos-Beneit, A.M., Macho, A., Lazaro, M.D.C., Hernandez-De Rojas, A., Modolell, M., Muñoz, E., & Mollinedo, F. (2000) Involvement of mitochondria and caspase-3 in ET-18-OCH3-induced apoptosis of human leukemic cells. *International Journal of Cancer*, **86**, 208–218.

Gallegos, L.L. & Newton, A.C. (2008) Spatiotemporal dynamics of lipid signaling: protein kinase C as a paradigm. *IUBMB Life*, **60**, 782–789.

Galluzzi, L., Blomgren, K., & Kroemer, G. (2009) Mitochondrial membrane permeabilization in neuronal injury. *Nature reviews. Neuroscience*, **10**, 481–494.

Galluzzi, L., Vitale, I., Abrams, J.M., Alnemri, E.S., Baehrecke, E.H., Blagosklonny, M.V., Dawson, T.M., Dawson, V.L., El-Deiry, W.S., Fulda, S., Gottlieb, E., Green, D.R., Hengartner, M.O., Kepp, O., Knight, R. a, Kumar, S., Lipton, S. a, Lu, X., Madeo, F., Malorni, W., Mehlen, P., Nuñez, G., Peter, M.E., Piacentini, M., Rubinsztein, D.C., Shi, Y., Simon, H.-U., Vandenabeele, P., White, E., Yuan, J., Zhivotovsky, B., Melino, G., & Kroemer, G. (2012) Molecular definitions of cell death subroutines: recommendations of the Nomenclature Committee on Cell Death 2012. *Cell death and differentiation*, **19**, 107–120.

Gan, H.K., Cvrljevic, A.N., & Johns, T.G. (2013) The epidermal growth factor receptor variant III (EGFRvIII): Where wild things are altered. *FEBS Journal*, **280**, 5350–5370.

Garcia, J., Ye, Y., Arranz, V., Letourneux, C., Pezeron, G., & Porteu, F. (2002) IEX-1: a new ERK substrate involved in both ERK survival activity and ERK activation. *The EMBO journal*, **21**, 5151–5163.

Georgakis, G.V., Li, Y., Rassidakis, G.Z., Martinez-Valdez, H., Medeiros, L.J., & Younes, A. (2006) Inhibition of heat shock protein 90 function by 17-allylamino-17-demethoxygeldanamycin in Hodgkin's lymphoma cells down-regulates Akt kinase, dephosphorylates extracellular signal-regulated kinase, and induces cell cycle arrest and cell death. *Clinical cancer research : an official journal of the American Association for Cancer Research*, **12**, 584–590.

Gilbert, M.R., Friedman, H.S., Kuttesch, J.F., Prados, M.D., Olson, J.J., Reaman, G.H., & Zaknoen, S.L. (2002) A phase II study of temozolomide in patients with newly diagnosed supratentorial malignant glioma before radiation therapy. *Neuro-oncology*, **4**, 261–267.

Goldschneider, D. & Mehlen, P. (2010) Dependence receptors: a new paradigm in cell signaling and cancer therapy. *Oncogene*, **29**, 1865–1882.

Golstein, P. & Kroemer, G. (2005) Redundant cell death mechanisms as relics and backups. *Cell death and differentiation*, **12 Suppl 2**, 1490–1496.

Golstein, P. & Kroemer, G. (2007) Cell death by necrosis: towards a molecular definition. *Trends in biochemical sciences*, **32**, 37–43.

Gomes, J., Al Zayadi, A., & Guzman, A. (2011) Occupational and environmental risk factors of adult primary brain cancers: a systematic review. *The international journal of occupational and environmental medicine*, **2**, 82–111.

Gonda, D.D., Warnke, P., Sanai, N., Taich, Z., Kasper, E.M., & Chen, C.C. (2013) The value of extended glioblastoma resection: Insights from randomized controlled trials. *Surgical neurology international*, **4**, 110.

Green, D.R. & Evan, G.I. (2002) A matter of life and death.

Green, D.R., Oberst, A., Dillon, C.P., Weinlich, R., & Salvesen, G.S. (2011) RIPK-dependent necrosis and its regulation by caspases: A mystery in five acts. *Molecular Cell*, **44**, 9–16.

Grier, J.T. & Batchelor, T. (2006) Low-Grade Gliomas in Adults 681–693.

Griner, E.M. & Kazanietz, M.G. (2007) Protein kinase C and other diacylglycerol effectors in cancer. *Nature reviews. Cancer*, **7**, 281–294.

Hac-Wydro, K., Dynarowicz-Łatka, P., Wydro, P., & Bak, K. (2011) Edelfosine disturbs the sphingomyelin-cholesterol model membrane system in a cholesterol-dependent way - The Langmuir monolayer study. *Colloids and Surfaces B: Biointerfaces*, **88**, 635–640.

Hamilton, S.R., Liu, B., Parsons, R.E., Papadopoulos, N., Jen, J., Powell, S.M., Krush, A.J., Berk, T., Cohen, Z., & Tetu, B. (1995) The molecular basis of Turcot's syndrome. *The New England journal of medicine*, **332**, 839–847.

Hanahan, D. & Weinberg, R.a. (2000) The hallmarks of cancer. *Cell*, **100**, 57–70.

Handrick, R., Rübel, A., Faltin, H., Eibl, H., Belka, C., & Jendrossek, V. (2006) Increased cytotoxicity of ionizing radiation in combination with membrane-targeted apoptosis modulators involves downregulation of protein kinase B/Akt-mediated survival-signaling. *Radiotherapy and Oncology*, **80**, 199–206.

He, S., Wang, L., Miao, L., Wang, T., Du, F., Zhao, L., & Wang, X. (2009) Receptor Interacting Protein Kinase-3 Determines Cellular Necrotic Response to TNF-α. *Cell*, **137**, 1100–1111.

Heerklotz, H. (2008) Interactions of surfactants with lipid membranes. *Quarterly reviews of biophysics*, **41**, 205–264.

Hegi, M.E., Diserens, A.-C., Gorlia, T., Hamou, M.-F., Tribolet, N. de, Weller, M., Kros, J.M., Hainfellner, J. a, Mason, W., Mariani, L., Bromberg, J.E.C., Hau, P., Mirimanoff, R.O., Cairncross, J.G., Janzer, R.C., & Stupp, R. (2005) MGMT gene silencing and benefit from temozolomide in glioblastoma. *The New England journal of medicine*, **352**,

997–1003.

Heiss, W.-D., Raab, P., & Lanfermann, H. (2011) Multimodality Assessment of Brain Tumors and Tumor Recurrence. *Journal of Nuclear Medicine*, **52**, 1585–1600.

Helfman, D.M., Barnes, K.C., & Kinkade, J.M. (1983) Phospholipid-sensitive Ca2+-dependent protein phosphorylation system in various types of leukemic cells from human patients and in human leukemic cell lines HL60 and K562, and its inhibition by alkyl-lysophospholipid.

Hentschel, S.J. & Sawaya, R. (2003) Optimizing outcomes with maximal surgical resection of malignant gliomas.

Hesselink, J.R. & Press, G.A. (1988) MR contrast enhancement of intracranial lesions with Gd-DTPA. *Radiologic clinics of North America*, **26**, 873–887.

Hitomi, J., Christofferson, D.E., Ng, A., Yao, J., Degterev, A., Xavier, R.J., & Yuan, J. (2008) Identification of a Molecular Signaling Network that Regulates a Cellular Necrotic Cell Death Pathway. *Cell*, **135**, 1311–1323.

Holdhoff, M. & Grossman, S.A. (2011) Controversies in the adjuvant therapy of high-grade gliomas. *The oncologist*, **16**, 351–358.

Holler, N., Zaru, R., Micheau, O., Thome, M., Attinger, A., Valitutti, S., Bodmer, J.L., Schneider, P., Seed, B., & Tschopp, J. (2000) Fas triggers an alternative, caspase-8-independent cell death pathway using the kinase RIP as effector molecule. *Nature immunology*, **1**, 489–495.

Holmström, T.H., Schmitz, I., Söderström, T.S., Poukkula, M., Johnson, V.L., Chow, S.C., Krammer, P.H., & Eriksson, J.E. (2000) MAPK/ERK signaling in activated T cells inhibits CD95/Fas-mediated apoptosis downstream of DISC assembly. *The EMBO journal*, **19**, 5418–5428.

Hong, S.J., Dawson, T.M., & Dawson, V.L. (2004) Nuclear and mitochondrial conversations in cell death: PARP-1 and AIF signaling. *Trends in pharmacological sciences*, **25**, 259–264.

Hong, S.J., Dawson, T.M., & Dawson, V.L. (2006) PARP and the release of apoptosis-inducing factor from mitochondria. In *Poly (ADP-Ribosyl)ation*. Springer US, pp. 103–117.

Hoover, J.M., Chang, S.M., & Parney, I.F. (2010) Clinical trials in brain tumor surgery. *Neuroimaging Clinics of North America*, **20**, 409–424.

Horská, A. & Barker, P.B. (2010) Imaging of brain tumors: MR spectroscopy and metabolic imaging.

Hostein, I., Robertson, D., DiStefano, F., Workman, P., & Clarke, P.A. (2001) Inhibition

of signal transduction by the Hsp90 inhibitor 17-allylamino-17-demethoxygeldanamycin results in cytostasis and apoptosis. *Cancer Research*, **61**, 4003–4009.

Hsu, H., Huang, J., Shu, H.B., Baichwal, V., & Goeddel, D.V. (1996) TNF-dependent recruitment of the protein kinase RIP to the TNF receptor-1 signaling complex. *Immunity*, **4**, 387–396.

Høyer-Hansen, M., Bastholm, L., Szyniarowski, P., Campanella, M., Szabadkai, G., Farkas, T., Bianchi, K., Fehrenbacher, N., Elling, F., Rizzuto, R., Mathiasen, I.S., & Jäättelä, M. (2007) Control of Macroautophagy by Calcium, Calmodulin-Dependent Kinase Kinase-β, and Bcl-2. *Molecular Cell*, **25**, 193–205.

Iacob, G. & Dinca, E.B. (2009) Current data and strategy in glioblastoma multiforme. *Journal of medicine and life*, **2**, 386–393.

IARC (2015) GLOBOCAN 2012:Estimated Cancer Incidence, Mortality and Prevalence Worlwide in 2012.

ICNIRP (1996) Health issues related to the use of hand-held radiotelephones and base transmitters. International Commission on Non-Ionizing Radiation Protection. *Health physics*, **70**, 587–593.

ICNIRP (2009) ICNIRP statement on the "Guidelines for limiting exposure to time-varying electric, magnetic, and electromagnetic fields (up to 300 GHz)". *Health physics*, **97**, 257–258.

Igney, F.H. & Krammer, P.H. (2002) Death and anti-death: tumour resistance to apoptosis. *Nature reviews. Cancer*, **2**, 277–288.

Jain, H.V. & Meyer-Hermann, M. (2011) The Molecular Basis of Synergism between Carboplatin and ABT-737 Therapy Targeting Ovarian Carcinomas. *Cancer research*, 705–715.

Jiang, Y.G., Peng, Y., & Koussougbo, K.S. (2011) Necroptosis: A novel therapeutic target for glioblastoma. *Medical Hypotheses*, **76**, 350–352.

Johnson, D.E. (2013) *Cell Death Signaling in Cancer Biology and Treatment.*

Johnson, D.R. & O'Neill, B.P. (2012) Glioblastoma survival in the United States before and during the temozolomide era. *Journal of Neuro-Oncology*, **107**, 359–364.

Kaiser, W.J., Daley-Bauer, L.P., Thapa, R.J., Mandal, P., Berger, S.B., Huang, C., Sundararajan, A., Guo, H., Roback, L., Speck, S.H., Bertin, J., Gough, P.J., Balachandran, S., & Mocarski, E.S. (2014) RIP1 suppresses innate immune necrotic as well as apoptotic cell death during mammalian parturition. *Proceedings of the National Academy of Sciences of the United States of America*, **111**, 7753–7758.

Kang, M.H. & Reynolds, C.P. (2009) Bcl-2 Inhibitors: Targeting Mitochondrial Apoptotic

Pathways in Cancer Therapy. *Clinical Cancer Research*, **15**, 1126–1132.

Kanu, O.O., Hughes, B., Di, C., Lin, N., Fu, J., Bigner, D.D., Yan, H., & Adamson, C. (2009) Glioblastoma Multiforme Oncogenomics and Signaling Pathways **3**, 39–52.

Kanzawa, T., Germano, I.M., Komata, T., Ito, H., Kondo, Y., & Kondo, S. (2004) Role of autophagy in temozolomide-induced cytotoxicity for malignant glioma cells. *Cell Death Differ*, **11**, 448–457.

Kataoka, T., Budd, R.C., Holler, N., Thome, M., Martinon, F., Irmler, M., Burns, K., Hahne, M., Kennedy, N., Kovacsovics, M., & Tschopp, J. (2000) The caspase-8 inhibitor FLIP promotes activation of NF-kappaB and Erk signaling pathways. *Current biology : CB*, **10**, 640–648.

Kearney, C.J., Cullen, S.P., Clancy, D., & Martin, S.J. (2014) RIPK1 can function as an inhibitor rather than an initiator of RIPK3-dependent necroptosis. *The FEBS journal*, **281**, 4921–4934.

Kim, J.W., Choi, E.J., & Joe, C.O. (2000) Activation of death-inducing signaling complex (DISC) by pro-apoptotic C-terminal fragment of RIP. *Oncogene*, **19**, 4491–4499.

Kim, R. (2005) Unknotting the roles of Bcl-2 and Bcl-xL in cell death. *Biochemical and biophysical research communications*, **333**, 336–343.

Kleihues, P. & Cavenee, W.K. (2000) *Pathology and Genetics of Tumours of the Nervous System*, Employment & social affairs. IARC Press.

Kleihues, P. & Ohgaki, H. (1999) Primary and secondary glioblastomas: from concept to clinical diagnosis. *Neuro-oncology*, **1**, 44–51.

Klionsky, D.J. (2014) Coming soon to a journal near you — the updated guidelines for the use and interpretation of assays for monitoring autophagy. *Autophagy*, 1691.

Knizhnik, A.V., Roos, W.P., Nikolova, T., Quiros, S., Tomaszowski, K.H., Christmann, M., & Kaina, B. (2013) Survival and Death Strategies in Glioma Cells: Autophagy, Senescence and Apoptosis Triggered by a Single Type of Temozolomide-Induced DNA Damage. *PLoS ONE*, **8**, 1–12.

Koenig, A., Buskiewicz, I.A., Fortner, K.A., Russell, J.Q., Asaoka, T., He, Y.-W., Hakem, R., Eriksson, J.E., & Budd, R.C. (2014) The c-FLIPL cleavage product p43FLIP promotes activation of extracellular signal-regulated kinase (ERK), nuclear factor κB (NF-κB), and caspase-8 and T cell survival. *The Journal of biological chemistry*, **289**, 1183–1191.

Kool, M., Linden, M. van der, Haas, M. de, Scheffer, G.L., Vree, J.M. de, Smith, A.J., Jansen, G., Peters, G.J., Ponne, N., Scheper, R.J., Elferink, R.P., Baas, F., & Borst, P. (1999) MRP3, an organic anion transporter able to transport anti-cancer drugs. *Proceedings of the National Academy of Sciences of the United States of America*, **96**, 6914–6919.

Kögel, D., Fulda, S., & Mittelbronn, M. (2010) Therapeutic exploitation of apoptosis and autophagy for glioblastoma. *Anti-cancer agents in medicinal chemistry*, **10**, 438–449.

Krakstad, C. & Chekenya, M. (2010) Survival signalling and apoptosis resistance in glioblastomas: opportunities for targeted therapeutics. *Molecular cancer*, **9**, 135.

Kroemer, G. & Levine, B. (2008) Autophagic cell death: the story of a misnomer. *Nature reviews. Molecular cell biology*, **9**, 1004–1010.

Kroemer, G., Galluzzi, L., & Brenner, C. (2007) Mitochondrial membrane permeabilization in cell death. *Physiological reviews*, **87**, 99–163.

Kurhanewicz, J., Vigneron, D.B., & Nelson, S.J. (2000) Three-Dimensional Magnetic Resonance Spectroscopic Imaging of Brain and Prostate Cancer1. *Neoplasia (New York, N.Y.)*, **2**, 166–189.

Lacroix, M., Abi-Said, D., Fourney, D.R., Gokaslan, Z.L., Shi, W., DeMonte, F., Lang, F.F., McCutcheon, I.E., Hassenbusch, S.J., Holland, E., Hess, K., Michael, C., Miller, D., & Sawaya, R. (2001) A multivariate analysis of 416 patients with glioblastoma multiforme: prognosis, extent of resection, and survival. *Journal of neurosurgery*, **95**, 190–198.

Lafitte, F., Morel-Precetti, S., Martin-Duverneuil, N., Guermazi, A., Brunet, E., Heran, F., & Chiras, J. (2001) Multiple glioblastomas: CT and MR features. *European Radiology*, **11**, 131–136.

Lanzetta, G. & Minniti, G. (2010) Treatment of glioblastoma in elderly patients: An overview of current treatments and future perspective. *Tumori*, **96**, 650–658.

Lavieu, G., Scarlatti, F., Sala, G., Levade, T., Ghidoni, R., Botti, J., & Codogno, P. (2007) Is autophagy the key mechanism by which the sphingolipid rheostat controls the cell fate decision? *Autophagy*, **3**, 45–47.

Lavrik, I.N., Golks, A., Riess, D., Bentele, M., Eils, R., & Krammer, P.H. (2007) Analysis of CD95 threshold signaling: triggering of CD95 (FAS/APO-1) at low concentrations primarily results in survival signaling. *The Journal of biological chemistry*, **282**, 13664–13671.

Lazova, R., Camp, R.L., Klump, V., Siddiqui, S.F., Amaravadi, R.K., & Pawelek, J.M. (2012) Punctate LC3B expression is a common feature of solid tumors and associated with proliferation, metastasis, and poor outcome. *Clinical Cancer Research*, **18**, 370–379.

Lefranc, F. & Kiss, R. (2006) Autophagy, the Trojan horse to combat glioblastomas. *Neurosurgical focus*, **20**, E7.

Leszczynski, D. & Xu, Z. (2010) Mobile phone radiation health risk controversy: the reliability and sufficiency of science behind the safety standards. *Health research policy and systems / BioMed Central*, **8**, 2.

Lewis, J., Devin, A., Miller, A., Lin, Y., Rodriguez, Y., Neckers, L., & Liu, Z.G. (2000) Disruption of Hsp96 function results in degradation of the death domain kinase, receptor-interacting protein (RIP), and blockage of tumor necrosis factor-induced nuclear factor-κB activation. *Journal of Biological Chemistry*, **275**, 10519–10526.

Li, J., McQuade, T., Siemer, A.B., Napetschnig, J., Moriwaki, K., Hsiao, Y.S., Damko, E., Moquin, D., Walz, T., McDermott, A., Chan, F.K.M., & Wu, H. (2012) The RIP1/RIP3 necrosome forms a functional amyloid signaling complex required for programmed necrosis. *Cell*, **150**, 339–350.

Li, J.H., Kluger, M.S., Madge, L.A., Zheng, L., Bothwell, A.L.M., & Pober, J.S. (2002) Interferon-gamma augments CD95(APO-1/Fas) and pro-caspase-8 expression and sensitizes human vascular endothelial cells to CD95-mediated apoptosis. *The American journal of pathology*, **161**, 1485–1495.

Li, L., Han, W., Gu, Y., Qiu, S., Lu, Q., Jin, J., Luo, J., & Hu, X. (2007) Honokiol induces a necrotic cell death through the mitochondrial permeability transition pore. *Cancer Research*, **67**, 4894–4903.

Li, Z., Tan, F., Liewehr, D.J., Steinberg, S.M., & Thiele, C.J. (2010) In vitro and in vivo inhibition of neuroblastoma tumor cell growth by AKT inhibitor perifosine. *Journal of the National Cancer Institute*, **102**, 758–770.

Liang, Y., Diehn, M., Watson, N., Bollen, A.W., Aldape, K.D., Nicholas, M.K., Lamborn, K.R., Berger, M.S., Botstein, D., Brown, P.O., & Israel, M. a (2005) Gene expression profiling reveals molecularly and clinically distinct subtypes of glioblastoma multiforme. *Proceedings of the National Academy of Sciences of the United States of America*, **102**, 5814–5819.

Lin, Y., Devin, A., Rodriguez, Y., & Liu, Z.G. (1999a) Cleavage of the death domain kinase RIP by Caspase-8 prompts TNF-induced apoptosis. *Genes and Development*, **13**, 2514–2526.

Lin, Y., Devin, A., Rodriguez, Y., & Liu, Z.G. (1999b) Cleavage of the death domain kinase RIP by Caspase-8 prompts TNF-induced apoptosis. *Genes and Development*, **13**, 2514–2526.

Liu, D.-h., Yuan, H.-y., Cao, C.-y., Gao, Z.-p., Zhu, B.-y., Huang, H.-l., & Liao, D.-f. (2007) Heat shock protein 90 acts as a molecular chaperone in late-phase activation of extracellular signal-regulated kinase 1/2 stimulated by oxidative stress in vascular smooth muscle cells. *Acta pharmacologica Sinica*, **28**, 1907–1913.

Long, J.S. & Ryan, K.M. (2012) New frontiers in promoting tumour cell death: targeting apoptosis, necroptosis and autophagy. *Oncogene*, **31**, 1–16.

Louis, D.N., Ohgaki, H., Wiestler, O.D., Cavenee, W.K., Burger, P.C., Jouvet, A., Schei-

thauer, B.W., & Kleihues, P. (2007) The 2007 WHO classification of tumours of the central nervous system. *Acta neuropathologica*, **114**, 97–109.

Lowe, S.W. & Lin, A.W. (2000) Apoptosis in cancer. *Carcinogenesis*, **21**, 485–495.

Lu, J.V., Weist, B.M., Raam, B.J. van, Marro, B.S., Nguyen, L.V., Srinivas, P., Bell, B.D., Luhrs, K.A., Lane, T.E., Salvesen, G.S., & Walsh, C.M. (2011) Complementary roles of Fas-associated death domain (FADD) and receptor interacting protein kinase-3 (RIPK3) in T-cell homeostasis and antiviral immunity. *Proceedings of the National Academy of Sciences of the United States of America*, **108**, 15312–15317.

Lu, Z. & Xu, S. (2006) ERK1/2 MAP kinases in cell survival and apoptosis. *IUBMB life*, **58**, 621–631.

Luo, X. & Kraus, W.L. (2012) On PAR with PARP: cellular stress signaling through poly(ADP-ribose) and PARP-1. *Genes & development*, **26**, 417–432.

Luo, X., Budihardjo, I., Zou, H., Slaughter, C., & Wang, X. (1998) Bid, a Bcl2 interacting protein, mediates cytochrome c release from mitochondria in response to activation of cell surface death receptors. *Cell*, **94**, 481–490.

Lwin, Z., MacFadden, D., Al-Zahrani, A., Atenafu, E., Miller, B.A., Sahgal, A., Menard, C., Laperriere, N., & Mason, W.P. (2013) Glioblastoma management in the temozolomide era: Have we improved outcome? *Journal of Neuro-Oncology*, **115**, 303–310.

Ly, J.D., Grubb, D.R., & Lawen, A. (2003) The mitochondrial membrane potential ($\delta\psi$m) in apoptosis; an update.

Mackillop, W.J. (2006) The Importance of Prognosis in Cancer Medicine. In *TNM Online*. John Wiley & Sons, Inc., Hoboken, NJ, USA.

Mao, H., LeBrun, D.G., Yang, J., Zhu, V.F., & Li, M. (2013) Deregulated Signaling Pathways in Glioblastoma Multiforme: Molecular Mechanisms and Therapeutic Targets. *Cancer investigation*, **30**, 48–56.

Marbán, Á.C. (2013) Mecanismos de toxicidad de lípidos antitumorales sintéticos en Saccharomyces cerevisiae (PhD thesis).

Marco, C., Ríos-Marco, P., Jiménez-López, J., Segovia, J., & Carrasco, M. (2014) Antitumoral Alkylphospholipids Alter Cell Lipid Metabolism. *Anti-Cancer Agents in Medicinal Chemistry*, **14**, 545–558.

Martinez, R., Setien, F., Voelter, C., Casado, S., Quesada, M.P., Schackert, G., & Esteller, M. (2007) CpG island promoter hypermethylation of the pro-apoptotic gene caspase-8 is a common hallmark of relapsed glioblastoma multiforme. *Carcinogenesis*, **28**, 1264–1268.

Martín-Oliva, D., Ferrer-Martín, R.M., Santos, A.M., Carrasco, M.C., Sierra, A., Marín-Teva,

J.L., Calvente, R., Navascués, J., & Cuadros, M.A. (2011) Simultaneous cell death and upregulation of poly(ADP-ribose) polymerase-1 expression in early postnatal mouse retina. *Investigative ophthalmology & visual science*, **52**, 7445–7454.

Masui, K., Gini, B., Wykosky, J., Zanca, C., Mischel, P.S., Furnari, F.B., & Cavenee, W.K. (2013) A tale of two approaches: Complementary mechanisms of cytotoxic and targeted therapy resistance may inform next-generation cancer treatments. *Carcinogenesis*, **34**, 725–738.

McCubrey, J. a, Steelman, L.S., Chappell, W.H., Abrams, S.L., Montalto, G., Cervello, M., Nicoletti, F., Fagone, P., Malaponte, G., Mazzarino, M.C., Candido, S., Libra, M., Bäsecke, J., Mijatovic, S., Maksimovic-Ivanic, D., Milella, M., Tafuri, A., Cocco, L., Evangelisti, C., Chiarini, F., & Martelli, A.M. (2012) Mutations and deregulation of Ras/Raf/MEK/ERK and PI3K/PTEN/Akt/mTOR cascades which alter therapy response. *Oncotarget*, **3**, 954–987.

Mechtler, L. (2009) Neuroimaging in Neuro-Oncology. *Neurologic Clinics*, **27**, 171–201.

Mellinghoff, I.K., Wang, M.Y., Vivanco, I., Haas-Kogan, D. a, Zhu, S., Dia, E.Q., Lu, K.V., Yoshimoto, K., Huang, J.H.Y., Chute, D.J., Riggs, B.L., Horvath, S., Liau, L.M., Cavenee, W.K., Rao, P.N., Beroukhim, R., Peck, T.C., Lee, J.C., Sellers, W.R., Stokoe, D., Prados, M., Cloughesy, T.F., Sawyers, C.L., & Mischel, P.S. (2005) Molecular determinants of the response of glioblastomas to EGFR kinase inhibitors. *The New England journal of medicine*, **353**, 2012–2024.

Melo-Lima, S., Celeste Lopes, M., & Mollinedo, F. (2014) Necroptosis is associated with low procaspase-8 and active RIPK1 and -3 in human glioma cells. *Oncoscience*, **1**, 649–664.

Melo-Lima, S., Lopes, M.C., & Mollinedo, F. (2015) ERK1/2 acts as a switch between necrotic and apoptotic cell death in ether phospholipid edelfosine-treated glioblastoma cells. *Pharmacol Res*, **95-96**, 2–11.

Michels, J., Kepp, O., Senovilla, L., Lissa, D., Castedo, M., Kroemer, G., & Galluzzi, L. (2013) Functions of BCL-X L at the Interface between Cell Death and Metabolism. *International journal of cell biology*, **2013**, 705294.

Minn, A.J., Boise, L.H., & Thompson, C.B. (1996) Expression of Bcl-x(L) and loss of p53 can cooperate to overcome a cell cycle checkpoint induced by mitotic spindle damage. *Genes and Development*, **10**, 2621–2631.

Minn, A.J., Rudin, C.M., Boise, L.H., & Thompson, C.B. (1995) Expression of bcl-xL can confer a multidrug resistance phenotype. *Blood*, **86**, 1903–1910.

Misra, A., Ganesh, S., Shahiwala, A., & Shah, S.P. (2003) Drug delivery to the central nervous system: A review. *Journal of Pharmacy and Pharmaceutical Sciences*, **6**, 252–273.

Modolell, M., Andreesen, R., Pahlke, W., Brugger, U., & Munder, P.G. (1979) Disturbance of phospholipid metabolism during the selective destruction of tumor cells induced by alkyl-lysophospholipids. *Cancer Research*, **39**, 4681–4686.

Mollinedo, F. (2014) Editorial: Antitumor alkylphospholipid analogs: a promising and growing family of synthetic cell membrane-targeting molecules for cancer treatment). *Anti-cancer agents in medicinal chemistry*, **14**, 495–498.

Mollinedo, F. & Gajate, C. (2006a) Fas/CD95 death receptor and lipid rafts: New targets for apoptosis-directed cancer therapy. *Drug Resistance Updates*, **9**, 51–73.

Mollinedo, F. & Gajate, C. (2006b) FasL-Independent Activation of Fas. In *Fas Signaling*. Springer US, Boston, MA, pp. 13–27.

Mollinedo, F. & Gajate, C. (2015) Lipid rafts as major platforms for signaling regulation in cancer. *Advances in biological regulation*, **57**, 130–146.

Mollinedo, F., Fernández, M., Hornillos, V., Delgado, J., Amat-Guerri, F., Acuña, a U., Nieto-Miguel, T., Villa-Pulgarín, J. a, González-García, C., Ceña, V., & Gajate, C. (2011) Involvement of lipid rafts in the localization and dysfunction effect of the antitumor ether phospholipid edelfosine in mitochondria. *Cell death & disease*, **2**, e158.

Mollinedo, F., Fernández-Luna, J.L., Gajate, C., Martín-Martín, B., Benito, A., Martínez-Dalmau, R., & Modolell, M. (1997) Selective induction of apoptosis in cancer cells by the ether lipid ET- 18-OCH3 (edelfosine): Molecular structure requirements, cellular uptake, and protection by bcl-2 and bcl-x(L). *Cancer Research*, **57**, 1320–1328.

Mollinedo, F., Gajate, C., & Modolell, M. (1994) The ether lipid 1-octadecyl-2-methyl-rac-glycero-3-phosphocholine induces expression of fos and jun proto-oncogenes and activates AP-1 transcription factor in human leukaemic cells. *The Biochemical journal*, **302 (Pt 2**, 325–329.

Mollinedo, F., Gajate, C., Martín-Santamaría, S., & Gago, F. (2004) ET-18-OCH3 (edelfosine): a selective antitumour lipid targeting apoptosis through intracellular activation of Fas/CD95 death receptor. *Current medicinal chemistry*, **11**, 3163–3184.

Mollinedo, F., Iglesia-Vicente, J. de la, Gajate, C., Estella-Hermoso de Mendoza, A., Villa-Pulgarin, J.A., Campanero, M.A., & Blanco-Prieto, M.J. (2010) Lipid raft-targeted therapy in multiple myeloma. *Oncogene*, **29**, 3748–3757.

Mollinedo, F., Martínez-Dalmau, R., & Modolell, M. (1993) Early and selective induction of apoptosis in human leukemic cells by the alkyl-lysophospholipid ET-18-OCH3. *Biochemical and biophysical research communications*, **192**, 603–609.

Moser, C., Lang, S.A., & Stoeltzing, O. (2009) Heat-shock protein 90 (Hsp90) as a molecular target for therapy of gastrointestinal cancer.

Moujalled, D.M., Cook, W.D., Okamoto, T., Murphy, J., Lawlor, K.E., Vince, J.E., & Vaux, D.L. (2013) TNF can activate RIPK3 and cause programmed necrosis in the absence of RIPK1. *Cell death & disease*, **4**, e465.

Mrugala, M.M. (2013) Advances and challenges in the treatment of glioblastoma: a clinician's perspective. *Discovery medicine*, **15**, 221–230.

Mulder, E. & Deenen, L.L. van (1965) Metabolism of red-cell lipids. 3. Pathways for phospholipid renewal. *Biochimica et biophysica acta*, **106**, 348–356.

Muller, A.J., DuHadaway, J.B., Donover, P.S., Sutanto-Ward, E., & Prendergast, G.C. (2005) Inhibition of indoleamine 2,3-dioxygenase, an immunoregulatory target of the cancer suppression gene Bin1, potentiates cancer chemotherapy. *Nature medicine*, **11**, 312–319.

Munder, P.G. & Modolell, M. (1973) Adjuvant induced formation of lysophosphatides and their role in the immune response. *International archives of allergy and applied immunology*, **45**, 133–135.

Munder, P.G., Ferber, E., Modolell, M., & Fischer, H. (1969) The influence of various adjuvants on the metabolism of phospholipids in macrophages. *International archives of allergy and applied immunology*, **36**, 117–128.

Munder, P.G., Modolell, M., Andreesen, R., Weltzien, H.U., & Westphal, O. (1979) Lysophosphatidylcholine (lysolecithin) and its synthetic analogues. Immunemodulating and other biologic effects. *Springer Seminars in Immunopathology*, **2**, 187–203.

Muñoz-Martínez, F., Torres, C., Castanys, S., & Gamarro, F. (2010) CDC50A plays a key role in the uptake of the anticancer drug perifosine in human carcinoma cells. *Biochemical Pharmacology*, **80**, 793–800.

Murphy, J.M., Czabotar, P.E., Hildebrand, J.M., Lucet, I.S., Zhang, J.G., Alvarez-Diaz, S., Lewis, R., Lalaoui, N., Metcalf, D., Webb, A.I., Young, S.N., Varghese, L.N., Tannahill, G.M., Hatchell, E.C., Majewski, I.J., Okamoto, T., Dobson, R.C.J., Hilton, D.J., Babon, J.J., Nicola, N.A., Strasser, A., Silke, J., & Alexander, W.S. (2013) The pseudokinase MLKL mediates necroptosis via a molecular switch mechanism. *Immunity*, **39**, 443–453.

Naumann, U., Bähr, O., Wolburg, H., Altenberend, S., Wick, W., Liston, P., Ashkenazi, A., & Weller, M. (2007) Adenoviral expression of XIAP antisense RNA induces apoptosis in glioma cells and suppresses the growth of xenografts in nude mice. *Gene therapy*, **14**, 147–161.

Naumann, U., Wischhusen, J., Weit, S., Rieger, J., Wolburg, H., Massing, U., & Weller, M. (2004) Alkylphosphocholine-induced glioma cell death is BCL-X(L)-sensitive, caspase-independent and characterized by massive cytoplasmic vacuole formation. *Cell death and differentiation*, **11**, 1326–1341.

NCI (2015) NCT01051557.

Neglia, J.P., Robison, L.L., Stovall, M., Liu, Y., Packer, R.J., Hammond, S., Yasui, Y., Kasper, C.E., Mertens, A.C., Donaldson, S.S., Meadows, A.T., & Inskip, P.D. (2006) New primary neoplasms of the central nervous system in survivors of childhood cancer: A report from the childhood cancer survivor study. *Journal of the National Cancer Institute*, **98**, 1528–1537.

Nelson, L.M., Tanner, C.M., Van Den Eeden, S.K., & McGuire, V.M. (2004) *Neuroepidemiology: from principles to practice.* Oxford University Press, Oxford.

Neuwelt, E.A., Bauer, B., Fahlke, C., Fricker, G., Iadecola, C., Janigro, D., Leybaert, L., Molnár, Z., O'Donnell, M.E., Povlishock, J.T., Saunders, N.R., Sharp, F., Stanimirovic, D., Watts, R.J., & Drewes, L.R. (2011) Engaging neuroscience to advance translational research in brain barrier biology. *Nature reviews. Neuroscience*, **12**, 169–182.

Nicotera, P., Leist, M., & Ferrando-May, E. (1999) Apoptosis and necrosis: different execution of the same death. *Biochemical Society symposium*, **66**, 69–73.

Nieto-Miguel, T., Fonteriz, R.I., Vay, L., Gajate, C., López-Hernández, S., & Mollinedo, F. (2007) Endoplasmic reticulum stress in the proapoptotic action of edelfosine in solid tumor cells. *Cancer Research*, **67**, 10368–10378.

Nieto-Miguel, T., Gajate, C., & Mollinedo, F. (2006) Differential targets and subcellular localization of antitumor alkyl-lysophospholipid in leukemic versus solid tumor cells. *Journal of Biological Chemistry*, **281**, 14833–14840.

Nogales-Cadenas, R., Carmona-Saez, P., Vazquez, M., Vicente, C., Yang, X., Tirado, F., Carazo, J.M., & Pascual-Montano, A. (2009) GeneCodis: interpreting gene lists through enrichment analysis and integration of diverse biological information. *Nucleic acids research*, **37**, W317–22.

Nuydens, R., Dispersyn, G., Van Den Kieboom, G., De Jong, M., Connors, R., Ramaekers, F., Borgers, M., & Geerts, H. (2000) Bcl-2 protects neuronal cells against taxol-induced apoptosis by inducing multi-nucleation. *Apoptosis*, **5**, 335–343.

Ofengeim, D. & Yuan, J. (2013) Regulation of RIP1 kinase signalling at the crossroads of inflammation and cell death. *Nature reviews. Molecular cell biology*, **14**, 727–736.

Ohgaki, H. & Kleihues, P. (2005) Epidemiology and etiology of gliomas. *Acta Neuropathologica*, **109**, 93–108.

Ohgaki, H. & Kleihues, P. (2007) Genetic pathways to primary and secondary glioblastoma. *The American journal of pathology*, **170**, 1445–1453.

Ohgaki, H. & Kleihues, P. (2013) The definition of primary and secondary glioblastoma. *Clinical Cancer Research*, **19**, 764–772.

Omuro, A. & DeAngelis, L.M. (2013) Glioblastoma and other malignant gliomas: a clinical review. *JAMA : the journal of the American Medical Association*, **310**, 1842–1850.

Ono, K., Wang, X., & Han, J. (2001) Resistance to tumor necrosis factor-induced cell death mediated by PMCA4 deficiency. *Molecular and cellular biology*, **21**, 8276–8288.

Orozco, S., Yatim, N., Werner, M.R., Tran, H., Gunja, S.Y., Tait, S.W.G., Albert, M.L., Green, D.R., & Oberst, A. (2014) RIPK1 both positively and negatively regulates RIPK3 oligomerization and necroptosis. *Cell death and differentiation*, **21**, 1511–1521.

Ostermann, S., Csajka, C., Buclin, T., Leyvraz, S., Lejeune, F., Decosterd, L. a, & Stupp, R. (2004) Plasma and cerebrospinal fluid population pharmacokinetics of temozolomide in malignant glioma patients. *Clinical cancer research : an official journal of the American Association for Cancer Research*, **10**, 3728–3736.

Ostrom, Q.T., Gittleman, H., Liao, P., Rouse, C., Chen, Y., Dowling, J., Wolinsky, Y., Kruchko, C. and, & Barnholtz-Sloan, J. (2012) CBTRUS Statistical Report: Primary Brain and Central Nervous System Tumors Diagnosed in the United States in 2004–2008. *Neuro-oncology*, **16**, Source: Central Brain Tumor Registry of the United.

O'Donnell, M.A. & Ting, A.T. (2011) RIP1 comes back to life as a cell death regulator in TNFR1 signaling. *The FEBS journal*, **278**, 877–887.

O'Donnell, M.A., Legarda-Addison, D., Skountzos, P., Yeh, W.C., & Ting, A.T. (2007) Ubiquitination of RIP1 regulates an NF-kappaB-independent cell-death switch in TNF signaling. *Current biology : CB*, **17**, 418–424.

Pachioni, J.D.A., Magalhães, J.G., Juliane, E., Lima, C., & Bueno, L.D.M. (2013) Alkylphospholipids – A Promising Class of Chemotherapeutic Agents with a Broad Pharmacological Spectrum **16**, 742–759.

Paglin, S., Hollister, T., Delohery, T., Hackett, N., McMahill, M., Sphicas, E., Domingo, D., & Yahalom, J. (2001) A novel response of cancer cells to radiation involves autophagy and formation of acidic vesicles. *Cancer Research*, **61**, 439–444.

Palacios, C., López-Pérez, A.I., & López-Rivas, A. (2010) Down-regulation of RIP expression by 17-dimethylaminoethylamino-17-demethoxygeldanamycin promotes TRAIL-induced apoptosis in breast tumor cells. *Cancer Letters*, **287**, 207–215.

Paris, C., Bertoglio, J., & Bréard, J. (2007) Lysosomal and mitochondrial pathways in miltefosine-induced apoptosis in U937 cells. *Apoptosis*, **12**, 1257–1267.

Pasparakis, M. & Vandenabeele, P. (2015) Necroptosis and its role in inflammation. *Nature*, **517**, 311–320.

PathologyOutlines.com (2013) CNS tumor Astrocytic tumors Glioblastoma multiforme.

Pattingre, S., Bauvy, C., Levade, T., Levine, B., & Codogno, P. (2009) Ceramide-induced autophagy: to junk or to protect cells? *Autophagy*, **5**, 558–560.

Pelloski, C.E. & Gilbert, M.R. (2007) Current Treatment Options in Adult Glioblastoma. *US Oncological Disease*, **1**, 105–109.

Peña, L. de la, Burgan, W.E., Carter, D.J., Hollingshead, M.G., Satyamitra, M., Camphausen, K., & Tofilon, P.J. (2006) Inhibition of Akt by the alkylphospholipid perifosine does not enhance the radiosensitivity of human glioma cells. *Molecular cancer therapeutics*, **5**, 1504–1510.

Peter, M.E., Hadji, A., Murmann, A.E., Brockway, S., Putzbach, W., Pattanayak, A., & Ceppi, P. (2015) The role of CD95 and CD95 ligand in cancer. *Cell death and differentiation*, **22**, 885–886.

Piqué, M., Barragán, M., Dalmau, M., Bellosillo, B., Pons, G., & Gil, J. (2000) Aspirin induces apoptosis through mitochondrial cytochrome c release. *FEBS letters*, **480**, 193–196.

Pisco, A.O. & Huang, S. (2015) Non-genetic cancer cell plasticity and therapy-induced stemness in tumour relapse: "What does not kill me strengthens me". *British Journal of Cancer*, **112**, 1725–1732.

Pisetsky, D.S. (2014) The Expression of HMGB1 on microparticles released during cell activation and cell death in vitro and in vivo. *Molecular medicine (Cambridge, Mass.)*, **20**, 158–163.

Ponnusamy, S., Meyers-Needham, M., Senkal, C.E., Saddoughi, S.A., Sentelle, D., Selvam, S.P., Salas, A., & Ogretmen, B. (2010) Sphingolipids and cancer: ceramide and sphingosine-1-phosphate in the regulation of cell death and drug resistance. *Future oncology (London, England)*, **6**, 1603–1624.

Portnow, J., Badie, B., Chen, M., Liu, A., Blanchard, S., & Synold, T.W. (2009) The neuropharmacokinetics of temozolomide in patients with resectable brain tumors: Potential implications for the current approach to chemoradiation. *Clinical Cancer Research*, **15**, 7092–7098.

Preté, P.S.C., Gomes, K., Malheiros, S.V.P., Meirelles, N.C., & De Paula, E. (2002) Solubilization of human erythrocyte membranes by non-ionic surfactants of the polyoxyethylene alkyl ethers series. *Biophysical Chemistry*, **97**, 45–54.

Qu, X., Zou, Z., Sun, Q., Luby-Phelps, K., Cheng, P., Hogan, R.N., Gilpin, C., & Levine, B. (2007) Autophagy Gene-Dependent Clearance of Apoptotic Cells during Embryonic Development. *Cell*, **128**, 931–946.

Quick, J., Gessler, F., Dützmann, S., Hattingen, E., Harter, P.N., Weise, L.M., Franz, K.,

Seifert, V., & Senft, C. (2014) Benefit of tumor resection for recurrent glioblastoma. *Journal of Neuro-Oncology*, **117**, 365–372.

Raj, A. & Oudenaarden, A. van (2008) Nature, nurture, or chance: stochastic gene expression and its consequences. *Cell*, **135**, 216–226.

Ramirez, Y.P., Weatherbee, J.L., Wheelhouse, R.T., & Ross, A.H. (2013) Glioblastoma multiforme therapy and mechanisms of resistance. *Pharmaceuticals*, **6**, 1475–1506.

Rangel-Yagui, C.D.O., Pessoa, A., & Tavares, L.C. (2005) Micellar solubilization of drugs. *Journal of Pharmacy and Pharmaceutical Sciences*, **8**, 147–163.

Reid, G.S.D., Shan, X., Coughlin, C.M., Lassoued, W., Pawel, B.R., Wexler, L.H., Thiele, C.J., Tsokos, M., Pinkus, J.L., Pinkus, G.S., Grupp, S.A., & Vonderheide, R.H. (2009) Interferon-gamma-dependent infiltration of human T cells into neuroblastoma tumors in vivo. *Clinical cancer research : an official journal of the American Association for Cancer Research*, **15**, 6602–6608.

Reilly, K.M. (2009) Brain tumor susceptibility: The role of genetic factors and uses of mouse models to unravel risk. In *Brain Pathology*. pp. 121–131.

Reis-Sobreiro, M., Roué, G., Moros, a, Gajate, C., Iglesia-Vicente, J. de la, Colomer, D., & Mollinedo, F. (2013) Lipid raft-mediated Akt signaling as a therapeutic target in mantle cell lymphoma. *Blood cancer journal*, **3**, e118.

Reitman, Z.J. & Yan, H. (2010) Isocitrate dehydrogenase 1 and 2 mutations in cancer: Alterations at a crossroads of cellular metabolism. *Journal of the National Cancer Institute*, **102**, 932–941.

Remijsen, Q., Goossens, V., Grootjans, S., Van den Haute, C., Vanlangenakker, N., Dondelinger, Y., Roelandt, R., Bruggeman, I., Goncalves, A., Bertrand, M.J.M., Baekelandt, V., Takahashi, N., Berghe, T.V., & Vandenabeele, P. (2014) Depletion of RIPK3 or MLKL blocks TNF-driven necroptosis and switches towards a delayed RIPK1 kinase-dependent apoptosis. *Cell death & disease*, **5**, e1004.

Rengstl, B., Newrzela, S., Heinrich, T., Weiser, C., Thalheimer, F.B., Schmid, F., Warner, K., Hartmann, S., Schroeder, T., Küppers, R., Rieger, M. a, & Hansmann, M.-L. (2013) Incomplete cytokinesis and re-fusion of small mononucleated Hodgkin cells lead to giant multinucleated Reed-Sternberg cells. *Proceedings of the National Academy of Sciences of the United States of America*, **110**, 20729–20734.

Rébé, C., Cathelin, S., Launay, S., Filomenko, R., Prévotat, L., L'Ollivier, C., Gyan, E., Micheau, O., Grant, S., Dubart-Kupperschmitt, A., Fontenay, M., & Solary, E. (2007) Caspase-8 prevents sustained activation of NF-B in monocytes undergoing macrophagic differentiation. *Blood*, **109**, 1442–1450.

Richardson, P.G., Eng, C., Kolesar, J., Hideshima, T., & Anderson, K.C. (2012) Perifosine , an oral, anti-cancer agent and inhibitor of the Akt pathway: mechanistic actions, pharmacodynamics, pharmacokinetics, and clinical activity. *Expert opinion on drug metabolism & toxicology*, **8**, 623–633.

Rodriguez-Viciana, P., Warne, P.H., Dhand, R., Vanhaesebroeck, B., Gout, I., Fry, M.J., Waterfield, M.D., & Downward, J. (1994) Phosphatidylinositol-3-OH kinase as a direct target of Ras. *Nature*, **370**, 527–532.

Rodríguez, A., Webster, P., Ortego, J., & Andrews, N.W. (1997) Lysosomes behave as Ca2+-regulated exocytic vesicles in fibroblasts and epithelial cells. *Journal of Cell Biology*, **137**, 93–104.

Ronellenfitsch, M.W., Brucker, D.P., Burger, M.C., Wolking, S., Tritschler, F., Rieger, J., Wick, W., Weller, M., & Steinbach, J.P. (2009) Antagonism of the mammalian target of rapamycin selectively mediates metabolic effects of epidermal growth factor receptor inhibition and protects human malignant glioma cells from hypoxia-induced cell death. *Brain : a journal of neurology*, **132**, 1509–1522.

Rong, Y., Durden, D.L., Van Meir, E.G., & Brat, D.J. (2006) 'Pseudopalisading' necrosis in glioblastoma: a familiar morphologic feature that links vascular pathology, hypoxia, and angiogenesis. *Journal of neuropathology and experimental neurology*, **65**, 529–539.

Ruano, Y., Mollejo, M., Camacho, F.I., De Lope, A.R., Fiaño, C., Ribalta, T., Martínez, P., Hernández-Moneo, J.L., & Meléndez, B. (2008) Identification of survival-related genes of the phosphatidylinositol 3-kinase signaling pathway in glioblastoma multiforme. *Cancer*, **112**, 1575–1584.

Ruiter, G.A., Zerp, S.F., Bartelink, H., Blitterswijk, W.J. van, & Verheij, M. (2003) Anti-cancer alkyl-lysophospholipids inhibit the phosphatidylinositol 3-kinase-Akt/PKB survival pathway. *Anti-cancer drugs*, **14**, 167–173.

Rübel, A., Handrick, R., Lindner, L.H., Steiger, M., Eibl, H., Budach, W., Belka, C., & Jendrossek, V. (2006) The membrane targeted apoptosis modulators erucylphosphocholine and erucylphosphohomocholine increase the radiation response of human glioblastoma cell lines in vitro. *Radiation oncology (London, England)*, **1**, 6.

Ryter, S.W., Mizumura, K., & Choi, A.M.K. (2014) The impact of autophagy on cell death modalities. *International Journal of Cell Biology*, **2014**, 17–19.

Safa, A.R., Day, T.W., & Wu, C.-H. (2008) Cellular FLICE-like inhibitory protein (C-FLIP): a novel target for cancer therapy. *Current cancer drug targets*, **8**, 37–46.

Samadder, P., Richards, C., Bittman, R., Bhullar, R.P., & Arthur, G. (2003) The antitumor ether lipid 1-O-Octadecyl-2-O-methyl-rac-glycerophosphocholine (ET-18-OCH3) inhibits the association between Ras and Raf-1. *Anticancer Research*, **23**, 2291–2295.

Sanden, M.H.M. van der, Houweling, M., Golde, L.M.G. van, & Vaandrager, A.B. (2003) Inhibition of phosphatidylcholine synthesis induces expression of the endoplasmic reticulum stress and apoptosis-related protein CCAAT/enhancer-binding protein-homologous protein (CHOP/GADD153). *The Biochemical journal*, **369**, 643–650.

Schilling, R., Geserick, P., & Leverkus, M. (2014) Characterization of the ripoptosome and its components: implications for anti-inflammatory and cancer therapy. *Methods in enzymology*, **545**, 83–102.

Schmidt, N.O., Westphal, M., Hagel, C., Ergün, S., Stavrou, D., Rosen, E.M., & Lamszus, K. (1999) Levels of vascular endothelial growth factor, hepatocyte growth factor/scatter factor and basic fibroblast growth factor in human gliomas and their relation to angiogenesis. *International journal of cancer. Journal international du cancer*, **84**, 10–18.

Schubert, K.M., Scheid, M.P., & Duronio, V. (2000) Ceramide inhibits protein kinase B/Akt by promoting dephosphorylation of serine 473. *The Journal of biological chemistry*, **275**, 13330–13335.

Schwartzbaum, J. a, Fisher, J.L., Aldape, K.D., & Wrensch, M. (2006) Epidemiology and molecular pathology of glioma. *Nature clinical practice. Neurology*, **2**, 494–503; quiz 1 p following 516.

SEER (2014) SEER Stat Fact Sheets: Brain and Other Nervous System Cancer.

Segui, B. & Legembre, P. (2010) Redistribution of CD95 into the lipid rafts to treat cancer cells? *Recent patents on anti-cancer drug discovery*, **5**, 22–28.

Sevrioukova, I.F. (2011) Apoptosis-inducing factor: structure, function, and redox regulation. *Antioxidants & redox signaling*, **14**, 2545–2579.

Shapiro, W.R., Green, S.B., Burger, P.C., Mahaley, M.S., Selker, R.G., VanGilder, J.C., Robertson, J.T., Ransohoff, J., Mealey, J., & Strike, T.A. (1989) Randomized trial of three chemotherapy regimens and two radiotherapy regimens and two radiotherapy regimens in postoperative treatment of malignant glioma. Brain Tumor Cooperative Group Trial 8001. (No. 1).

Siegel, R., Naishadham, D., & Jemal, A. (2013) Cancer statistics, 2013. *CA: a cancer journal for clinicians*, **63**, 11–30.

Siegmund, D., Wicovsky, A., Schmitz, I., Schulze-Osthoff, K., Kreuz, S., Leverkus, M., Dittrich-Breiholz, O., Kracht, M., & Wajant, H. (2005) Death receptor-induced signaling pathways are differentially regulated by gamma interferon upstream of caspase 8 processing. *Molecular and cellular biology*, **25**, 6363–6379.

Simmons, M.L., Lamborn, K.R., Takahashi, M., Chen, P., Israel, M.a., Berger, M.S., Godfrey, T., Nigro, J., Prados, M., Chang, S., Barker, F.G., & Aldape, K. (2001) Analysis of

complex relationships between age, p53, epidermal growth factor receptor, and survival in glioblastoma patients. *Cancer Research*, **61**, 1122–1128.

Stadlbauer, A., Hammen, T., Grummich, P., Buchfelder, M., Kuwert, T., Dörfler, A., Nimsky, C., & Ganslandt, O. (2011) Classification of peritumoral fiber tract alterations in gliomas using metabolic and structural neuroimaging. *Journal of nuclear medicine : official publication, Society of Nuclear Medicine*, **52**, 1227–1234.

Stambolsky, P., Weisz, L., Shats, I., Klein, Y., Goldfinger, N., Oren, M., & Rotter, V. (2006) Regulation of AIF expression by p53. *Cell death and differentiation*, **13**, 2140–2149.

Stegh, A.H., Barnhart, B.C., Volkland, J., Algeciras-Schimnich, A., Ke, N., Reed, J.C., & Peter, M.E. (2002) Inactivation of Caspase-8 on Mitochondria of Bcl-xL-expressing MCF7-Fas Cells: ROLE FOR THE BIFUNCTIONAL APOPTOSIS REGULATOR PROTEIN. *Journal of Biological Chemistry*, **277**, 4351–4360.

Stummer, W., Pichlmeier, U., Meinel, T., Wiestler, O.D., Zanella, F., & Reulen, H.J. (2006) Fluorescence-guided surgery with 5-aminolevulinic acid for resection of malignant glioma: a randomised controlled multicentre phase III trial. *Lancet Oncology*, **7**, 392–401.

Sun, K., Deng, W., Zhang, S., Cai, N., Jiao, S., Song, J., & Wei, L. (2013) Paradoxical roles of autophagy in different stages of tumorigenesis: protector for normal or cancer cells. *Cell & bioscience*, **3**, 35.

Sun, L., Wang, H., Wang, Z., He, S., Chen, S., Liao, D., Wang, L., Yan, J., Liu, W., Lei, X., & Wang, X. (2012) Mixed lineage kinase domain-like protein mediates necrosis signaling downstream of RIP3 kinase. *Cell*, **148**, 213–227.

Sundar, S., Jha, T.K., Thakur, C.P., Bhattacharya, S.K., & Rai, M. (2006) Oral miltefosine for the treatment of Indian visceral leishmaniasis. *Transactions of the Royal Society of Tropical Medicine and Hygiene*, **100 Suppl**, S26–S33.

Sundar, S., Jha, T.K., Thakur, C.P., Engel, J., Sindermann, H., Fischer, C., Junge, K., Bryceson, A., & Berman, J. (2002) Oral miltefosine for Indian visceral leishmaniasis. *The New England journal of medicine*, **347**, 1739–1746.

Sundeep Deorah, M., Lynch, C.F., Sibenaller, Z.A., & Ryken, T.C. (2006) Trends in brain cancer incidence and survival in the United States: Surveillance, Epidemiology, and End Results Program, 1973 to 2001. *Neurosurgical focus*, **20**, E1.

Susin, S.A., Zamzami, N., Castedo, M., Hirsch, T., Marchetti, P., Macho, A., Daugas, E., Geuskens, M., & Kroemer, G. (1996) Bcl-2 inhibits the mitochondrial release of an apoptogenic protease. *The Journal of experimental medicine*, **184**, 1331–1341.

Sylvester, P.W. (2011) Optimization of the tetrazolium dye (MTT) colorimetric assay for cellular growth and viability. *Methods in molecular biology (Clifton, N.J.)*, **716**, 157–168.

Tabas-Madrid, D., Nogales-Cadenas, R., & Pascual-Montano, A. (2012) GeneCodis3: a non-redundant and modular enrichment analysis tool for functional genomics. *Nucleic acids research*, **40**, W478–W483.

Tait, S.W.G., Ichim, G., & Green, D.R. (2014) Die another way–non-apoptotic mechanisms of cell death. *Journal of cell science*, **127**, 2135–2144.

Takahashi, N., Duprez, L., Grootjans, S., Cauwels, A., Nerinckx, W., DuHadaway, J.B., Goossens, V., Roelandt, R., Van Hauwermeiren, F., Libert, C., Declercq, W., Callewaert, N., Prendergast, G.C., Degterev, A., Yuan, J., & Vandenabeele, P. (2012) Necrostatin-1 analogues: critical issues on the specificity, activity and in vivo use in experimental disease models. *Cell death & disease*, **3**, e437.

Tanaka, K., Babic, I., Nathanson, D., Akhavan, D., Guo, D., Gini, B., Dang, J., Zhu, S., Yang, H., Jesus, J. de, Amzajerdi, A.N., Zhang, Y., Dibble, C.C., Dan, H., Rinkenbaugh, A., Yong, W.H., Vinters, H.V., Gera, J.F., Cavenee, W.K., Cloughesy, T.F., Manning, B.D., Baldwin, A.S., & Mischel, P.S. (2011) Oncogenic EGFR signaling activates an mTORC2-NF-κB pathway that promotes chemotherapy resistance. *Cancer Discovery*, **1**, 524–538.

Tarnowski, G.S., Mountain, I.M., Stock, C.C., Munder, P.G., Weltzien, H.U., & Westphal, O. (1978) Effect of lysolecithin and analogs on mouse ascites tumors. *Cancer Research*, **38**, 339–344.

TCGA (2008) The Cancer Genome Atlas.

Teicher, B. a (2006) Protein kinase C as a therapeutic target. *Clinical cancer research : an official journal of the American Association for Cancer Research*, **12**, 5336–5345.

Tekedereli, I., Alpay, S.N., Akar, U., Yuca, E., Ayugo-Rodriguez, C., Han, H.-D., Sood, A.K., Lopez-Berestein, G., & Ozpolat, B. (2013) Therapeutic Silencing of Bcl-2 by Systemically Administered siRNA Nanotherapeutics Inhibits Tumor Growth by Autophagy and Apoptosis and Enhances the Efficacy of Chemotherapy in Orthotopic Xenograft Models of ER (-) and ER (+) Breast Cancer. *Molecular therapy. Nucleic acids*, **2**, e121.

Temkin, V., Huang, Q., Liu, H., Osada, H., & Pope, R.M. (2006) Inhibition of ADP/ATP exchange in receptor-interacting protein-mediated necrosis. *Molecular and cellular biology*, **26**, 2215–2225.

Thakur, A., Joshi, N., Shanmugam, T., & Banerjee, R. (2013) Proapoptotic miltefosine nanovesicles show synergism with paclitaxel: Implications for glioblastoma multiforme therapy. *Cancer Letters*, **334**, 274–283.

Torok, J.A., Wegner, R.E., Mintz, A.H., Heron, D.E., & Burton, S.A. (2011) Re-irradiation with radiosurgery for recurrent glioblastoma multiforme. *Technology in cancer research & treatment*, **10**, 253–258.

Traganos, F. & Darzynkiewicz, Z. (1994) Lysosomal proton pump activity: supravital cell staining with acridine orange differentiates leukocyte subpopulations. *Methods in cell biology*, **41**, 185–194.

Tran, S.E., Holmstrom, T.H., Ahonen, M., Kahari, V.M., & Eriksson, J.E. (2001) MAPK/ERK overrides the apoptotic signaling from Fas, TNF, and TRAIL receptors. *The Journal of biological chemistry*, **276**, 16484–16490.

Tsuchiya, Y., Nakabayashi, O., & Nakano, H. (2015) FLIP the Switch: Regulation of Apoptosis and Necroptosis by cFLIP. *International journal of molecular sciences*, **16**, 30321–30341.

Turke, A.B., Song, Y., Costa, C., Cook, R., Arteaga, C.L., Asara, J.M., & Engelman, J.A. (2012) MEK inhibition leads to PI3K/AKT activation by relieving a negative feedback on ERBB receptors. *Cancer research*, **72**, 3228–3237.

Uchiumi, T., Hinoshita, E., Haga, S., Nakamura, T., Tanaka, T., Toh, S., Furukawa, M., Kawabe, T., Wada, M., Kagotani, K., Okumura, K., Kohno, K., Akiyama, S., & Kuwano, M. (1998) Isolation of a novel human canalicular multispecific organic anion transporter, cMOAT2/MRP3, and its expression in cisplatin-resistant cancer cells with decreased ATP-dependent drug transport. *Biochemical and biophysical research communications*, **252**, 103–110.

Urbańska, K., Sokołowska, J., Szmidt, M., & Sysa, P. (2014) Review Glioblastoma multiforme – an overview. *Współczesna Onkologia*, **5**, 307–312.

Van Blitterswijk, W.J. & Verheij, M. (2013) Anticancer mechanisms and clinical application of alkylphospholipids. *Biochimica et Biophysica Acta - Molecular and Cell Biology of Lipids*, **1831**, 663–674.

Van Brocklyn, J.R. & Williams, J.B. (2012) The control of the balance between ceramide and sphingosine-1-phosphate by sphingosine kinase: oxidative stress and the seesaw of cell survival and death. *Comparative biochemistry and physiology. Part B, Biochemistry & molecular biology*, **163**, 26–36.

Van Meir, E.G., Hadjipanayis, C.G., Norden, A.D., Shu, H.-K., Wen, P.Y., & Olson, J.J. (2009) Exciting new advances in neuro-oncology: the avenue to a cure for malignant glioma. *CA: a cancer journal for clinicians*, **60**, 166–193.

Vanden Berghe, T., Kaiser, W.J., Bertrand, M.J., & Vandenabeele, P. (2015) Molecular crosstalk between apoptosis, necroptosis, and survival signaling. *Molecular & Cellular Oncology*, **2**, e975093.

Vanden Berghe, T., Linkermann, A., Jouan-Lanhouet, S., Walczak, H., & Vandenabeele, P. (2014) Regulated necrosis: the expanding network of non-apoptotic cell death pathways. *Nature reviews. Molecular cell biology*, **15**, 135–147.

Vanlangenakker, N., Bertrand, M.J.M., Bogaert, P., Vandenabeele, P., & Vanden Berghe, T. (2011) TNF-induced necroptosis in L929 cells is tightly regulated by multiple TNFR1 complex I and II members. *Cell Death and Disease*, **2**, e230.

Vanlangenakker, N., Vanden Berghe, T., & Vandenabeele, P. (2012) Many stimuli pull the necrotic trigger, an overview. *Cell Death and Differentiation*, **19**, 75–86.

Varadhachary, a S., Edidin, M., Hanlon, a M., Peter, M.E., Krammer, P.H., & Salgame, P. (2001) Phosphatidylinositol 3'-kinase blocks CD95 aggregation and caspase-8 cleavage at the death-inducing signaling complex by modulating lateral diffusion of CD95. *Journal of immunology (Baltimore, Md. : 1950)*, **166**, 6564–6569.

Varfolomeev, E., Goncharov, T., Fedorova, A.V., Dynek, J.N., Zobel, K., Deshayes, K., Fairbrother, W.J., & Vucic, D. (2008) c-IAP1 and c-IAP2 are critical mediators of tumor necrosis factor alpha (TNFalpha)-induced NF-kappaB activation. *The Journal of biological chemistry*, **283**, 24295–24299.

Vercammen, D., Brouckaert, G., Denecker, G., Van de Craen, M., Declercq, W., Fiers, W., & Vandenabeele, P. (1998) Dual signaling of the Fas receptor: initiation of both apoptotic and necrotic cell death pathways. *The Journal of experimental medicine*, **188**, 919–930.

Verhaak, R.G.W., Hoadley, K.A., Purdom, E., Wang, V., Qi, Y., Wilkerson, M.D., Miller, C.R., Ding, L., Golub, T., Mesirov, J.P., Alexe, G., Lawrence, M., O'Kelly, M., Tamayo, P., Weir, B.A., Gabriel, S., Winckler, W., Gupta, S., Jakkula, L., Feiler, H.S., Hodgson, J.G., James, C.D., Sarkaria, J.N., Brennan, C., Kahn, A., Spellman, P.T., Wilson, R.K., Speed, T.P., Gray, J.W., Meyerson, M., Getz, G., Perou, C.M., & Hayes, D.N. (2010) Integrated Genomic Analysis Identifies Clinically Relevant Subtypes of Glioblastoma Characterized by Abnormalities in PDGFRA, IDH1, EGFR, and NF1. *Cancer Cell*, **17**, 98–110.

Vivanco, I. & Sawyers, C.L. (2002) The phosphatidylinositol 3-Kinase AKT pathway in human cancer. *Nature reviews. Cancer*, **2**, 489–501.

Vordermark, D., Kölbl, O., Ruprecht, K., Vince, G.H., Bratengeier, K., & Flentje, M. (2005) Hypofractionated stereotactic re-irradiation: treatment option in recurrent malignant glioma. *BMC cancer*, **5**, 55.

Walsh, C.M. (2014) Grand challenges in cell death and survival: apoptosis vs. necroptosis. *Frontiers in Cell and Developmental Biology*, **2**.

Wang, X., Zhang, J., Kim, H.P., Wang, Y., Choi, A.M.K., & Ryter, S.W. (2004) Bcl-XL disrupts death-inducing signal complex formation in plasma membrane induced by hypoxia/reoxygenation. *FASEB journal : official publication of the Federation of American Societies for Experimental Biology*, **18**, 1826–1833.

Wang, Z., Jiang, H., Chen, S., Du, F., & Wang, X. (2012) The mitochondrial phosphatase PGAM5 functions at the convergence point of multiple necrotic death pathways. *Cell*,

148, 228–243.

Watanabe, K., Tachibana, O., Sata, K., Yonekawa, Y., Kleihues, P., & Ohgaki, H. (1996) Overexpression of the EGF receptor and p53 mutations are mutually exclusive in the evolution of primary and secondary glioblastomas. *Brain pathology (Zurich, Switzerland)*, **6**, 217–223; discussion 23–24.

Weller, M., Fisher, B., Taphoorn, M.J.B., Belanger, K., Brandes, A.A., Marosi, C., Bogdahn, U., Curschmann, J., & Janzer, R.C. (2005) Radiotherapy plus concomitant and adjuvant temozolomide for glioblastoma. *Cancer/Radiothérapie*, **9**, 196–197.

WHO (2006) Framework for Developing Health-Based EMF Standards.

Wick, W., Steinbach, J.P., Küker, W.M., Dichgans, J., Bamberg, M., & Weller, M. (2004) One week on/one week off: a novel active regimen of temozolomide for recurrent glioblastoma. *Neurology*, **62**, 2113–2115.

Wick, W., Wagner, S., Kerkau, S., Dichgans, J., Tonn, J.C., & Weller, M. (1998) BCL-2 promotes migration and invasiveness of human glioma cells. *FEBS Letters*, **440**, 419–424.

Wieder, T., Orfanos, C.E., & Geilen, C.C. (1998) Induction of ceramide-mediated apoptosis by the anticancer phospholipid analog, hexadecylphosphocholine. *The Journal of biological chemistry*, **273**, 11025–11031.

Wiemels, J., Wrensch, M., & Claus, E.B. (2010) Epidemiology and etiology of meningioma. *Journal of Neuro-Oncology*, **99**, 307–314.

Will, M., Qin, A.C.R., Toy, W., Yao, Z., Rodrik-Outmezguine, V., Schneider, C., Huang, X., Monian, P., Jiang, X., De Stanchina, E., Baselga, J., Liu, N., Chandarlapaty, S., & Rosen, N. (2014) Rapid induction of apoptosis by PI3K inhibitors is dependent upon their transient inhibition of RAS-ERK signaling. *Cancer Discovery*, **4**, 334–348.

Wilson, T., Karajannis, M., & Harter, D.H. (2014) Glioblastoma multiforme: State of the art and future therapeutics. *Surgical neurology international*, **5**, 64.

Wolbers, J.G. (2014) Novel strategies in glioblastoma surgery aim at safe, super-maximum resection in conjunction with local therapies.

Wong, E.T., Hess, K.R., Gleason, M.J., Jaeckle, K.A., Kyritsis, A.P., Prados, M.D., Levin, V.A., & Yung, W.K. (1999) Outcomes and prognostic factors in recurrent glioma patients enrolled onto phase II clinical trials. *Journal of clinical oncology : official journal of the American Society of Clinical Oncology*, **17**, 2572–2578.

Wrensch, M., Minn, Y., Chew, T., Bondy, M., & Berger, M.S. (2001) Epidemiology of primary brain tumors: Current concepts and review of the literature 1. *Neuro-Oncology*, 278–299.

Wu, H., Che, X., Zheng, Q., Wu, A., Pan, K., Shao, A., Wu, Q., & Zhang, J. (2014) Cas-

pases : A Molecular Switch Node in the Crosstalk between Autophagy and Apoptosis. *International Journal of Biological Sciences*, **10**, 1072–1083.

Wu, W., Liu, P., & Li, J. (2012) Necroptosis: An emerging form of programmed cell death. *Critical Reviews in Oncology/Hematology*, **82**, 249–258.

Yang, S., Wang, X., Contino, G., Liesa, M., Sahin, E., Ying, H., Bause, A., Li, Y., Stomme, J.M., Dell'Antonio, G., Mautner, J., Tonon, G., Haigis, M., Shirihai, O.S., Doglioni, C., Bardeesy, N., & Kimmelman, A.C. (2011) Pancreatic cancers require autophagy for tumor growth. *Genes and Development*, **25**, 717–729.

Youle, R.J. & Strasser, A. (2008) The BCL-2 protein family: opposing activities that mediate cell death. *Nature reviews. Molecular cell biology*, **9**, 47–59.

Young, N. & Van Brocklyn, J.R. (2006) Signal transduction of sphingosine-1-phosphate G protein-coupled receptors. *TheScientificWorldJournal*, **6**, 946–966.

Yung, W.K.A., Prados, M.D., Yaya-Tur, R., Rosenfeld, S.S., Brada, M., Friedman, H.S., Albright, R., Olson, J., Chang, S.M., O'Neill, A.M., Friedman, A.H., Bruner, J., Yue, N., Dugan, M., Zaknoen, S., & Levin, V.A. (1999) Multicenter phase II trial of temozolomide in patients with anaplastic astrocytoma or anaplastic oligoastrocytoma at first relapse. *Journal of Clinical Oncology*, **17**, 2762–2771.

Zelcer, N., Saeki, T., Reid, G., Beijnen, J.H., & Borst, P. (2001) Characterization of drug transport by the human multidrug resistance protein 3 (ABCC3). *The Journal of biological chemistry*, **276**, 46400–46407.

Zentaris, A. (2012) Press release.

Zhang, D.-W., Shao, J., Lin, J., Zhang, N., Lu, B.-J., Lin, S.-C., Dong, M.-Q., & Han, J. (2009) RIP3, an energy metabolism regulator that switches TNF-induced cell death from apoptosis to necrosis. *Science (New York, N.Y.)*, **325**, 332–336.

Zhang, H. & Burrows, F. (2004) Targeting multiple signal transduction pathways through inhibition of Hsp90. *Journal of Molecular Medicine*, **82**, 488–499.

Zhang, X., Zhang, W., Cao, W., Cheng, G., & Zhan, Y. (2012) Glioblastoma multiforme: Molecular characterization and current treatment strategy (Review). *Experimental and Therapeutic Medicine*, **3**, 9–14.

Zheng, B., Fiumara, P., Li, Y.V., Georgakis, G., Snell, V., Younes, M., Vauthey, J.N., Carbone, A., & Younes, A. (2003) MEK/ERK pathway is aberrantly active in Hodgkin disease: a signaling pathway shared by CD30, CD40, and RANK that regulates cell proliferation and survival. *Blood*, **102**, 1019–1027.

Zheng, H., Luo, R.-C., Zhang, L.-S., & Mai, G.-F. (2002) Interferon-gamma up-regulates Fas expression and increases Fas-mediated apoptosis in tumor cell lines. *Di 1 jun yi da xue*

xue bao = Academic journal of the first medical college of PLA, **22**, 1090–1092.

Zhou, X., Lu, X., Richard, C., Xiong, W., Litchfield, D.W., Bittman, R., & Arthur, G. (1996) 1-O-octadecyl-2-O-methyl-glycerophosphocholine inhibits the transduction of growth signals via the MAPK cascade in cultured MCF-7 cells. *Journal of Clinical Investigation*, **98**, 937–944.

Zhu, H., Woolfenden, S., Bronson, R.T., Jaffer, Z.M., Barluenga, S., Winssinger, N., Rubenstein, A.E., Chen, R., & Charest, A. (2010) The novel Hsp90 inhibitor NXD30001 induces tumor regression in a genetically engineered mouse model of glioblastoma multiforme. *Molecular cancer therapeutics*, **9**, 2618–2626.